2mit

NASA CR- 132354

ANALYSIS OF AEROELASTIC MODEL STABILITY AUGMENTATION SYSTEMS

FINAL REPORT

(NASA-CR-132354) ANALYSIS OF AEROELASTIC MODEL STABILITY AUGMENTATION SYSTEMS Final Report (Boeing Co., Wichita, Kans.) ~~202~~ p HC $12.25 CSCL 01C
200
N74-11829
Unclas
G3/02 22988

D3-8390-4

MARCH 1971

THE BOEING COMPANY
WICHITA DIVISION - WICHITA, KANSAS, 67210

IG710274

1.0 INTRODUCTION

This final report describes assistance provided the NASA-Langley Research Center from 10 February 1970 to 9 February 1971 under Contract NAS 1-9808 in the analysis of aeroelastic model stability augmentation systems. All previously published documents and Coordination Sheets prepared under the contract are contained in this single document.

Section 2.0 contains Boeing Document D3-8390-1 which presents results of an analytical and mechanization study conducted for two flutter SAS concepts developed by Dr. Eliahu Nissim of the NASA-Langley Aeroelasticity Branch.

Section 3.0 is a work statement for a proposed design and mechanization of a ride control system for the B-52 aeroelastic model. This work statement was previously released as Boeing Document D3-8390-2.

Boeing Document D3-8390-3, presented in Section 4.0, contains results of a study conducted to evaluate the B-52 aeroelastic model aileron and elevator actuation systems and proposed modifications to provide satisfactory performance.

Section 5.0 contains Boeing Coordination Sheet SDF-79-0. This report describes a study conducted to provide a basis for comparing B-52 aeroelastic model wind tunnel gust response data to flight test data.

Section 6.0 contains Boeing Coordination Sheet 3-7560-70-76 which presents a summary of technical support provided for mechanizing a flutter suppression system on the SST wing aeroelastic model.

NASA CR- 132354

THE BOEING COMPANY
WICHITA DIVISION

CODE IDENT. NO. 81205

NUMBER D3-8390-4 REV LTR

INITIAL RELEASE DATE 4 March 1971

TITLE ANALYSIS OF AEROELASTIC MODEL STABILITY AUGMENTATION SYSTEMS - FINAL REPORT

FOR LIMITATIONS IMPOSED ON THE USE OF THE INFORMATION CONTAINED IN THIS DOCUMENT AND ON THE DISTRIBUTION OF THIS DOCUMENT, SEE LIMITATIONS SHEET.

MODEL CONTRACT NAS1-9808

ISSUE NO. ISSUED TO

PREPARED BY Frank D. Sevart

SUPERVISED BY Dr. Gerald E. Bergmann

APPROVED BY Glenn O. Thompson

APPROVED BY

ABSTRACT

This document discusses analysis results of stability augmentation systems for aeroelastic models, accomplished under NASA-Langley Research Center Contract NAS 1-9808.

RETRIEVAL REFERENCE WORDS:

Aeroelastic Models
Flutter Suppression Systems
Ride Control Systems

CONTENTS

ABSTRACT

1.0 INTRODUCTION

2.0 ANALYSIS AND MECHANIZATION OF NASA-LANGLEY FLUTTER SAS CONCEPTS (BOEING DOCUMENT D3-8390-1)

3.0 DESIGN AND MECHANIZATION OF RIDE CONTROL SYSTEM FOR B-52 AEROELASTIC MODEL - WORK STATEMENT (BOEING DOCUMENT D3-8390-2)

4.0 EVALUATION OF B-52 AEROELASTIC MODEL CONTROL SURFACE ACTUATION SYSTEMS (BOEING DOCUMENT D3-8390-3)

5.0 B-52 AEROELASTIC MODEL PROGRAM (NASA-LANGLEY), EFFECTS OF TURBULENCE SCALE ON FLIGHT TEST FREQUENCY RESPONSE FUNCTIONS, EWI 4850 (BOEING COORDINATION SHEET SDF-79-0)

6.0 CONTROL TECHNOLOGY SUPPORT PROVIDED AT NASA-LANGLEY RESEARCH CENTER (BOEING COORDINATION SHEET 3-7560-70-76)

THE BOEING COMPANY
WICHITA DIVISION

CODE IDENT. NO. 81205

NUMBER D3-8390-1 REV LTR

INITIAL RELEASE DATE 21 SEPTEMBER 1970

TITLE ANALYSIS AND MECHANIZATION OF NASA-LANGLEY FLUTTER SAS CONCEPTS

FOR LIMITATIONS IMPOSED ON THE USE OF THE INFORMATION CONTAINED IN THIS DOCUMENT AND ON THE DISTRIBUTION OF THIS DOCUMENT, SEE LIMITATIONS SHEET.

MODEL 969-300 CONTRACT

ISSUE NO. ISSUED TO

PREPARED BY Garold E. Hodges Frank D. Sevart

SUPERVISED BY Dr. Gerald E. Bergmann

APPROVED BY Glenn O. Thompson

APPROVED BY

E-3039 RS

ABSTRACT

This document discusses results of an active flutter suppression system analysis using a Boeing Supersonic Transport 969-300 configuration. The work was accomplished under NASA-Langley Contract NAS1-9808. Dr. Eliahu Nissim of the NASA-Langley Aeroelasticity Branch, Dynamic Loads Division, developed the two concepts analyzed.

RETRIEVAL REFERENCE WORDS:

REV LTR:

TABLE OF CONTENTS

SECTION		PAGE
1.0	INTRODUCTION AND SUMMARY	1
2.0	FLUTTER ANALYSIS	6
2.1	Full Scale SST Equations of Motion	6
2.2	Results	6
3.0	FLUTTER SAS MECHANIZATION	15
3.1	Description of Computer Circuit for Measuring Frequency	15
3.2	Frequency Measuring Circuit Performance	18
3.3	Period Measuring Mechanization and Performance	18

1.0 INTRODUCTION AND SUMMARY

This report presents the results of an analytical and mechanization study conducted for two flutter SAS concepts developed by Dr. Eliahu Nissim of the NASA-Langley Aeroelasticity Branch, Dynamic Loads Division. Concept No. 1 utilizes only the wing trailing edge control surface(s). Concept No. 2 utilizes leading and trailing edge control surfaces operating simultaneously. Theoretically, the combined use of leading and trailing edge control surfaces will improve the surface coupling (controllability) with vertical bending and torsional structural modes and decrease the coupling between bending and torsional modes.

The purpose of this study was:

- To determine flutter speed using full scale 969-300 SST equations of motion augmented with flutter SAS concepts No. 1 and No. 2.
- To develop a method of implementing these concepts for wind tunnel testing.

The wing is configured with three leading edge control surfaces (outboard, mid-span and inboard) and three corresponding trailing edge control surfaces. Five combinations of control surfaces and SAS concepts were analyzed during this study. These combinations and corresponding flutter speed improvements are as follows:

- 4.5 percent for the outboard trailing edge surface with flutter SAS No. 1.
- 11 percent for the leading/trailing (L/T) edge outboard surfaces with SAS No. 2.
- 28 percent for the L/T edge mid-span surfaces with SAS No. 2.
- 21 percent for the L/T edge inboard surfaces with SAS No. 2.
- Greater than 41 percent for the combined L/T edge inboard and mid-span surfaces with SAS No. 2.

Figure 1 illustrates the flutter problem on an airspeed root locus plot for the combined inboard and mid-span L/T edge surfaces at a constant Mach No. = 0.9. Airspeed was varied by changing altitude while holding Mach number constant. The free airplane encounters instability at 422 KCAS. The airplane augmented with flutter concept No. 2 using both inboard and mid-span surfaces is flutter free for airspeeds up to 595 KCAS (altitude: sea level). Figure 2 presents the third and fourth elastic mode damping ratio as a function of airspeed for the combined surface cofiguration. Similar plots for each of the other flutter SAS concepts are included in Section 2.0.

NOTES:
1) M = 0.9
2) —— FREE AIRPIANE
3) --- WITH SAS FLUTTER NO. 2
4) FLUTTER SPEED (3RD MODE)
   FREE AIRPLANE: 422 KCAS
   WITH SAS: 595 KCAS

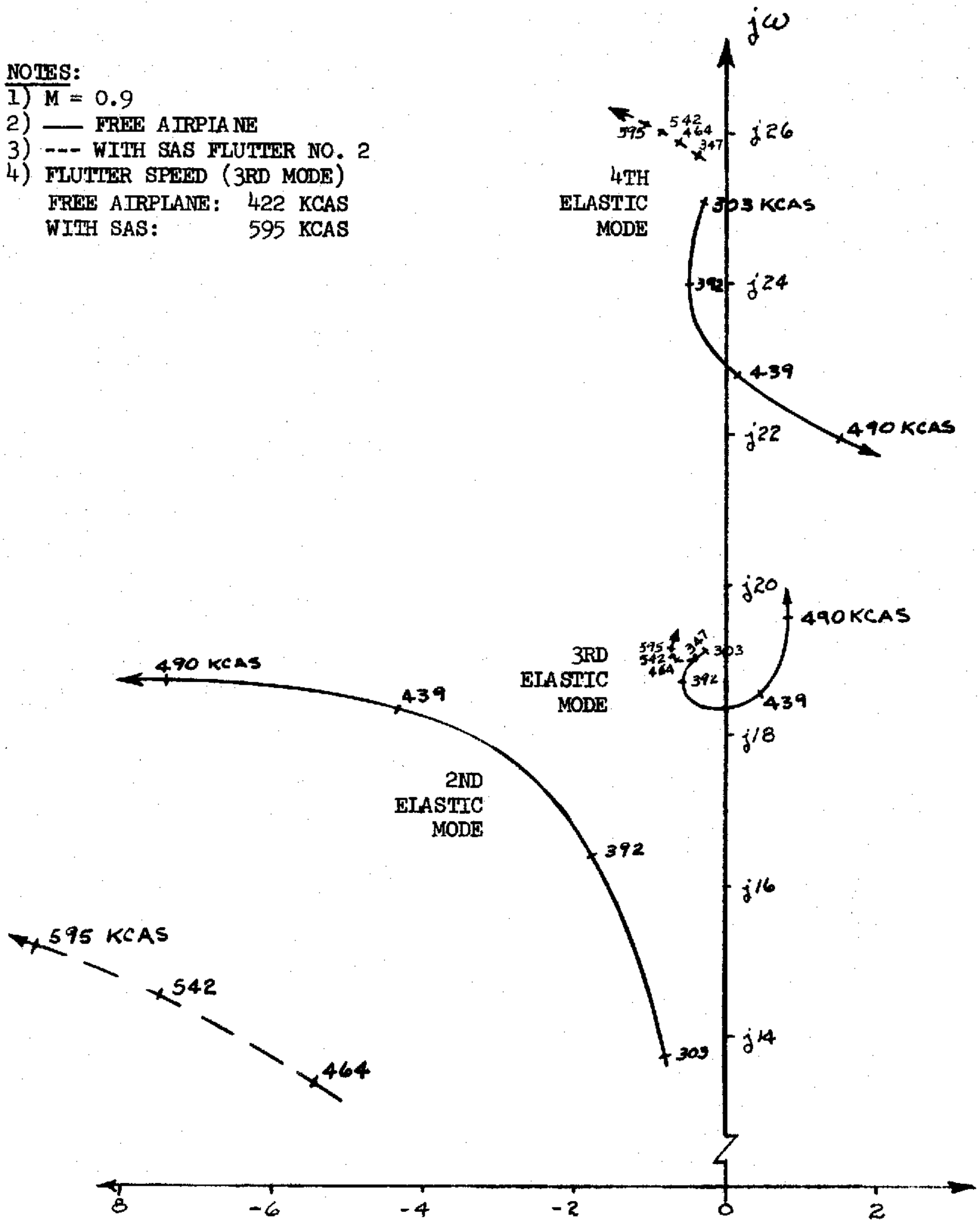

FLUTTER SAS ROOT LOCUS WITH MID-SPAN
AND INBOARD L/T EDGE SURFACES

Figure 1

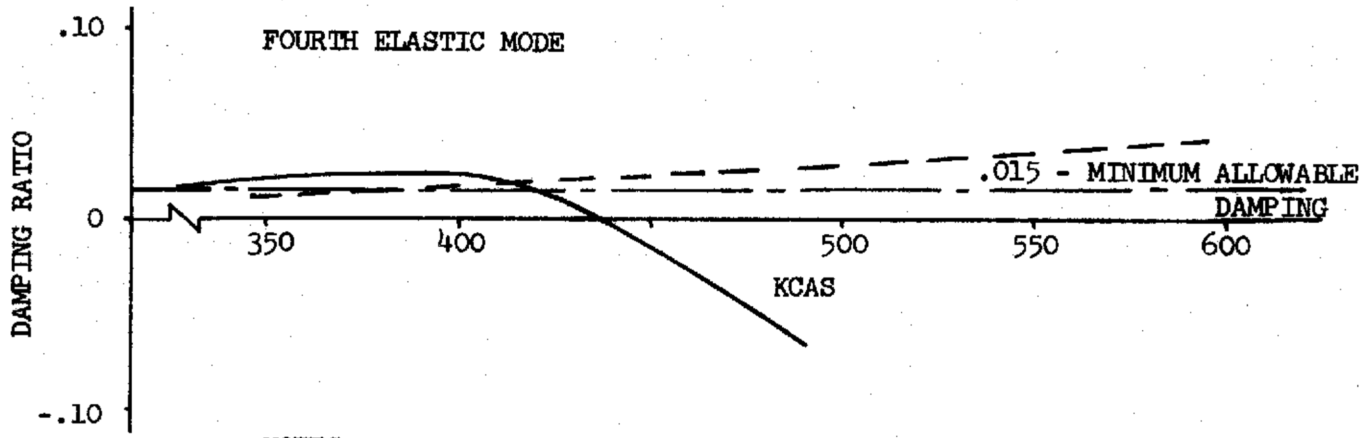

NOTES:
1) ——— FREE AIRPLANE
 - - - FLUTTER SAS NO. 2 WITH MID-SPAN AND INBOARD L/T SURFACES
2) M = 0.9
3) STRUCTURAL MODE STABILITY ONLY

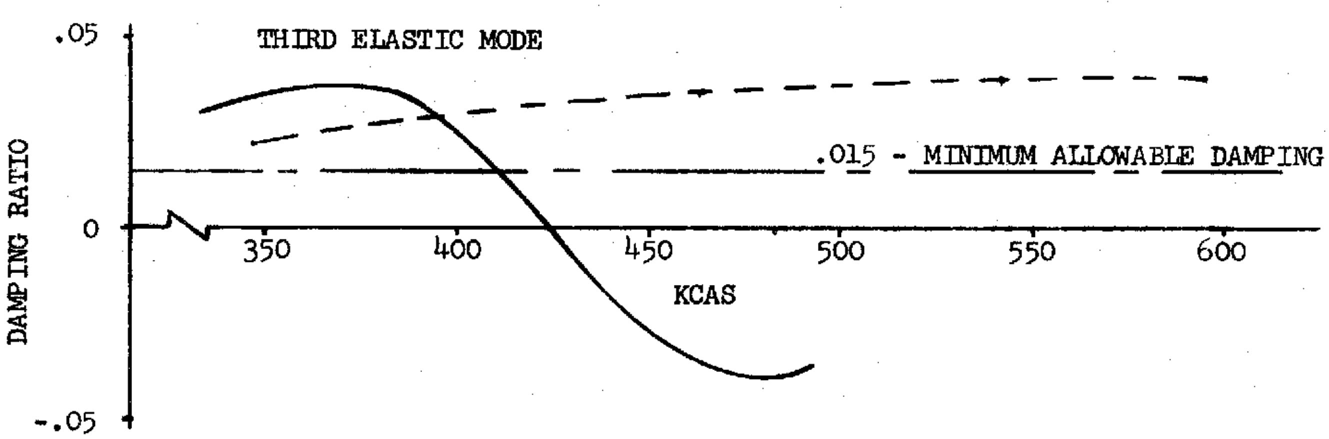

EFFECT OF SAS ON FLUTTER SPEED

Figure 2

All flutter concepts and surface combinations cause a low frequency (phugoid mode) instability at the selected gains. Stability results indicate that phase lead and a decrease in amplitude at this frequency, obtained with a high-pass filter, would stabilize this mode.

Flutter SAS concept No. 1 using an outboard control surface is scheduled to be mechanized and tested on NASA-Langley's 1/17 scale SST wing model.

A block diagram of the system to be mechanized is shown in Figure 3. The primary problem associated with mechanization is that the systems require the rate signal to be divided by frequency. Two methods of mechanizing the flutter augmentation systems were tested on an analog computer to assess the feasibility of measuring instantaneous frequency (period) based on the simple harmonic motion relationship: $\omega^2 = |\text{acceleration}|/|\text{displacement}|$. The other method measures "period" by detecting zero-crossings. Both mechanizations adequately measure the steady-state frequency over the frequency range of primary interest (5 to 25 Hz).

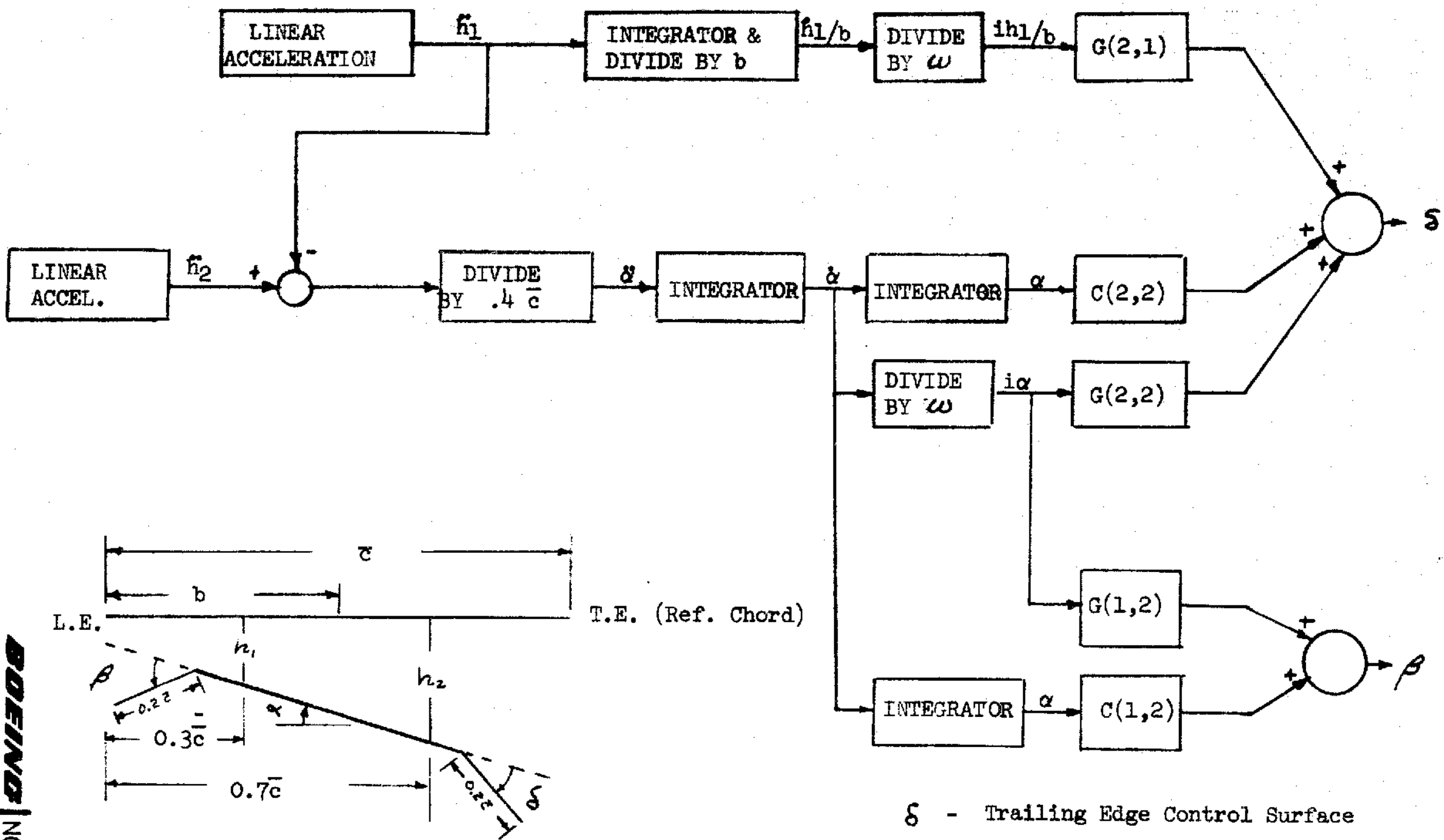

δ - Trailing Edge Control Surface

β - Leading Edge Control Surface

FLUTTER SAS BLOCK DIAGRAM

Figure 3

2.0 FLUTTER ANALYSIS

2.1 Full Scale SST Equations of Motion

Flutter analyses were conducted using the 969-300 SST configuration at Mach 0.9 and a gross weight of 395,000 pounds. The equations were modified to incorporate a 20 percent chord leading edge control surface. Figure 4 shows the location of the control surfaces, and Z (vertical translation) and θ (pitch angle) response stations for the wing. Vertical acceleration was sensed at chord (panel) stations that correspond to 30 and 70 percent chord.

The linear differential equations representing the 969-300 SST airplane configuration were written with forward speed and air density as explicit functions. This permitted varying the forward velocity as a function of altitude at constant Mach number to determine flutter speed. The math model includes two rigid body and ten structural modes. The aerodynamic theory used for the leading and trailing edge control surfaces was steady-state lifting surface with first-order lift growth approximations (Wagner functions) to represent unsteady aerodynamics.

2.2 Results

Both flutter SAS concepts employ a signal which has the same amplitude as displacement but is in phase with rate. This signal was generated for the stability study by using phase root locus to introduce a phase shift ($e^{j\theta}$) without changing the signal amplitude as a function of frequency. A block diagram of the system as arranged for stability analysis is shown in Figure 5.

Free airplane flutter is encountered when the third elastic mode crosses the imaginary axis at 422 KCAS. As speed is increased further the fourth elastic mode becomes unstable at 435 KCAS. The trailing edge control surface primarily stabilizes the fourth elastic mode whereas stability of the third mode is predominantly controlled with the leading/trailing edge surfaces. This conclusion is illustrated in Figure 6 by comparing the results for SAS No. 1 and No. 2 with outboard surfaces. Figure 7 shows the third and fourth mode damping ratio as a function of airspeed for the mid-span and inboard surfaces. Airspeed root locus plots for SAS No. 1 using a trailing edge surface and for SAS No. 2 using outboard, mid-span and inboard L/T edge surfaces are portrayed in Figures 8 through 11.

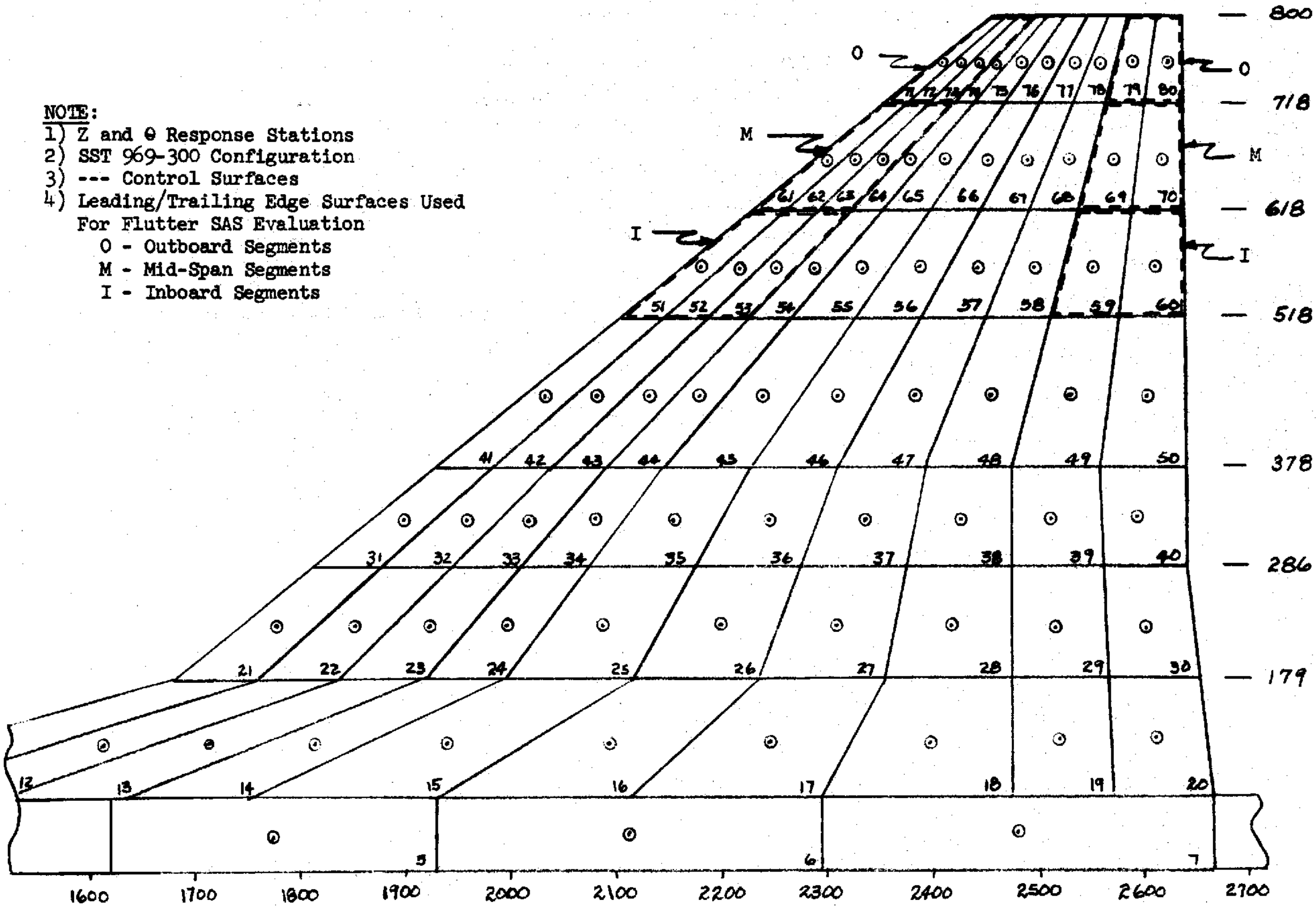

WING PANELING DIAGRAM

Figure 4

FLUTTER SAS DIAGRAM FOR STABILITY ANALYSIS
(Leading/Trailing Edge Control Surfaces)

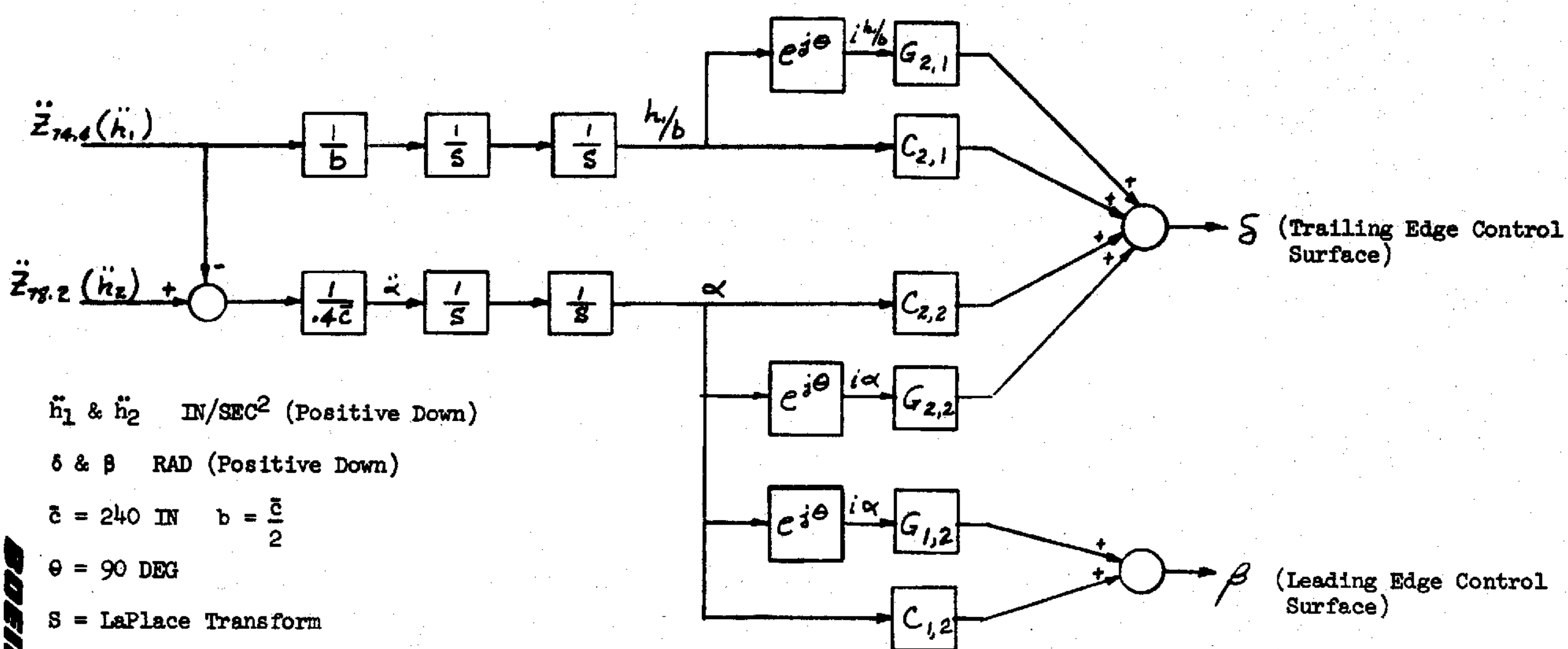

$\ddot{h}_1$ & $\ddot{h}_2$ IN/SEC^2 (Positive Down)

δ & β RAD (Positive Down)

$\bar{c}$ = 240 IN $b = \frac{\bar{c}}{2}$

θ = 90 DEG

S = LaPlace Transform

$$\begin{Bmatrix}\beta\\ \delta\end{Bmatrix} = \overset{C}{\begin{bmatrix}0 & 0\\ -0.35 & -1.9\end{bmatrix}}\begin{Bmatrix}h_1/b\\ \alpha\end{Bmatrix} + e^{j\theta}\overset{G}{\begin{bmatrix}0 & 0\\ 0.35 & 0.1\end{bmatrix}}\begin{Bmatrix}h_1/b\\ \alpha\end{Bmatrix}$$

FLUTTER SAS NO. 1
TRAILING EDGE CONTROL ONLY

$$\begin{Bmatrix}\beta\\ \delta\end{Bmatrix} = \begin{bmatrix}0 & 5.6\\ 0 & -1.4\end{bmatrix}\begin{Bmatrix}h_1/b\\ \alpha\end{Bmatrix} + e^{j\theta}\begin{bmatrix}0 & 1.5\\ 0.6 & 0.2\end{bmatrix}\begin{Bmatrix}h_1/b\\ \alpha\end{Bmatrix}$$

FLUTTER SAS NO. 2
TRAILING AND LEADING EDGE CONTROL

Figure 5

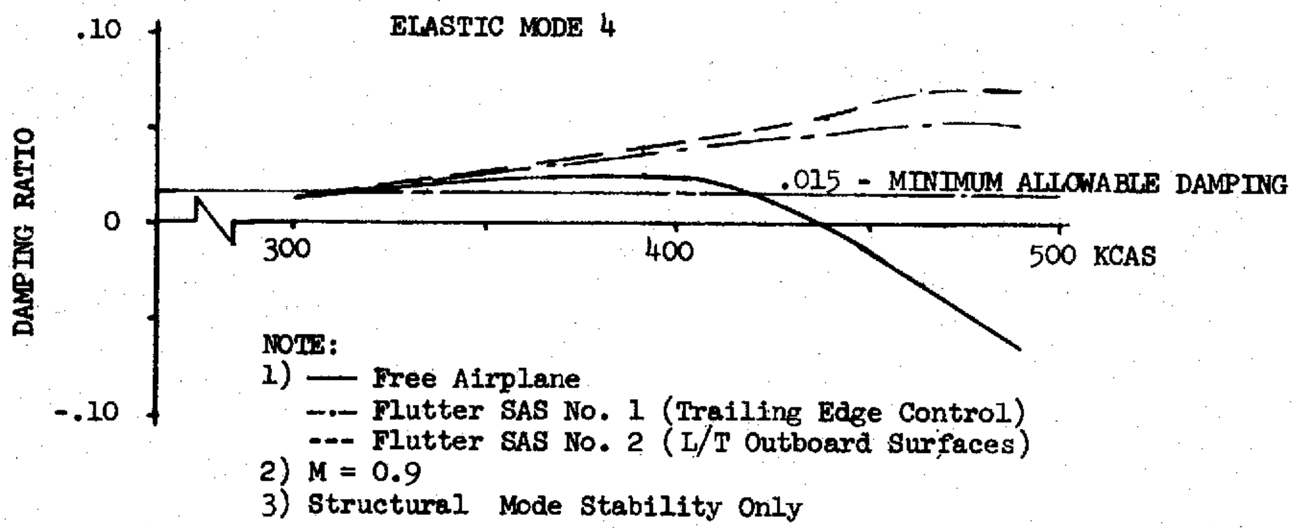

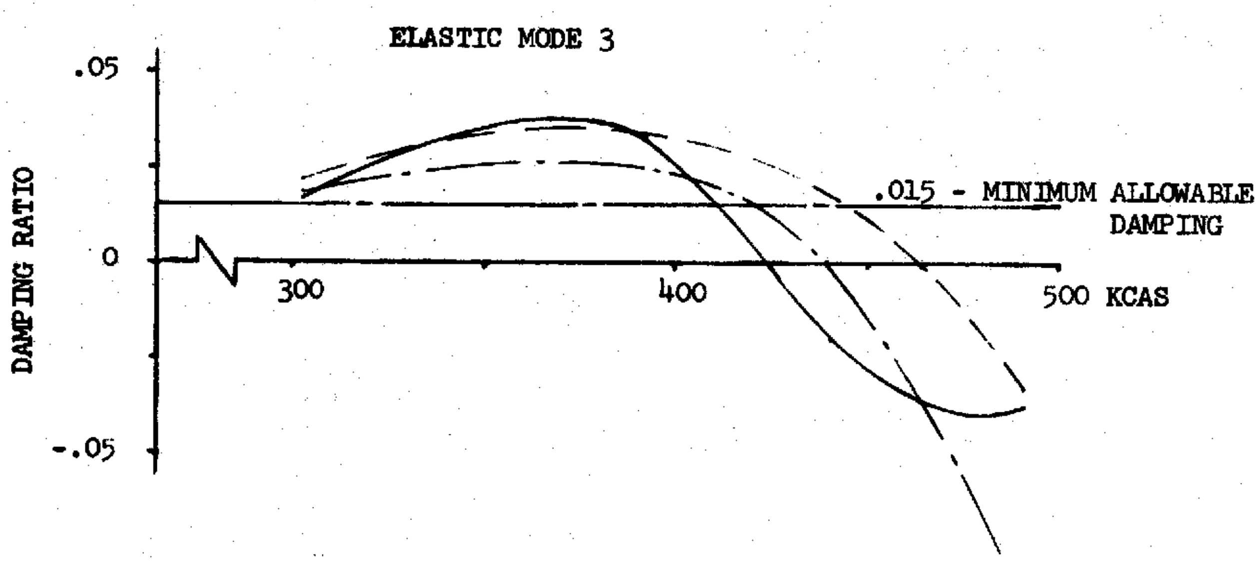

EFFECT OF SAS ON FLUTTER SPEED

Figure 6

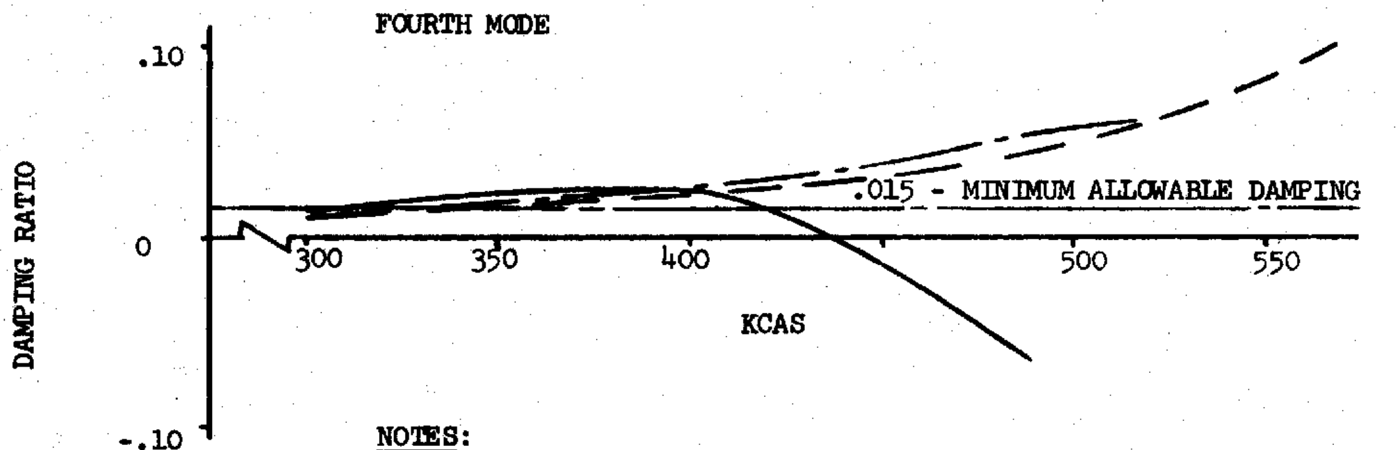

NOTES:
(1) M = 0.9
(2) —— FREE AIRPLANE
--- MID SPAN SURFACES
-·- INBOARD SURFACE
(3) FLUTTER SAS NO. 2 (L/T EDGE CONTROL)

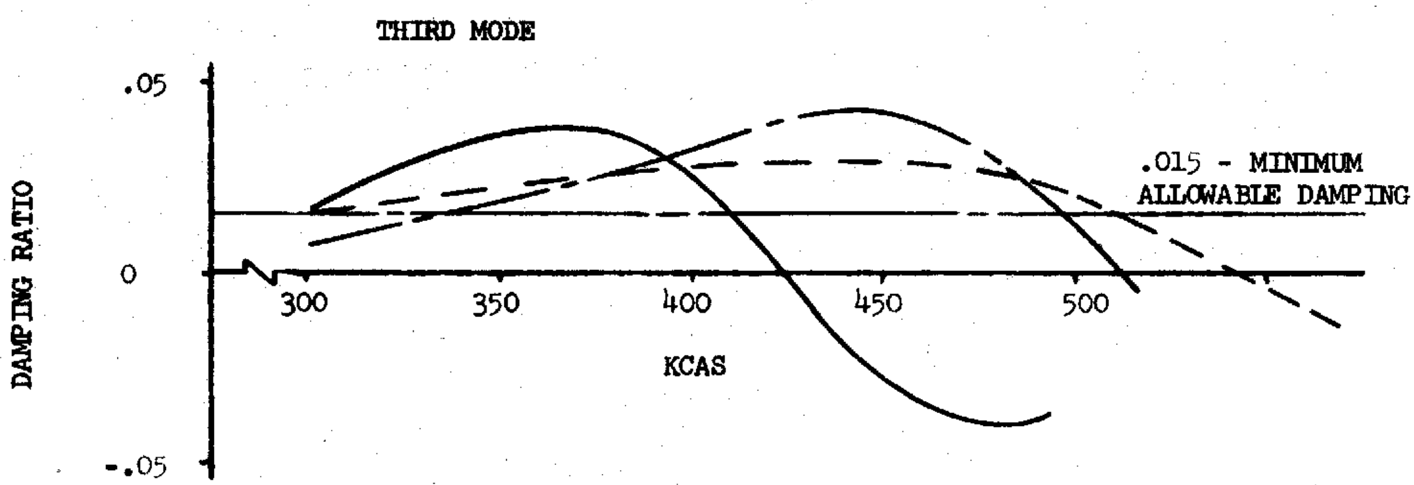

EFFECT OF SAS ON FLUTTER SPEED

Figure 7

NOTE:

1) M = 0.9
2) —— Free Airplane
3) --- With Flutter SAS No. 1
4) Flutter Speed (3rd Mode)
   FREE AIRPLANE: 422 KCAS
   WITH SAS: 440 KCAS

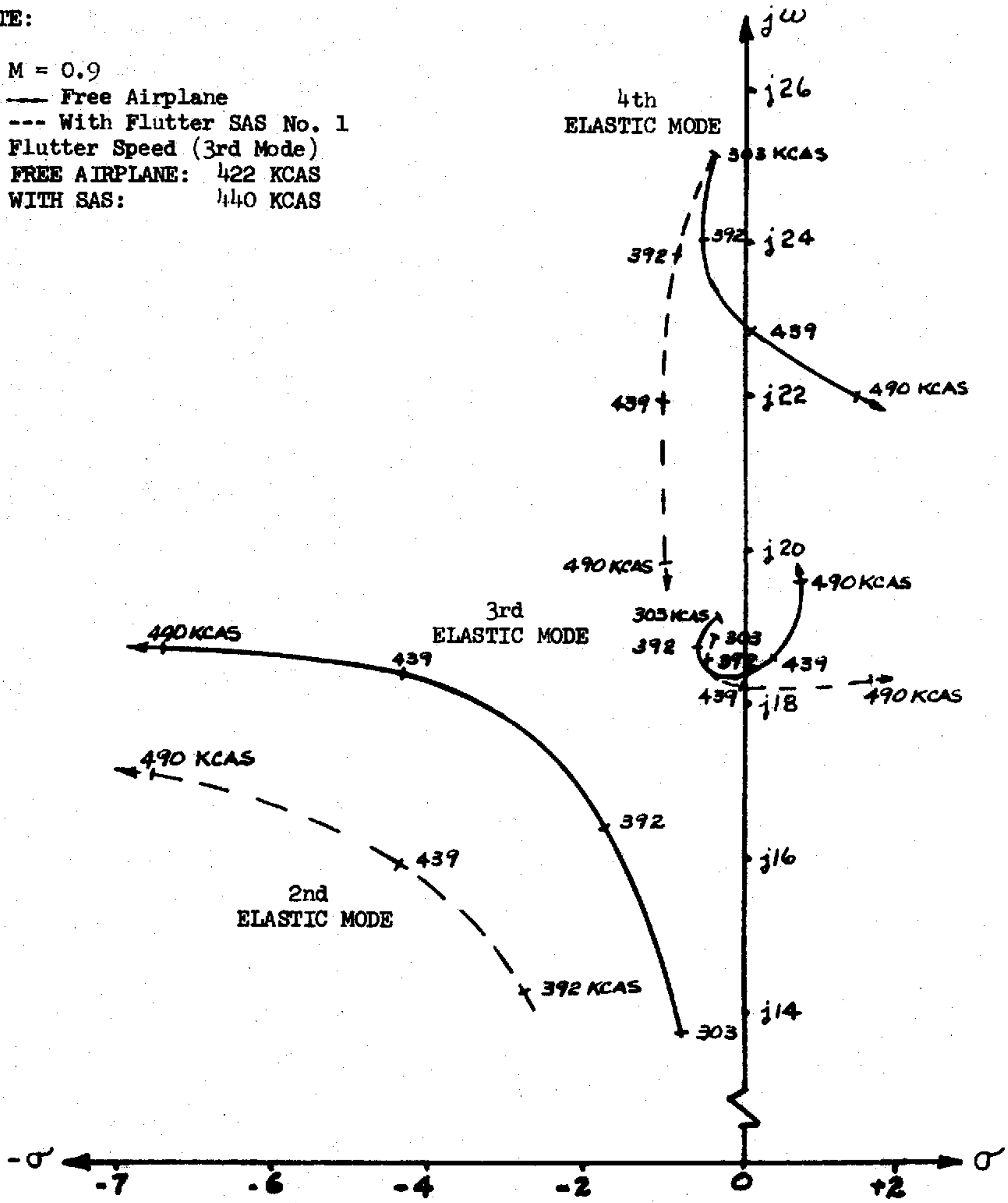

FLUTTER SAS ROOT LOCUS
WITH TRAILING EDGE CONTROL SURFACE

Figure 8

NOTES:

1) M = 0.9
2) ___ Free Airplane
3) --- With Flutter SAS No. 2
4) Flutter Speed (3rd Mode)
   Free Airplane: 422 KCAS
   With SAS: 464 KCAS

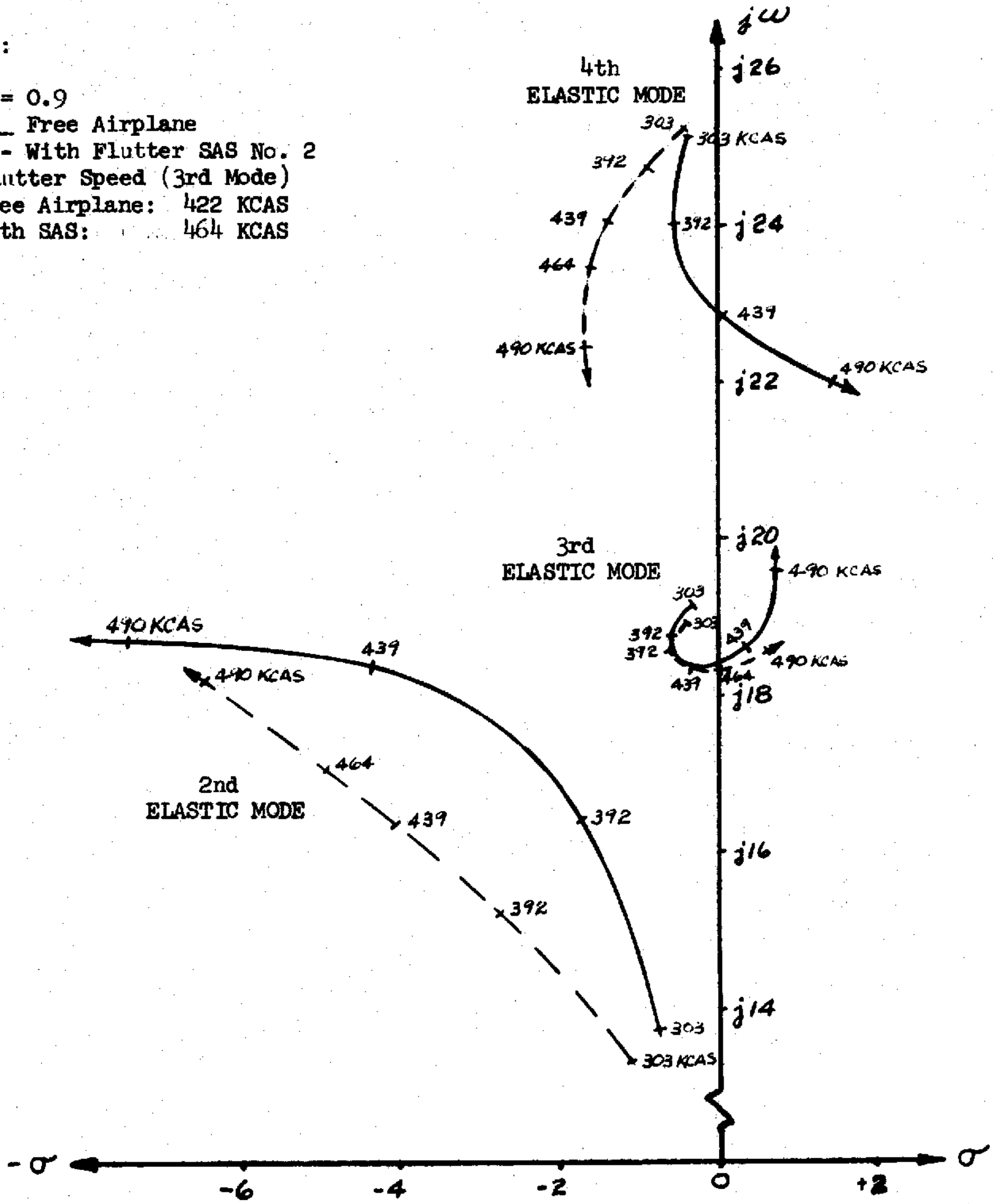

FLUTTER SAS ROOT LOCUS
WITH OUTBOARD L/T EDGE CONTROL SURFACES

Figure 9

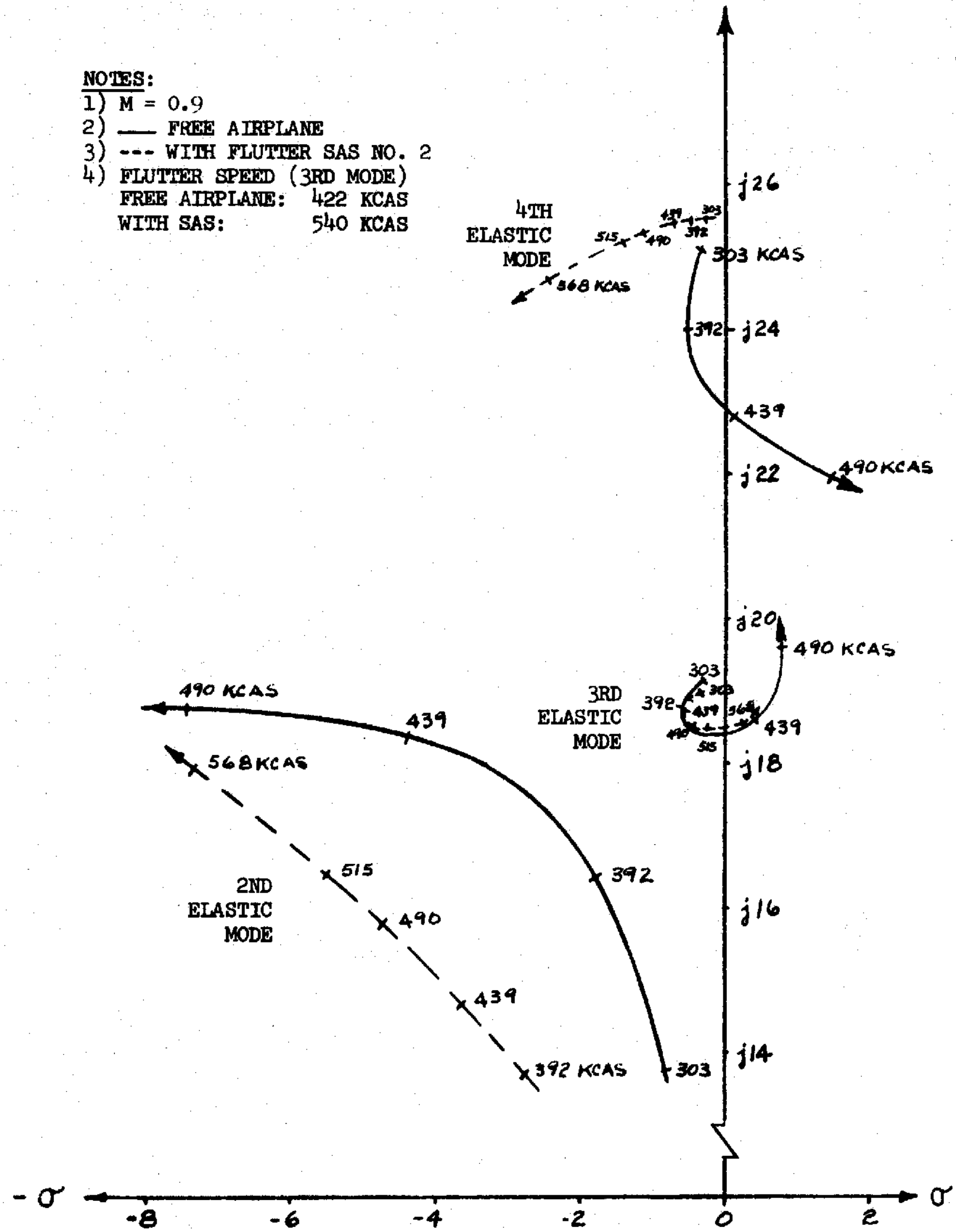

FLUTTER SAS ROOT LOCUS
WITH MID-SPAN L/T EDGE SURFACES

FIGURE 10

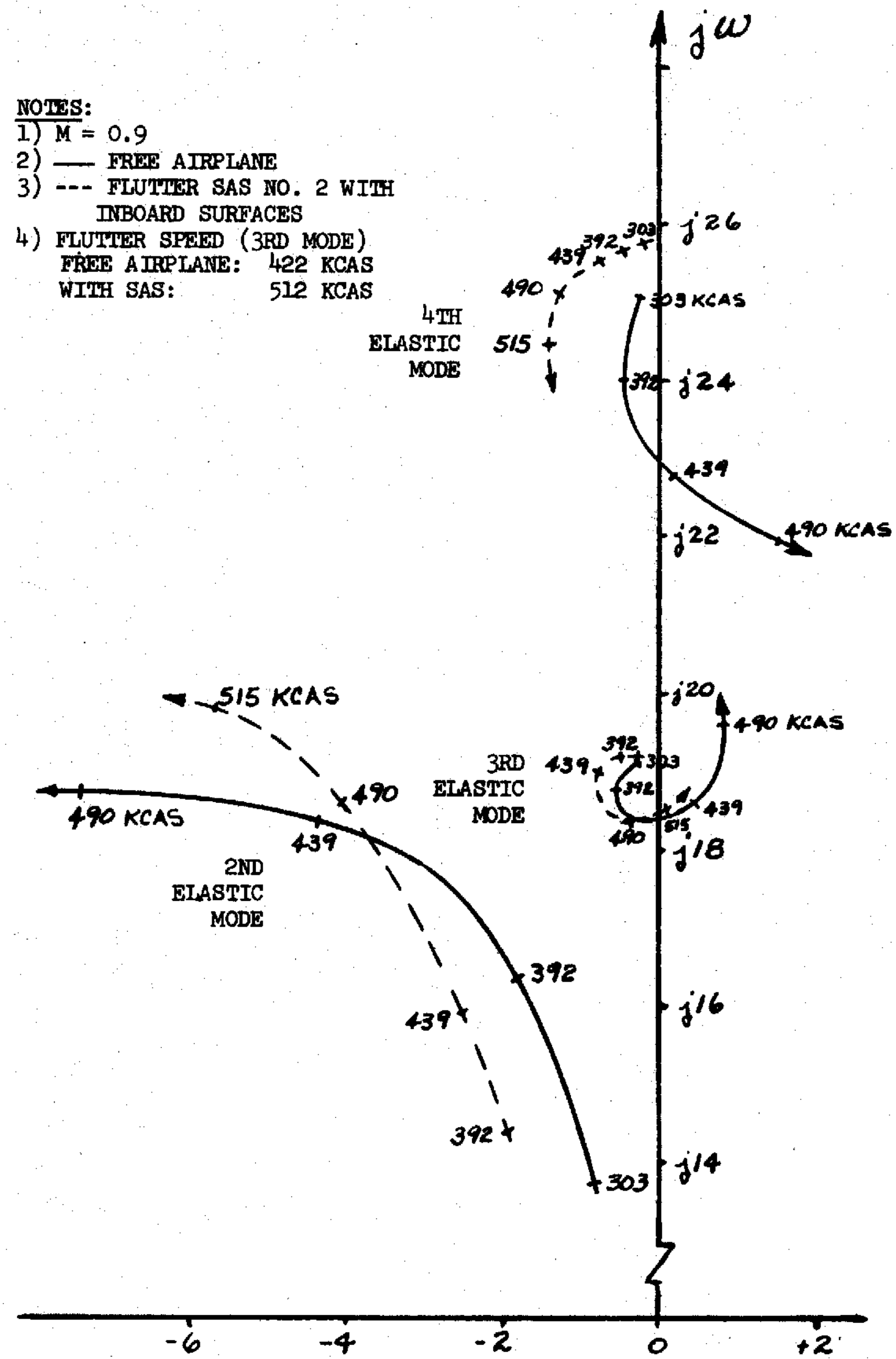

FLUTTER SAS ROOT LOCUS
WITH INBOARD L/T EDGE SURFACES

Figure 11

3.0 FLUTTER SAS MECHANIZATION

To mechanize these flutter SAS concepts it is necessary to measure the feedback signal frequency (or period) or to generate 90 degrees phase lead. An analog computer simulation was developed to assess the feasibility of measuring frequency using analog components. The "frequency" measurement was based on the simple harmonic motion relationship: $\omega^2 = |\text{acceleration}|/|\text{displacement}|$. Sections 3.1 and 3.2 describe the mechanization and performance of this technique.

A second analog simulation was utilized to evaluate a technique that measures the signal "period". This method eliminates some division and square root circuits associated with the frequency method. Section 3.3 describes the mechanization and performance of this system.

3.1 Description of Computer Circuit for Measuring Frequency

An analog computer diagram for one channel of the SAS is shown in Figure 12. The numerator and denominator terms which form the radian frequency (ω) are passed through approximate derivative circuits to eliminate any d.c. bias in either signal. The voltage signals from the derivative circuits are then rectified to accommodate the electronic multiplier division circuit producing ω_1^2.

Threshold logic was mechanized using a relay comparator to alleviate the noise amplification produced by the division circuit when the numerator and denominator voltages are small. When the voltage representing the denominator, $|Z_2|$, is above the threshold value the frequency is formed by the equation $\omega_1^2 = |\ddot{Z}_2 / Z_2|$. When this voltage is less than the threshold, the value of ω_1^2 before the relay switches is stored. This mechanization also eliminates division by zero when the oscillatory transient solution of the plant equations decays to zero, leaving only the steady state solution (as for a step plant disturbance).

While the relay comparator is switching, the numerator and denominator voltages are both momentarily zero which causes the amplifiers in the division circuit to saturate. This produces the spikes on the time history for ω_1^2 shown in Figure 13 and, without filtering, these spikes appear in the square root as well. Several first order filters were tried to alleviate this difficulty. The time histories shown in Figure 13 were recorded with the filter $G(S) = \frac{10}{S+10}$.

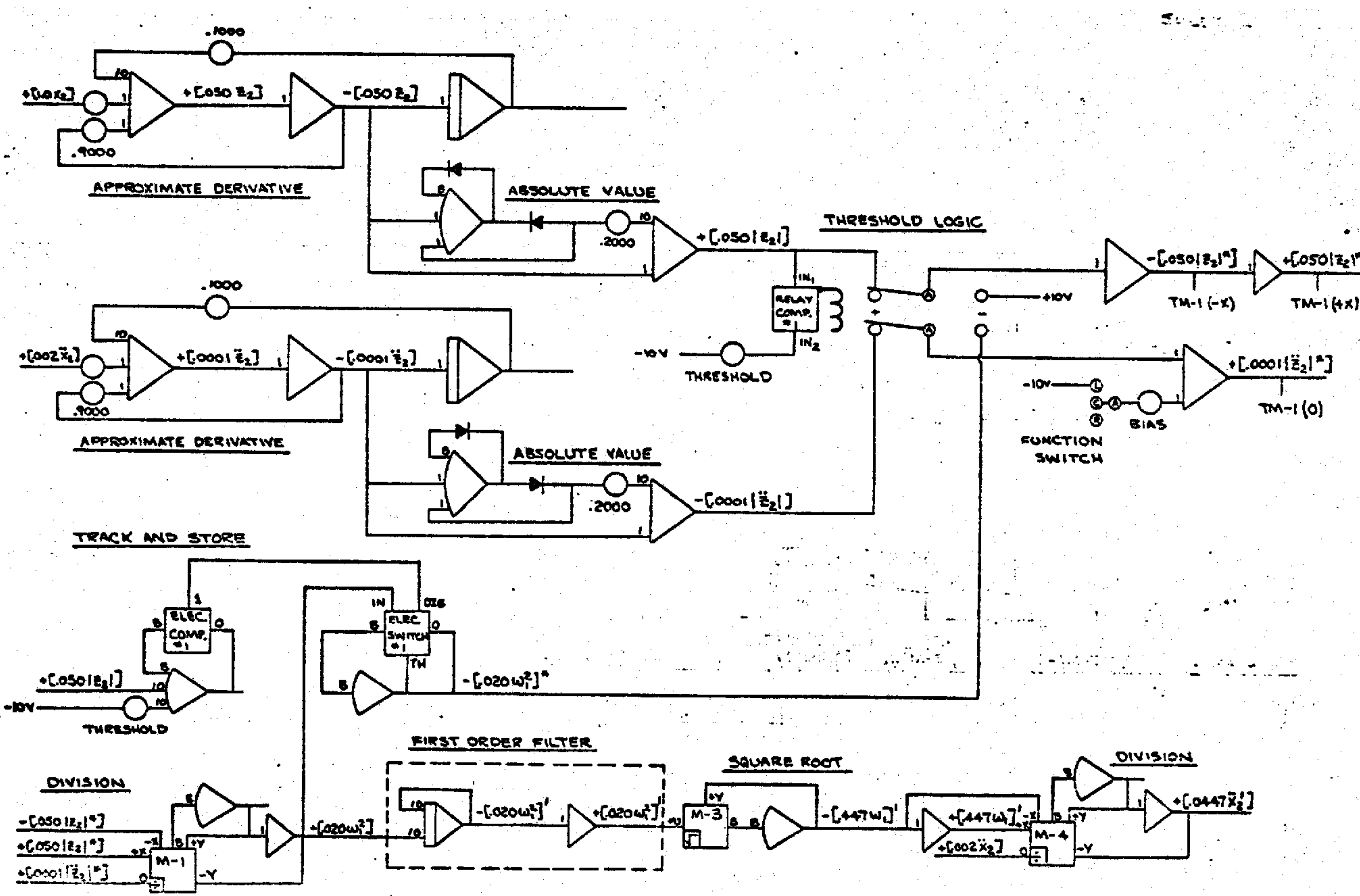

FIGURE 12. ANALOG CIRCUIT DIAGRAM (SINGLE CHANNEL)

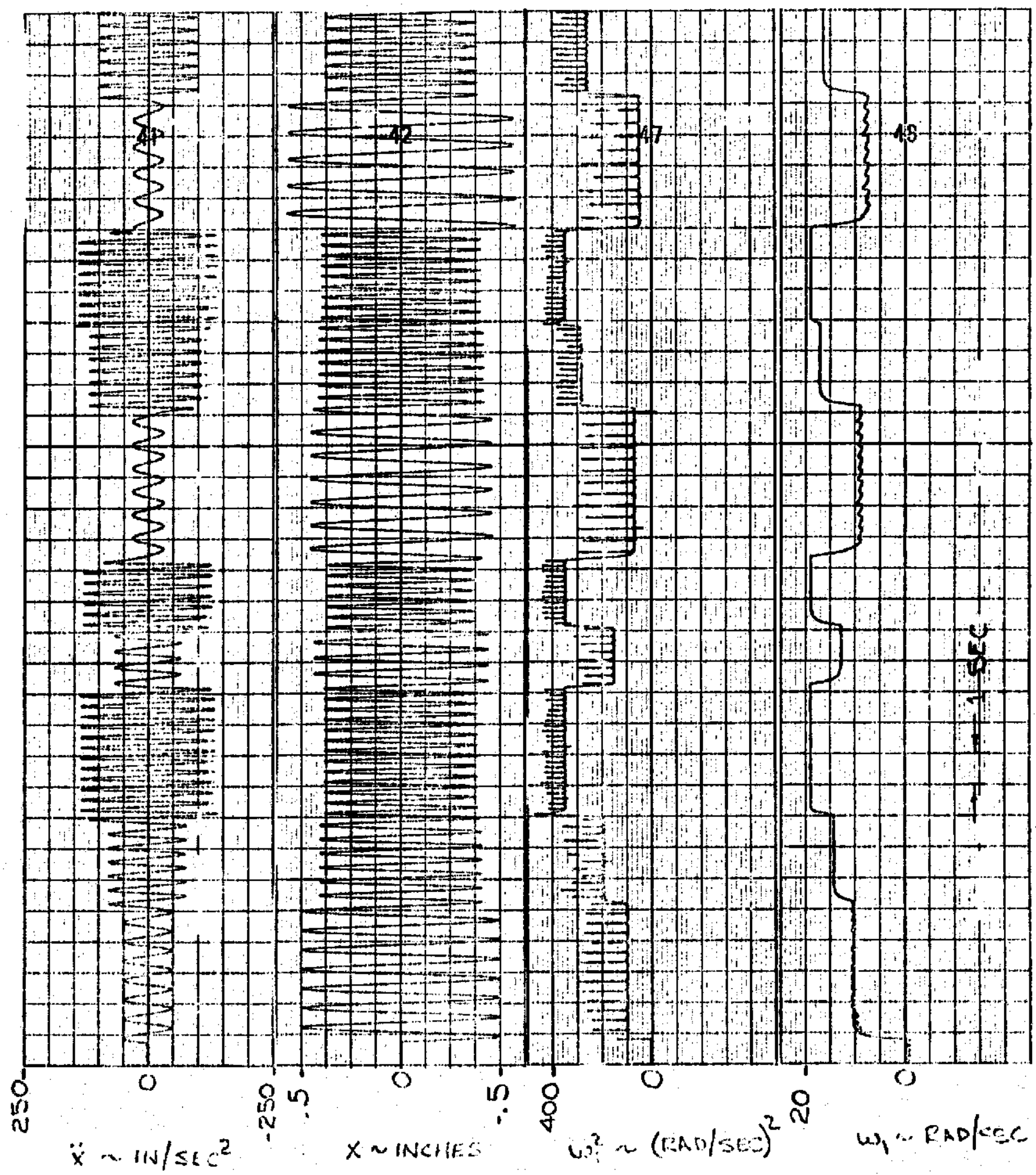

FIGURE 13

FREQUENCY MEASURING CIRCUIT PERFORMANCE

The analog components required to mechanize this single channel on the TR-48 computer are tabulated below:

20 Summing Amplifiers
3 Integrating Amplifiers
1 Relay Comparator
1 Electronic Comparator and Switch
3 Electronic Multipliers
11 Potentiometers

3.2 Frequency Measuring Circuit Performance

The capability of the mechanization to measure instantaneous frequency for simple harmonic motion is illustrated in Figure 14. This figure shows the acceleration, displacement, radian frequency squared, and the radian frequency for step changes in frequency.

The ratio which forms the radian "frequency" is not constant, in general, for a multi-degree-of-freedom plant containing more than one oscillatory mode. This is due to each degree-of-freedom consisting of a weighted sum of all the oscillatory modes. Figure 14 shows this for a coupled two degree-of-freedom plant with two lightly damped modes. This figure shows the two displacements and the radian "frequency" formed by the ratio $|\ddot{x}_3 - \ddot{x}_2|/|x_3 - x_2|$.

3.3 Period Measuring Mechanization and Performance

Figure 15 illustrates the performance of the "period" measuring mechanization for simple harmonic motion. The figure shows the system response for input oscillations of 5 and 50 Hz. This method measures the "period" by detecting zero-crossings. The system updates after each zero-crossing and holds this value until the next crossing. Therefore, the measured "period" is not instantaneous. An analog circuit diagram and signal sketches for one channel of the SAS is presented in Figure 16. This approach to measuring the period forces a trade-off between accuracy at low frequency and speed of response since a first-order lag is used as an approximate integrator. Its associated time constant determines how fast the voltage on the integrator changes.

The data indicates that the steady-state error in the frequency range of interest (5 to 25 Hz) is less than 3 percent. The transient response for a step change in frequency has a nominal rise time of approximately 0.25 seconds. This value increases approximately 50 percent when the step change occurs at the maximum integrator voltage.

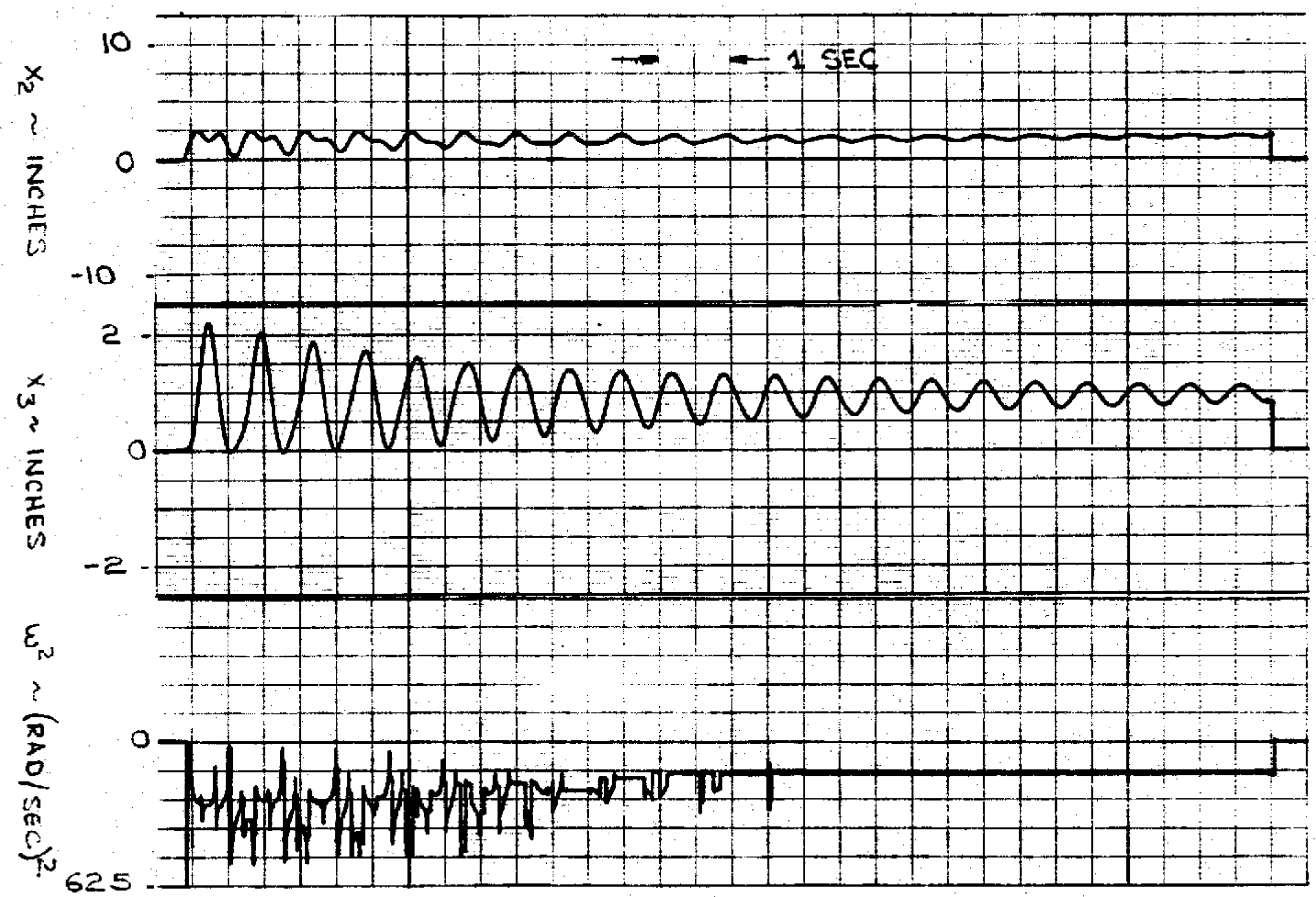

FREQUENCY MEASURING CIRCUIT PERFORMANCE
FOR TWO DOF PLANT

FIGURE 14

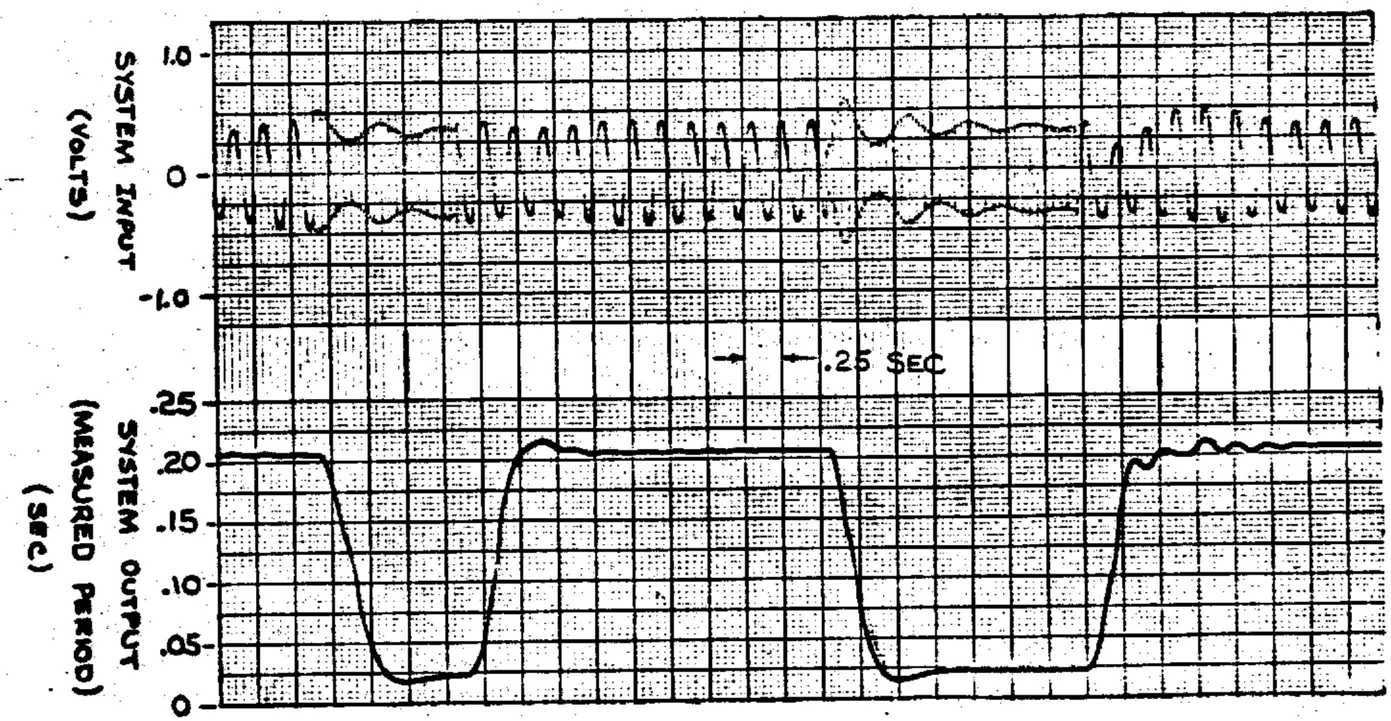

PERIOD MEASURING CIRCUIT PERFORMANCE

FIGURE 15

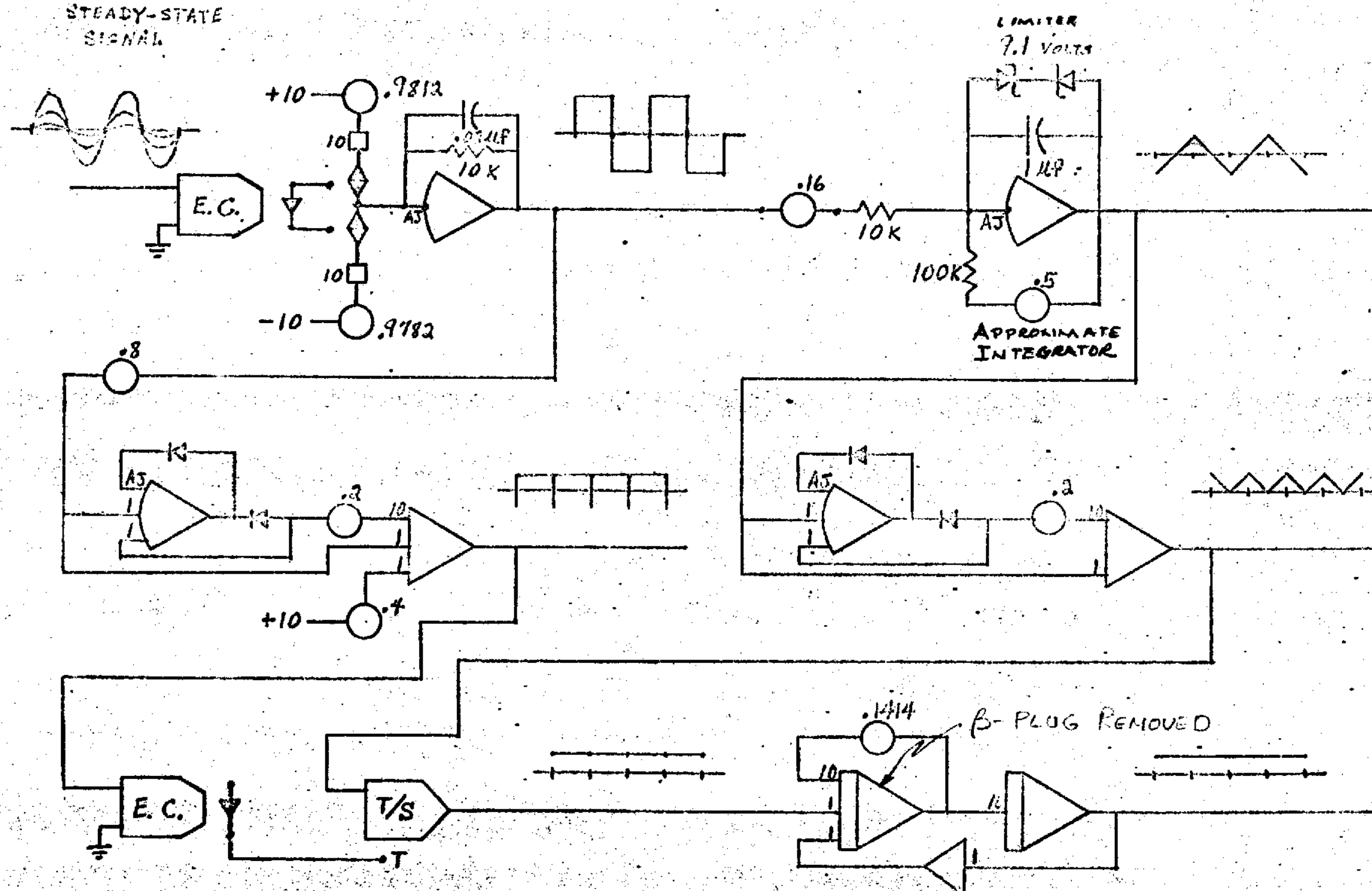

NOTE: 1) SCALE FACTOR: .025 SEC/VOLT

FIGURE 16. PERIOD MEASURING SYSTEM

ANALOG DIAGRAM AND SIGNAL SKETCHES

THE **BOEING** COMPANY
WICHITA DIVISION

CODE IDENT. NO. 81205

NUMBER D3-8390-2 REV LTR

INITIAL RELEASE DATE 20 August 1970

TITLE DESIGN AND MECHANIZATION OF RIDE CONTROL SYSTEM FOR B-52 AEROELASTIC MODEL - WORK STATEMENT

MODEL CONTRACT

ISSUE NO. ISSUED TO

PREPARED BY Garold E. Hodges
Garold E. Hodges

SUPERVISED BY Gerald E. Bergmann
Dr. Gerald E. Bergmann

APPROVED BY G. O. Thompson
G. O. Thompson

APPROVED BY

E-3039 R4

FOREWORD

This work statement describes the proposed design and mechanization of a ride control system for a B-52 aeroelastic model. The work will be accomplished under NASA Contract No. NAS1-9808.

TABLE OF CONTENTS

SECTION		PAGE
1.0	INTRODUCTION	1
2.0	DESIGN OF RIDE CONTROL SYSTEM	5
2.1	Phase I - Existing Control Surfaces	5
2.2	Phase II - Canard Surfaces	5
2.2.1	Math Model	8
2.2.2	SAS Synthesis	8
2.2.3	SAS Mechanization	9
2.3	Phase III - Canard and Flaperon Surfaces	10
2.3.1	Math Model	10
2.3.2	SAS Synthesis	10
2.3.3	SAS Mechanization	10
3.0	REFERENCES	10

1.0 INTRODUCTION

A Boeing-Wichita IR & D analytical research program is being conducted to determine the ride improvement attainable with a ride control system (RCS) on the CCV B-52 airplane. The objective of this program is to reduce RMS vertical accelerations along the fuselage with maximum emphasis on reducing acceleration at the pilot station. Preliminary results from this study indicate that a forward body canard surface is required to achieve a significant reduction in forward body vertical acceleration as illustrated in Figures 1 and 2. These studies also show the maximum reduction in acceleration along the entire fuselage is obtained with a combined canard and flaperon system as depicted in Figure 3. A simplified analysis conducted in a previous study to identify the optimum control surface location for gust alleviation indicates that a control force applied at the airplane center of pressure provides maximum vertical acceleration reductions along the fuselage (see Reference 1).

The objective of this study is to design and evaluate a RCS for the B-52E aeroelastic model with maximum performance for minimum model modifications. To realize this objective, the RCS synthesis will be accomplished in phases with the design processes terminating when a satisfactory design is obtained. Langley will review and judge system performance periodically.

Phase I will evaluate and summarize the ride improvement attainable with the existing elevator and aileron surfaces. Results of previous Boeing RCS studies will be reviewed. Additional analytical work will be conducted only as required to determine what ride improvement is achievable with these surfaces. Phase II will investigate the improvement feasible with a canard/elevator system or canard/aileron system. Studies to date have not thoroughly evaluated this combination of surfaces. Phase III will apply the canard/flaperon system, designed for the CCV airplane, to the B-52 model.

Results for each phase of work described herein will be informally transmitted to NASA-Langley at their completion. The final design, mechanization and wind tunnel test results will be documented as a dash number to this basic document at the completion of RCS testing.

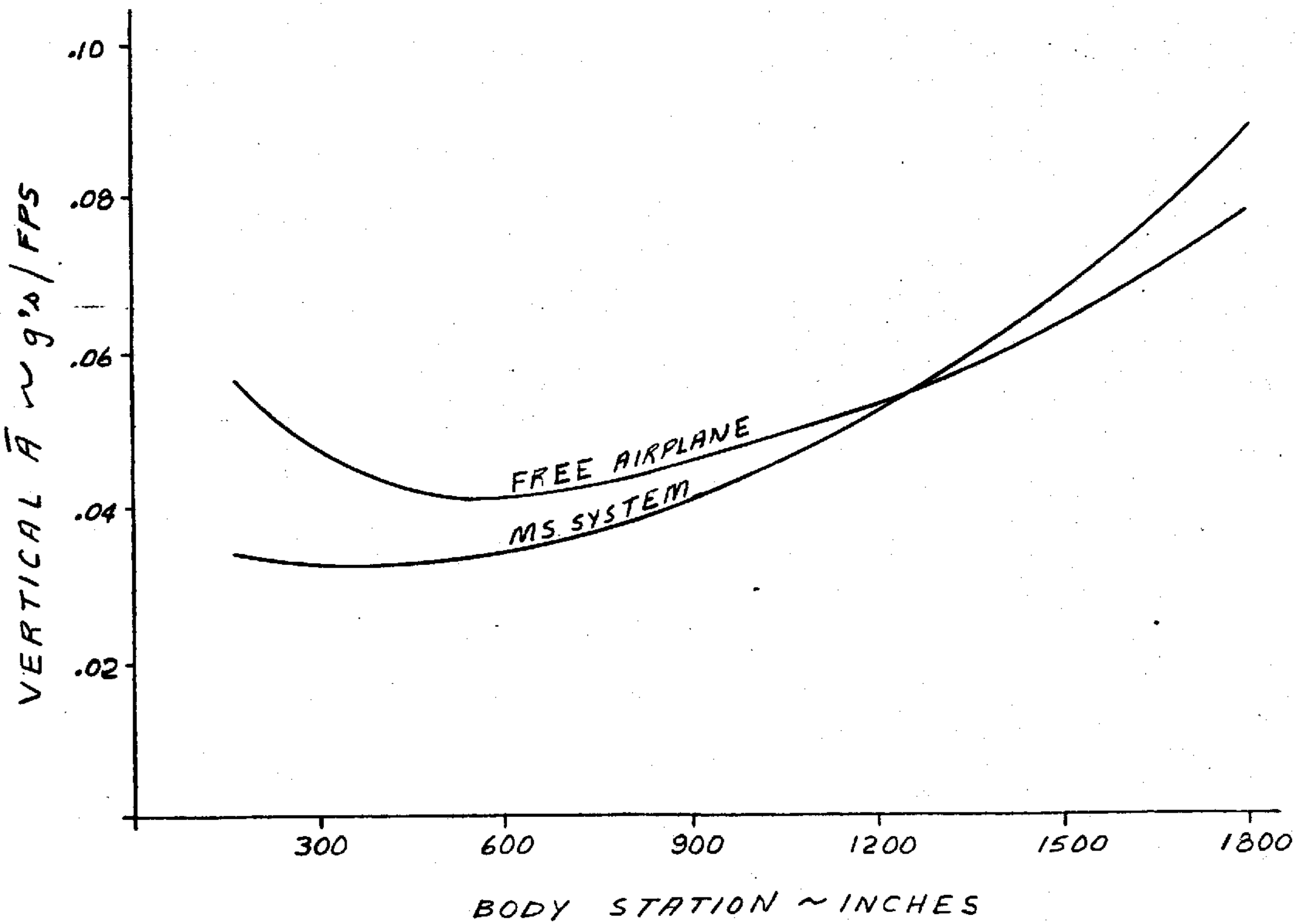

FUSELAGE VERTICAL ACCELERATION WITH MODE SUPPRESSION SYSTEM

FIGURE 1

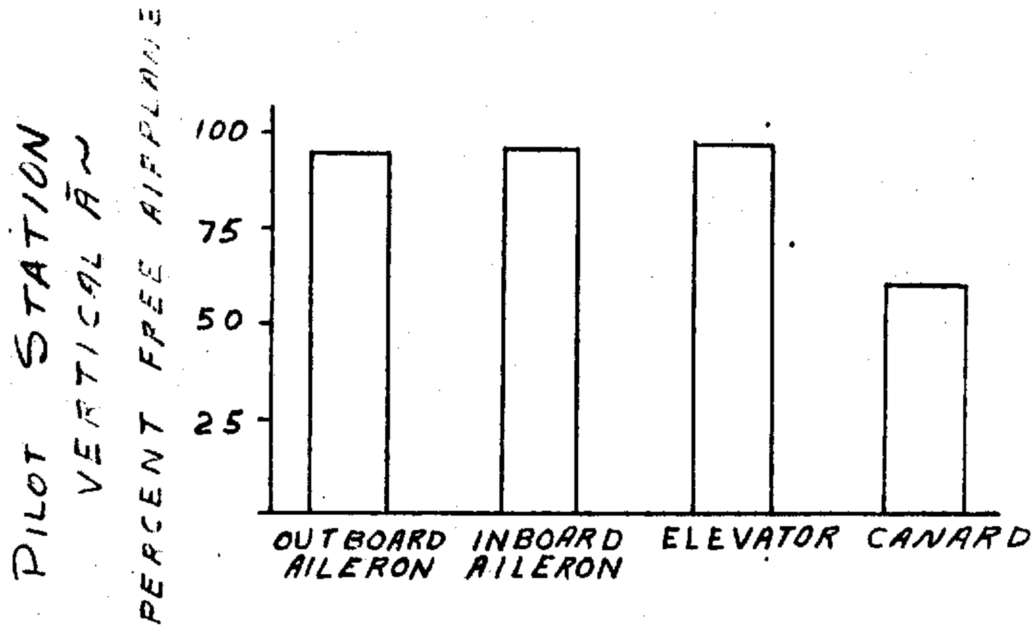

VERTICAL Ā REDUCTIONS WITH MODE SUPPRESSION SYSTEMS

FIGURE 2

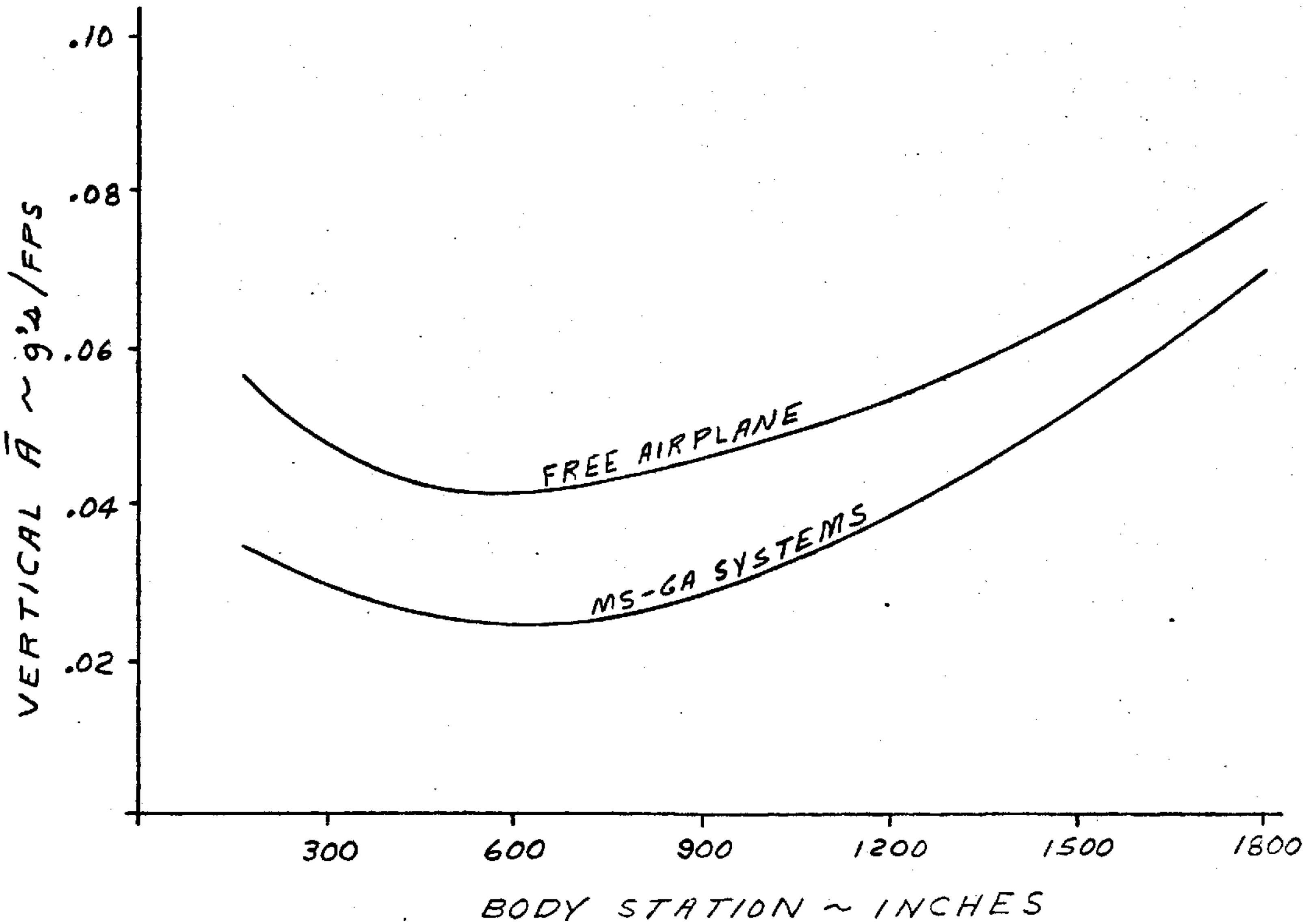

FUSELAGE VERTICAL ACCELERATION WITH MODE SUPPRESSION – GUST ALLEVIATION SYSTEMS

FIGURE 3

2.0 DESIGN OF RIDE CONTROL SYSTEM

A ride control system will be designed which analytically demonstrates the feasibility of improving passenger/pilot ride using active controls. Another parallel effort currently underway is directed toward mechanizing the system on the B-52 model. Control surfaces and control surface locations to be considered in the study are shown in Figure 4.

The goal for system design will be to obtain a minimum of 30 percent reduction in RMS vertical accelerations along the fuselage as illustrated in Figure 5. This is judged to be a realistic goal since the ride problem is less severe for the two heavy-weight model flight conditions as compared to the CCV condition (400 KEAS and 222 KIPS) and large percent reduction more difficult to obtain.

2.1 Phase I - Existing Control Surfaces

Indications from various B-52 stability and ride control studies are that the elevator, employing aft body sensors, primarily damps the short period with some improvement in aft fuselage acceleration. The aft fuselage acceleration reduction obtained during the 1195 program using elevator surfaces controlled with aft body pitch rate is presented in Figure 6. However, it should be noted that most of the ride control design efforts on the B-52 airplane have emphasized improvement at the pilot station thereby locating the motion sensor near this station. This causes acceleration in the aft body to increase when using the elevator.

The mid-span aileron surfaces (existing on the B-52 model) couple with the aft body modes to reduce acceleration but these surfaces also excite wing modes.

During this phase previous Boeing RCS studies will be reviewed. Additional work will be accomplished as required (probably on the aileron surface) to determine what improvement is attainable with these surfaces.

2.2 Phase II - Canard Surfaces

Previous studies have not completely evaluated canard/elevator and canard/aileron type of systems which sense motion in the forward and aft body. These systems will be analyzed before considering a flaperon system for the model. Figure 2 indicates that the minimum addition of a canard surface will probably be required to reduce acceleration along the entire fuselage.

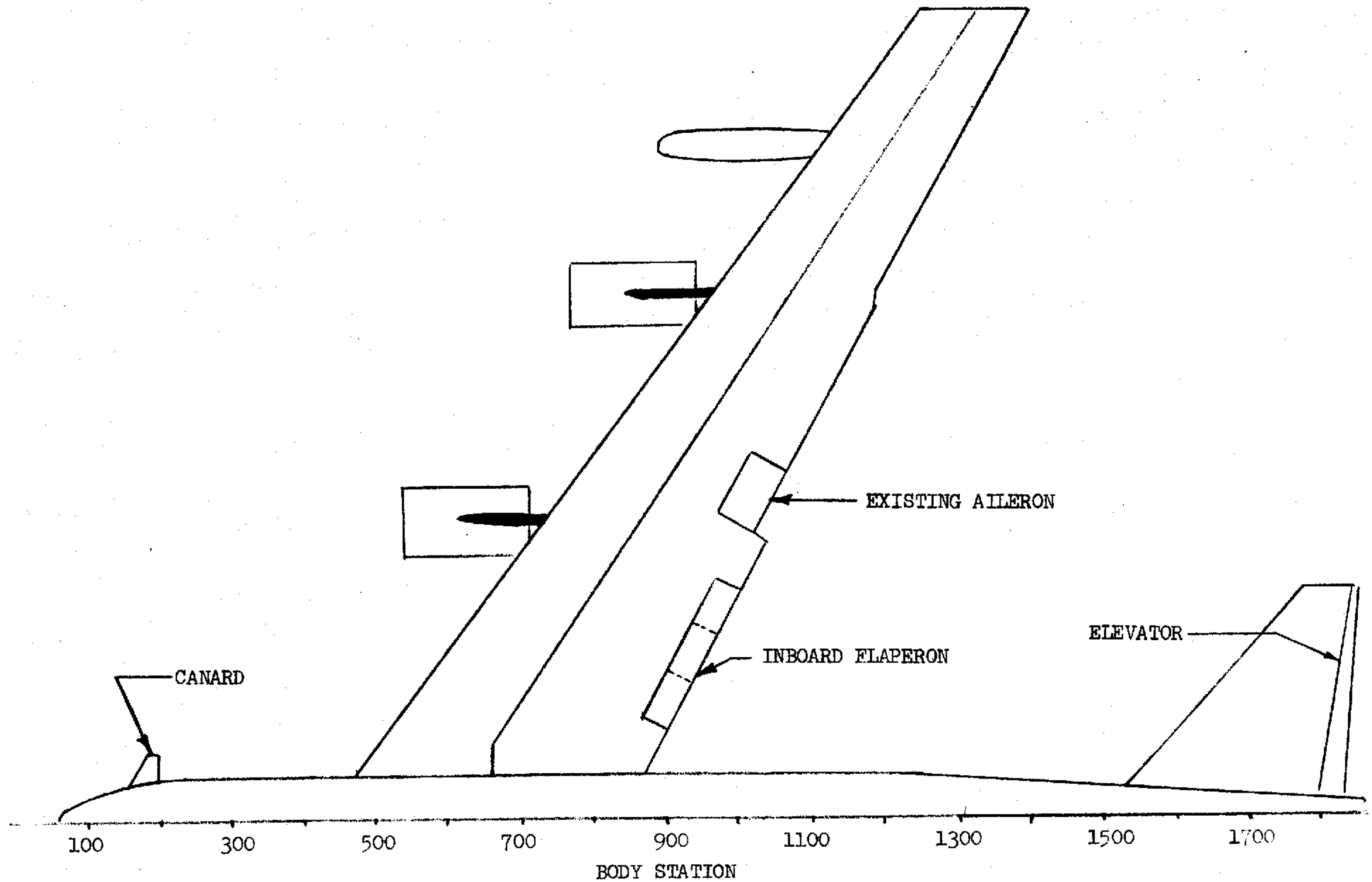

CONTROL SURFACES AND LOCATION
FIGURE 4

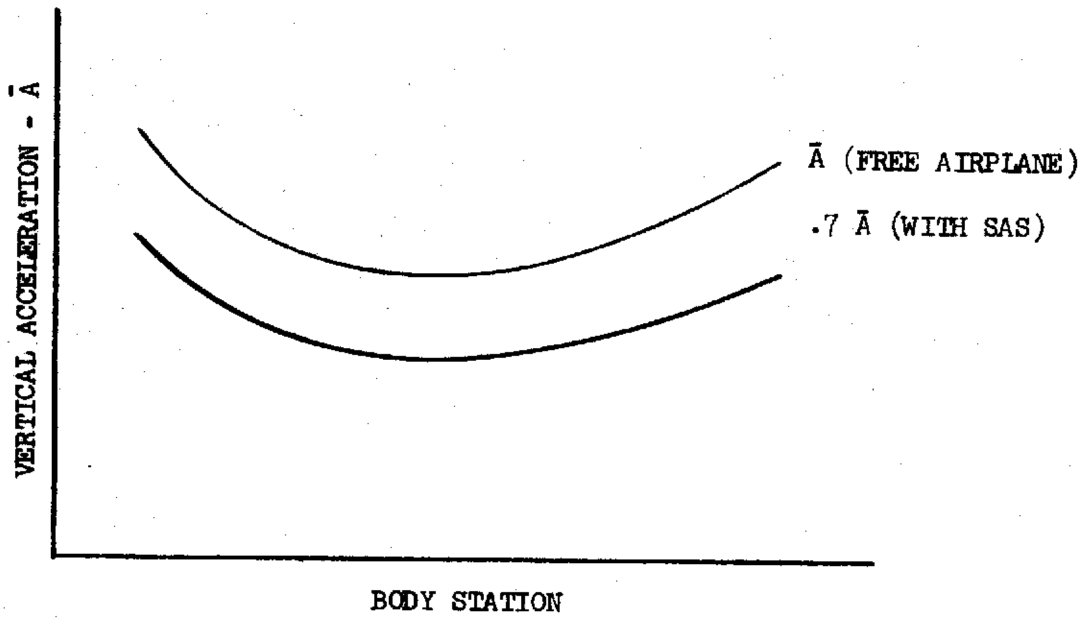

DESIGN GOAL FOR VERTICAL ACCELERATION
FIGURE 5

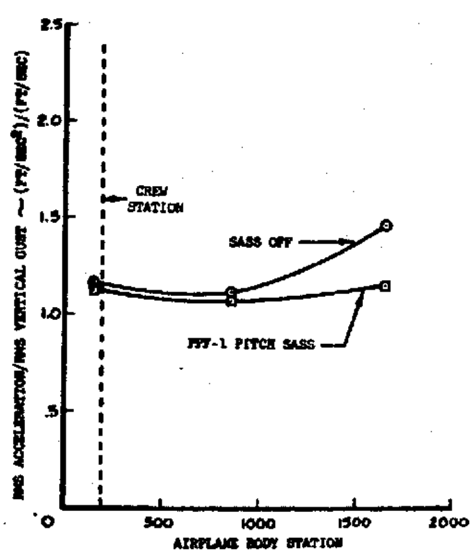

VERTICAL ACCELERATION (Ā)
ECP 1195 FLIGHT TEST RESULTS

FIGURE 6

2.2.1 Mathematical Model

The B-52 model equations of motion that exist for flight conditions 1 and 2 (defined in Reference 2) do not include canard surfaces. The canards will be represented by a point force at the appropriate body station for these initial studies to evaluate the combination of aileron/canard and elevator/canard surfaces. This technique is expected to provide a good representation of the canard surface with the existing equations. A 14 DOF math model will be utilized for SAS synthesis.

The atmospheric turbulence model for evaluating aircraft ride will be the von Karman spectrum having the following power spectral density:

$$\Phi(\omega) = \frac{\sigma_g^2 L}{\pi U_o} \frac{1 + 2.667(1.339 \frac{L\omega}{U_o})^2}{\left[1 + (1.339 \frac{L\omega}{U_o})^2\right]^{11/6}}$$

where: σ_g = RMS gust velocity, ft/sec
U_o = aircraft velocity, ft/sec
L = turbulence scale length, ft
ω = frequency, rad/sec

The RMS gust velocity will be 1 ft/sec with the turbulence scale as follows:

Turbulence Scale, L (ft)	Height Above Terrain (ft)
500	0 to 500
1000	500 to 2500
2500	Above 2500

2.2.2 SAS Synthesis

A conventional type of SAS design will be employed. Stability, gain values, gain margin and phase margin will be derived from root locus results. Ride improvement will be determined from power spectral density analyses.

Results of the RCS design will define the feedback signal (sensor type and location), gain and compensation for each control surface. This study will also establish theoretical reduction in vertical acceleration along the fuselage, and rate and displacement requirements for each surface.

2.2.3 SAS Mechanization

A preliminary estimate of the space and weight required to install a canard system in the model at the model station corresponding to B.S. 172 has been formulated based on an estimate of the size, inertia and deflection of the canard. From the CCV configuration an area of 10 ft^2/side and deflections of 10 degrees with the same frequency response (40 cps) as the aileron and elevator systems were assumed. Additional canard assumptions included a 4 foot semi-span, leading edge swept 30° trailing edge normal to the fuselage and a 10 percent maximum thickness to chord ratio. It was also assumed that the hinge line was located at approximately 25 percent of the mean aerodynamic chord to minimize torque requirements. Model airloads were assumed at .15 in-oz-/degree to allow for inaccuracies. The total load inertia derived for the surface, linkage, potentiometer, tachometer, shafts, etc. was .00054 in-oz-sec^2.

Two torque motors were considered for providing 10 degrees deflection out to 20 cps model frequency. These were Aeroflex motors TQ18-7 and TQG25-3 with a continuous torque of 8 and 10 in-oz respectively. The TQG25-3 motor is an integrated torque motor-tachometer package. Using a TA-42DC power amplifier with these motors will produce a displacement amplitude of 20 degrees at 20 cps. Therefore, these motors should give the required performance with rate and position feedback.

From the fuselage assembly drawing, it appears the area above the elastic member in the vicinity of B.S. 172 would offer sufficient space to mount the TQ18-7 motor, potentiometer and tachometer. This area has the following equipment presently mounted.

A. Accelerometer (Kistler 303T) - item 48
B. Converter 14V (P/N 93A236-1) - item 47
C. Support brackets for the above equipment.

Since a forward body accelerometer is probably required, it will be necessary to locate the canard aft at approximately B.S. 190 or to relocate the accelerometer. The area below the elastic member could possibly permit the installation of the canard system or the accelerometer. This would involve the relocation of:

A. Transducer selector (Model 1, S/N -100) - item 46
B. Support bracket for item 46.

It appears that this equipment could be relocated to the area below the aileron drive system, with the aileron trim system removed.

The estimated weight of the canard system is 18.5 oz for TQ18-7 motor and 23.5 oz for the TQG25-3 motor. The motor-tachometer combination (TQG25-3) is 2.5 inch diameter by 1.4 long. The dimensions of the TQ18-7 is 1.87 inches in diameter and the length is 1.10 inches.

Canard installation will require fabrication of surfaces and mounting brackets for the surfaces and equipment. Modification to the model should be minor.

2.3 Phase III - Canard and Flaperon Surfaces

The advantage of flaperons over the aileron surfaces is that they effectively reduce aft body vertical acceleration with a minimum excitation of wing modes. The flaperons are located near the airplane center of pressure and tend to provide ride improvement all along the fuselage except at the pilot station. This conclusion is illustrated by comparing Figure 2 (canard system) and Figure 3 (canard/flaperon system).

During this phase the canard/flaperon system, designed for the CCV airplane, will be applied to the B-52 model.

2.3.1 Math Model

The existing model equations do not include flaperon surfaces. It is questionable whether a point force representation for the aileron will provide the required accuracy. The equations will, therefore, be modified to include flaperon and canard surfaces. The turbulence model for this phase is described in Section 2.2.1.

2.3.2 SAS Synthesis

SAS design will be similar to the method described in Section 2.2.2.

2.3.3 SAS Mechanization

A preliminary evaluation was conducted to determine the effect of changing from the existing aileron surfaces to flaperon surfaces. Installing flaperon surfaces will require a modification to the model wings and minor changes in mechanization to convert the aileron control system to the flaperon. Flaperon surfaces and support structure will have to be fabricated and installed in the wing. Mechanization will require new pushrods, brackets and shafts as a minimum.

3.0 REFERENCES

1. Coordination Sheet No. 3-7560-70-9, "Results of B-52H Vertical Ride Smoothing SAS Conceptual Studies--EWI 6107 Final Report", from JIArnold and GOThompson to EJSullivan, dated 23 January 1970.

2. Boeing Document D3-7055-2, "Wind Tunnel Measurement of Dynamic Airplane Response Control System Performance".

THE BOEING COMPANY
WICHITA DIVISION

CODE IDENT. NO. 81205

NUMBER D3-8390-3 REV LTR

INITIAL RELEASE DATE 4 March 1971

TITLE EVALUATION OF B-52 AEROELASTIC MODEL CONTROL SURFACE ACTUATION SYSTEMS

FOR LIMITATIONS IMPOSED ON THE USE OF THE INFORMATION CONTAINED IN THIS DOCUMENT AND ON THE DISTRIBUTION OF THIS DOCUMENT, SEE LIMITATIONS SHEET.

MODEL ______ CONTRACT ______

ISSUE NO. ______ ISSUED TO ______

PREPARED BY Frank D. Sevart

SUPERVISED BY Dr. Gerald E. Bergmann

APPROVED BY Glenn O. Thompson

APPROVED BY ______

E-3033 RS

ABSTRACT

This document discusses the results of an evaluation of the NASA B-52 aeroelastic model aileron and elevator actuation systems. This work was accomplished under NASA Contract NAS 1-9808. The results indicate that the existing model actuation systems can be modified to give satisfactory performance.

RETRIEVAL REFERENCE WORDS:

REV SYM:

CONTENTS

		PAGE
	ABSTRACT	2
1.0	SUMMARY	4
2.0	INTRODUCTION	5
3.0	BASELINE ACTUATION SYSTEM	7
3.1	Linear Analysis	7
3.2	Laboratory Testing	19
3.2.1	Description of Baseline System	19
3.2.2	Test Results	19
3.3	Conclusions of Baseline System Testing	26
4.0	AILERON AND ELEVATOR SIMULATIONS	29
4.1	Description of Existing Aileron Actuation System	29
4.1.1	Description of Aileron Simulation	29
4.1.2	Test Results	32
4.2	Description of Existing Elevator Actuation System	38
4.2.1	Description of Elevator Simulation	38
4.2.2	Test Results	42
5.0	RECOMMENDATIONS AND CONCLUSIONS	47
6.0	REFERENCES	49
APPENDIX A	SUMMARY OF MODIFICATIONS OF THE B-52 AEROELASTIC MODEL AILERON AND ELEVATOR ACTUATION SYSTEMS AND THE RESULTANT PERFORMANCE	50

1.0 SUMMARY

This document contains the results of an evaluation of the aileron and elevator actuation systems installed in the B-52 aeroelastic model. This work was accomplished under NASA-Langley Research Center Contract NAS 1-9808.

This evaluation consisted of an analytical assessment of the capability of the actuation systems and laboratory tests of breadboard simulations to identify modifications which provided satisfactory performance.

The results of this study indicate that the existing actuation systems will meet performance and stability requirements with a minimum of modifications. Rate feedback capability is required to provide stability at the high system bandpass necessary to attain the desired performance. Other modifications are required to minimize friction and inertia. No attempt was made to optimize the actuation systems, but modifications were identified which permit the systems to meet the performance and stability requirements.

The right hand aileron and the elevator actuation systems in the model were modified during January 1971. The modified aileron system performance was satisfactory, but additional modifications are required to reduce friction in the elevator system (see Appendix A).

2.0 INTRODUCTION

The Aeroelasticity Branch of NASA-Langley Research Center has procured a 1/30th scale aeroelastic model of a B-52E airplane with active aileron and elevator systems installed. NASA has initiated a research program to demonstrate a gust alleviation stability augmentation system on this model in the Langley transonic wind tunnel. This document describes an evaluation of the aileron and elevator actuation systems conducted under NASA Contract NAS 1-9808 to determine if modifications of these systems were required to accomplish the program goal.

The mass and stiffness properties of this model were scaled to produce aeroelastic characteristics equivalent to the airplane from 0 to 4.5 Hz (model frequency 0 to 25 Hz). The desired performance of the model aileron and elevator actuation systems was equivalent to the actuation systems of the B-52E LAMS airplane in this primary frequency band. The performance and stability requirements for these systems are summarized below, from Reference 1.

- Usable angle of rotation of each actuation system must be at least ±25 degrees
- Each actuation system must be capable of at least 25 in.-oz. peak torque at ±19 degrees rotation and 15 to 20 in.-oz. continuous torque
- Each actuation system most possess rate capability of at least 750 deg./sec.
- Frequency response of each actuation system shall not exceed three db amplitude attenuation and 45 degrees phase lag at 25 Hz for ±3 degree sinusoidal input. The motor-load resonance shall have a nominal damping ratio of 0.3, and a minimum of 0.15
- Each actuation system shall have an input capability of at least ±6 degrees (without power amplifier saturation) up to a frequency of 20 Hz
- The total actuation system hysteresis shall not exceed ±0.20 degrees measured at the control surface

The initial phase of this study was an evaluation of baseline actuation systems, using the torque motors and power amplifiers from the model. The torque motor was directly coupled to the simulated surface inertia in each system, as described in Section 3.0.

Section 4.0 discusses the testing of simulations of the model actuation systems to evaluate the mechanical linkage used to transmit torque from the motor to the surface.

Specific modifications to the aileron and elevator actuation systems are recommended in Section 5.0. These modifications will permit the systems to meet the performance and stability requirements outlined above.

A summary of the modifications, accomplished during January 1971 after the body of this document was written, is included in Appendix A. This appendix includes a detailed setup and checkout procedure for the aileron and elevator actuation systems. The performance attained with these modifications is discussed and recommendations are made of methods to further improve the performance of the systems.

3.0 BASELINE ACTUATION SYSTEM

The analysis of the B-52 aeroelastic model control surface actuation systems began with a linear analysis and laboratory testing of a baseline system. This system differs from the actual actuation systems in that the torque motor was directly coupled to the simulated surface inertia, rather than torque being transmitted to the surface through mechanical linkage. This analysis was conducted to determine the capability of the Aeroflex TQ20-1 torque motor and TA-100DC power amplifier combination, and to determine the feedback compensation required to meet the performance criteria.

3.1 Linear Analysis

The linear analysis was based on a mathematical model derived from the simplified, lumped parameter representation of the torque motor and load inertia shown in Figure 3-1. This representation shows the most general case with the load inertia elastically coupled to the motor shaft and aerodynamic damping and spring elements included for completeness. The three degrees-of-freedom in the system are the armature current, I_a; motor angular position, θ_M; and load angular position, θ_L. The system input is the power amplifier output voltage, V_a. A complete listing of nomenclature used in the analysis is presented in Table 3-I.

The dynamic equations of the system are referenced to the equilibrium state defined by zero motor and load angular position corresponding to zero amplifier output voltage. The three differential equations are derived for the electromechanical system by applying Kirchhoff's and Newton's fundamental laws:

$$I_a R_a + V_b + L_a \frac{dI_a}{dt} = V_a \tag{1}$$

$$J_M \frac{d^2 \theta_M}{dt^2} + F_M \frac{d\theta_M}{dt} + K_S \theta_M - K_S \theta_L = T_d \tag{2}$$

$$J_L \frac{d^2 \theta_L}{dt^2} + F_L \frac{d\theta_L}{dt} + (K_S + K_L) \theta_L - K_S \theta_M = 0. \tag{3}$$

The electromechanical coupling is provided through the torque sensitivity constant and the back electromotive force constant. This coupling may be expressed in equation form

$$T_d = K_i I_a \quad \text{and} \quad V_b = K_b \frac{d\theta_M}{dt} .$$

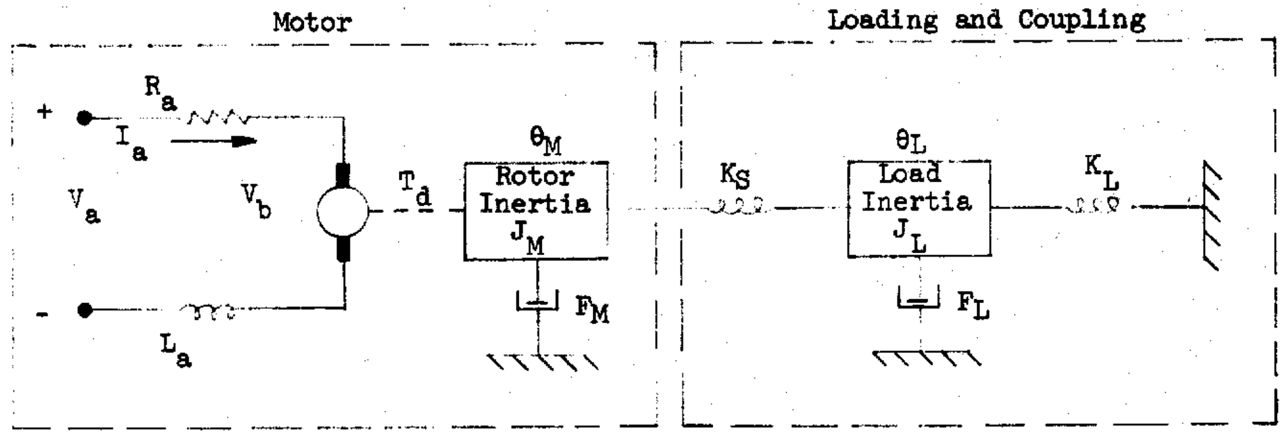

Transfer Functions:

$$\frac{\theta_M}{V_a}(S) = \frac{K_T\left[J_L S^2 + F_L S + (K_S + K_L)\right]}{\left[\left(J_M S^2 + F_M S + K_S\right)\left(\tau_a S + 1\right) + DS\right]\left[J_L S^2 + F_L S + \left(K_S + K_L\right)\right] - K_S^2\left(\tau_a S + 1\right)}$$

$$\frac{\theta_L}{\theta_M}(S) = \frac{K_S}{J_L S^2 + F_L S + \left(K_S + K_L\right)}$$

Baseline System $K_S \approx \infty$, $K_L = 0$, $F_L = 0$, $F_M = 0$

$$\frac{\theta_M}{V_a}(S) = \frac{K_T/\tau_a\left(J_M + J_L\right)}{S\left[S^2 + \frac{S}{\tau_a} + \frac{D}{\tau_a\left(J_M + J_L\right)}\right]} \quad \text{and} \quad \frac{\theta_L}{\theta_M} = 1$$

SIMPLIFIED REPRESENTATION OF MOTOR AND LOAD

FIGURE 3-1

TABLE 3-I

NOMENCLATURE

SYMBOL	DEFINITION	UNITS
D	Equivalent viscous damping coefficient due back electromotive force	in-oz/rad/sec
F_L	Load viscous damping coefficient due to aerodynamic damping	in-oz/rad/sec
F_M	Mechanical viscous damping coefficient of the motor	in-oz/rad/sec
I_a	Armature current	amp
J_L	Load inertia (simulated surface inertia)	in-oz-sec^2
J_M	Rotor inertia	in-oz-sec^2
K_b	Back electromotive-force constant	volt/rad/sec
K_i	Torque sensitivity constant	in-oz/amp
K_L	Load elastic spring coefficient due to aerodynamic restoring force	in-oz/rad
K_S	Elastic spring coefficient of shafts and couplings	in-oz/rad
K_T	Torque sensitivity to applied voltage	in-oz/volt
L_a	Armature inductance	henry
R_a	Armature resistance	ohm
T_d	Developed torque	in-oz
V_a	Power amplifier output voltage (input voltage to motor)	volt
V_b	Back electromotive force	volt
θ_L	Load angular displacement	radian
θ_M	Motor angular displacement	radian
τ_a	Motor electrical time constant	second

Substitution of these identities into the two motor equations produces the desired form

$$I_a R_a + K_b \frac{d\theta_M}{dt} + L_a \frac{dI_a}{dt} = V_a \tag{4}$$

$$J_M \frac{d^2\theta_M}{dt^2} + F_M \frac{d\theta_M}{dt} + K_S\theta_M - K_S\theta_L = K_i I_a \ . \tag{5}$$

With the system at rest in the equilibrium condition, the Laplace transformation of the system equations produces the form

$$\left(L_a S + R_a\right) I_a(S) + K_b S\ \theta_M(S) = V_a(S) \tag{6}$$

$$- K_i\ I_a(S) + \left(J_M\ S^2 + F_M\ S + K_S\right)\ \theta_M(S) - K_S\ \theta_L(S) = 0 \tag{7}$$

$$- K_S\ \theta_M(S) + \left(J_L\ S^2 + F_L\ S + K_S + K_L\right)\ \theta_L(S) = 0. \tag{8}$$

The system of equations may be solved for the transfer function of motor angular position due to amplifier voltage using Cramer's rule. This transfer function may be expressed as

$$\frac{\theta_M}{V_a}(S) = \frac{K_T\left[J_L S^2 + F_L S + K_S + K_L\right] \text{ (Rad/Volt)}}{\left[\left(J_M S^2 + F_M S + K_S\right)\left(\tau_a S+1\right) + DS\right]\left[J_L S^2 + F_L S + K_S + K_L\right] - K_S^{\ 2}\left(\tau_a S+1\right)} \tag{9}$$

where $K_T = K_i/R_a$, $D = K_i\ K_b/R_a$, and $\tau_a = L_a/R_a$. The transfer function of load angular position to motor angular position can be determined directly from Equation (8).

$$\frac{\theta_L}{\theta_M}(S) = \frac{K_S}{J_L\ S^2 + F_L\ S + \left(K_S + K_L\right)} \tag{10}$$

The baseline system transfer functions are defined by assuming $K_S \approx \infty$, with the aerodynamic terms and motor mechanical damping coefficient set to zero. The baseline system transfer functions are

$$\frac{\theta_M}{V_a}(S) = \frac{K_T/\tau_a \left(J_M + J_L\right)}{S\left[S^2 + \frac{1}{\tau_a}S + \frac{D}{\tau_a\left(J_M + J_L\right)}\right]} \quad \text{and} \quad \frac{\theta_L}{\theta_M} = 1.$$

The characteristics of the TQ20-1 torque motor and TA-100DC power amplifier are shown in Table 3-II, as summarized from the manufacturer's data. The open loop steady state capability of the motor and amplifier combination is shown in Figure 3-2, assuming simple harmonic motion. The maximum operating range of the motor is ±25 degrees and the maximum accelerations shown correspond to amplifier saturation.

The transfer functions for the open loop motor show that position feedback is required for a position command system. A stability analysis of the system with position feedback shows that rate feedback is required to meet stability and damping requirements. Without rate feedback, the system is unstable above a closed loop natural frequency of 174 rad/sec for a .0035 in-oz-sec^2 load inertia. The frequency response criteria requires a closed loop natural frequency of approximately 250 rad/sec. An induction potentiometer was selected for the laboratory test due to its low friction and inertia. This provided a more accurate determination of the torque motor/power amplifier by eliminating nonlinearities introduced by potentiometer friction.

Figure 3-3 shows the closed loop block diagram of the elevator control system. This block diagram includes the approximate transfer function of a pulse sample demodulator required for the induction potentiometer used in laboratory testing. The characteristics of this potentiometer and the dc tachometer used are shown in Table 3-II. The root locus for this system, shown in Figure 3-4, illustrates the stabilization provided by the rate feedback loop.

Figures 3-5 and 3-6 show the rate and position feedback gains required for a range of closed loop natural frequencies and damping ratios, for the two assumed surface inertia values. These plots were obtained through a root locus analysis.

The predicted hysteresis due to one in-oz of friction and residual torque is shown in Figure 3-7 as a function of closed loop natural frequency for a nominal damping ratio of 0.30. The hysteresis for the system with the larger

TABLE 3-II

ACTUATION SYSTEM DESIGN VALUES

DESCRIPTION	SYMBOL	VALUES	UNITS
1. Torque Motor, TQ20-1			
Armature Resistance	R_a	5.0	ohms
Torque Sensitivity	K_i	8.0	in-oz/amp
Motor Inertia	J_M	.002	in-oz-sec^2
Viscous Damping	D	.100	$\frac{\text{in-oz}}{\text{rad/sec}}$
Electrical Time Constant	τ_a	6×10^{-4}	sec
Torque Output, Continous	T	30	in-oz
2. Power Amplifier, TA-100DC			
Output (Maximum)	V_a(max)	20	VDC
Voltage Gain	K_a	9.96	volt/volt
Rated Load	--	3.2-5.6	ohms
3. Tachometer, TG 10Y-5			
Output Sensitivity	--	.18	$\frac{\text{Volt}}{\text{rad/sec}}$
Rotor Inertia	J_T	4×10^{-5}	in-oz-sec^2
4. Position Transducer			
Linear Transformer Sensitivity	--	.332	$\frac{\text{VRMS}}{\text{Deg}}$
Solar Cell	--	Variable	$\frac{\text{Volt}}{\text{Deg}}$
5. Demodulator (PSD)			
Sensitivity	--	1.0	$\frac{\text{VDC}}{\text{VRMS}}$
6. Control Surfaces (Including Linkage)			
Aileron Inertia	J_A	.0035	in-oz-sec^2
Elevator Inertia	J_E	.002	in-oz-sec^2

REV LTR:

E-3033 R1

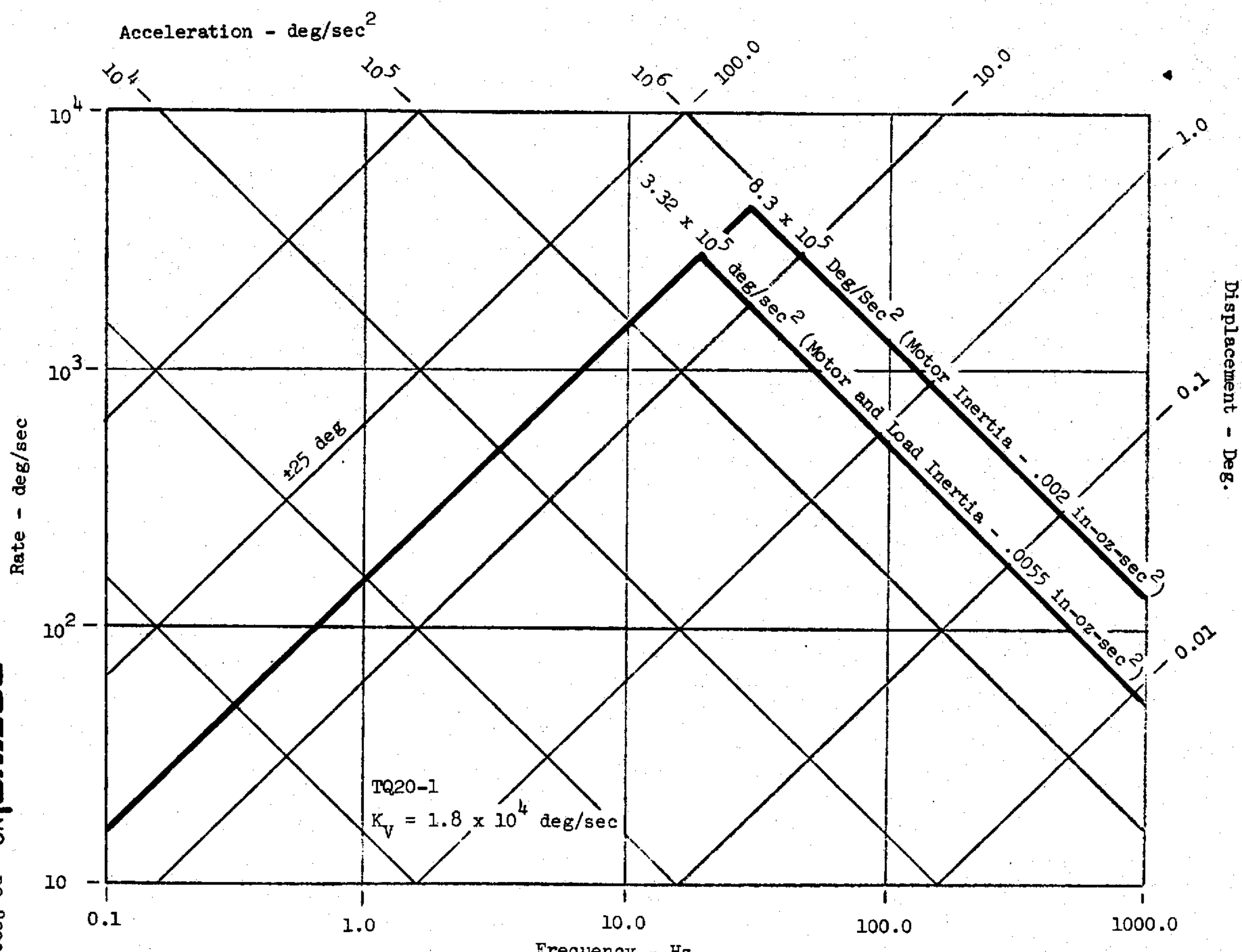

TORQUE MOTOR AND CONTROL SURFACE CHARACTERISTICS

FIGURE 3-2

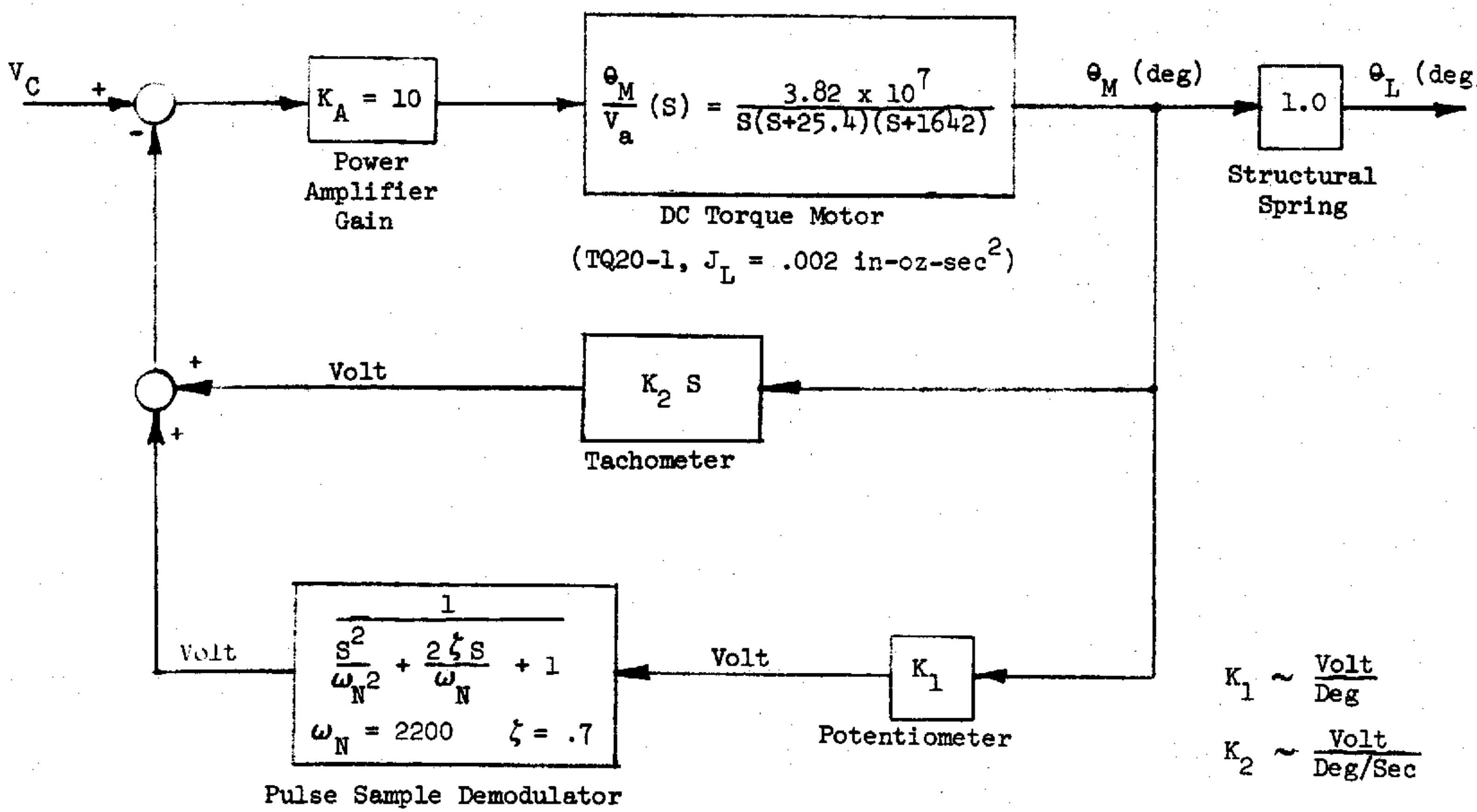

BLOCK DIAGRAM FOR BASELINE SYSTEM

FIGURE 3-3

NOTE:

(1) Torque Motor TQ20-1

(2) Load Inertia: .002 in-oz-sec^2

(3) ▲ - K_1 = .253 volt/deg

$K_2 = 8.2 \times 10^{-4} \frac{\text{volt}}{\text{deg/sec}}$

ω_N = 250 rad/sec

ζ = .3

(4) Demodulator Dynamics Included

(5) Poles not shown

S = -1641

S = -1540 ± j 1571

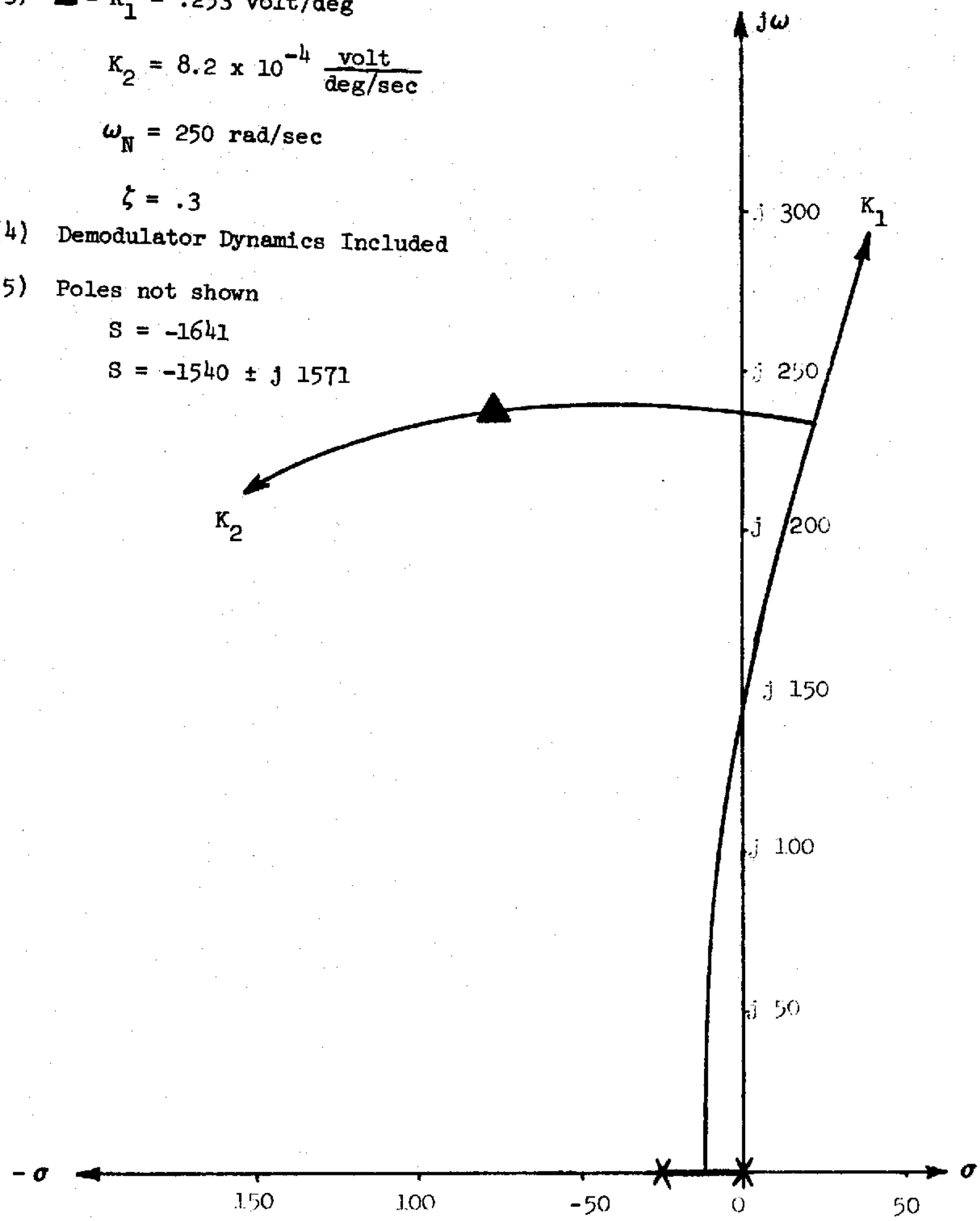

B-52 MODEL CONTROL SYSTEM STABILITY
AILERON AND ELEVATOR SYSTEMS

FIGURE 3-4

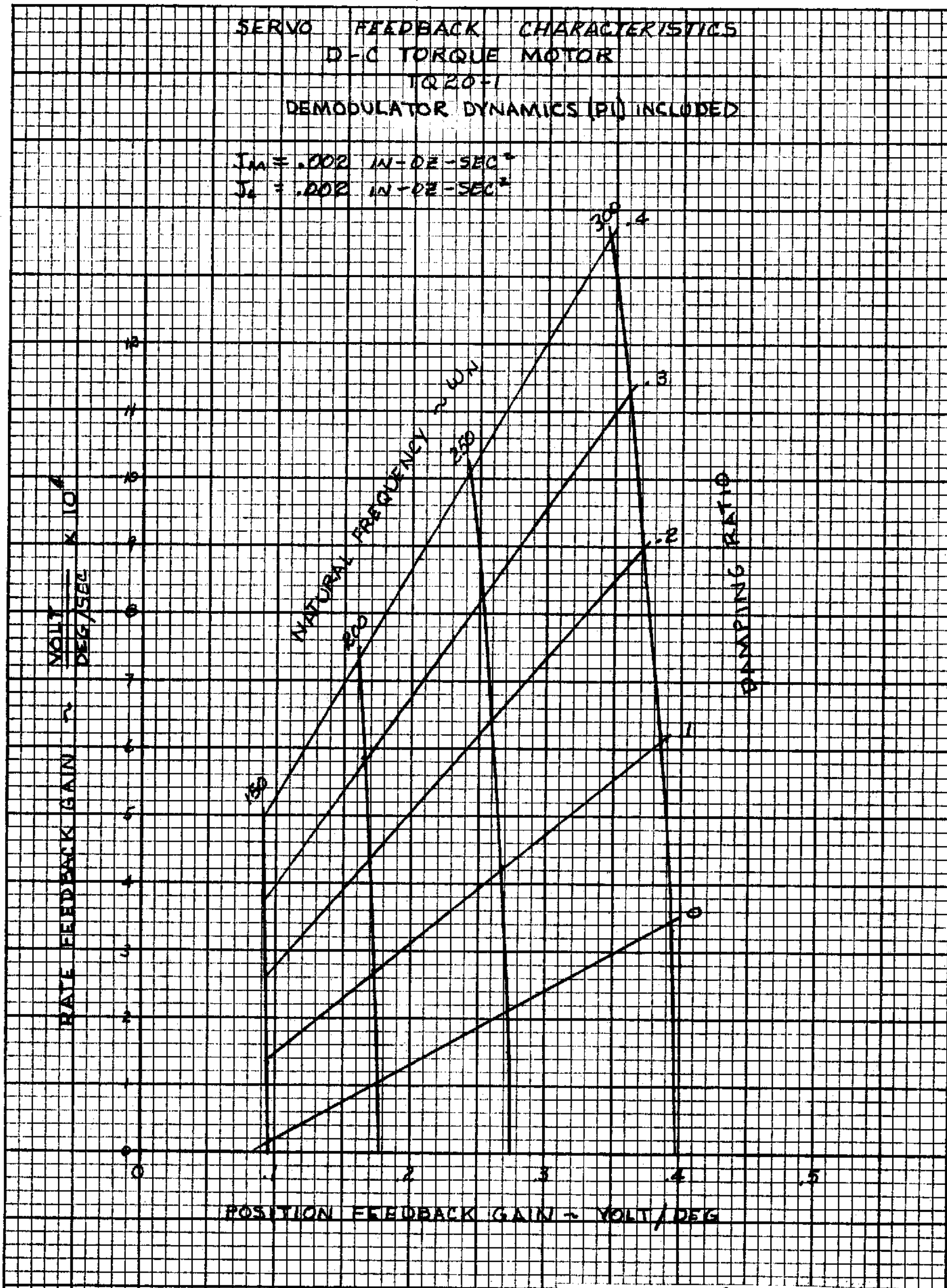
SERVO FEEDBACK CHARACTERISTICS
D-C TORQUE MOTOR
TQ 20-1
DEMODULATOR DYNAMICS (PI) INCLUDED
JM = .002 IN-OZ-SEC²
JL = .002 IN-OZ-SEC²
NATURAL FREQUENCY ~ ωN
150
200
250
300
DAMPING RATIO
.4
.3
.2
.1
0
RATE FEEDBACK GAIN ~ VOLT / DEG/SEC x 10⁴
0
1
2
3
4
5
6
7
8
9
10
11
12
.1
.2
.3
.4
.5
POSITION FEEDBACK GAIN ~ VOLT/DEG

FIGURE 3-5

SERVO FEEDBACK CHARACTERISTICS
TORQUE MOTOR: TQ20-1
DEMODULATOR DYNAMICS (P1) INCLUDED
J_M = .002 IN-OZ-SEC²
J_L = .0035 IN-OZ-SEC²

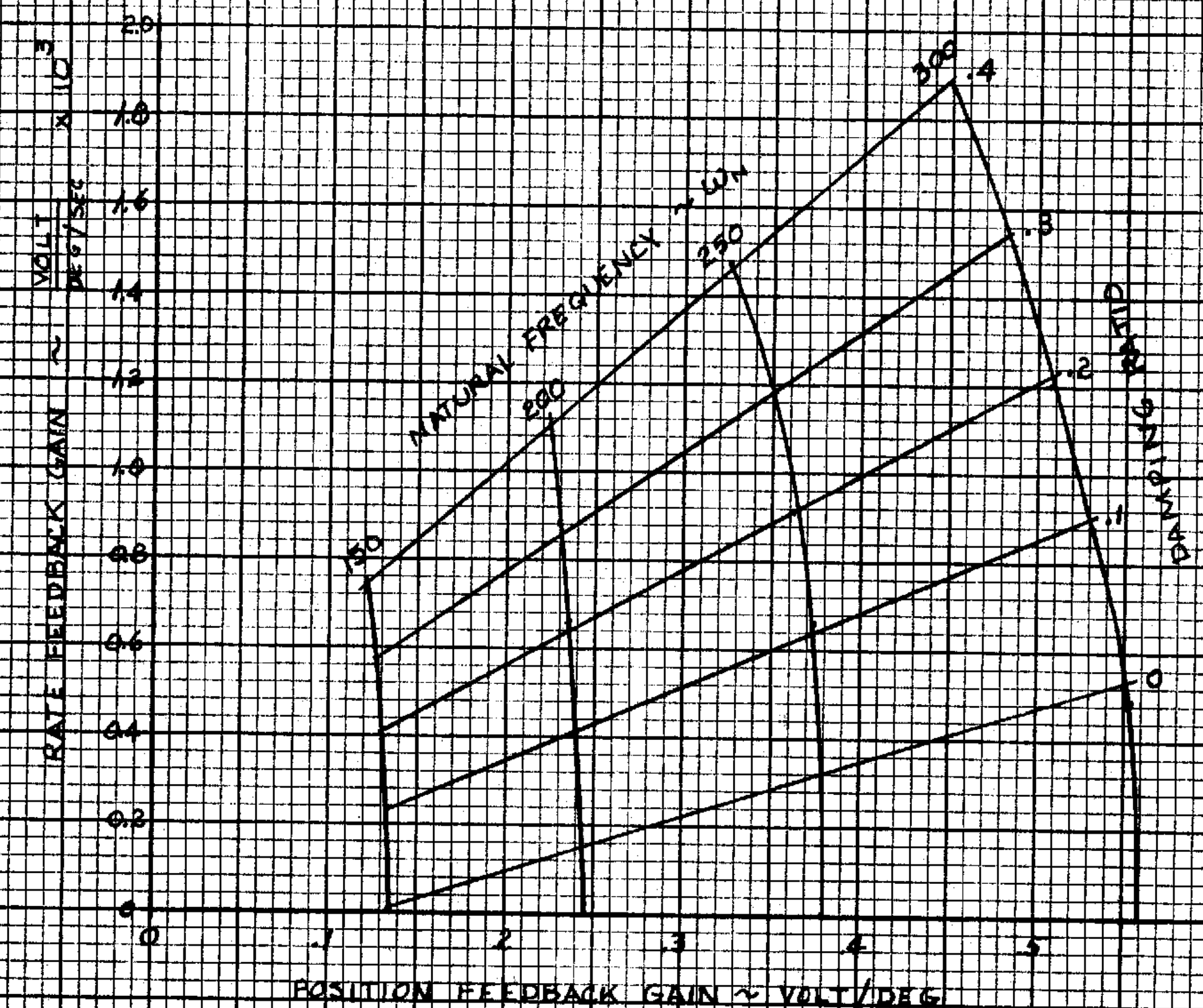

FIGURE 3-6

NOTE:

(1) $J_M = .002$ in-oz-sec^2
$J_{L_1} = .002$ in-oz-sec^2
$J_{L_2} = .0035$ in-oz-sec^2

(2) Torque Motor TQ20-1

(3) Demodulator Dynamics (P1) Included

(4) Damping Ratio: .3

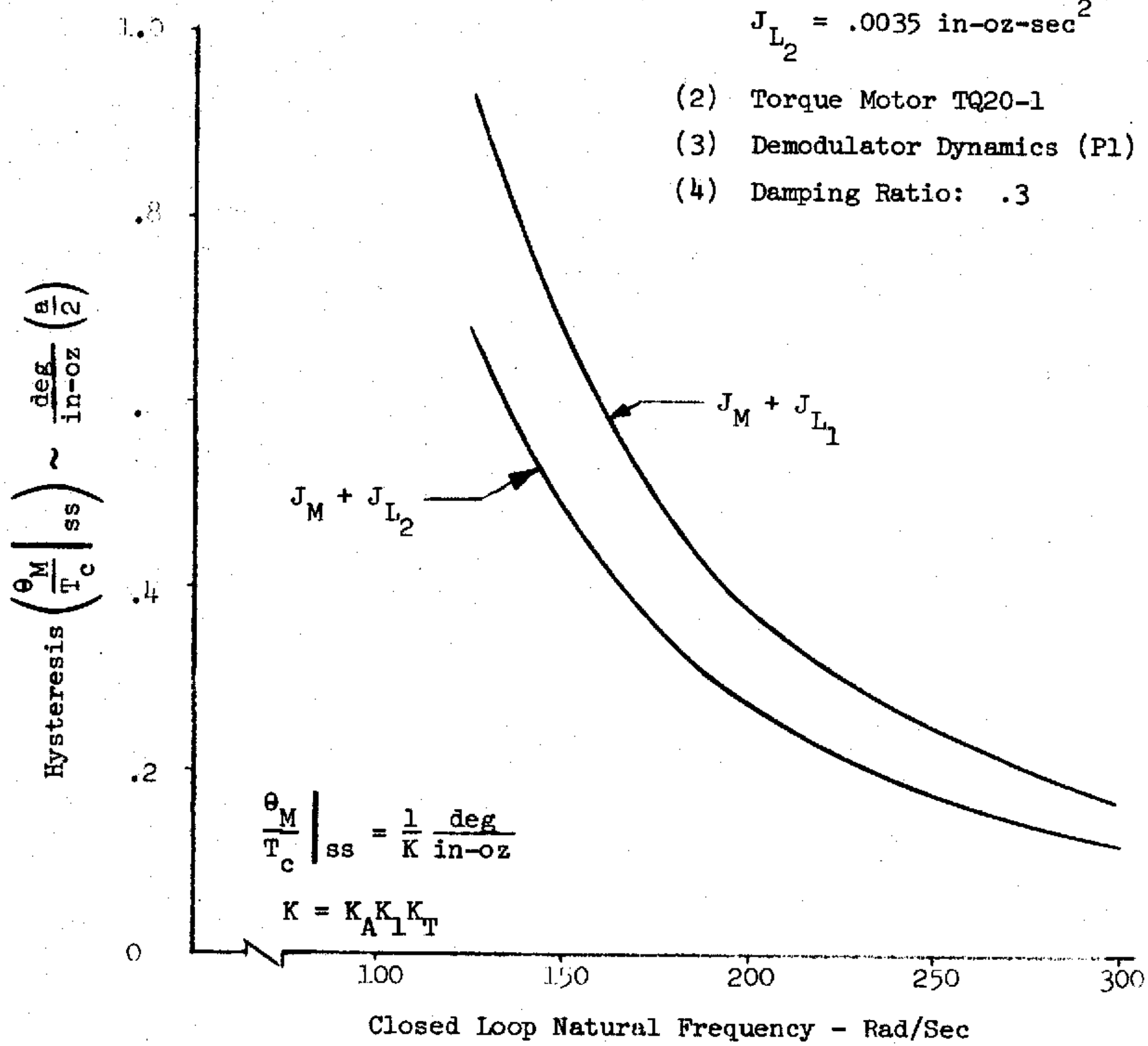

CONTROL SYSTEM HYSTERESIS
(FRICTION AND RESIDUAL TORQUE)

FIGURE 3-7

inertia is smaller since the position feedback gain, K_1, must be larger to produce the same closed loop natural frequency. These plots show that friction must be minimized to meet the system hysteresis requirement of no more than ±0.20 degrees at the control surface.

3.2 Laboratory Testing

Laboratory testing was conducted on breadboard baseline systems utilizing the torque motors and power amplifiers from the B-52 model. Three Aeroflex TQ20-1 torque motors and two Aeroflex TA-100DC power amplifiers were received from NASA for this testing. One of the torque motors, Serial Number 68F0050, was found to have one of its three windings open and was returned to NASA for repair.

3.2.1 Description of Baseline Systems

The baseline systems had the torque motor coupled directly to the load inertia, as shown in Figure 3-8. An Aeroflex TG10Y-5H DC tachometer was coupled to the motor shaft, and a Clifton LTH-11-B-3 induction potentiometer coupled to the load shaft. Testing was conducted for simulated load inertias of the aileron and elevator control surfaces. A TR-48 analog computer was used to provide input/output functions and to shape the position and rate feedback signals. The computer patching diagram is shown in Figure 3-9.

The tachometer and induction potentiometer were selected to minimize inertia and friction drag in the system. A full wave pulse sample demodulator (PSD) was used with the 400 Hz carrier induction potentiometer. Figure 3-10 shows the frequency response of the demodulator, and the theoretical approximation used in the linear analysis. The demodulator gain was adjustable through a 10,000 ohm handset potentiometer across the output terminals of the induction potentiometer, in series with the demodulator. The voltage gain of the TA-100DC power amplifiers was reduced from the nominal 100 volt/volt to 9.96 volt/volt by replacing the 250,000 ohm pre-amplifier feedback resistor with a 24,900 ohm resistor. This was done to ease scaling requirements on the 10 volt reference analog computer.

3.2.2 Test Results

The two torque motor and power amplifier combinations were found to be essentially identical during testing. A comparison of actual system performance to the theoretical performance is shown in Figures 3-11 and 3-12 for the two combinations with the simulated elevator inertia. Figure 3-13 shows the comparison with the simulated aileron inertia. The load inertias used in the laboratory testing were slightly smaller than the values listed in Table 3-II which include the linkage inertias.

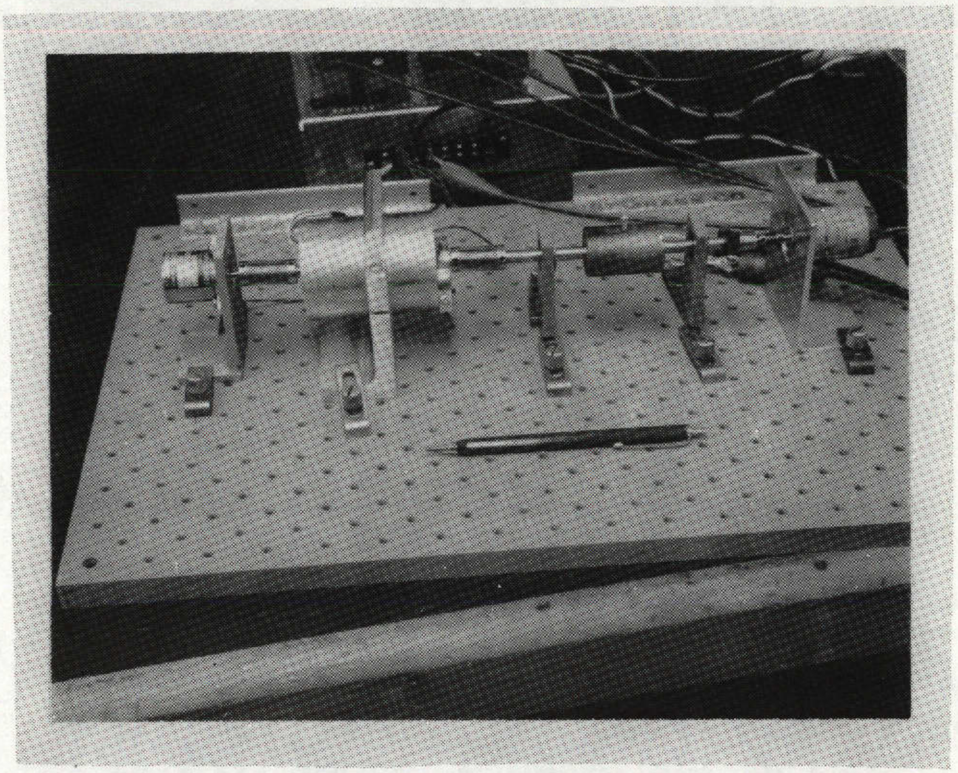

Aeroflex TG10Y-5 Tachometer	Aeroflex TQ20-1 Torque Motor	Simulated Aileron Inertia	Clifton LTH-11-B-3 Induction Potentiometer

AEROELASTIC MODEL CONTROL SURFACE ACTUATOR
BASELINE SYSTEM

FIGURE 3-8

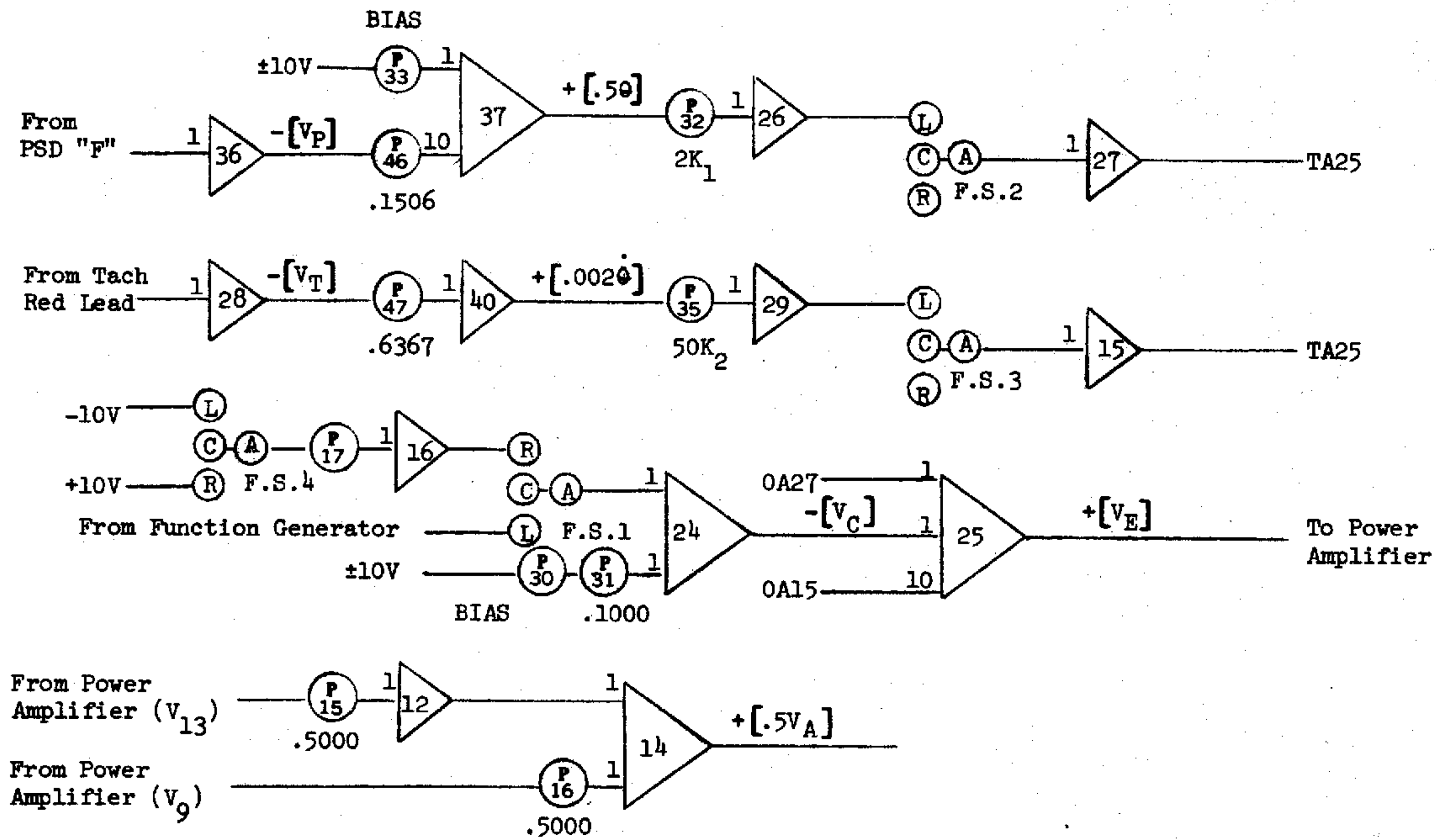

AEROELASTIC MODEL CONTROL SURFACE ACTUATOR STUDY
ANALOG COMPUTER PATCHING DIAGRAM

FIGURE 3-9

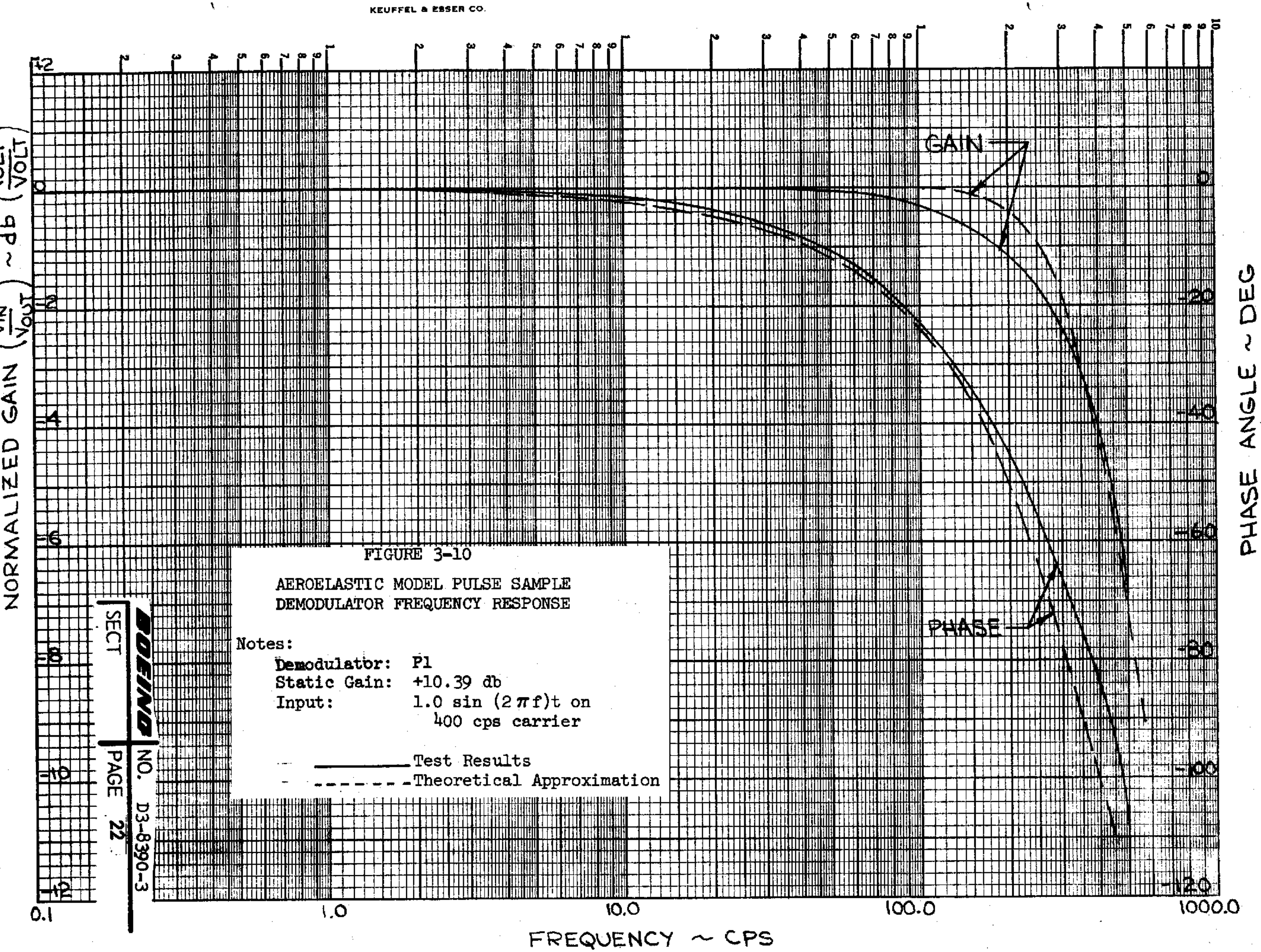

FIGURE 3-10

AEROELASTIC MODEL PULSE SAMPLE
DEMODULATOR FREQUENCY RESPONSE

Notes:

Demodulator: P1
Static Gain: +10.39 db
Input: 1.0 sin $(2\pi f)t$ on 400 cps carrier

———— Test Results
- - - - - - Theoretical Approximation

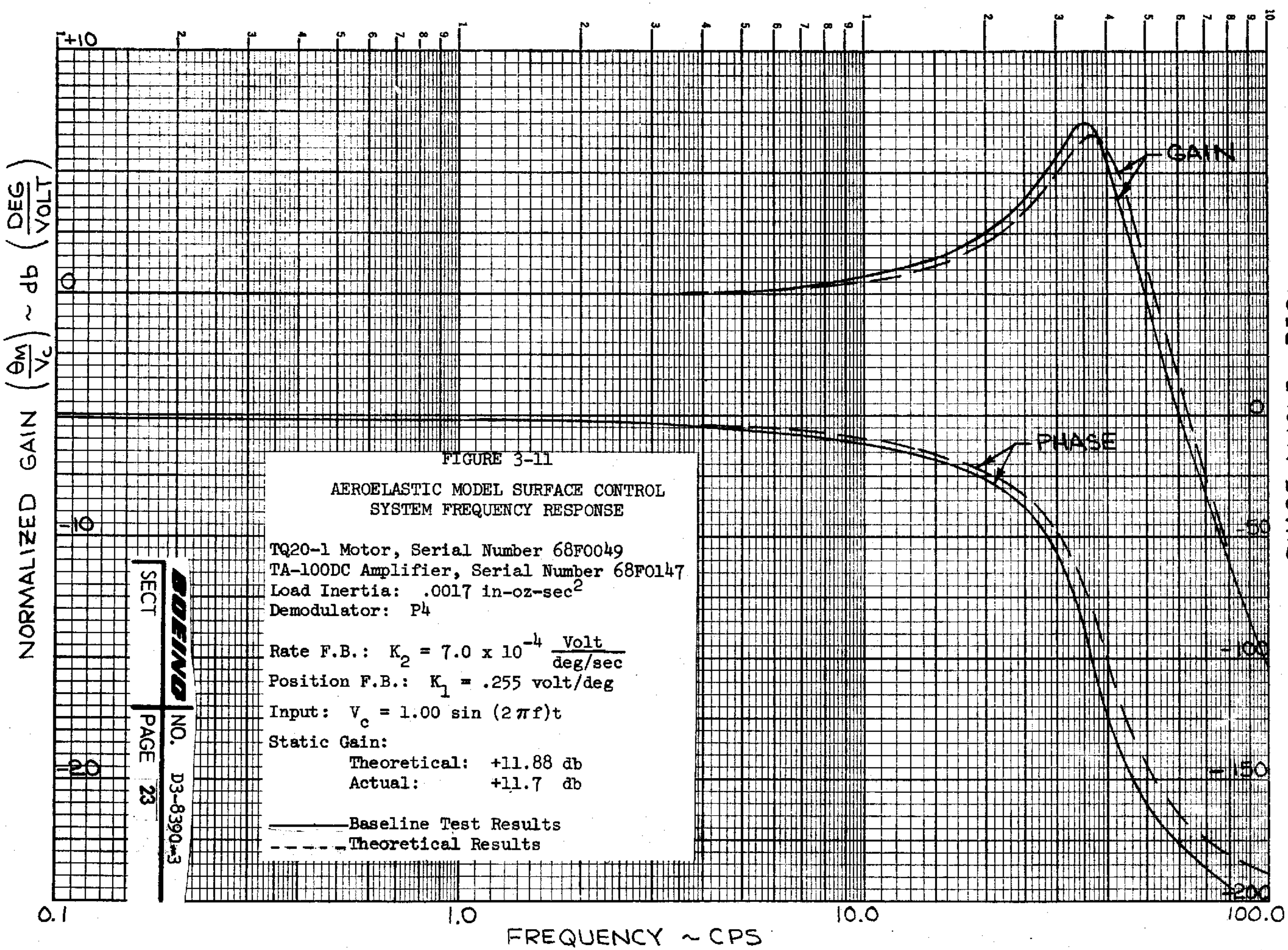

FIGURE 3-11

AEROELASTIC MODEL SURFACE CONTROL SYSTEM FREQUENCY RESPONSE

TQ20-1 Motor, Serial Number 68F0049
TA-100DC Amplifier, Serial Number 68F0147
Load Inertia: .0017 in-oz-sec^2
Demodulator: P4

Rate F.B.: $K_2 = 7.0 \times 10^{-4} \frac{\text{Volt}}{\text{deg/sec}}$
Position F.B.: K_1 = .255 volt/deg
Input: $V_c = 1.00 \sin(2\pi f)t$
Static Gain:
Theoretical: +11.88 db
Actual: +11.7 db

——— Baseline Test Results
- - - - Theoretical Results

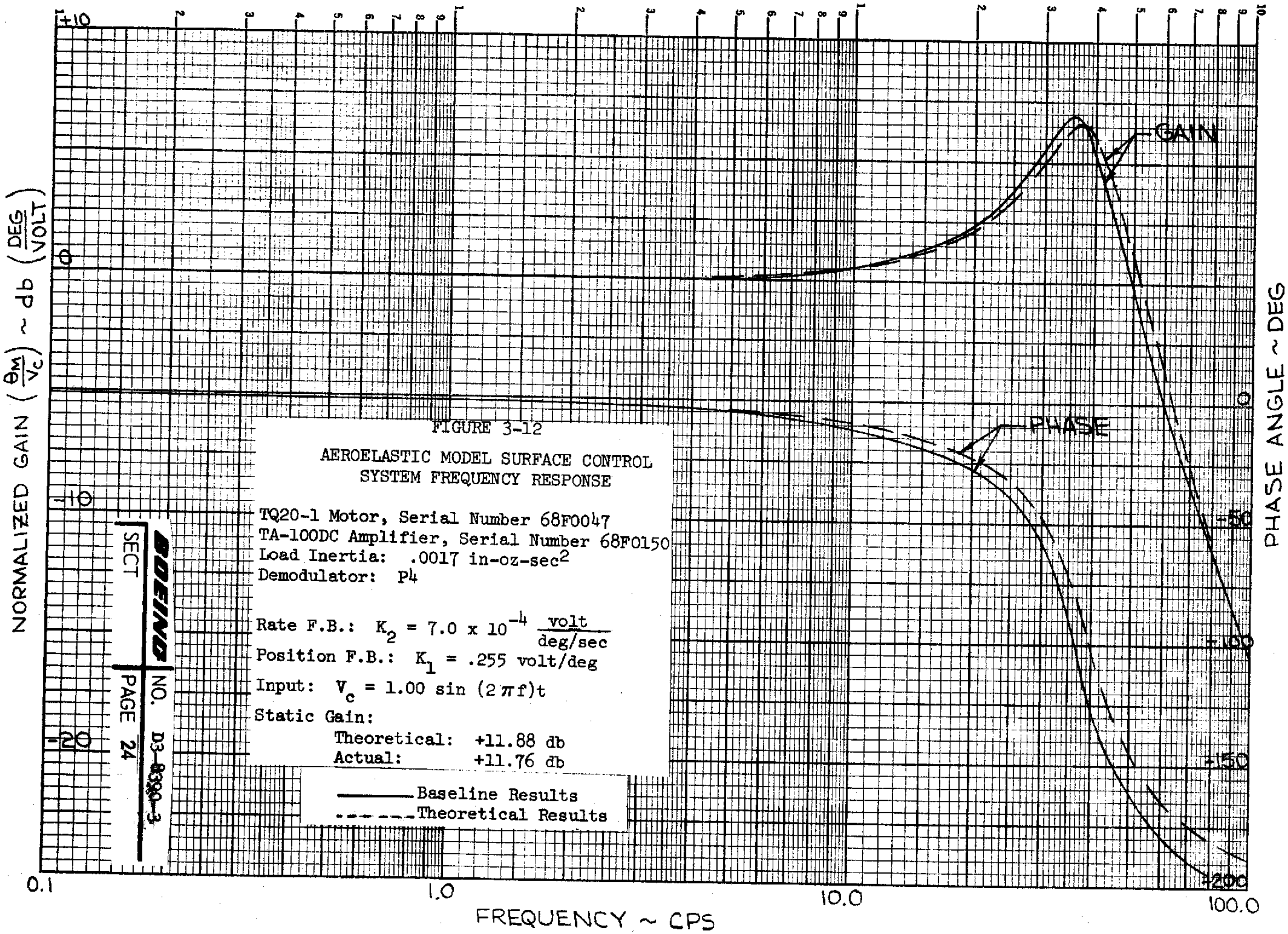

FIGURE 3-12

AEROELASTIC MODEL SURFACE CONTROL SYSTEM FREQUENCY RESPONSE

TQ20-1 Motor, Serial Number 68F0047
TA-100DC Amplifier, Serial Number 68F0150
Load Inertia: .0017 in-oz-sec^2
Demodulator: P4

Rate F.B.: $K_2 = 7.0 \times 10^{-4}$ $\frac{\text{volt}}{\text{deg/sec}}$
Position F.B.: K_1 = .255 volt/deg
Input: $V_c = 1.00 \sin (2\pi f)t$
Static Gain:
Theoretical: +11.88 db
Actual: +11.76 db

——— Baseline Results
- - - - Theoretical Results

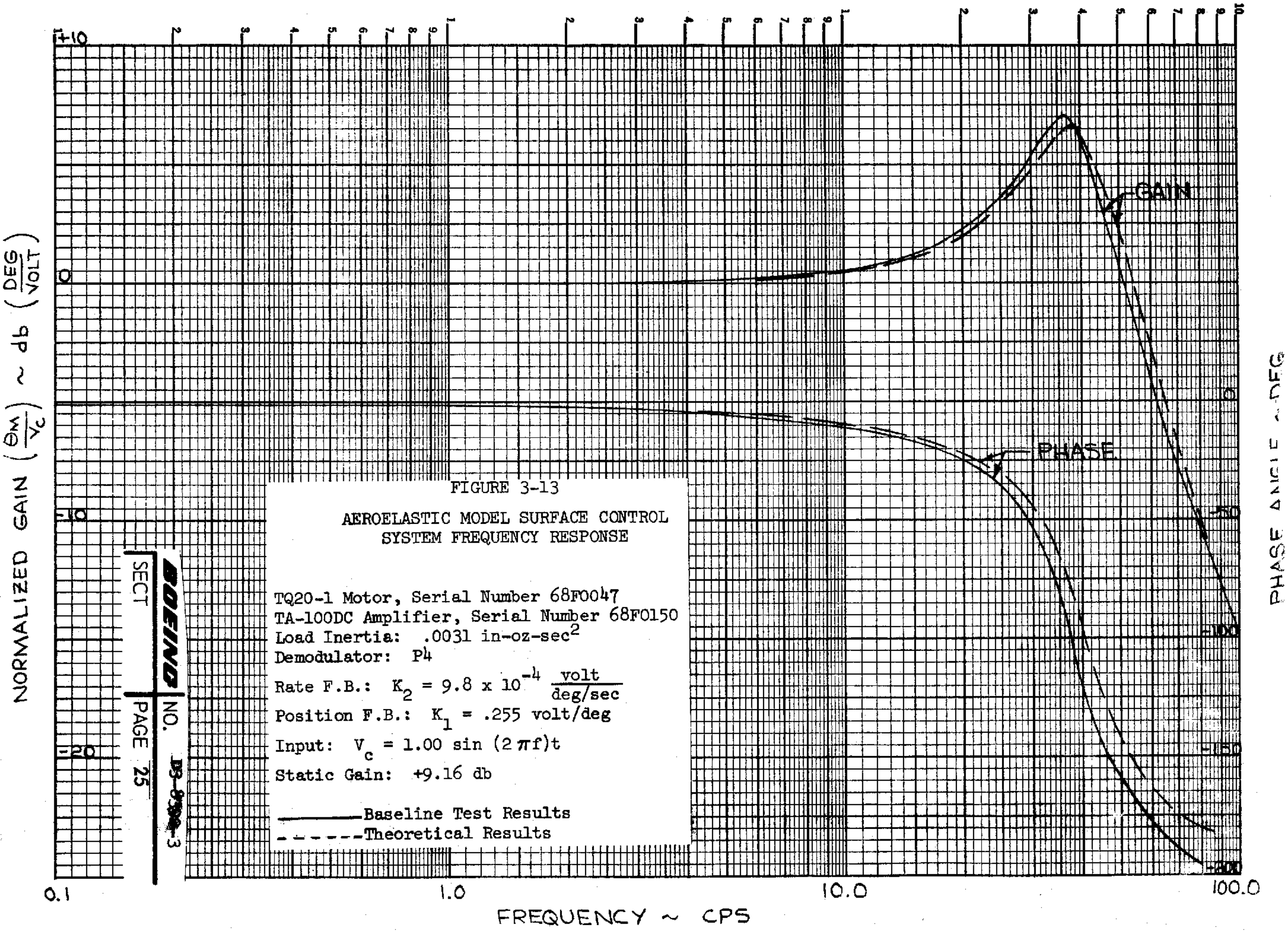

FIGURE 3-13

AEROELASTIC MODEL SURFACE CONTROL SYSTEM FREQUENCY RESPONSE

TQ20-1 Motor, Serial Number 68F0047
TA-100DC Amplifier, Serial Number 68F0150
Load Inertia: .0031 in-oz-sec^2
Demodulator: P4
Rate F.B.: $K_2 = 9.8 \times 10^{-4} \frac{\text{volt}}{\text{deg/sec}}$
Position F.B.: K_1 = .255 volt/deg
Input: $V_c = 1.00 \sin (2\pi f)t$
Static Gain: +9.16 db

——— Baseline Test Results
– – – – Theoretical Results

The hysteresis of the baseline aileron actuation system is shown in Figure 3-14. This plot of motor angular position versus voltage input command indicates a hysteresis of ±0.032 degrees, with the simulated aileron inertia. Hysteresis increases as elevator inertia increases at a constant closed loop natural frequency (see Figure 3-7).

The transient responses of Figure 3-15 indicate a damping ratio of 0.24 and a damped natural frequency of 38 Hz. The frequency response of this system, shown in Figure 3-13, indicates 0.23 damping ratio with a peak frequency of 37 Hz. This shows good agreement between the two testing methods.

3.3 Conclusions of Baseline System Testing

The theoretical analysis and laboratory testing of the baseline surface actuation systems indicate the TQ20-1 torque motor and TA-100DC power amplifier combinations possess the capability of meeting the performance and stability requirements. Both rate and position feedback are required to attain this performance.

To meet these requirements with the actual control surface actuation systems, the friction and inertia of the mechanical linkage must be minimized. Testing of simulations of the model aileron and elevator actuation systems is discussed in Section 4.0.

NOTES: TQ20-1 Motor, Serial Number 68F0047
TA-100DC Amplifier, Serial Number 68F0150
Load Inertia: .0031 in-oz-sec^2
Feedback Gains: K_1 = .348 volt/deg, K_2 = .00098 volt/deg/sec
Input: 0.1 Hz Triangular Wave

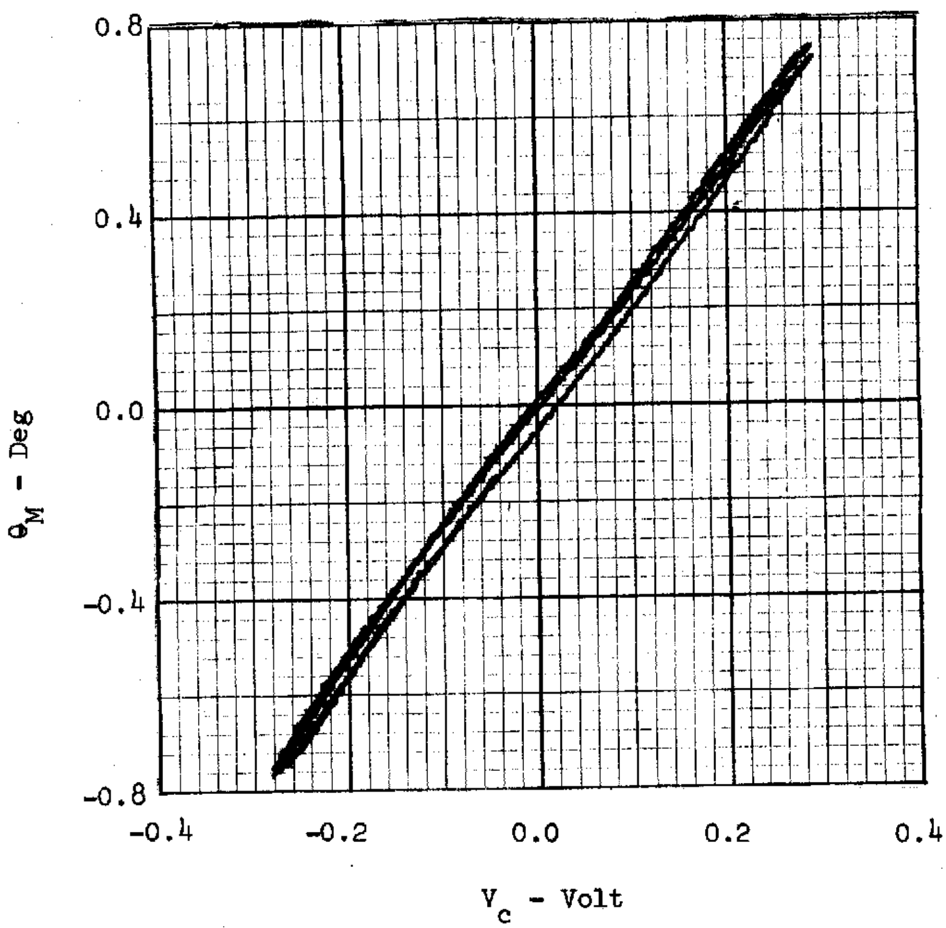

AEROELASTIC MODEL CONTROL SURFACE
ACTUATOR HYSTERESIS

FIGURE 3-14

NOTES: TQ20-1 Motor, Serial Number 68F0047
TA-100DC Amplifier, Serial Number 68F0150
Load Inertia: .0031 in-oz-sec^2
Feedback Gains: K_1 = .348 volt/deg, K_2 = .00098 volt/deg/sec

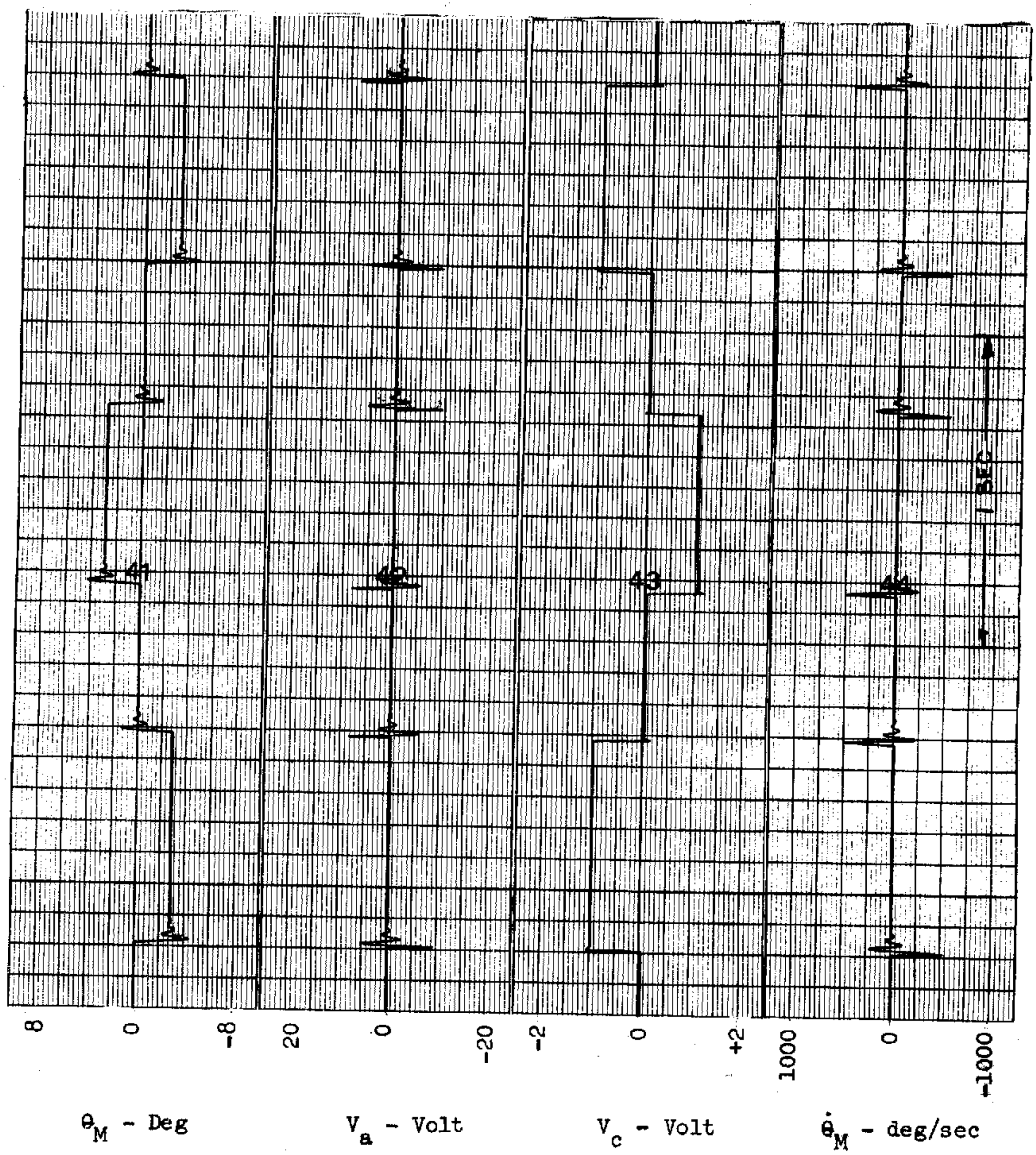

AEROELASTIC MODEL CONTROL
SURFACE ACTUATOR TRANSIENT RESPONSES

FIGURE 3-15

4.0 AILERON AND ELEVATOR SIMULATIONS

The analysis and laboratory tests of the baseline control surface actuation systems proved that the B-52 model torque motor and power amplifier combinations could meet performance and stability requirements with position and rate feedback. The final step in the evaluation of the model actuation systems was to determine the effects on performance of the mechanical linkage from torque motor to the control surface. For this part of the evaluation, breadboard simulations of the model aileron and elevator actuation systems were designed and assembled for laboratory tests. The geometric constraints imposed by the model were retained within practical limits in the simulations.

4.1 Description of Existing Aileron Actuation System

The aileron mechanization installed in the model utilizes a TQ20-1 torque motor to drive each of the two surfaces. The motors mount in the model fuselage, normal to the fuselage centerline. Torque is transmitted from each motor through a crank-pushrod assembly to a shaft routed approximately out each wing elastic axis. The torque then is transmitted from this shaft to the trailing edge surface through another crank-pushrod assembly. A dc potentiometer, in the fuselage, is driven through gears off the shaft. A 0.50 inch diameter potentiometer is coupled directly to the aileron hinge shaft to measure the surface angular position.

The 30 degree change of direction of the shaft is accomplished in the model by two miniature universal joints. Flexible bellows couplings in the shaft permit flexing of the wing. All bearings used to support the shaft and the surface are oil-less bronze type. No provisions were made in the model for the installation of a tachometer.

A more detailed description of the aileron actuation system installed in the model is contained in Reference 2.

4.1.1 Description of Aileron Simulation.

Figure 4-1 is a photograph of the aileron simulation tested in the laboratory. To adequately simulate the vertical bending of the model wing, a wing plate was fabricated which approximated the vertical stiffness of the wing. The routing of the drive shaft is identical to the routing in the model, except in the vertical plane. The shaft in the model is approximately in the same horizontal plane as the wing elastic axis. The effects of vertical bending of the wing are amplified in the simulation since the shaft is located 0.875 inch above the wing plate neutral axis.

A close-up view of the simulated aileron drive assembly is shown in Figure 4-2. This photograph illustrates the torque transmission from the torque motor out along the wing plate. The brushless, permanent magnet dc tachometer is coupled directly to the motor shaft through a bellows coupling which permits some shaft misalignment. The induction potentiometer is gear driven from the aileron drive shaft. This potentiometer and the tachometer provide the position and rate feedback signals which are scaled on the analog computer.

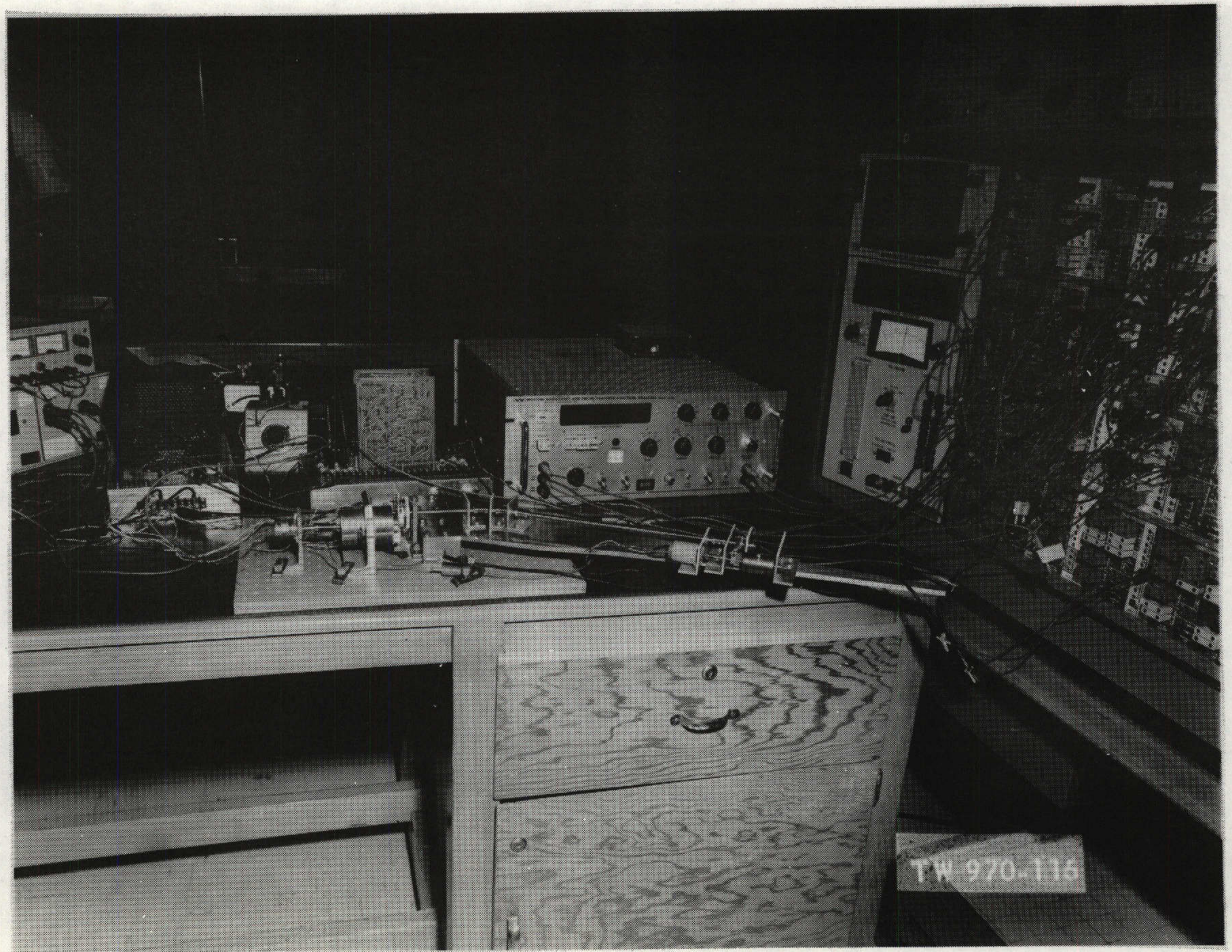

B-52 AEROELASTIC MODEL AILERON SIMULATION

FIGURE 4-1

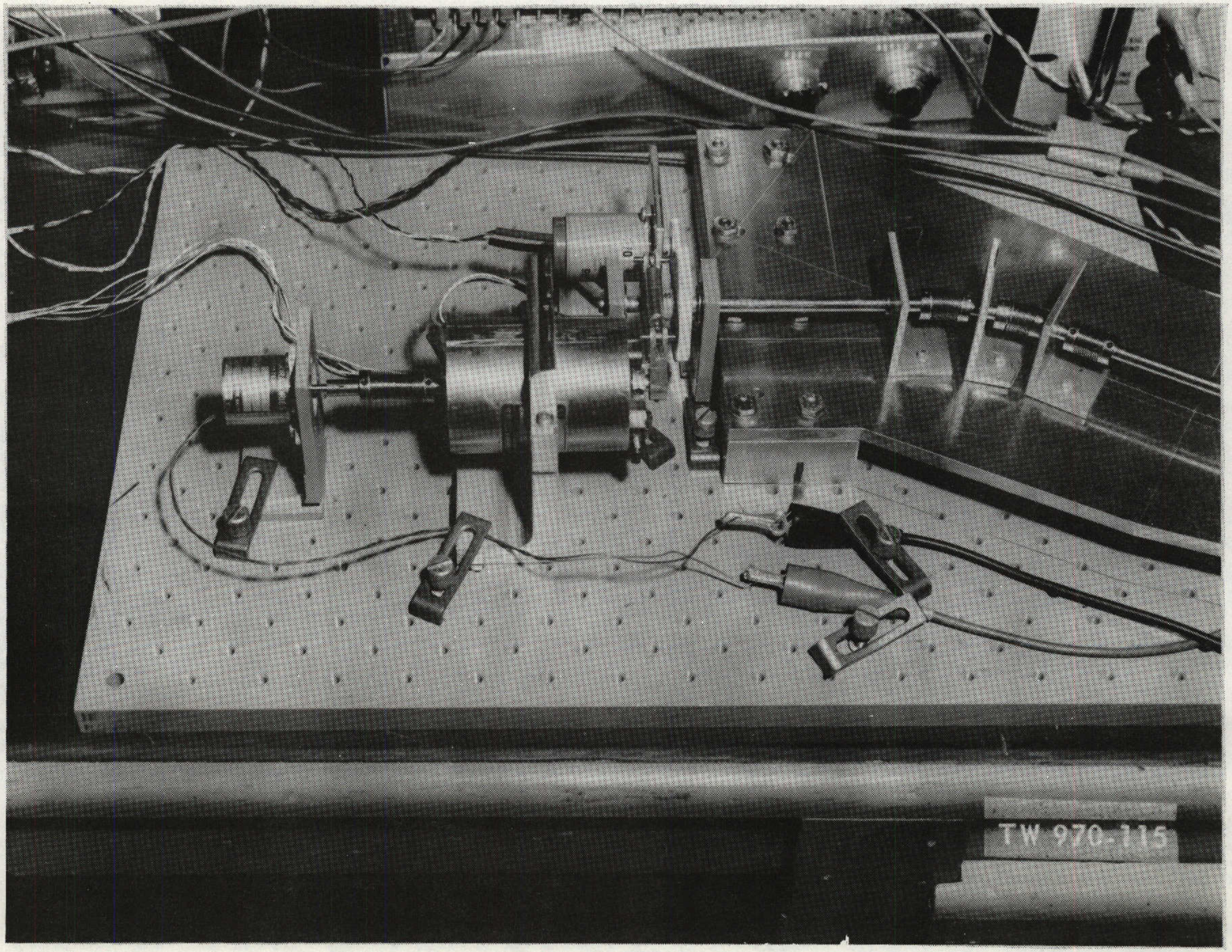

SIMULATED AILERON DRIVE ASSEMBLY

FIGURE 4-2

Two Sterling Instrument G404-56 bellows couplings are used to accomplish the 30 degree change in shaft direction. The shaft support between the two couplings was necessary to increase the torsional stiffness. Bellows couplings tend to buckle in the vertical plane under a torsional load, which appeared during testing as a vertical vibration of the two couplings. The added shaft support restrained the vibration and increased the torsional stiffness.

A close-up view of the simulated aileron surface is shown in Figure 4-3. The fabricated crank-pushrod assembly utilizes precision fit pins through the cranks and Southwest Products Company 2-DREM-1 miniature low friction rod ends. Teflon washers were inserted between the rod ends and the clevises to eliminate binding experienced during tests. An induction potentiometer is coupled directly to the simulated aileron shaft to provide a means of evaluating the linkage dynamic behavior.

Stainless steel precision shafting is used for all shafts in the simulation. All shaft supports utilize stainless steel precision ball bearings to minimize friction.

It will be necessary to mount the tachometer either below or aft of the torque motor in the model driven by a crank-pushrod assembly from the motor shaft. This method of driving the tachometer was not evaluated, but no difficulty should occur if low friction rod ends are used and the inertia of the crank-pushrod assembly is minimized.

4.1.2 Test Results

Testing of the aileron simulation shows that satisfactory performance can be attained with a minimum of modifications to the existing actuation system mechanization. Figure 4-4 shows the frequency response of the aileron angular position due to a 3 degree sinusoidal input command. This plot indicates a damping ratio of 0.21 and 44.7 degrees phase lag at 25 Hz, which satisfies the frequency response requirement. The linkage frequency response, Figure 4-5, illustrates two linkage vibration modes, at about 85 Hz and 95 Hz. These modes are lightly damped, which is typical of structural modes. The frequencies of these modes are well above the primary frequency band of normal operation of the aileron actuation system.

The hysteresis measured at the simulated aileron surface is shown in Figure 4-6. The ± .13 degree hysteresis width illustrates the degree that friction has been minimized. The positional accuracy of the actuation system is shown in the transient responses of Figure 4-7.

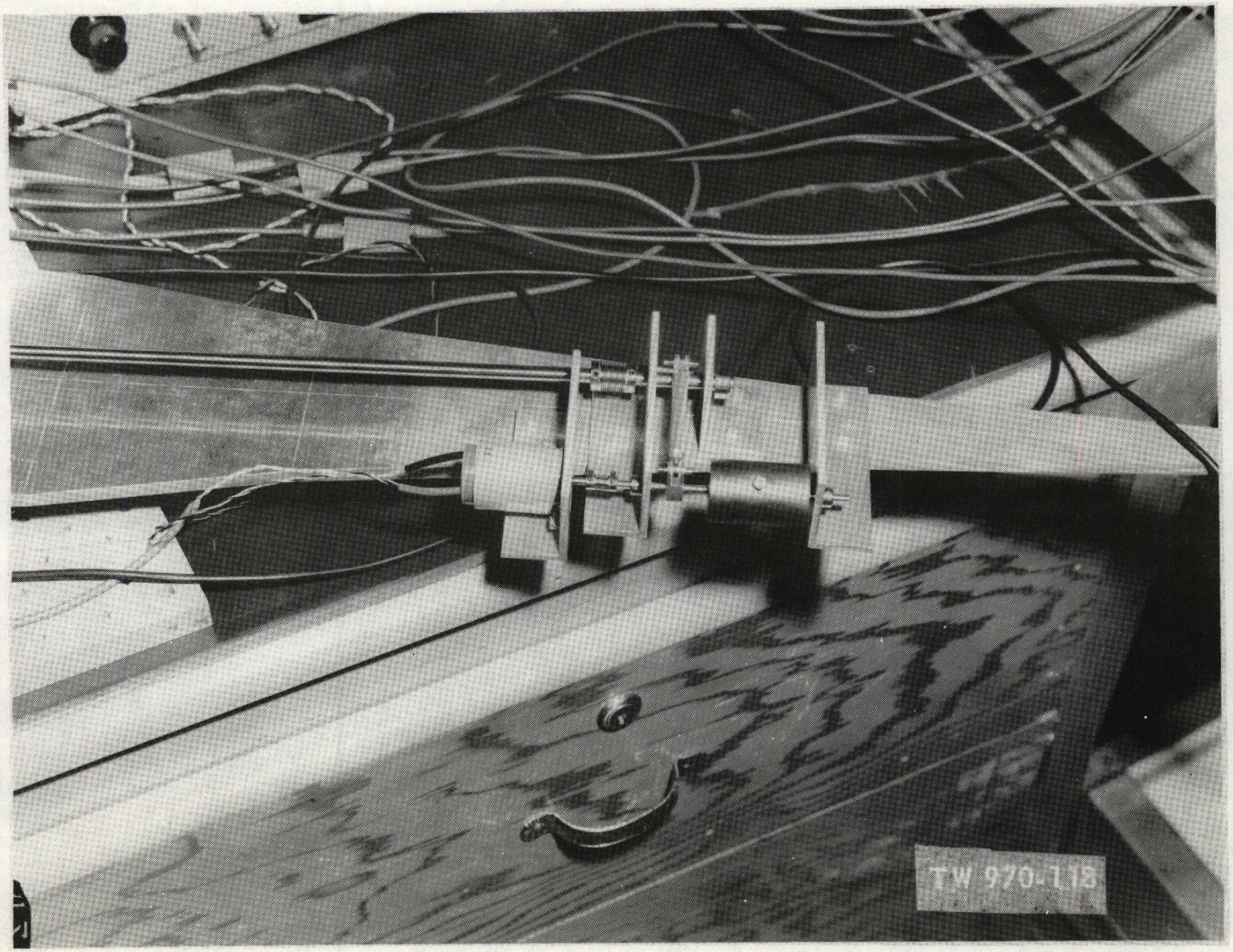

SIMULATED AILERON SURFACE

FIGURE 4-3

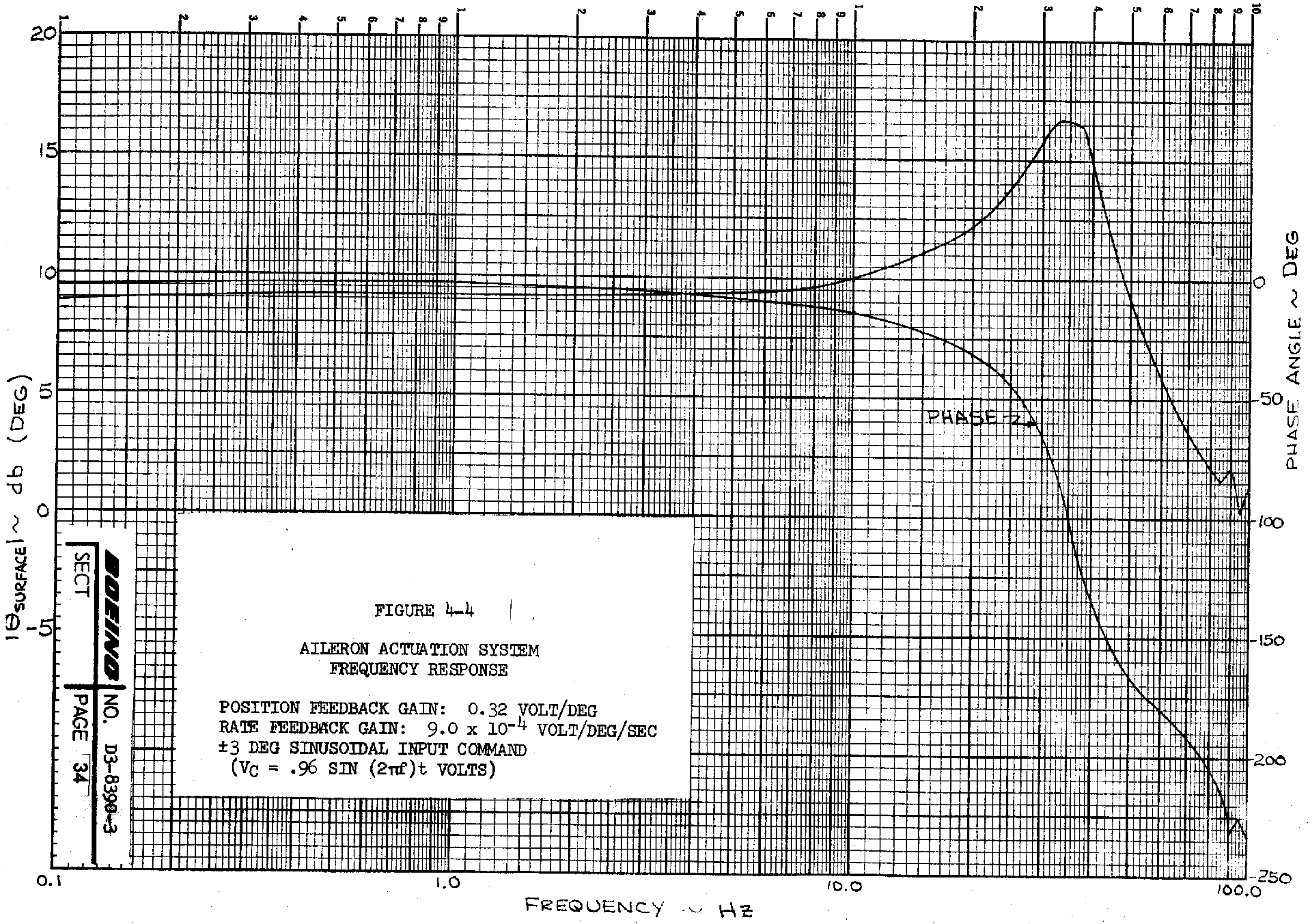

FIGURE 4-4

AILERON ACTUATION SYSTEM
FREQUENCY RESPONSE

POSITION FEEDBACK GAIN: 0.32 VOLT/DEG
RATE FEEDBACK GAIN: 9.0×10^{-4} VOLT/DEG/SEC
±3 DEG SINUSOIDAL INPUT COMMAND
(V_C = .96 SIN ($2\pi f$)t VOLTS)

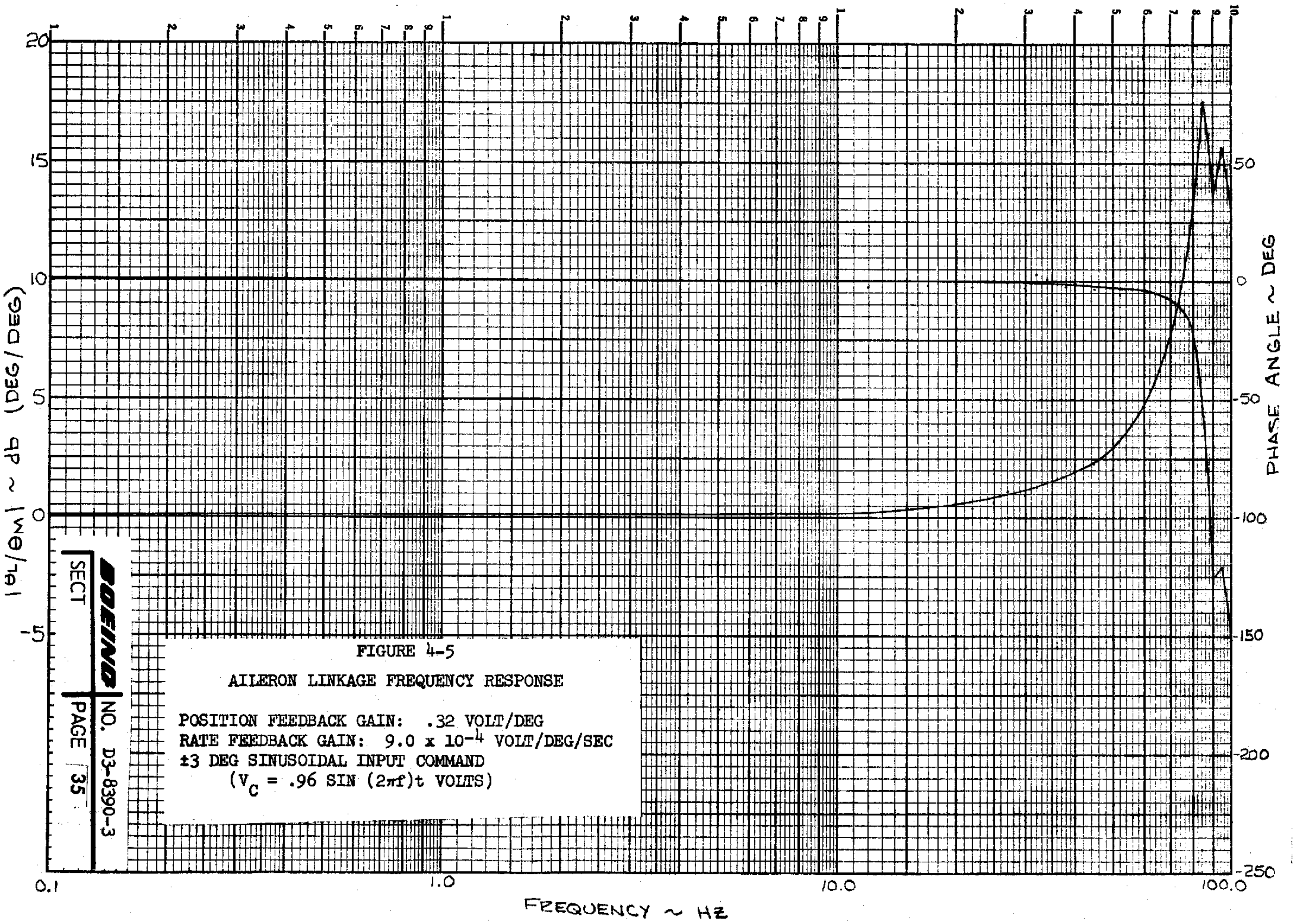

FIGURE 4-5

AILERON LINKAGE FREQUENCY RESPONSE

POSITION FEEDBACK GAIN: .32 VOLT/DEG
RATE FEEDBACK GAIN: 9.0×10^{-4} VOLT/DEG/SEC
±3 DEG SINUSOIDAL INPUT COMMAND
(V_C = .96 SIN ($2\pi f$)t VOLTS)

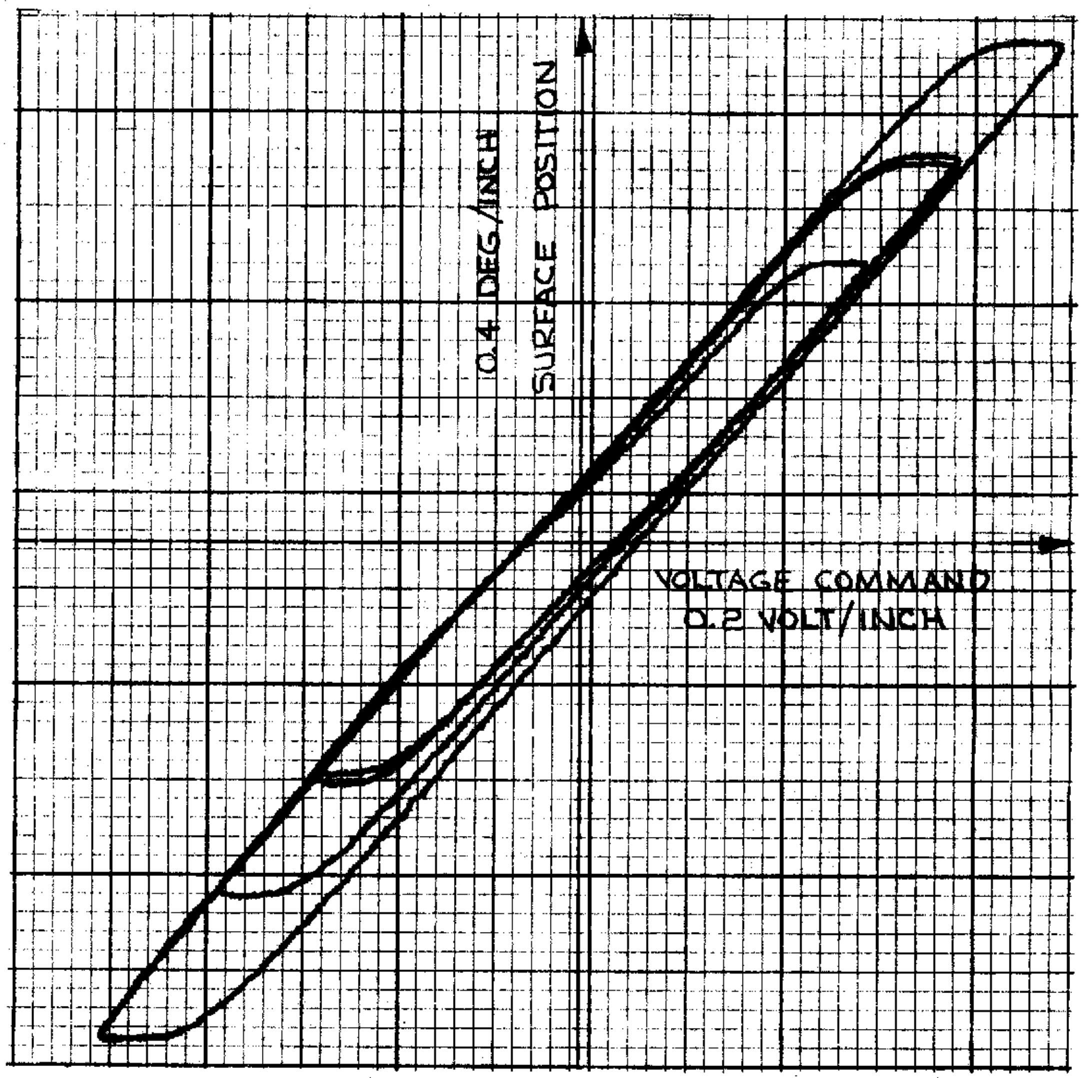

FIGURE 4-6

AILERON ACTUATION SYSTEM HYSTERESIS

POSITION FEEDBACK GAIN: 0.32 VOLT/DEG
RATE FEEDBACK GAIN: 9.0×10^{-4} VOLT/DEG/SEC
INPUT: 0.1 HZ TRIANGULAR WAVE, VARYING AMPLITUDE

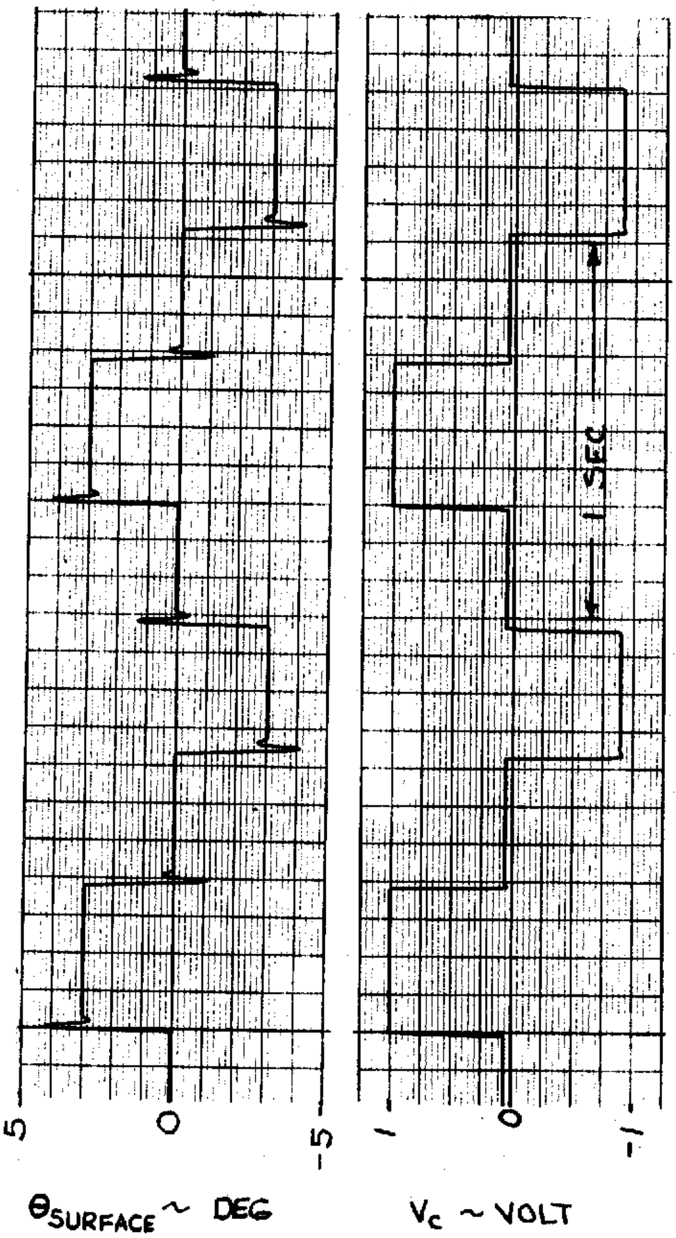

FIGURE 4-7

AILERON ACTUATION SYSTEM
TIME HISTORIES

NOTE: POSITION FEEDBACK GAIN 0.32 VOLT/DEG
RATE FEEDBACK GAIN 9.0×10^{-4} VOLT/DEG/SEC

4.2 Description of Existing Elevator Actuation System

The elevator actuation system installed in the B-52 aeroelastic model utilizes an Aeroflex TQ20-1 torque motor mounted normal to the fuselage centerline. Torque is transmitted aft approximately 20 inches through a crank-pushrod linkage that includes a movable pushrod support about mid-way between the torque motor and the elevator hinge line. A dc potentiometer is gear driven by the motor to measure motor angular position. Another dc potentiometer is gear driven by the elevator shaft to measure the elevator angular position relative to the horizontal stabilizer. No provisions were made for the installation of a tachometer.

The inboard support of each elevator surface is provided by the stainless steel elevator shaft supported by an aluminum horizontal stabilizer spar, without a bearing or bushing. Each surface is hinged on the outboard end by a 0.032 inch diameter steel pin riding on an aluminum bearing surface. Flexible bellows couplings permit flexing of the horizontal stabilizer relative to the model fuselage without binding the elevator shaft. Oil-less bronze bearings are used in the fuselage shaft supports.

A more detailed description of the elevator actuation system installed in the model is contained in Reference 2.

4.2.1 Description of Elevator Simulation

An overall view of the elevator simulation tested in the laboratory is shown in Figure 4-8. This photograph shows the crank-pushrod assembly which was installed in the model. This linkage was later redesigned to reduce the inertia reflected to the motor shaft. This was accomplished by reducing the length of the two cranks and the pushrod support to provide a crank radius of 0.50 inch. The elevator surfaces shown are simplified versions of the actual surfaces, with the hinge method retained.

The close-up view of the simulated elevator drive assembly, Figure 4-9, shows the induction potentiometer gear driven by the motor, and the tachometer connected to the motor shaft through a bellows coupling. These sensors provided position and rate feedback signals which were scaled on the analog computer.

The simulated elevator surfaces and supports are shown in Figure 4-10. Stainless steel precision ball bearings were used in the simulation to minimize friction.

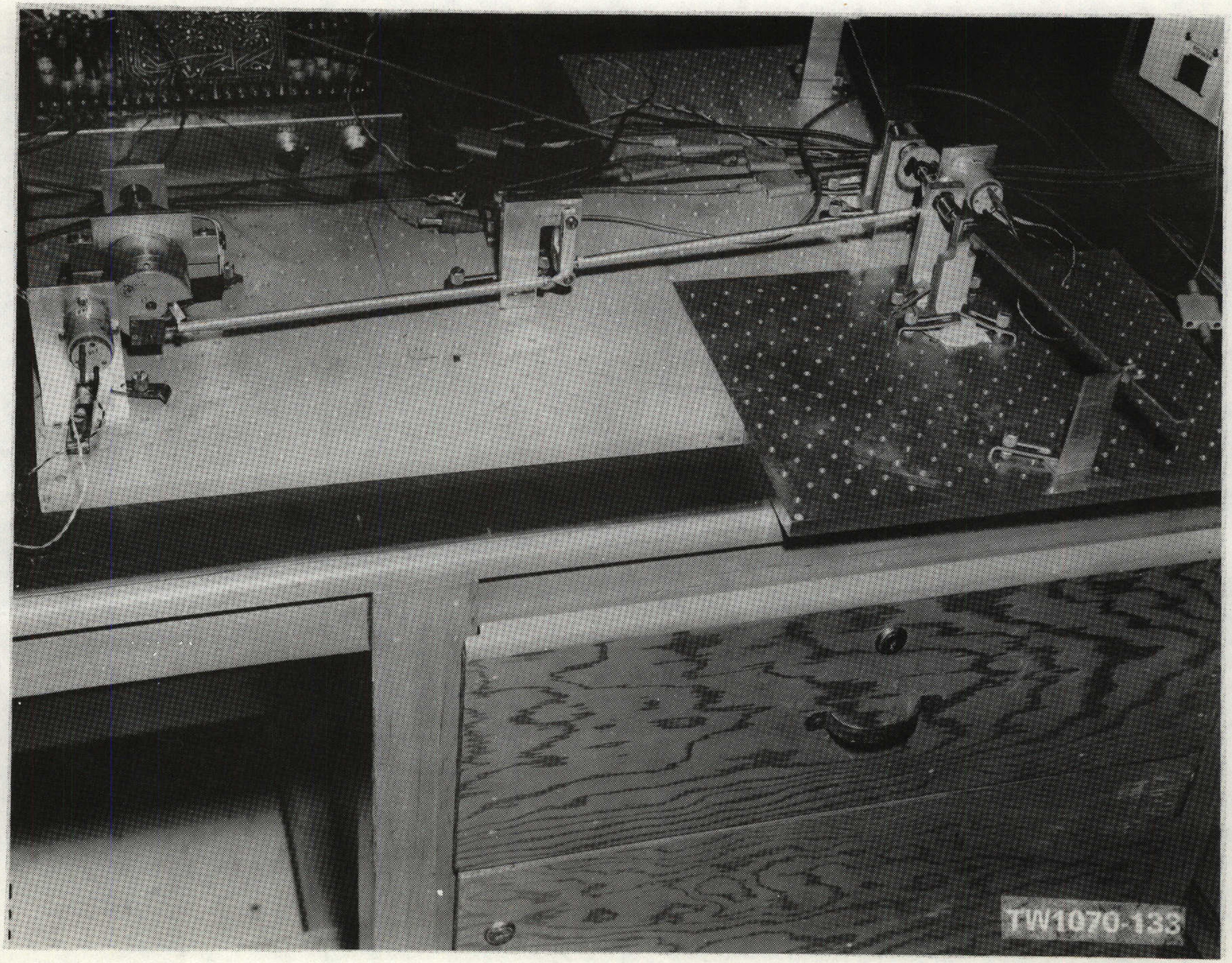

B-52 AEROELASTIC MODEL ELEVATOR SIMULATION

FIGURE 4-8

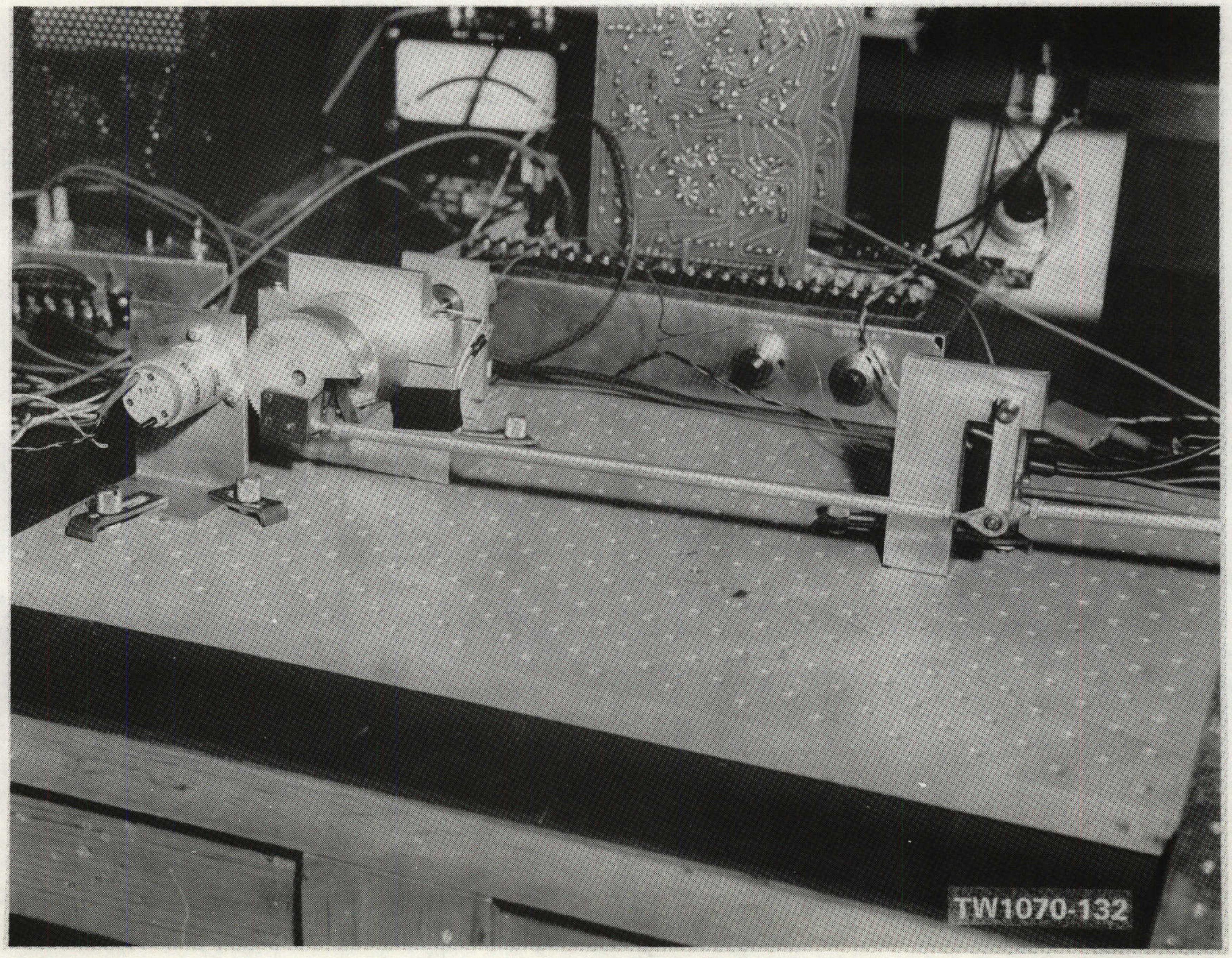

SIMULATED ELEVATOR DRIVE ASSEMBLY

FIGURE 4-9

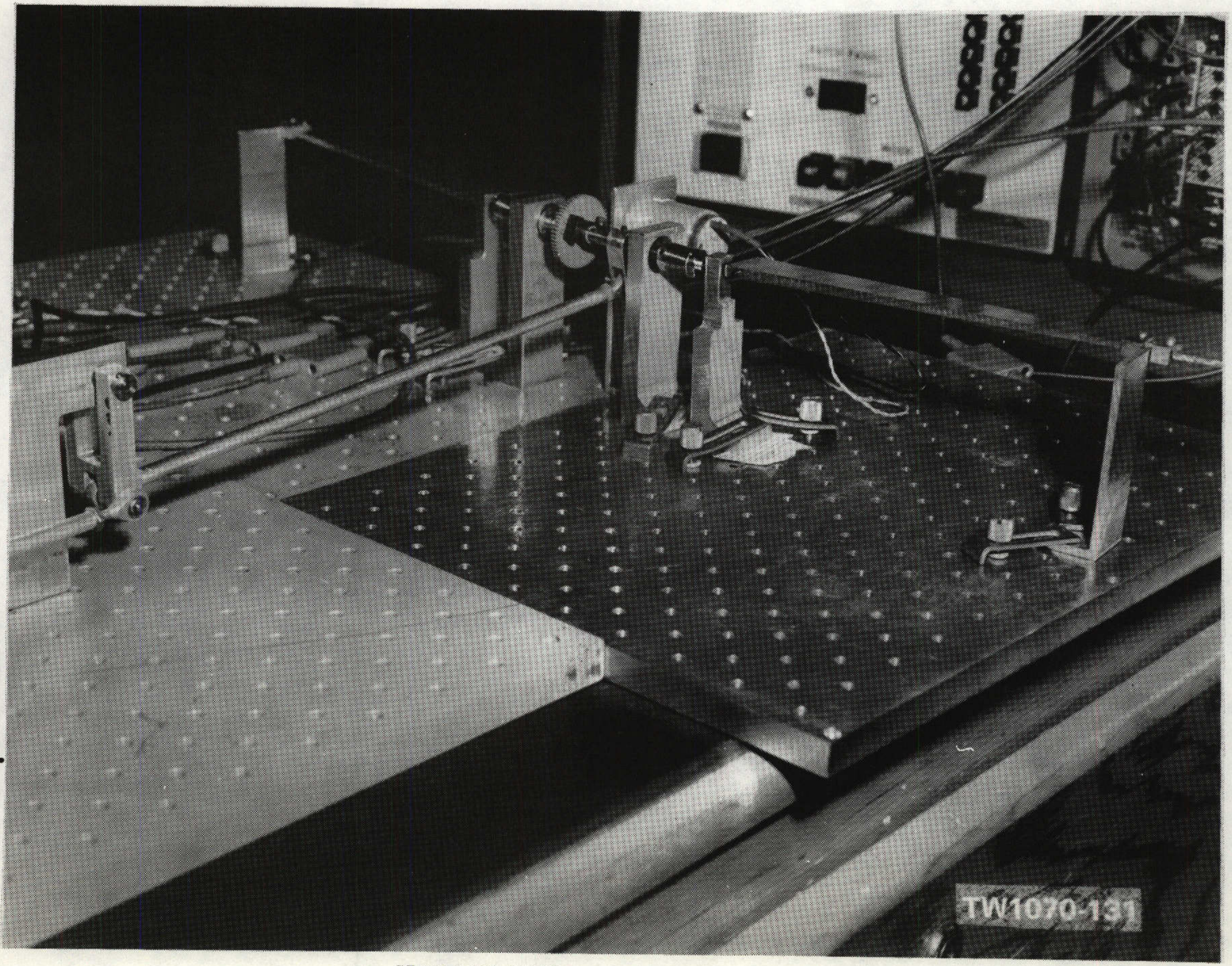

SIMULATED ELEVATOR SURFACES

FIGURE 4-10

4.2.2 Test Results

Laboratory testing of the simulated elevator actuation system shows that the linkage inertia must be reduced to meet performance and stability requirements. With the effective crank radius reduced to 0.50 inch, satisfactory performance was attained with the TQ20-1 torque motor and TA-100 dc power amplifier combination with motor position and rate feedback. The frequency response of elevator position due to a 3 degree sinusoidal input command shown in Figure 4-11 indicates a damping ratio of 0.21 with peak frequency of 35 Hz and 43.5 degrees phase lag at 25 Hz. This satisfies the frequency response criteria for the elevator actuation system. The linkage frequency response, Figure 4-12, shows a linkage vibration mode with a peak frequency above 100 Hz, which is well above the nominal frequency band of normal operation.

The system hysteresis plot of Figure 4-13 indicates friction is excessive. Part of this hysteresis is due to poor pin fit in the pushrod support arm, but most is due to friction in the surface hinges. The ±0.45 degree hysteresis width does not meet the requirement, but the hysteresis will be considerably less with the reduced friction in the model surface hinges. The transient responses of Figure 4-14 illustrate the effect of relatively high hysteresis in the actuation system.

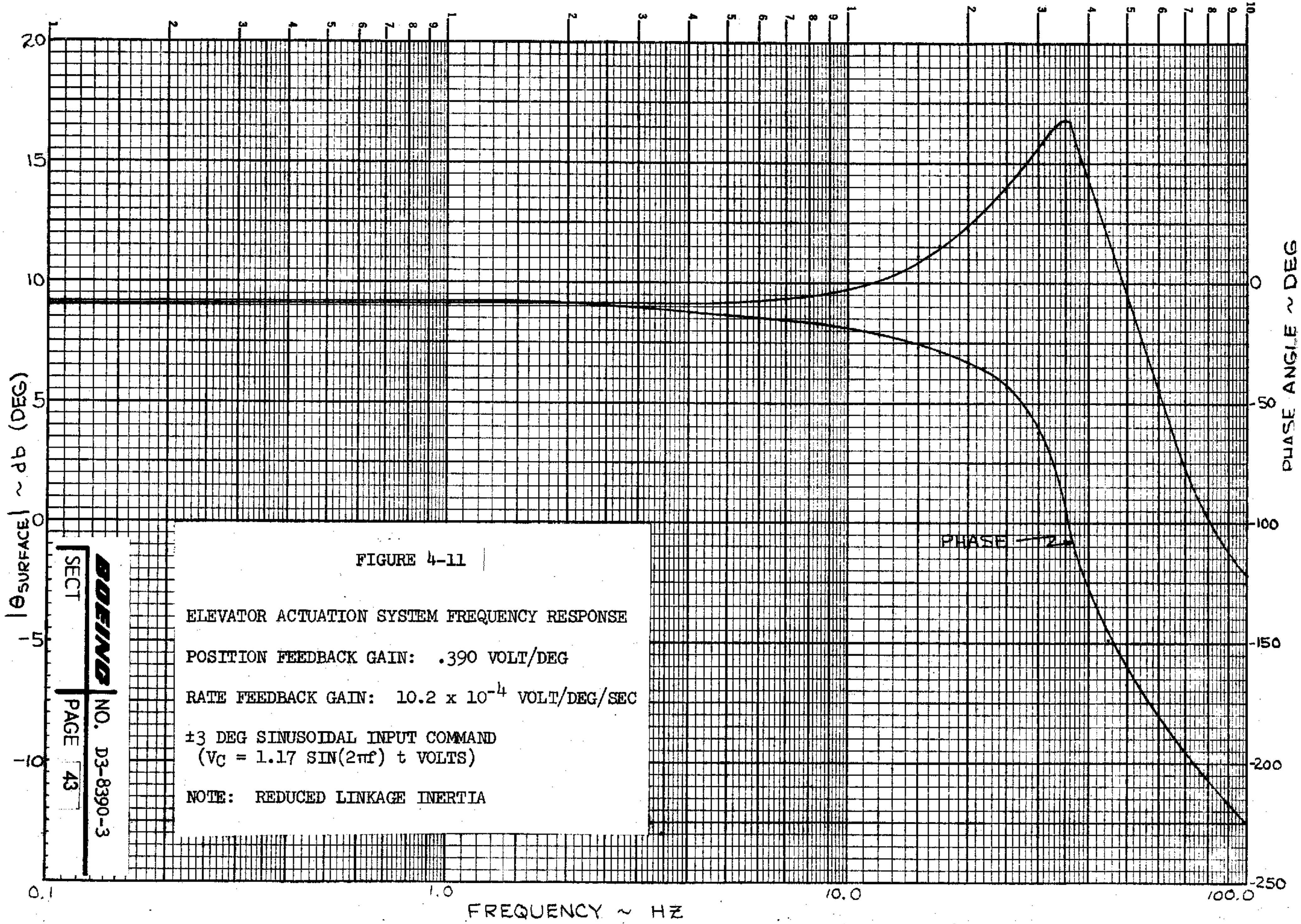

FIGURE 4-11

ELEVATOR ACTUATION SYSTEM FREQUENCY RESPONSE

POSITION FEEDBACK GAIN: .390 VOLT/DEG

RATE FEEDBACK GAIN: 10.2×10^{-4} VOLT/DEG/SEC

±3 DEG SINUSOIDAL INPUT COMMAND
($V_C = 1.17 \sin(2\pi f)\, t$ VOLTS)

NOTE: REDUCED LINKAGE INERTIA

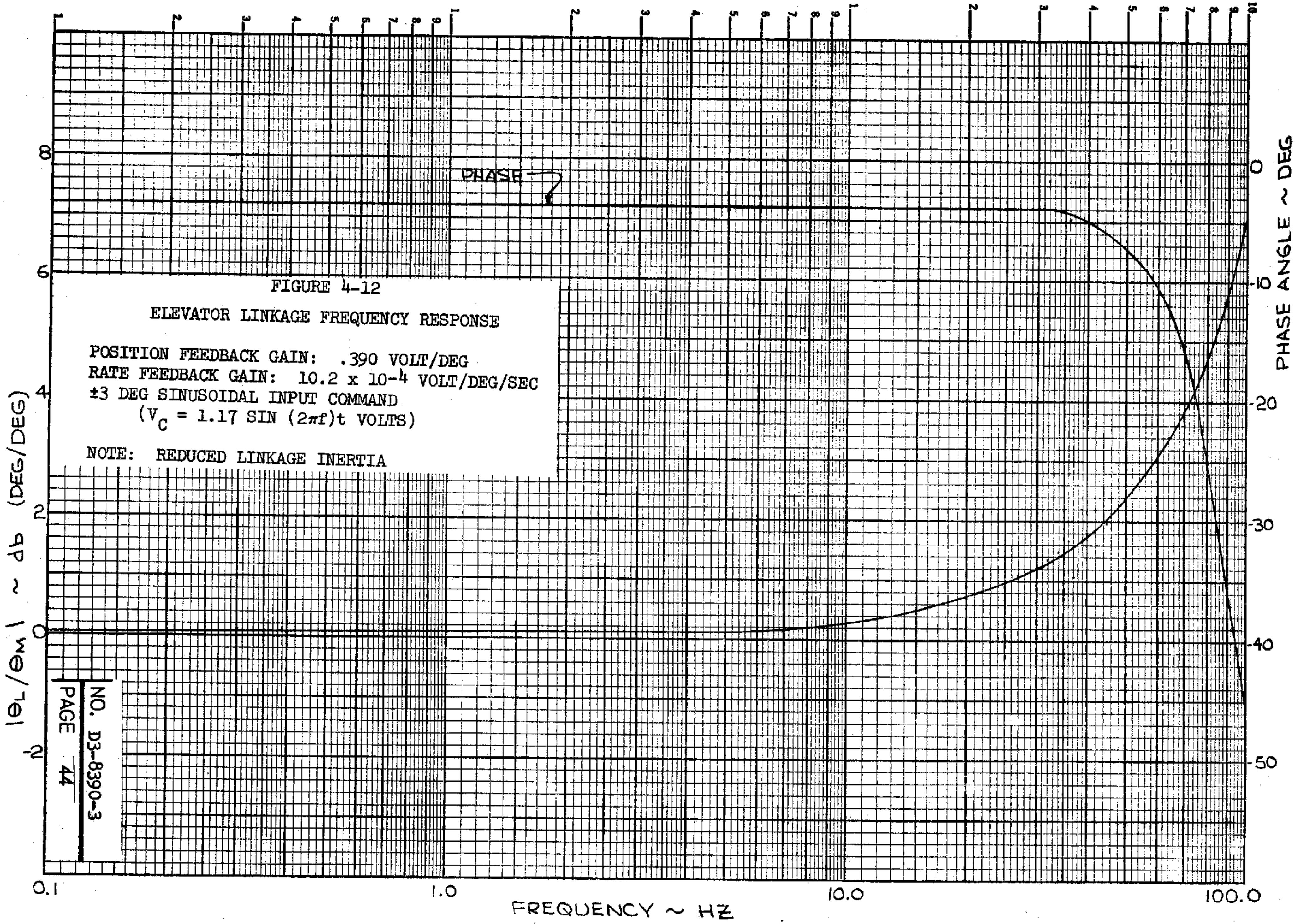

FIGURE 4-12

ELEVATOR LINKAGE FREQUENCY RESPONSE

POSITION FEEDBACK GAIN: .390 VOLT/DEG
RATE FEEDBACK GAIN: 10.2×10^{-4} VOLT/DEG/SEC
±3 DEG SINUSOIDAL INPUT COMMAND
(V_C = 1.17 SIN $(2\pi f)$t VOLTS)

NOTE: REDUCED LINKAGE INERTIA

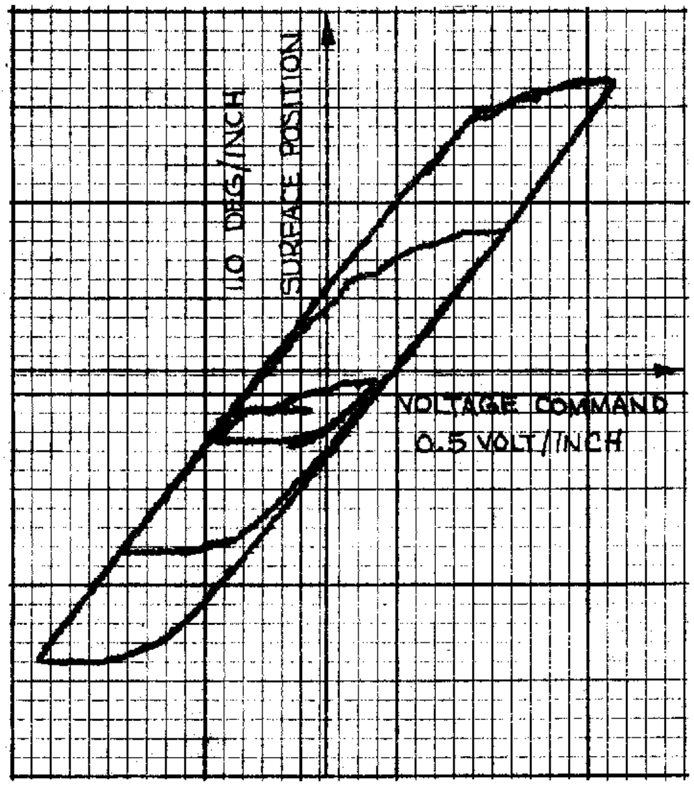

FIGURE 4-13

ELEVATOR ACTUATION SYSTEM
HYSTERESIS

POSITION FEEDBACK GAIN: .390 VOLT/DEG
RATE FEEDBACK GAIN: 10.2×10^{-4} VOLT/DEG/SEC
INPUT: 0.1 HZ TRIANGULAR WAVE, VARYING AMPLITUDE
NOTE: REDUCED LINKAGE INERTIA

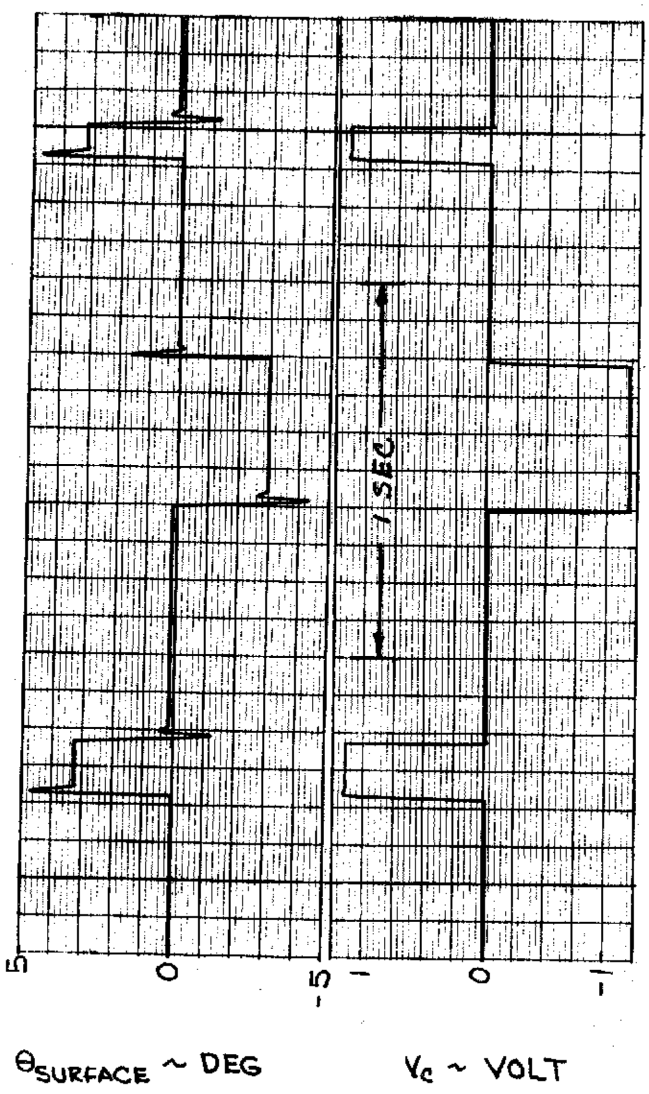

FIGURE 4-14

ELEVATOR ACTUATION SYSTEM
TIME HISTORIES

NOTE: POSITION FEEDBACK GAIN .390 VOLT/DEG
RATE FEEDBACK GAIN 10.2×10^{-4} VOLT/DEG/SEC
REDUCED LINKAGE INERTIA

5.0 RECOMMENDATIONS AND CONCLUSIONS

This evaluation of the B-52 aeroelastic model aileron and elevator actuation systems shows that satisfactory performance can be attained with a minimum of modifications. As a minimum, a tachometer will have to be added to provide motor rate feedback for each of the three actuation systems installed in the model. Every effort should also be made to minimize friction through ball bearings and low drag position and rate sensors.

The friction drag of the 0.5 inch diameter potentiometers coupled to the aileron hinge shafts is unknown. If this friction is excessive, a solar cell assembly could be utilized as the surface angular position sensor in the small space available in the wing trailing edge. The assembly would consist of two semi-circular cells mounted on a common base, separated by a 0.010 gap. A lamp and shield would be required to produce a semi-circular area of illumination on the cells such that equal potential is generated by the cells in the null position, with the cell assembly mounted on the end of the aileron hinge shaft. Some testing was done with a 0.160 inch diameter assembly, but inaccuracies in positioning the assembly on the shaft and locating the shield and lamp did not permit satisfactory performance. An accurate positioning method would have to be developed if this type of angular position sensor were used in the model.

The following modifications to the model actuation systems are recommended:

a. Install a low drag, dc tachometer for each actuation system, to be driven by the motor shafts through crank-pushrod assemblies, or other linkage. It is essential for system stability that motor rate be sensed for rate feedback.

b. Replace all bronze bearings with stainless steel, precision ball bearings.

c. Replace the universal joints in the aileron drive shaft with Sterling Instrument G404-56 Hi-Flex bellows couplings, and if required to increase stiffness, install a shaft support between each pair of bellows couplings, as shown in Figure 4-2.

d. Replace the fabricated rod ends in the pushrod assembly at the aileron surfaces with Southwest Products Company 2-DREM-1, or equivalent, low friction miniature rod ends.

e. Replace the dc potentiometers with induction potentiometers or a solar cell assembly. A standard Size 8 induction potentiometer could be used in all locations except the wing trailing edge. The dc potentiometers already installed in this location should be used unless their friction drag is excessive. Demodulators would be required for the induction potentiometers, but these would be external to the model.

f. Redesign the elevator crank-pushrod linkage to reduce its inertia reflected back to the motor shaft.

Other modifications may be required to make the modifications listed above compatible with the remaining parts of the actuation systems. All bearings and the elevator hinges should be lubricated properly to reduce friction to the maximum extent possible. Precision fit pins should be used at all crank-rod end connections to minimize mechanical deadzone.

6.0 REFERENCES

1. Boeing Coordination Sheet 3-7560-70-53, "Performance Criteria for B-52 Aeroelastic Model Aileron and Elevator Control Systems", G. E. Hodges to G. E. Bergmann, 24 July 1970.

2. Boeing Coordination Sheet 3-7560-70-48, "B-52 Aeroelastic Model Controls Mechanization", F. D. Sevart to G. E. Bergmann, 20 July 1970.

APPENDIX A

SUMMARY OF MODIFICATIONS OF THE B-52 AEROELASTIC MODEL AILERON AND ELEVATOR ACTUATION SYSTEMS AND THE RESULTANT PERFORMANCE

This appendix contains an informal report prepared after the aileron and elevator actuation systems were modified and tested in the model. The primary purpose of this report was to provide NASA personnel with a detailed set-up, checkout, and operation procedure for the model control surface actuation systems.

▼ 1.0 INTRODUCTION ▼

This appendix summarizes the modifications of the B-52 aeroelastic model elevator and aileron actuation systems and the resultant performance. Included in this appendix is a detailed wiring diagram of the analog computer circuits used and of the wiring from the computer and the 28 vdc power supply to the actuation systems. A detailed set-up and checkout procedure is also presented.

2.0 ELEVATOR ACTUATION SYSTEM

The elevator system was modified and tested before the aileron system since the parts required were readily available.

2.1 MODIFICATIONS

The modifications performed on the elevator actuation system were designed to reduce friction and inertia and to install a tachometer providing motor rate for feedback compensation of the motor.

The tachometer was installed aft and below the motor. The tachometer is driven directly by the motor through a crank-pushrod assembly. The pushrod utilizes two Southwest Products Company 2-DREM-1 miniature, low friction rod ends and a 3/16 inch diameter aluminum rod. The torque motor stop arm was extended and a clevis formed to mate with the rod end.

The two cranks and the idler arm in the elevator drive linkage were shortened to provide a crank radius of 0.50 inch. The drive gear was also modified to reduce it's inertia by leaving only a 90 degree segment of the gear teeth to drive the potentiometer. The pushrod rod end is bolted directly to the gear. The two pushrods were replaced with rods fabricated of 0.25 inch outside diameter tubing. The idler arm was also redesigned and fabricated to reduce weight. The bronze bushing which was used at the idler arm support shaft was replaced with two stainless steel precision ball bearings.

The model structure designed for mounting a vertical fin below the fuselage was trimmed to provide clearance for the aft pushrod. This was necessary due to the shorter cranks. More should be trimmed to allow operation of the elevator throughout the allowable horizontal stabilizer travel.

2.2 SYSTEM SET-UP AND CHECKOUT

Figure 1 shows a functional block diagram of the complete elevator actuation system and the equipment required for its operation and check out. Note that the horizontal stabilizer potentiometer is not shown in this figure. The analog computer patching diagram, Figure 2, shows the details of the wiring for all three potentiometers, as well as the analog computer circuits.

The d.c. power amplifier is mounted on a chassis for convenience. A terminal block is provided on the front of the chassis and the common ground and the output voltages are available at jack receptacles on top. The ground of the 28 vdc power supply connects to terminal #3 and +28 volts to terminal #8. The chassis contains an on-off switch and a 6 amp fuse for the 28 volt power. The power amplifier receives the voltage input, V_E, on terminal #4. The white motor leads connect to terminal #2, V_{13}; and the green leads to terminal #1, V_9. The power amplifier is such that when V_E is positive, the output voltage $V_{13}-V_9$ is positive. With the motor leads connected as described above, positive voltage V_E produces motor rotation in a positive direction (defined herein as elevator trailing edge up). Reversing the motor connections would produce the opposite direction of rotation for a given voltage polarity V_E. The gain of the power amplifier has been reduced to 10 volt/volt by changing the pre-amplifier feedback resistor to 24.9 KΩ. The power amplifiers with Serial Numbers 68F0147 and 68F0150 have this change already made.

Before the elevator and tach linkages are connected to the torque motor, the electrical zero of the motor must be determined so that the linkage can be connected such that the motor operates in its linear region (± 20 degrees about zero). The factory (Aeroflex) recommended method of determining the zero is to feed a small dc voltage (about 0.100 volt) directly to the motor terminals. The nominal motor resistance is only 5 ohm. This small voltage will cause the motor to rotate to a point of zero sensitivity, which for the 4-pole motor would be ± 45 degrees from zero, depending on the polarity of voltage used. Note that the voltage should not be passed through the power amplifier, to give the most accurate results. Rotation of the motor shaft 45 degrees in either direction should align the zero within one or two degrees, depending on the residual magnetism of the motor.

The elevator motor installed in the model has the motor zero marked on the shaft and stop bracket using a prick punch. This zero was established using the power amplifier and should be within ± 3 degrees of true electrical zero.

Once the electrical zero of the torque motor has been determined, the linkage can be connected to the motor. This has been done with the horizontal stabilizer in its zero position. The model has limit switches on the stabilizer at 10 ± 1 degree trailing edge down and 5 ± 1 degree trailing edge up. The zero position was determined by running the stabilizer trailing edge down until the limit switch engaged, then, back off 10 degrees as measured by the potentiometer geared to the stabilizer shaft. This appears close by visual inspection. In the zero position, the stabilizer chord plane should be parallel to the fuselage waterline planes.

The elevator drive linkage is nonlinear and the best way to adjust and set it is unknown. An analysis of the linkage kinematics to determine optimum pushrod lengths and positions of the cranks and idler arm at zero surface (and motor) position is strongly recommended. The performance index could be the difference between ideal (linear) case normally used for pushrod linkages and the actual relationship. This difference could be minimized using, for example, maxima-minima theory from the calculus. The primary objective is to set the linkage so that, as close as possible, one degree motor rotation produces one degree surface rotation (relative to the horizontal stabilizer) for the envelope of horizontal stabilizer positions.

With the linkage adjusted the way it is now, one degree motor rotation produces 1.03 (approximately) surface rotation relative to the horizontal stabilizer at the zero stabilizer position. This ratio changes with changing stabilizer position, though this was not pursued sufficiently to establish trends.

The power amplifiers will normally have a small dc offset. There are no provisions in the amplifiers themselves to null the amplifier output voltage. This can be done easily on the analog computer, using a bias voltage on V_E to cancel the power amplifier offset. With the offset not cancelled, the motor will operate about a point other than zero depending on the sign and magnitude of the power amplifier offset. The power amplifier voltage zero should correspond to the motor electrical zero as determined above, and the motor potentiometer zero should correspond to both zeros.

The strip chart recorder provides a convenient way to monitor the system behavior. The Boonshaft transfer function analyzer provides the sine wave input and measures amplitude and phase of voltage signal, patched to the left hand terminals. The triangular wave function generator provides the input for measuring hysteresis. The hysteresis is measured by plotting θ_S vertically and θ_{M_C} horizontally on the x-y plotter, using a 0.10 Hz triangular wave input. The oscillioscope is used in trouble shooting, for example, in monitoring the power amplifier output.

The analog computer (EAI 580) patching diagram and the wiring to and from the model potentiometers are shown in Figure 2. This diagram shows the wiring for the elevator system, with the changes required for the aileron system noted on the diagram. Note that no integrators are used in the circuit, hence the analog computer can be left in the IC mode, with no need to go to the operate (op) mode. No attempt has been made to minimize the number of analog amplifiers or potentiometers.

Amplifiers 78 and 79 are used to form ± 1.0 volt required for the potentiometers installed in the model. One volt was chosen since analog computer reference voltage was to be used and the amplifiers are current limited at approximately 2.5 ma. The New England Instrument Company and Waters potentiometers have only 1000 ± 10% resistive elements. The 2.5 ma current limit is at 10v out of the amplifier. The limit is higher at lower voltage. Satisfactory performance was attained with three potentiometers patched from these two amplifiers. Three potentiometers in parallel would require 6 ma total current through the resistive elements.

The power amplifier voltage, $V_{13}-V_9$, is formed as the output of amplifier 08. A scale factor of .5 volt analog/volt output is used since the maximum power amplifier voltage is around 20 volts and the saturation voltage on the computer is about 11.5 volts, depending on the amplifier loading.

The motor angular position is formed as the output of amplifier 29 and the surface position is formed as the output of amplifier 51. Both of these potentiometers are geared 2 to 1 to the shafts whose positions they measure. The NEI 78ESB102 potentiometers are designed for 340 ± 5 degrees of travel. Thus, with + 1.0 to one terminal and - 1.0 volt to the other, the potentiometer equation is

$$V_p = \frac{[+1.0 - (-1.0)]\text{ volt}}{340\text{ deg}} * \theta_p\text{ (deg)}, \quad \text{but } \theta_p = 2\theta_M \text{, or } \theta_p = 2\theta_S .$$

The scaling of the motor position equation then is

$$V_{P_M} = \frac{2\text{ volt}}{340\text{ deg}} * (2\theta_M)\text{ (deg)}$$

$$\theta_M\text{ (deg)} = \frac{340\text{ deg}}{4\text{ volt}} * V_{P_M}\text{ (volt)} .$$

Since the maximum excursion for the motor rotation is 20 degrees, a scale factor of .5 volt-analog/degree is used. Then,

$$[.5\theta_M] = .5\left(\frac{340}{4}\right)[1.0\, V_{P_M}] .$$

Finally, $[.5\theta_M] = .4250(10)(10)[1.0\, V_{P_M}]$.

And, $[.5\theta_S] = .4250(10)(10)[1.0\, V_{P_S}]$.

The dc potentiometers must be wired to 1-gains on the dual amplifiers to eliminate loading, which will give lower values of voltage than they should be. The 1-gains on the dual amplifiers are 100 KΩ whereas the 10-gains on the dual amplifiers and the 1-gains on the quad amplifiers are only 10 KΩ. The lower input resistors will give about 3% lower output voltages (taking into account the feedback resistors) than when the potentiometer outputs are patched to 100 KΩ input resistors.

The horizontal stabilizer potentiometer is geared 2.5 to 1 to the stabilizer shaft. Thus, $\theta_{POT} = 2.5\, \theta_{H.S.}$, and the scaling becomes

$$V_{P_{H.S.}} = \frac{2\text{ volt}}{340\text{ deg}} * 2.5\, \theta_{H.S.}\text{ (deg)} .$$

Or,

$$\theta_{H.S.} = \frac{340}{5} * V_{P_{H.S.}} .$$

And, keeping consistent scale factors,

$$[.5\theta_{H.S.}] = .5\left(\frac{340}{5}\right)[1.0\, V_{P_{H.S.}}] ,$$

Which produces

$$[.5\theta_{H.S.}] = .3400(10)(10)[1.0\, V_{P_{H.S.}}] .$$

This voltage is formed as the output of amplifier 38. Note that when this amplifier reads + 5 volts, we have

$$\left[.5 \frac{\text{volt-analog}}{\text{deg}} (\theta_{H.S.} \text{ deg})\right] = +5 \text{ volt-analog}$$

and the stabilizer position is (with the trailing edge up positive)

$$\theta_{H.S.} (\text{deg}) = \frac{+5 \text{ volt-analog}}{.5 \text{ volt-analog/deg}}$$

or simply,

$$\theta_{H.S.} = +10 \text{ degrees} .$$

The remaining wiring on the analog computer is the formation of the error voltage of classical servomechanism theory. By referring to the simplified block diagram shown in Figure 3, we can obtain the equation for the error voltage as

$$V_E = V_C - K_1 \theta_M - K_2 \dot{\theta}_M$$

where V_c is the voltage command to the servo system and may be a step, a sine wave, or a triangular wave depending upon the desired function. With the elevator actuation system, we have the additional complication of commanding elevator position relative to the moveable horizontal stabilizer, while only the motor can be controlled directly. One method of circumventing this difficulty is to bias the motor one way or the motor such that the elevator is (ideally) moving symmetrically with respect to the horizontal stabilizer.

The relative motion equation relating the motor, elevator, and horizontal stabilizer angular positions is, from elementary kinematic theory,

$$\theta_M = \theta_{H.S.} + \theta_{ELEVATOR/H.S.} = \theta_{ELEVATOR} \text{ (ABSOLUTE)} .$$

This equation assumes ideal, linear linkage characteristics and is only an approximation for this system. This may be rewritten with $\theta \text{elevator}/_{h.s.} = \theta s$:

$$\theta_M = \theta_{H.S.} + \theta_S .$$

Thus, if we think in terms of angular motor and surface commands, this equation becomes

$$\theta_{M_C} = \theta_{H.S.} + \theta_{S_C} .$$

Assuming we can command up to 20 degrees angular rotation, we will apply the scale factor 0.5 volt-analog/deg as before.

$$[.5\, \theta_{M_C}] = [.5\, \theta_{S_C}] + [.5\, \theta_{H.S.}] .$$

But, θ_{S_C} must be formed. The step command is formed by patching -1.0 volt to the top terminal of Functional Relay 01 (left hand switch), and +1.0 to the bottom terminal of the same switch. The amplitude of the sine wave is set on the Boonshaft at 1.00 sin wt and formed as the output of amplifier 09. The attenuator P05 provides a bias voltage to offset any bias on the sine wave from the Boonshaft. The motor command is formed as the output of amplifier 31. The equation programmed is

$$[.5\,\theta_{M_c}] = \frac{.5\theta_{SC}}{10} * 10 + [.5\,\theta_{H.S.}].$$

Thus, for the step command

$$[.5\theta_{M_c}] = (.05\theta_{S_C}) * 1.0 * 10 + [.5\theta_{H.S.}].$$

For example, a + 3 degree command would be formed by setting attenuator P31 at (.05 * 3 = .1500) and admitted to the system by setting Function Relay 01 to bottom terminal, F.R. 02 to top terminal and F.R. 03 to top terminal. Functional Relay 03 also admits the horizontal stabilizer position since it is set on the right hand switch. The amplitude of the sine wave is formed in the same manner, and is admitted with F.R. 02 set to bottom terminal, and F.R. 03 set also to bottom terminal.

The torque motor voltage command is merely the position feedback gain, K_1, times the motor angular position command, θ_{M_c}. Thus, the error voltage equation becomes

$$V_E = K_1\theta_{M_C} - K_1\theta_M - K_2\dot{\theta}_M.$$

Note that the voltage command is not formed explicitly as the output of an amplifier. The error voltage equation cannot be scaled, nor does it require scaling. A unity scale factor (1.0 volt-analog/volt) is used. Thus,

$$[1.0V_E] = \frac{(1.0)K_1}{.5}[.5\theta_{M_c}] - \frac{(1.0)K_1}{.5}[.5\theta_M] - \frac{(1.0)K_2}{.002}[.002\dot{\theta}_M].$$

Or simply,

$$[1.0V_E] = 2K_1[.5\theta_{M_c}] - 2K_1[.5\theta_M] - 500K_2[.002\dot{\theta}_M].$$

It might be well to take into account the sign change across each amplifier.

$$+[1.0V_E] = -1\left\{(2K_1)\{-[.5\theta_{M_c}]\} + (2K_1)\{+[.5\theta_M]\} + (500K_2)\{+[.002\dot{\theta}_M]\}\right\},$$

or, Output = -1 Times the inputs.

The motor rate scaling has been omitted, so it will be inserted at this point. The tachometer gradient is 0.18 volt/rad/sec as specified in manufacturer's data. Thus, the tachometer voltage generated is

$$V_T = 0.18\,\frac{\text{volt}}{\text{rad/sec}} * \dot{\theta}_M\,(\text{rad/sec}) = \frac{0.18}{57.3}\,\frac{\text{volt}}{\text{deg/sec}} * \dot{\theta}_M\,(\text{deg/sec}).$$

Then,

$$\dot{\theta}_M = \frac{57.3}{0.18} * V_T .$$

The maximum expected motor angular rate is 5000 deg/sec, and a scale factor of .002 volt-analog/deg/sec will keep the analog voltage no higher than 10 volts as long as this rate is not exceeded.

Then,

$$[.002\,\dot{\theta}_M] = .002\left(\frac{57.3}{0.18}\right)[1.0 V_T] .$$

Or,

$$[.002\,\dot{\theta}_M] = .6367\,[1.0 V_T] .$$

Note that the tachometer output must also be patched to a 100 KΩ input resistor to eliminate loading effects.

The position and rate feedback loops are closed around the motor by setting Function Relay 00 to the top terminal position. The relay contacts close simultaneously. If any other method is used, the rate feedback loop must be closed first since the system is unstable without rate feedback at the operating position feedback gain. Note also that there should be an odd number of amplifiers in both the rate and position feedback loops from the tachometer and potentiometer to the error voltage, V_E. This is true provided the motor is wired to the power amplifier such that positive voltage V_E gives a positive voltage on the motor potentiometer. The sign convention used for all surfaces, elevator, horizontal stabilizer, and aileron, is that trailing edge up is positive. The motor and potentiometer voltages should be wired to conform with this sign convention.

Attenuators P07 and P37 are patched in series into amplifier 39. This makes possible fine adjustment of the bias voltage required to cancel the power amplifier dc offset. Care should be taken to insure that the motor potentiometer reads zero when the motor shaft is aligned with its zero (and the tachometer aligned with its zero) and the power amplifier output voltage is zero before the position (and rate) feedback loops are closed. Otherwise, the motor will seek a new "zero" position to operate about. If the offset is excessive (4 or 5 degrees) the motor output can be distorted, due to operating out of the linear region of the motor. The amount of offset which can be tolerated is dependent on the oscillations demanded. The best way of eliminating this problem is to set the motor stops at ± 20 degrees from zero and leave them there.

Note that the inputs of amplifier 58 are "borrowed" by amplifier 39. The patching of an external feedback resistor for amplifier 58 is shown on the analog diagram.

During operation of the control systems, the motor will heat after a short period of time when at high frequency and amplitude. The motor will draw about 4 amps at its maximum torque, and the motor resistance decreases with increasing temperature. This lowers the motor sensitivity. This problem should not be encountered below 30 cps and motor amplitude of around 6 degrees.

When running a frequency response, it is best to switch out the sine wave while data is recorded and frequency is being changed. This also decreases wear on the system, and thus prolongs life of the components.

When closing the feedback loops for the first time after set up, it is best to start with the rate loop only, set at low gain, say, 1.0×10^{-4} volt/deg/sec. By oscillating the control system by hand, the action of the rate feedback should be felt opposing the motion. If it is helping, the feedback is positive and the system is unstable. After the rate feedback loop has been checked, keep it closed and repeat the procedure with the position loop. Start with a position feedback gain of about .05 volt/deg. As a further check on stability, increment both gains gradually up to the operating gains. If an instability should occur, immediately place the analog computer in the "Set Pot" (SP) mode, and check all wiring. If the gains are very high when the instability occurs, it will be obvious immediately when the feedback loops are closed.

One final comment. The torque motor does not produce much torque open loop and with friction in the system, it is about impossible to determine if the power amplifier and torque motor are behaving properly. Characteristically, the amplifier output and hence the motor angular motion will be somewhat distorted.

2.3 PERFORMANCE ATTAINED

Rate and position feedback gains were determined which permitted the elevator actuation system to meet the frequency response criteria of less than 3 db amplitude attentuation and 45 degrees phase lag at 25 Hz, for a 3 degree sinusoidal input command. The frequency response as measured is plotted in Figure 4. The plot was not normalized since the system is nonlinear. For reference, 3 degrees amplitude is 9.54 db. The equivalent linear second order damping ratio of the resonant peak is 0.252. No attempt was made to iterate on the feedback gains to satisfy the .30 damping ratio requirement, due to the excessive hysteresis present in the system.

The hysteresis is shown graphically in the plot of Figure 5. This plot of elevator displacement vs. motor angular displacement command shows a hysteresis width of approximately ± 0.51 degree. Note that for this plot no attempt was made to assure the motor commanded angle was symmetric. It is difficult to locate the origin of the coordinates exactly with the hysteresis width as wide as this. The hysteresis greatly exceeds the desired width of ± 0.20 degrees as measured at the elevator shaft.

The hysteresis is attributable to three things: residual magnetism of the motor; coulomb friction at shaft and elevator hinge supports and the two dc potentiometers; and physical mismatch (slop) in the linkage itself. The residual magnetism appears to be low. The hysteresis attributable to physical mismatch in the linkage measures about ± .16 degrees. Most of the remaining hysteresis is due to coulomb (dry) friction. This indicates a friction torque of 2 to 2.5 ounce-inches.

The total inertia of the linkage and the elevators appears to be slightly over .0035 in-oz-sec^2. Better performance could be attained with this lowered to even .0030 in-oz-sec^2. The largest improvement in performance would be brought about by the reduction of the coulomb friction to below 1.0 oz-in and elimination of the physical mismatch in the linkage.

2.4 RECOMMENDATIONS OF METHODS TO IMPROVE PERFORMANCE

If improved performance is desired, the following modifications should be helpful:

1. Fabricate thin oil-less bronze bushings to install in the inboard elevator hinge on both sides. Anything that can be done to reduce the friction coefficient here would be beneficial. The bending of the bellows couplings creates a sizable normal force in the hinge. No known ball bearings will fit in the space permitted in the hinge. Replacing the two G404-57 bellows couplings with G404-56 couplings will reduce the bearing normal force, and the friction, by 50%. These couplings are .12 inch longer and other modifications may be necessary to permit their installation.

2. Replace the four Heim HM-2C rod ends used in the pushrod linkage with rod ends manufactured to closer tolerance. With the crank radius at only 0.5 inch, any play in the rod ends significantly increases the hysteresis. A right hand thread rod end should be used on one end of each pushrod and one with left hand threads on the other. This would make pushrod length adjustments much easier.

3. As a last resort, in the interest of minimizing friction, the two New England Instrument Company 78ESB102 potentiometers could be replaced by low drag linear transformers (induction potentiometers) of an appropriate size and characteristics.

3.0 AILERON ACTUATION SYSTEM

The modifications performed on the aileron actuation system were aimed primarily at reducing coulomb friction in the torque transmission linkage, and to install a dc tachometer to provide the means for rate feedback compensation of the torque motor. The testing conducted on this system is the same as was conducted on the elevator system.

3.1 MODIFICATIONS

The Aeroflex TF10Y-5H d.c. tachometer was installed aft of the torque motor installation, on the same mounting frame. The aileron drive system is removable in one piece by separating the shafts on either side at the bellows couplings and removing two bolts that tie the assembly to the model fuselage structure. The tachometer is driven through a crank-pushrod assembly that utilizes Southwest Products Company 2-DREM-1 miniature, low friction end rods. The crank at the tachometer was fabricated with a 0.70 inch crank radius, instead of 0.75 inch as required. This will be taken into account in scaling the tachometer equation. The other end of the pushrod connects to the motor drive pushrod at the drive gear through the use of a compound bolt machined to mate with the Heim HM-2C rod end and threaded to bolt the drive pushrod to the drive gear. The other end is machined to mate with the 2-DREM-1 rod end and threaded for a #2-56 nut. A 3/16 diameter aluminum rod is utilized also in the pushrod. Only the right hand tachometer has been mounted, though everything required for installation of the left hand tachometer has been fabricated. The mounting arrangement is the same as the tachometer on the right hand side.

All bronze bushings used in the aileron system have been replaced on the right hand aileron with stainless steel precision ball bearings. Before this was done, the friction torque was high, an estimated 10 in-oz. The fabricated rod ends in the pushrod assembly at the aileron surface have been replaced with the 2-DREM-1 rod ends, also in the interest of reducing friction. This made necessary a new pushrod about 1/10 of an inch longer than before, and aluminum was used rather than steel. The friction of the entire aileron system is down to an estimated 1.0 in-oz, or less.

There was a mismatch of about 0.10 inch vertically between the aileron shaft in the wing and the shaft in the drive assembly. This problem was eliminated by inverting the inboard wing shaft support and placing a washer between it and the wing elastic member. The wing panels were checked and no interference was detected. This permitted better alignment of the two shafts in the vertical plane. Two Sterling Instrument Company G404-56 bellows couplings are used between the shaft in the wing and the shaft in the drive assembly to make the 30 degree change of direction. The two couplings are joined by a short segment of shaft. The shaft in the drive assembly was replaced by a slightly longer shaft to mate with the bellows couplings.

The 3/16 inch face steel drive gears were machined down about 0.10 inch and holes drilled through the remaining material to reduce its weight and, hence, reduce its inertia. The machining was done on the side opposite the gear hub, which is the outboard side. This makes the attachment of the pushrod a little difficult. It would be better to have the machining done on the hub side of the gear, or to replace the 3/16 face gear with a gear with an 1/8 inch face.

3.2 SYSTEM SET-UP AND CHECKOUT

Most of the set-up and checkout procedures outlined in Section 2.2 apply to the aileron actuation system. There are only two potentiometers in the aileron system, while there are three in the elevator system.

As before, the first step in the set-up should be the determination of the motor zero to assure linear operation of the motor. This has been done for the R.H. aileron torque motor, again by feeding about .1000 volt to the motor terminals through the power amplifier. The zero position has been marked in orange pencil on the shaft and the motor case. However, it is felt that the marked zero is accurate to only ± 5 or 6 degrees. Before the stop arm and drive crank are pinned to the motor shaft, a more accurate determination of the motor zero should be made. For small amplitude oscillations, the zero marked is of sufficient accuracy.

The wiring from the analog computer and the 28 vdc power supply to the power amplifier is identical to the elevator system. The motor leads are patched opposite to the elevator motor leads, to conform to the sign convention of positive error voltage, V_E, producing motor rotation in a positive sense (defined herein as aileron trailing edge up is positive). The green leads should be connected to the power amplifier terminal #2 (V_{13}) and the white leads connected to terminal #1 (V_9). The wiring to the potentiometers must conform to the sign convention. This wiring is shown on the analog computer diagram, Figure 2.

After the two potentiometers have been adjusted so that their zero voltage readings coincide with the motor zero, the tachometer must be aligned to operate about its zero. It's linear range extends about ± 40 degrees from its zero. Based on experience, care should be taken to align the tachometer as close as possible. The zero is scribed on the shaft end and on the case.

The next step is to check the analog computer wiring. The motor potentiometer is gear driven 2 to 1 by the motor and the scaling for θ_M is identical to that for the elevator system. The Waters WPS ½ potentiometer is direct driven 1 to 1, and the potentiometer is constructed for 300 degrees of travel. Thus, the equation for the potentiometer voltage is

$$V_{PS} = \frac{2.0 \text{ volt}}{300 \text{ deg}} * \theta_S \text{ (deg)}$$

or,

$$\theta_S = \frac{300}{2} * V_{PS} .$$

Since the aileron is designed for ± 20 degrees of travel, a scale factor of 0.5 volts-analog/deg will be used. Then,

$$[.5\theta_S] = .5\left(\frac{300}{2}\right) * [1.0 V_{PS}]$$

$$[.5\theta_S] = .7500(10)(10)[1.0 V_{PS}] .$$

The linearity of this potentiometer is unknown, but it does not appear good. The scaling given above produces low readings at the ± 20 degree stops. The readings for smaller angles are low, by as much as 15% at ± 3 degree amplitude. The crank and pushrod at the surface have been checked and appear correct. Since this potentiometer is for instrumentation only (and not feedback) it probably has sufficient accuracy. It may be difficult obtaining meaningful data from it, though.

The tachometer crank was made with a 0.70 inch radius, rather than the required 0.75. This can be taken into account by assuming the linear relationship

$$\dot{\theta}_T = \frac{.75}{.70} \dot{\theta}_M .$$

Then, the tachometer output voltage equation is

$$V_T = \frac{0.18}{57.3} \frac{\text{volt}}{\text{deg/sec}} * \left(\frac{.75}{.70}\right) \dot{\theta}_M \text{ (deg/sec)}.$$

Then $\theta_M = \frac{57.3\ (.70)}{0.18\ (.75)} V_T$, and with the same scale factor as before,

$$[.002\dot{\theta}_M] = .5942\,[1.0 V_T].$$

This attenuator setting (and all others required) are shown on the analog computer wiring diagram.

The setting of the rate and position feedback gains, and closing of the two feedback loops is identical to that described above for the elevator system. The setting of the motor command is also the same. The comments relating to the operation of the elevator system are equally applicable to the aileron system.

3.3 PERFORMANCE ATTAINED

During the initial set-up and checkout, the Waters WPS ½ potentiometer was found to have insufficient wiper pressure, and the output was erratic and noisy. This potentiometer possessed low friction drag. It was replaced by the spare WPS ½ potentiometer which gives a clean, smooth output, but the potentiometer has 3 to 4 in-oz of friction. In addition, the potentiometer gradient appears to be a function of position.

Figure 6 shows the hysteresis for the feedback gains K_1 = .34 volt/deg and K_2 = 7.0 x 10^{-4} volt/deg/sec, as measured by the Waters potentiometer at the surface. This plot of θ_S vs. θ_{M_C} shows a hysteresis width of nearly ± 2.1 degrees. With the potentiometer output voltage so erratic it is difficult to tell how accurate the plot is. It is apparent, though, that the hysteresis is high.

Figure 7(b) shows the hysteresis for this case, but measured at the motor potentiometer. The hysteresis width at the motor measures approximately ± .43 degrees. As a comparison, Figure 7(a) shows the hysteresis at the motor shaft, with aileron shaft separated at the two G404-56 bellows couplings, to be only ± .11 degree. And, the plot of Figure 8 shows the hysteresis at the motor with the surface connected, but with the WPS ½ potentiometer replaced by an 1/8th inch diameter precision steel shaft. Since there is no perceptible slack in the linkage, this plot represents the lowest hysteresis attainable for the right hand aileron system, for these feedback gains. This plot of θ_M vs. θ_{M_C} shows approximately ± 0.18 degree hysteresis width, which would satisfy the ± 0.20 degree criteria.

The effect of the high hysteresis is apparent in the motor frequency response shown in Figure 9, for the gains listed above. The high hysteresis shows up as a loss of low frequency gain. Three degrees is 9.54 db (deg). The motor-load resonant peak occurs at approximately 34 Hz, and a shaft vertical vibration mode appears at about 37 Hz. This vibration mode is clearly audible and prolonged operation near this frequency should be avoided. This plot shows 39.7 degrees phase lag at 25 Hz, and the second order damping is about 0.25.

Figure 10 shows the frequency response of motor position for the same feedback gains, but with the Waters WPS $\frac{1}{2}$ potentiometer replaced with an 1/8 inch diameter precision steel shaft. This plot shows a damping ratio of about 0.24 and only 35.2 degrees phase lag at 25 cps. The frequency response at the surface should show only 2 or 3 degrees more lag at this frequency, provided the angular position sensor has low friction. Thus, the rate feedback gain could be increased to bring the magnitude peak down some.

A frequency response was recorded for these gains at the surface, but the accuracy of the values is questionable due to the nonlinearities of the Waters WPS $\frac{1}{2}$ potentiometer.

3.4 RECOMMENDATIONS OF METHODS TO IMPROVE PERFORMANCE

The performance of the aileron system must be improved to be usable in the wind tunnel. The primary problem with the system is the high friction in the Waters WPS $\frac{1}{2}$ potentiometer at the surface. There are two alternatives to the solution of this problem:

1. Replace the Waters WPS $\frac{1}{2}$ potentiometer with an 1/8 inch diameter stainless steel precision shaft (to form the aileron inboard hinge) and not use an angular position sensor at the surface; or

2. Replace the Waters potentiometer as above and use an angular position sensor with much lower friction drag. One possibility is a solar cell assembly, but great care must be used in its installation to locate the cell assembly with sufficient accuracy on the end of the shaft togive good linearity.

It is not felt that an angular position sensor at the aileron surface is essential for the successful operation of the actuation system. Such a sensor at the elevator shaft is desirable, though, due to the linkage nonlinearities.

FUNCTIONAL BLOCK DIAGRAM

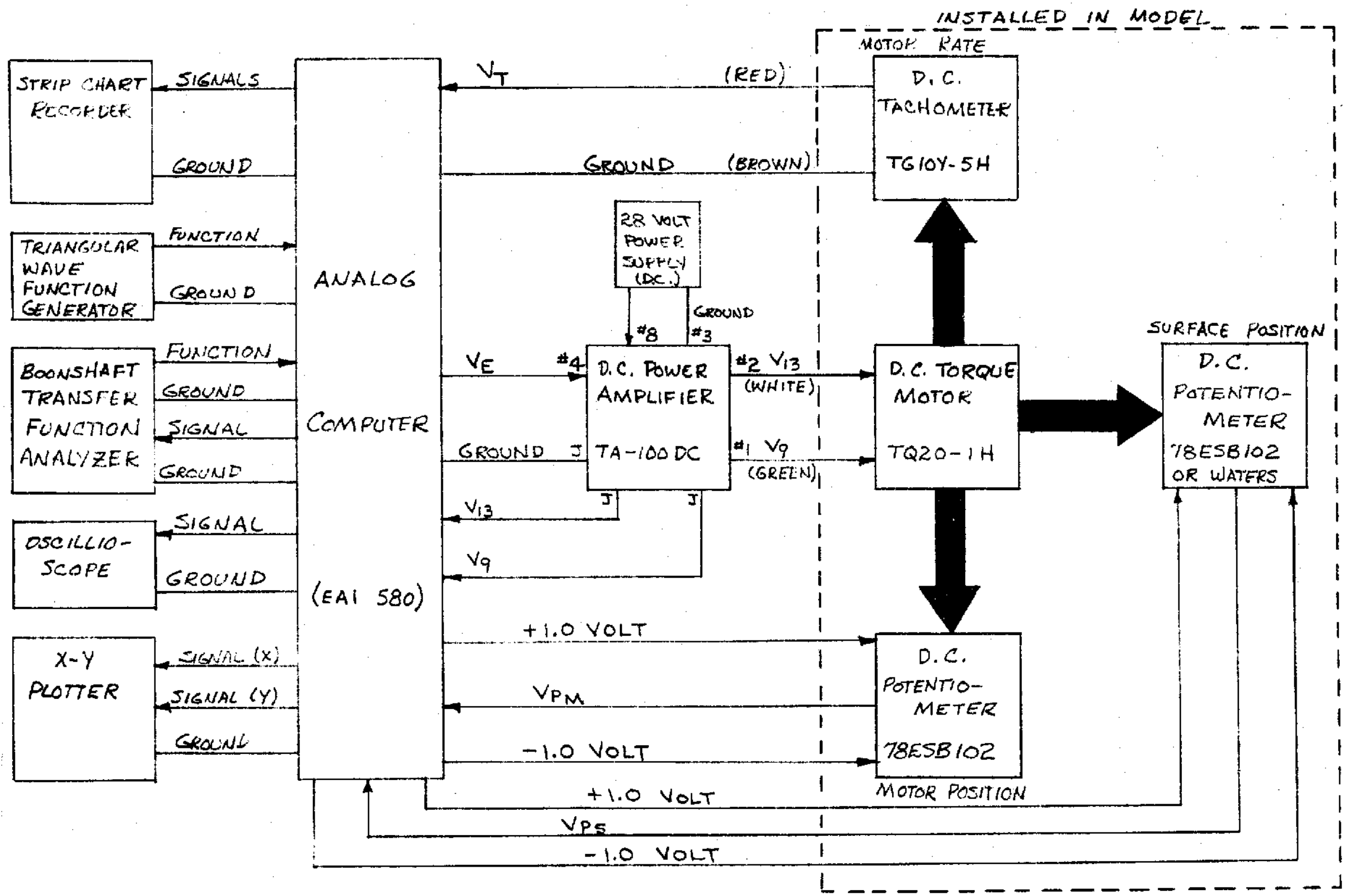

B-52 AEROELASTIC MODEL CONTROL SURFACE ACTUATION SYSTEMS TEST SET-UP

FIGURE 1

NOTE: MOTOR TERMINAL CONNECTIONS SHOWN ARE FOR ELEVATOR SYSTEM.

FIGURE 2 - ANALOG COMPUTER PATCHING DIAGRAM (SHEET 1 OF 2)

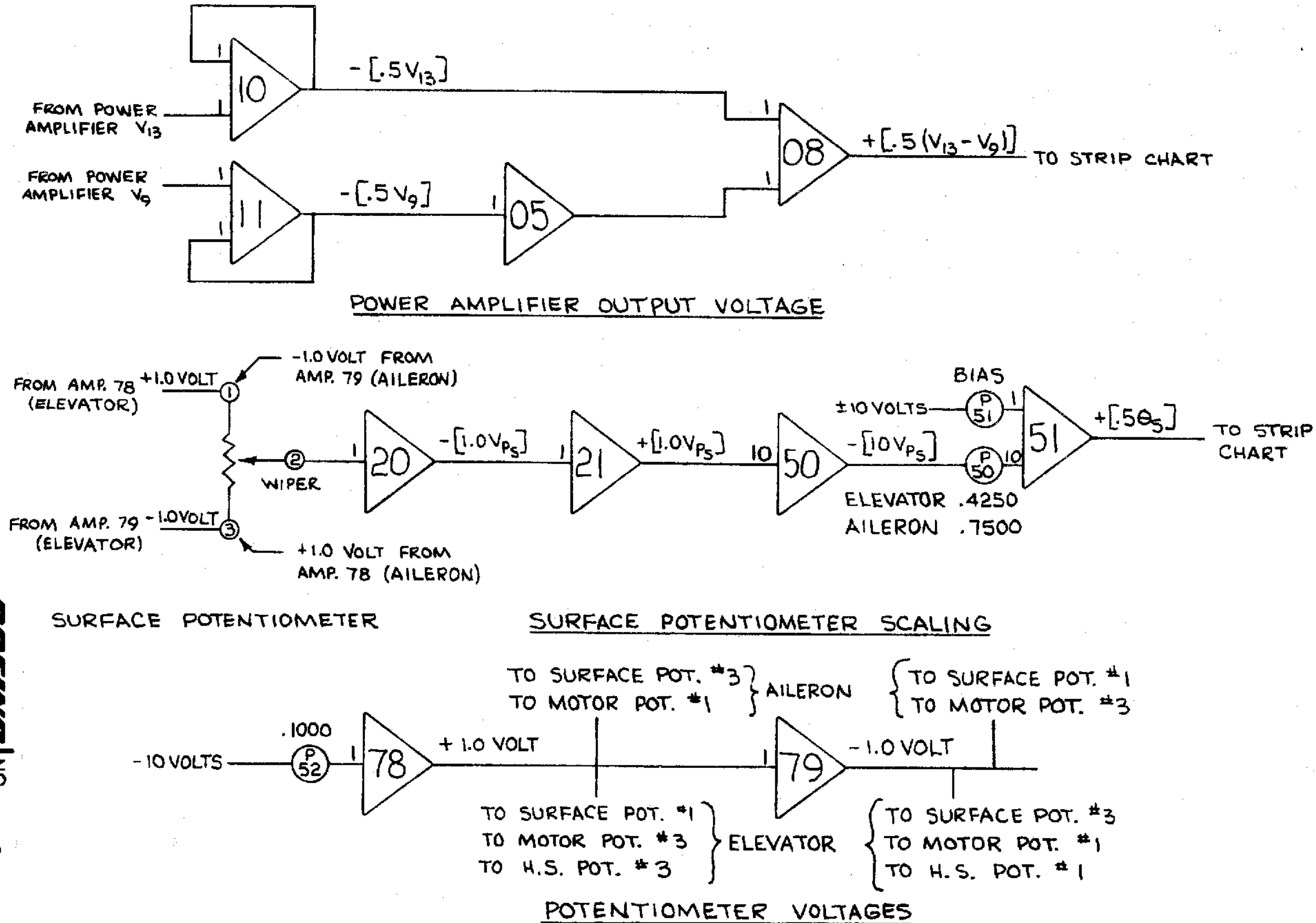

FIGURE 2 — ANALOG COMPUTER PATCHING DIAGRAM (SHEET 2 OF 2)

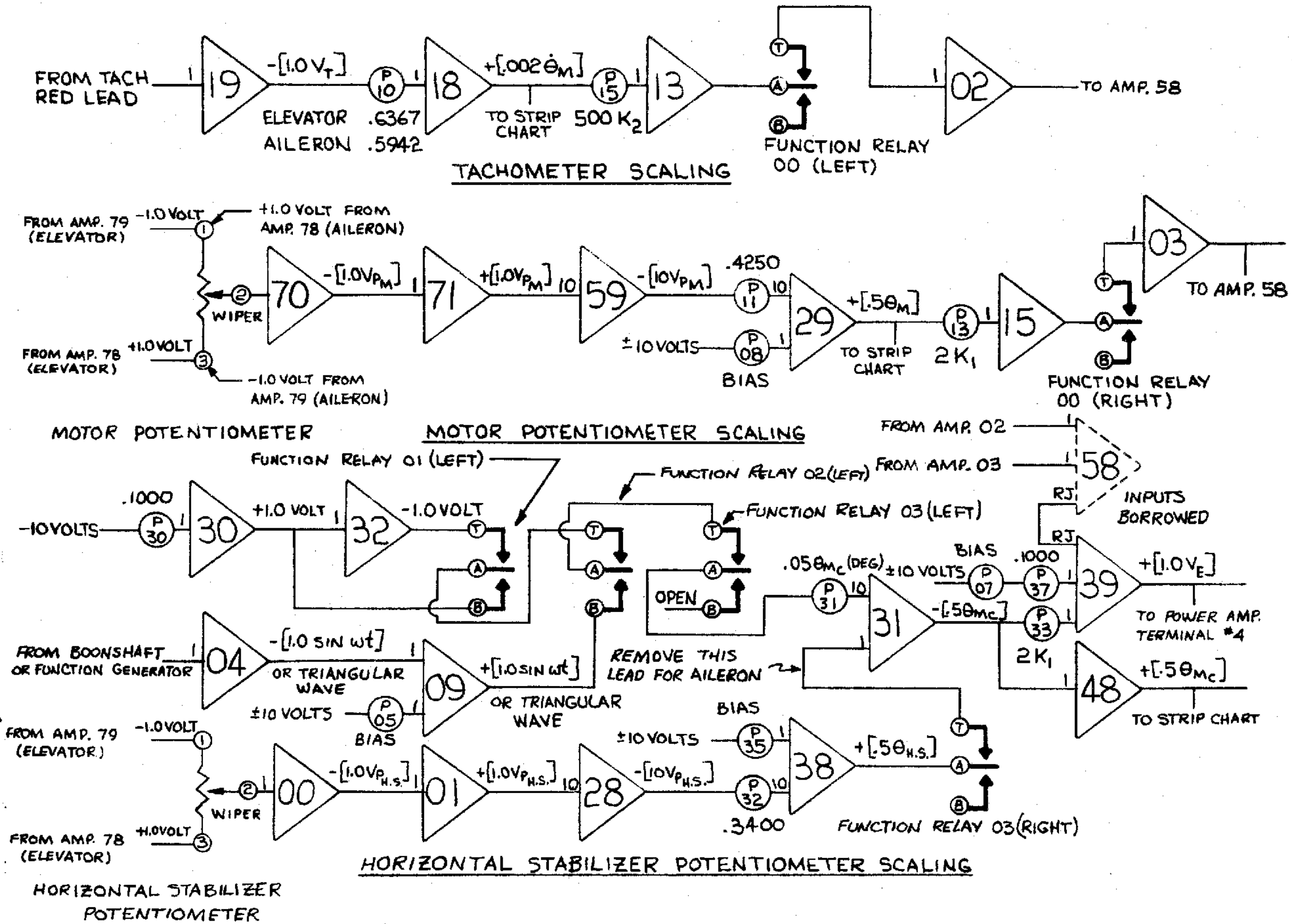

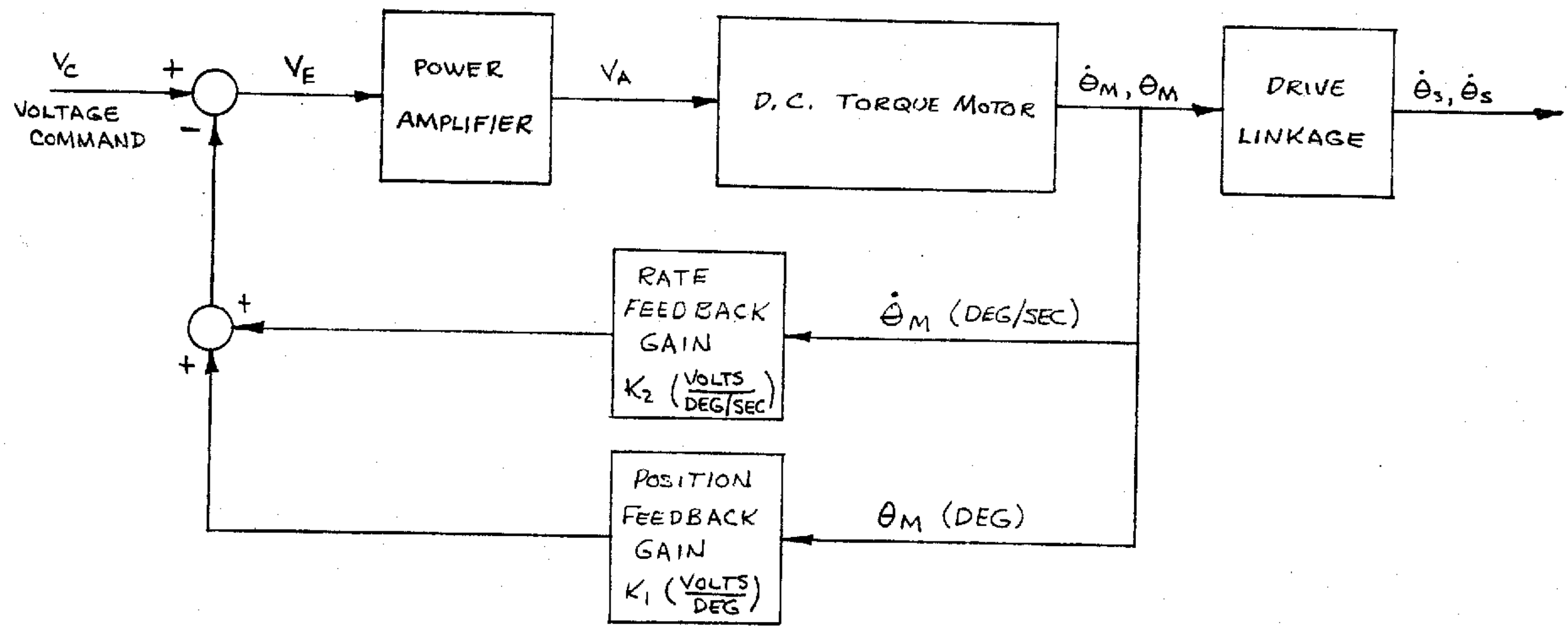

CONTROL SURFACE ACTUATION SYSTEMS

BLOCK DIAGRAM

FIGURE 3

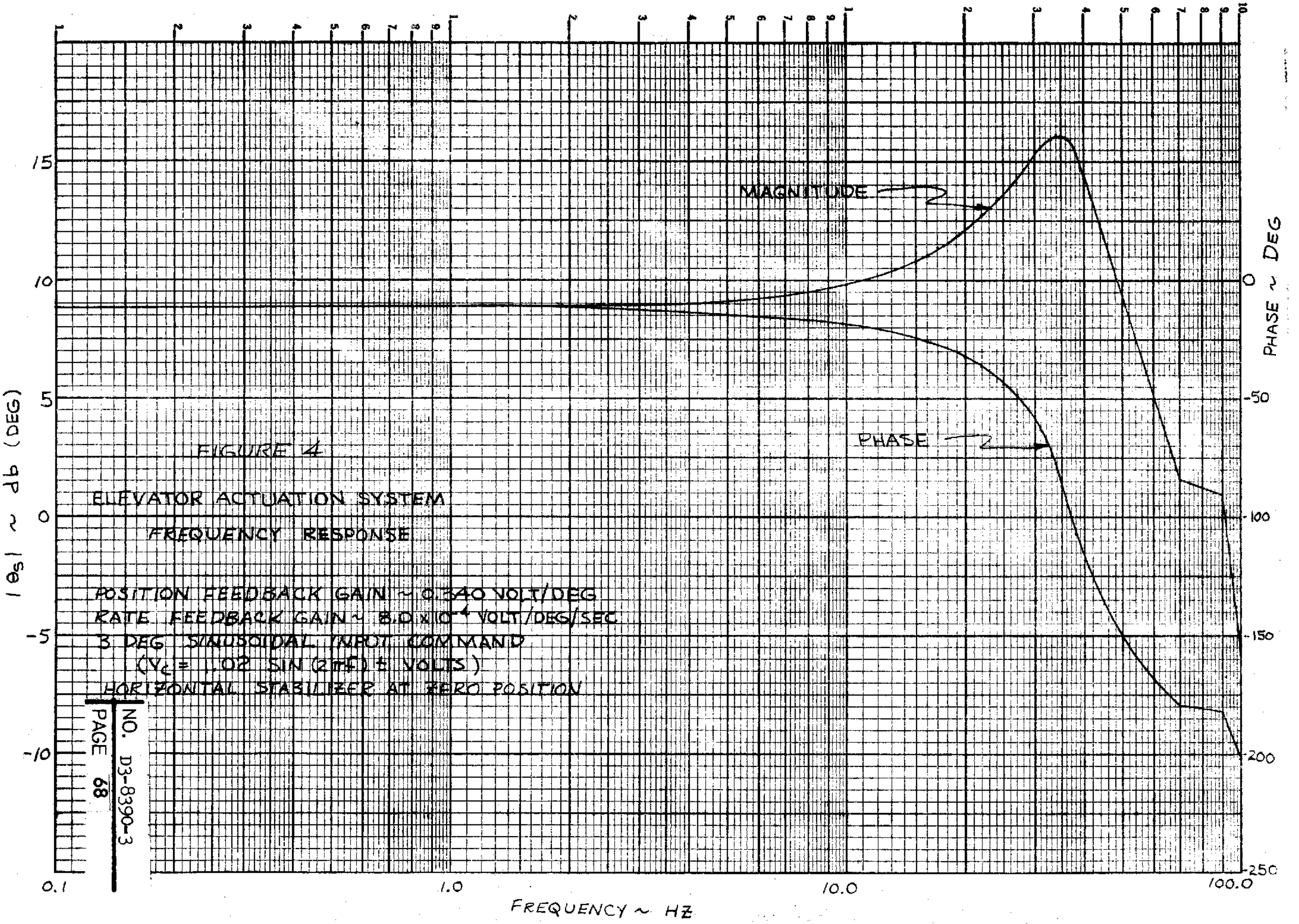
FIGURE 4
ELEVATOR ACTUATION SYSTEM
FREQUENCY RESPONSE
POSITION FEEDBACK GAIN ~ 0.340 VOLT/DEG
RATE FEEDBACK GAIN ~ 8.0 x 10^-4 VOLT/DEG/SEC
3 DEG SINUSOIDAL INPUT COMMAND
(Vc = .02 SIN (2πf) t VOLTS)
HORIZONTAL STABILIZER AT ZERO POSITION
MAGNITUDE
PHASE
|θs| ~ db (DEG)
PHASE ~ DEG
FREQUENCY ~ HZ
0.1
1.0
10.0
100.0
15
10
5
0
-5
-10
0
-50
-100
-150
-200
-250

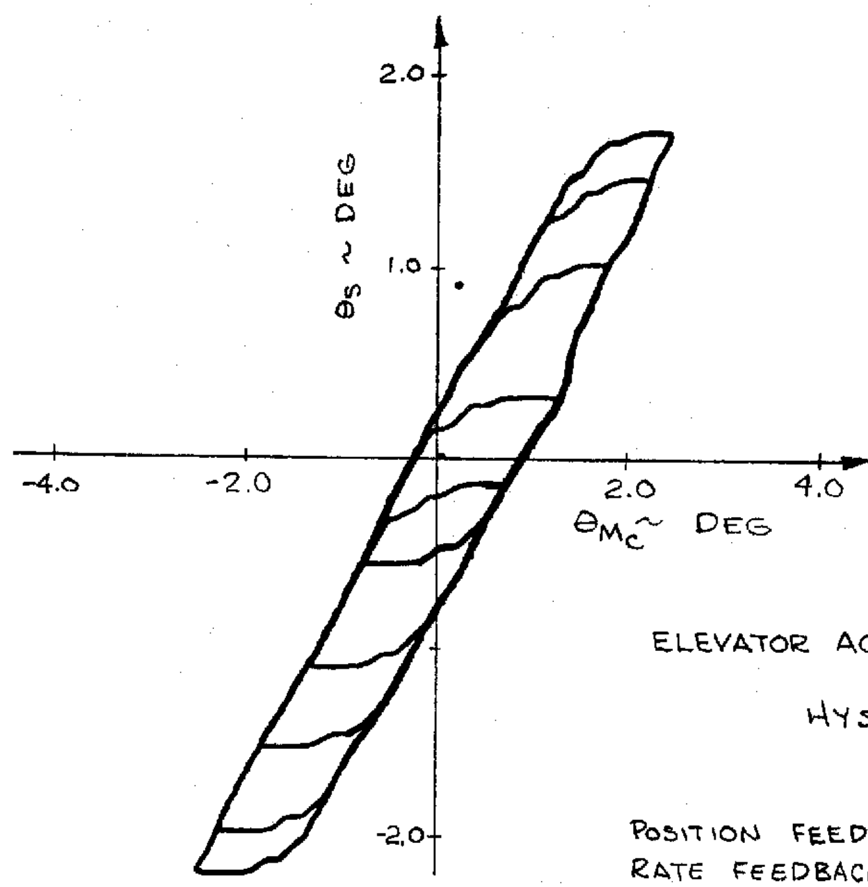

ELEVATOR ACTUATION SYSTEM

HYSTERESIS

POSITION FEEDBACK GAIN ~ 0.340 VOLT/DEG
RATE FEEDBACK GAIN ~ 8.0×10^{-4} VOLT/DEG/SEC
INPUT ~ 0.1 HZ TRIANGULAR WAVE WITH VARYING AMPLITUDE
HORIZONTAL STABILIZER AT ZERO POSITION

FIGURE 5

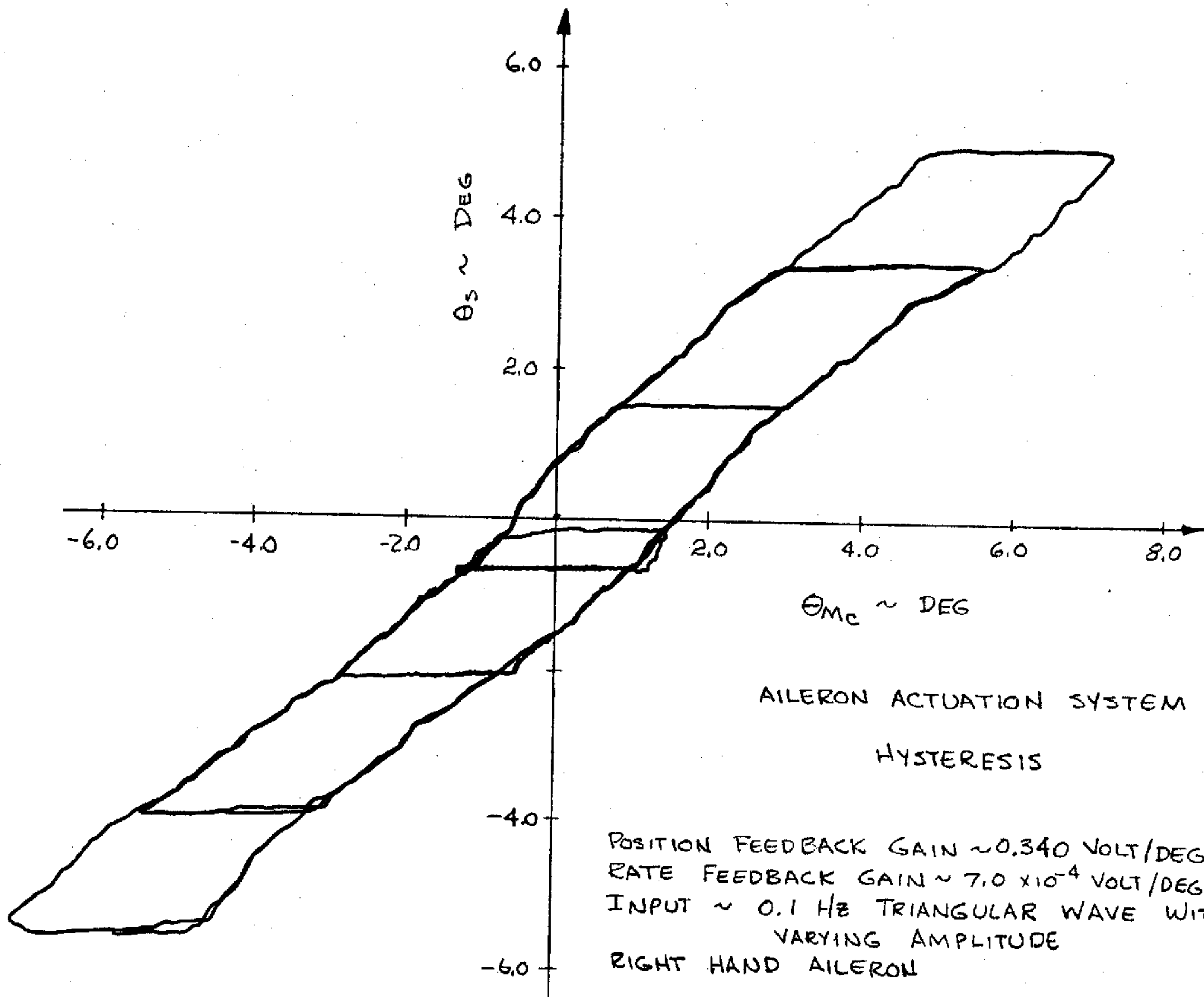

AILERON ACTUATION SYSTEM

HYSTERESIS

POSITION FEEDBACK GAIN ~0.340 VOLT/DEG
RATE FEEDBACK GAIN ~ 7.0 $\times 10^{-4}$ VOLT/DEG/SEC
INPUT ~ 0.1 Hz TRIANGULAR WAVE WITH VARYING AMPLITUDE
RIGHT HAND AILERON

FIGURE 6

AILERON ACTUATION SYSTEM HYSTERESIS

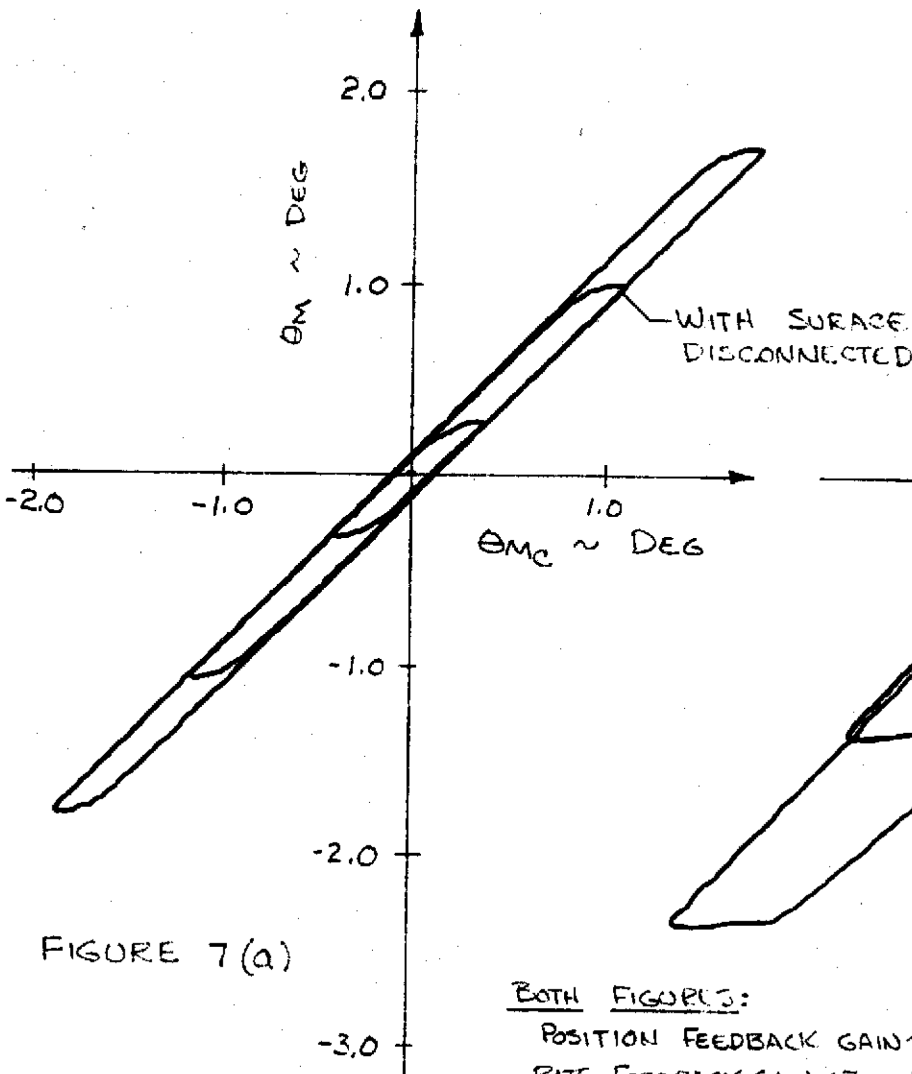

FIGURE 7(a)

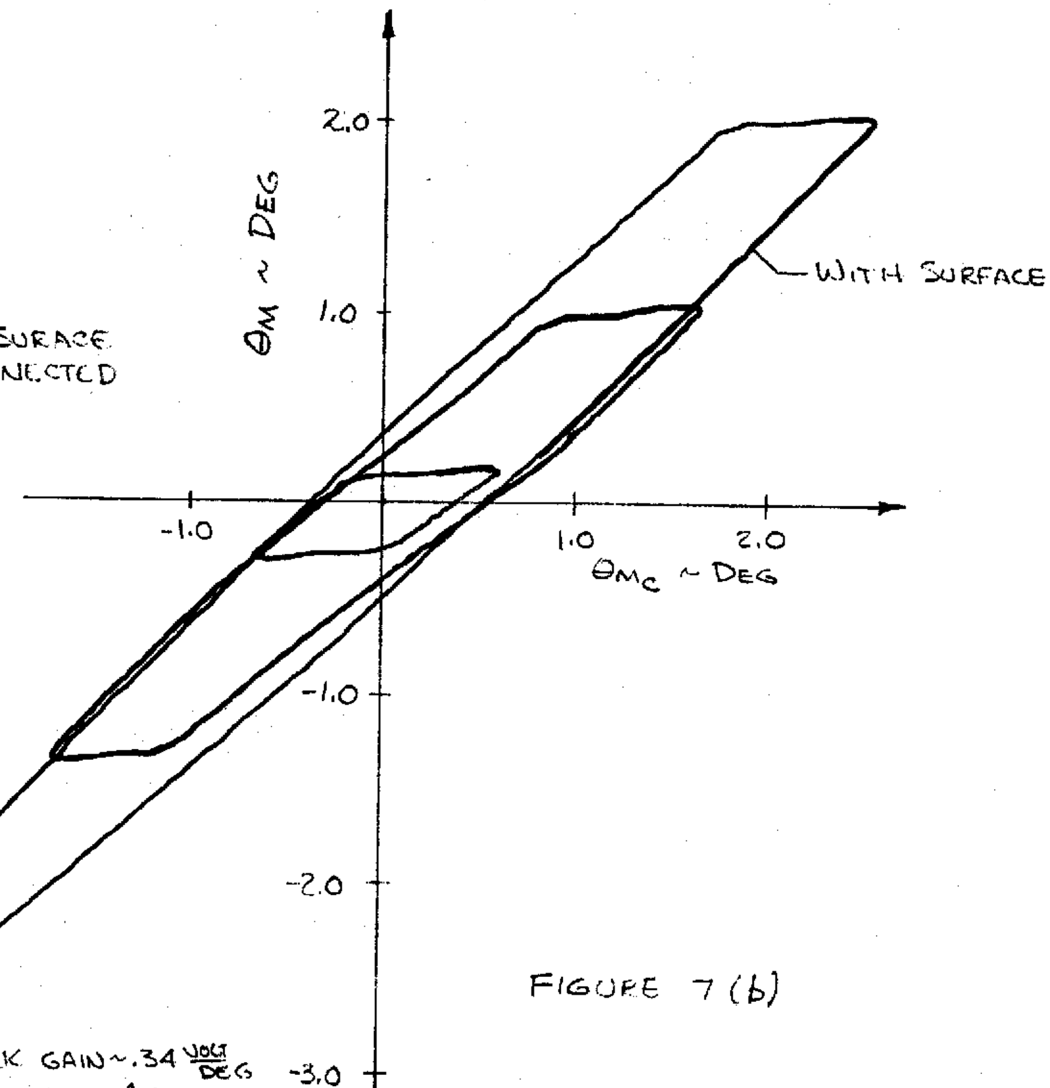

FIGURE 7(b)

<u>BOTH</u> <u>FIGURES</u>:

POSITION FEEDBACK GAIN ~ .34 VOLT/DEG
RATE FEEDBACK GAIN ~ 7.0×10^{-4} VOLT/DEG/SEC
INPUT ~ 0.1 Hz TRIANGULAR WAVE
RIGHT HAND AILERON

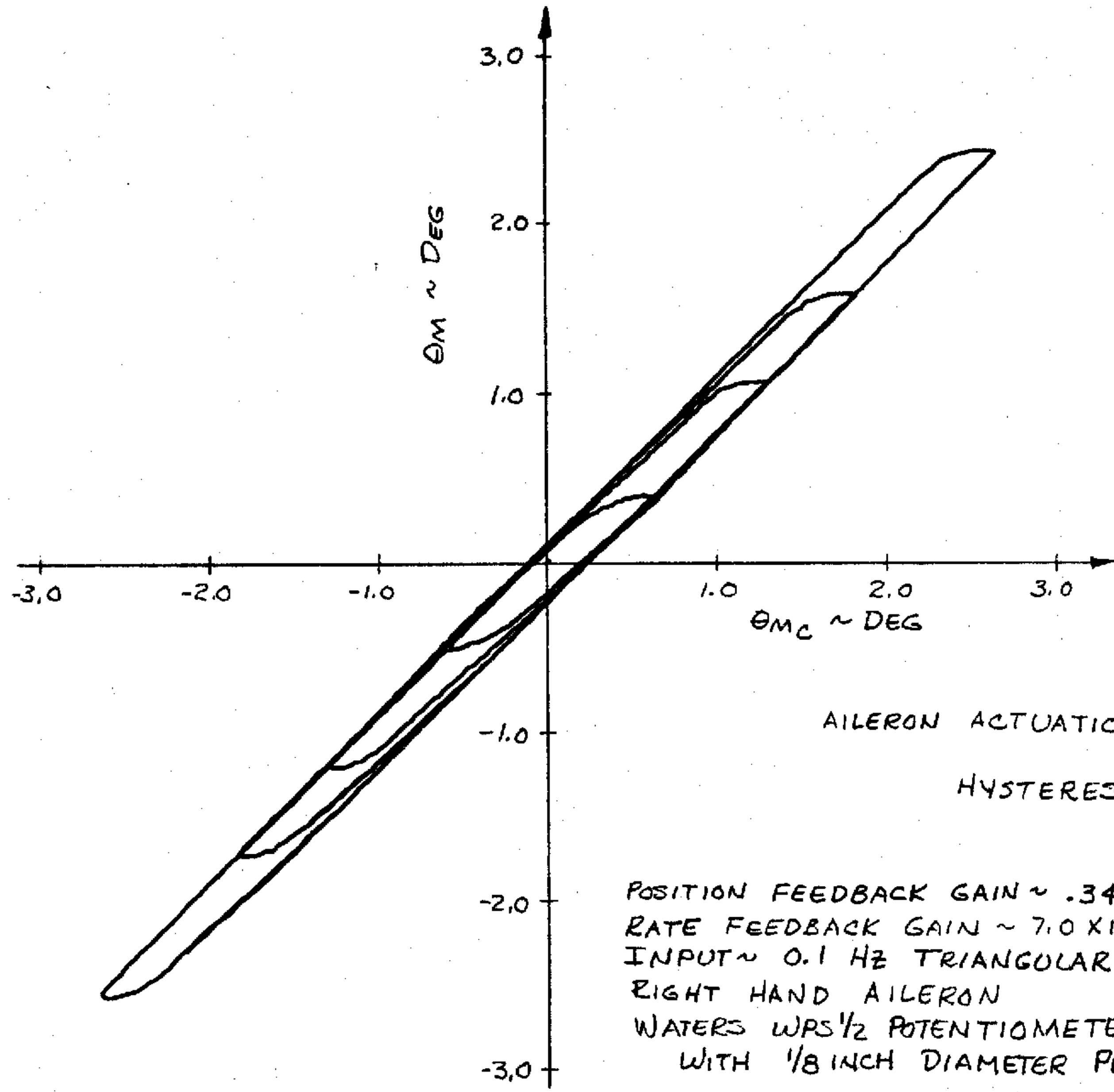

AILERON ACTUATION SYSTEM

HYSTERESIS

POSITION FEEDBACK GAIN ~ .34 VOLT / DEG
RATE FEEDBACK GAIN ~ 7.0×10^{-4} VOLT / DEG / SEC
INPUT ~ 0.1 HZ TRIANGULAR WAVE
RIGHT HAND AILERON
WATERS WPS 1/2 POTENTIOMETER REPLACED
WITH 1/8 INCH DIAMETER PRECISION STEEL SHAFT

FIGURE 8

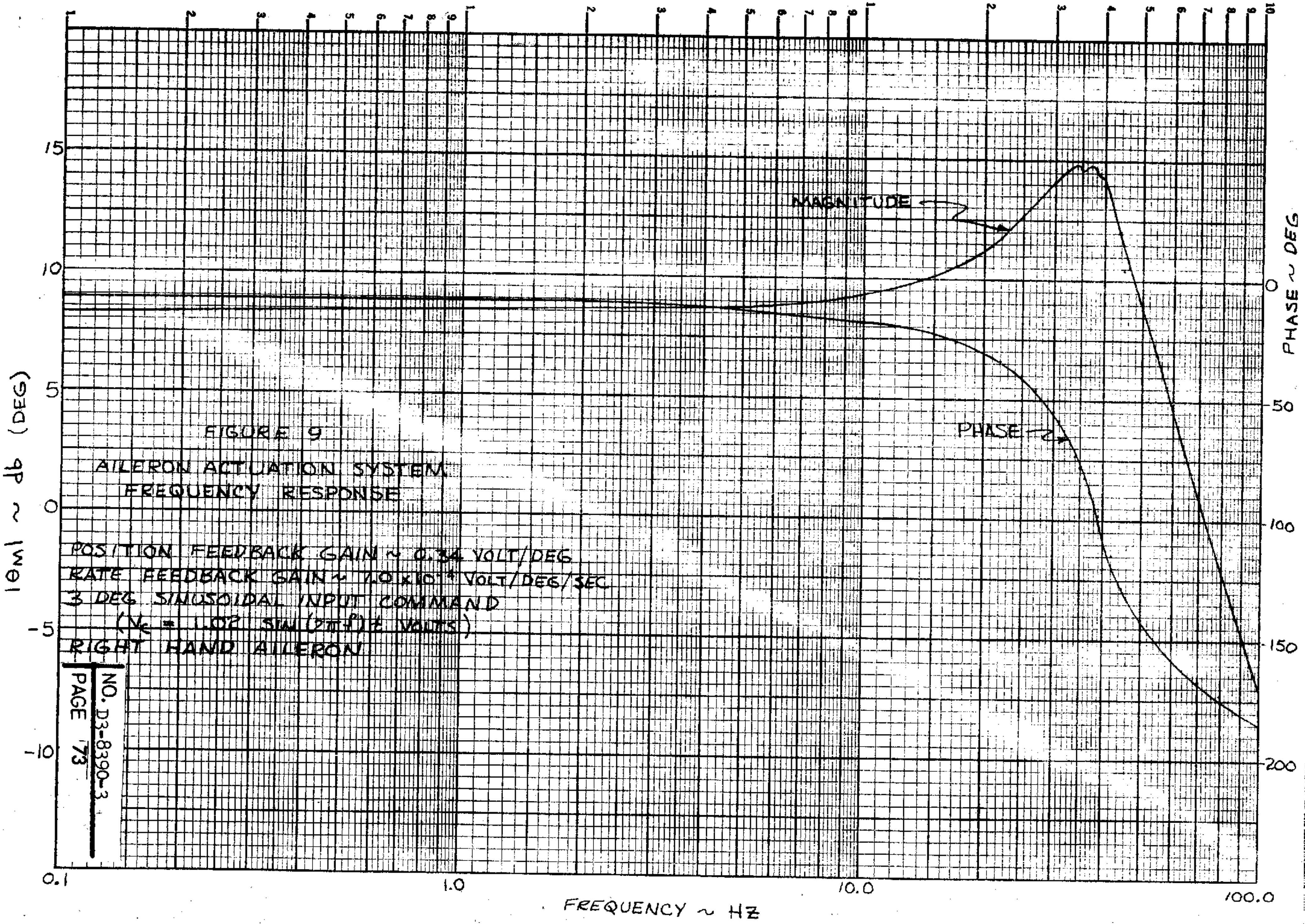

FIGURE 9
AILERON ACTUATION SYSTEM
FREQUENCY RESPONSE
POSITION FEEDBACK GAIN ~ 0.34 VOLT/DEG
RATE FEEDBACK GAIN ~ 1.0 x 10^-4 VOLT/DEG/SEC
3 DEG SINUSOIDAL INPUT COMMAND
(Vc = 1.02 SIN(2πf)t VOLTS)
RIGHT HAND AILERON
MAGNITUDE
PHASE
|θ| ~ db (DEG)
15
10
5
0
-5
-10
PHASE ~ DEG
0
50
100
150
200
0.1
1.0
10.0
100.0
FREQUENCY ~ HZ

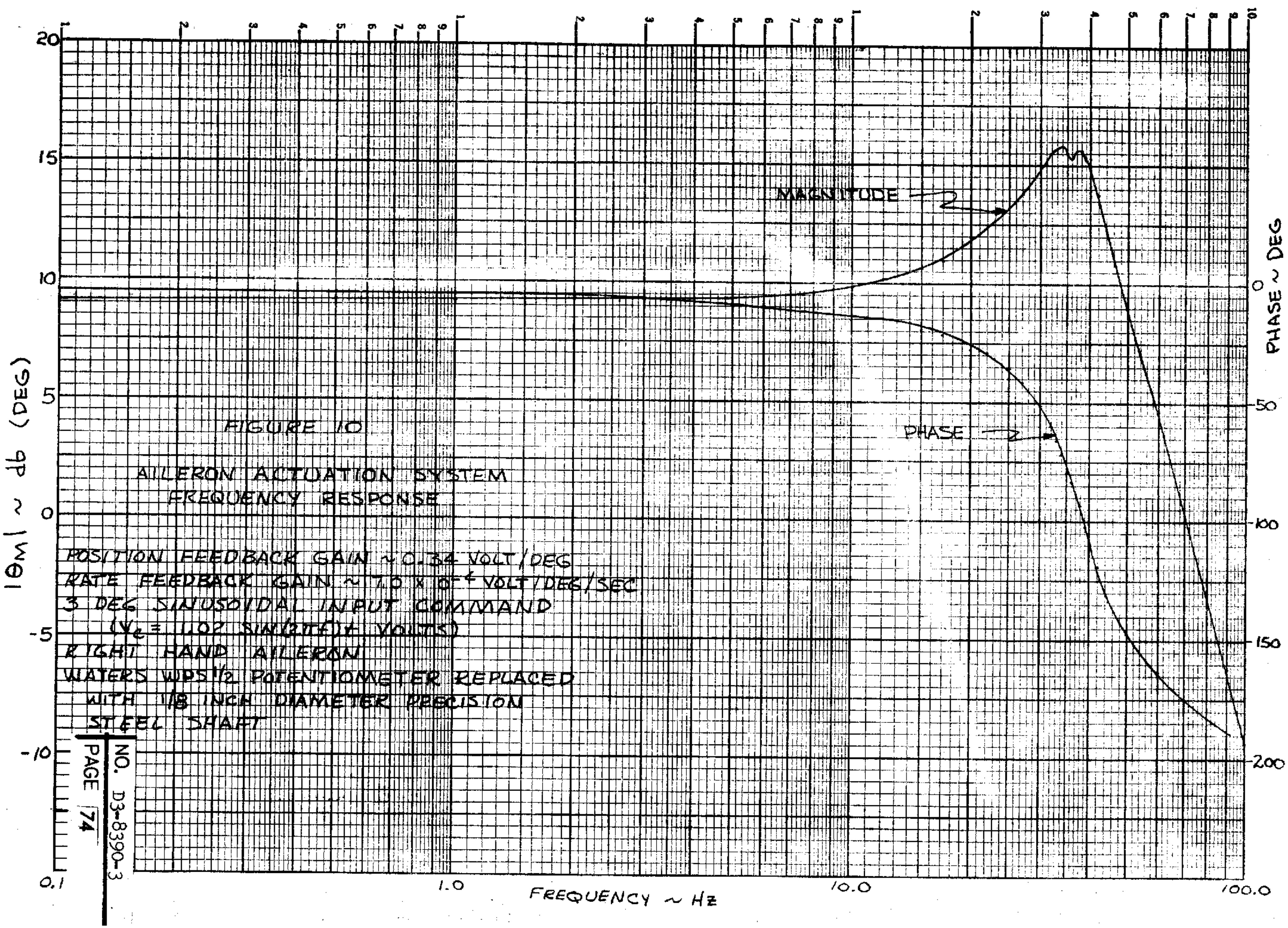
FIGURE 10
AILERON ACTUATION SYSTEM
FREQUENCY RESPONSE
POSITION FEEDBACK GAIN ~ 0.34 VOLT/DEG
RATE FEEDBACK GAIN ~ 7.0 x 10⁻⁴ VOLT/DEG/SEC
3 DEG SINUSOIDAL INPUT COMMAND
(V_c = 1.02 SIN(2πf)t VOLTS)
RIGHT HAND AILERON
WATERS WPS 1/2 POTENTIOMETER REPLACED
WITH 1/8 INCH DIAMETER PRECISION
STEEL SHAFT
MAGNITUDE
PHASE
|θ_M| ~ db (DEG)
PHASE ~ DEG
FREQUENCY ~ Hz
20
15
10
5
0
-5
-10
0
50
100
150
200
0.1
1.0
10.0
100.0

COORDINATION SHEET

TO 7564 - Gerald E. Bergmann - 16-18

NO. SDF-79-0

ITEM NO.

GROUP INDEX Structural Dynamics and Fatigue - Dynamics

DATE 5/18/70

SUBJECT B-52 Aeroelastic Model Program (NASA-Langley), Effects of Turbulence Scale on Flight Test Frequency Response Functions, EWI 4850

MODEL

The attachments to this coordination sheet are a report of the work performed by Structural Dynamics (7583) on part 1 of EWI 4850, "Analysis of Aeroelastic Model Stability Augmentation Systems," Contract No. NAS 1-9808. Part 1 is --

> "Compute theoretical airplane responses to vertical gusts with spanwise turbulence variations using the von Karman turbulence model for the B-52 configuration corresponding to WFT 1293, condition 3. Compare with computed responses to one-dimensional turbulence and flight test data."

The release of this report is milestone No. 1 on EWI 4850. Extra copies are attached to be forwarded to NASA-Langley.

Prepared By: Kenneth L. Roger
Kenneth L. Roger

Approved By: D. D. Norby
D. D. Norby

Attachments:
(A) Background and Summary of Results
(B) Theoretical and Test Responses
(C) Choice of Theoretical Gust Spectra
(D) Summary of Spectral Relationships and Nomenclature
(E) Method of Response Calculations with Spanwise Gust Variations
(F) Equations of Motion and Response Equations

cc: JDempster/JWherry
GKass
DSawdy

Attachment (A)

BACKGROUND AND SUMMARY OF RESULTS

References:
(a) Boeing Document D3-7763-1, B-52 Aeroelastic Model - Summary Report, 1968
(b) Mitchell, C. G. B., "Assessment of the Accuracy of Gust Response Calculations by Comparison with Experiments," J. Aircraft, March-April 1970
(c) Sawdy, D. T., "On the Two-Dimensional Atmospheric Turbulence Response of an Airplane," Doctoral Thesis, University of Kansas, 1966

Background

The B-52 Aeroelastic Model Program is a wind tunnel study being conducted by the National Aeronautics and Space Administration (NASA). The study will evaluate the feasibility of using a dynamically scaled elastic model in a wind tunnel to obtain gust response data. The model represents a B-52E flight test airplane which carried a nose-mounted probe instrumented to measure gusts, and for which a large amount of flight test gust response data is available.

The Boeing Company furnished design data for the model design, theoretical equations of motion for the airplane and model, flight test gust response data, and theoretical gust response data. These items were included in the four volumes summarized in Reference (a).

The theoretical gust responses were based on the assumption that atmospheric turbulence would vary along the flight path in a statistically describable manner, but that no spanwise variations would occur -- at a given instant the vertical gust at the left wing tip would be exactly the same as the vertical gust at the right wing tip. This is referred to as one dimensional random turbulence. The theoretical method of predicting responses to turbulence with random spanwise variations, referred to as two-dimensional random turbulence, was known but was considered too expensive to use. An application of 2-D gust theory to a similar problem is given by D. Sawdy in Reference (c).

The present study was begun because of obvious disagreement between theoretical and test responses, and because of the development of more economical computer programs to perform the 2-D gust computations. The problem we are addressing is well stated by C. Mitchell in Reference (b). Quoting from his conclusions,

> "The standard of the gust response calculations described in this paper is believed to be typical of those made to date. Improvements that can be immediately foreseen are the inclusion of the unsteady aerodynamic interference between the wing and tailplane, and the extension of calculations to include the variation of turbulence across the span of the airplane. Both these improvements will increase the amount of computing significantly.
>
> "It has been shown, by comparison with flight measurements, that the present day calculations -- overestimate the excitation of the higher frequency elastic modes appreciably. --The accelerations at the extremities of flexible aircraft are lower in flight than would be predicted."

The first problem stated by Mr. Mitchell, wing and tailplane unsteady interference, can be approached through wind tunnel investigations. However, the the second problem, variation of turbulence across the span of the airplane, refers to a type of turbulence fundamentally different from that which will be generated in the wind tunnel. The differences between response to 2-D turbulence and 1-D turbulence, since they are appreciable, must be theoretically estimated and applied as corrections to wind tunnel data before comparison with flight test data can be made. The purpose of this report is to present the results of such a theoretical study for the B-52 flight condition simulated by the B-52 aeroelastic model.

Summary of Results

The theoretical amplitudes of B-52 responses in atmospheric turbulence are considerably different using two-dimensional turbulence models than when using one-dimensional turbulence models. The phase angle between response and gust is not appreciably different, 1-D vs. 2-D. Low coherency between gust and response (less than .01 at some frequencies less than 7 Hertz) is predicted by the two-dimensional gust theory.

Response amplitude to gust amplitude ratios versus frequency for the 1-D gust theory tend to be higher than for 2-D theory and this difference increases with frequency. Bending moment at wing station 222, for example, at 0.65 Hz is 40% higher for 1-D gusts than for 2-D gusts. (The figures in Attachment (B) show squared amplitudes which show a factor of 2 difference.) The trends are not invariable, however. The effects of mode coupling, tuning from penetration effects, and peculiarities of the mode shapes preclude "rule-of-thumb" forecasting here, as in most multiple freedom problems.

The differences between responses to 2-D and 1-D turbulence, as shown on the figures of Attachment (B), should be interpreted as expected differences between flight test results (2-D turbulence) and wind tunnel results (1-D turbulence). This information is presented for each of the airplane responses considered in the Boeing aeroelastic model documents, Reference (a). Actual flight test responses are shown for comparison.

An important result is that the ratios of response amplitude to gust amplitude obtained using 2-D gust theory do not change greatly vs. turbulence scale length and do not approach the 1-D theory ratios for any of the scale lengths commonly used for aircraft analysis. An equivalent effect was noted by D. Sawdy, Reference (c). Typical gust spectral densities are plotted in Figure A-1 in a way which illustrates this property of the von Karman isotropic gust spectrum. In Figure A-1, the cross spectral density of two gusts at points with spanwise separation Δy has been normalized by the gust auto-spectral density ($\Delta y = 0$). Flag 1 is plotted at $\Delta y/L = .2$ and $\omega L/V = 4$ and is representative of the turbulence which drives B-52 low frequency modes at low altitudes (L = approx. 500 ft.). If the scale of turbulence "L" were doubled, the point would be replotted by flag 2. Notice that it does not move appreciably upward toward the 1-D gust value. If the scale of turbulence were 4 times the original, the point would be at flag 3. If the scale were 10 times the original the point

would be at flag 4, where the spectral ratio is still not significantly higher than for the original scale. A similar trend can be shown for higher frequency responses. As a matter of fact, only responses near zero frequency can be expected to converge to 1-D gust values for reasonable scale lengths. This excludes almost all responses of structural interest unless the airplane is without rigid body freedoms.

EFFECT OF SPANWISE SEPARATION ON VERTICAL GUST CROSS-SPECTRAL DENSITY

VON KARMAN CORRELATION FUNCTION
$$\left\{ \begin{aligned} & R(\tau, \Delta y) = .59253\,(z)^{1/3}\left[K_{1/3}(z) - .5z\,K_{2/3}(z)\right] \\ & z = \sqrt{(V\tau/L)^2 + (\Delta y/L)^2}\;/\;1.339 \end{aligned} \right\}$$

▷ SEE "SUMMARY OF RESULTS" FOR A DISCUSSION OF THE FLAGS.

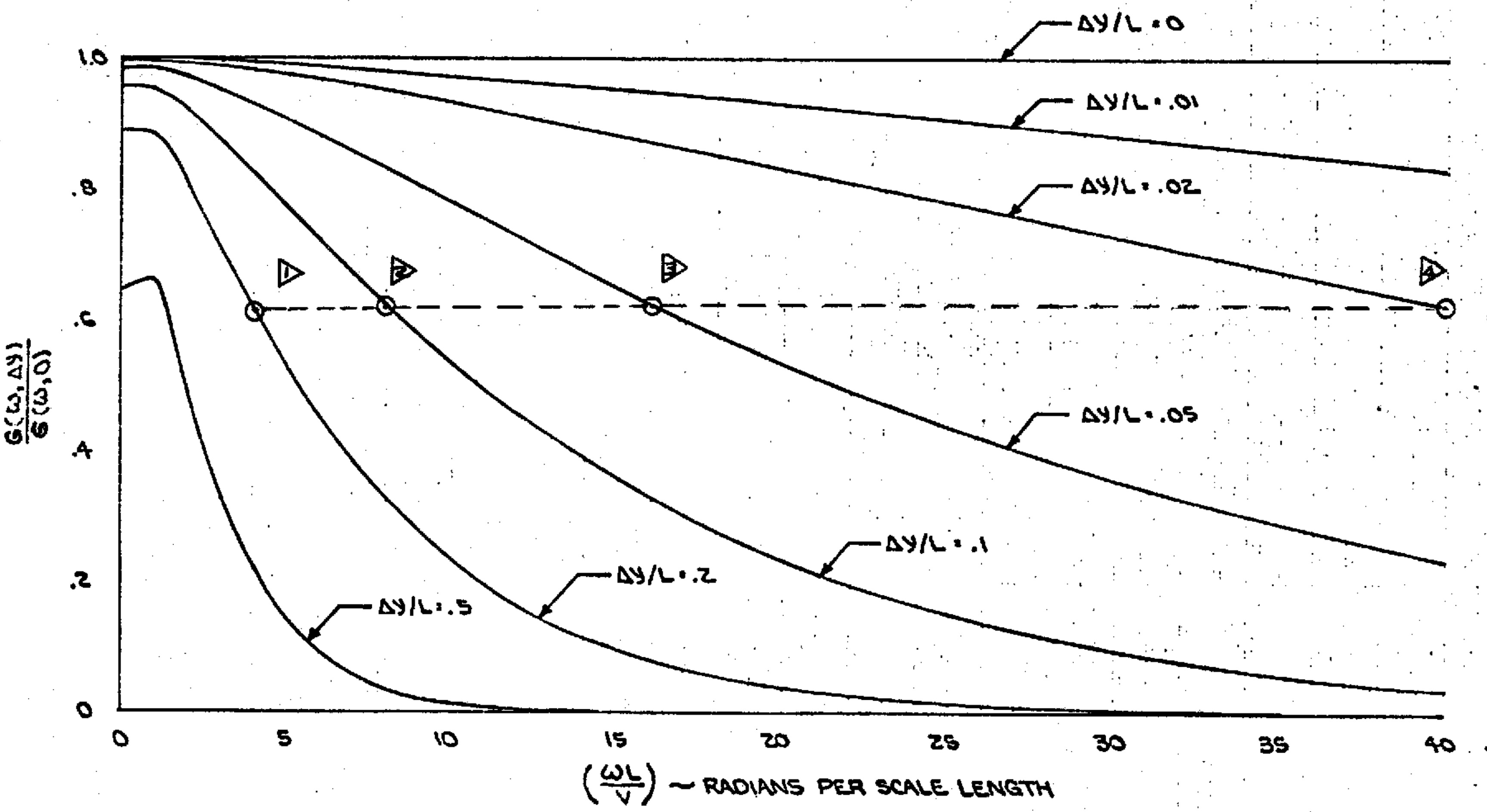

CALC			
CHECK			
APPD			
APPD			
		REVISED	DATE

REV LTR:

FIGURE A-1

SECT | NO. | PAGE A-4

Attachment (B)

THEORETICAL AND TEST RESPONSES

Reference Boeing Document D3-7763-4, B-52 Aeroelastic Model--Frequency Response Function Data

The test responses plotted in this section are tabulated in the above reference. No changes were made except the algebraic sign of the phase angles was reversed so that response lag would correspond to a negative angle.

The theoretical responses were computed to correspond precisely with the items measured in flight testing. The three items plotted are phase angle of the cross-spectral density (response and gust), coherence of response and gust, and amplitude ratios of response to gust by the cross-spectral method. All are plotted versus frequency from 0.1 to 7.0 Hertz.

Four sets of theoretical data are plotted--the response to one-dimensional turbulence (the items plotted will be independent of turbulence scale "L" for 1-D turbulence) and the responses to two-dimensional turbulence for L = 250, 500, and 1000 feet. The effect of scale length "L" for two-dimensional turbulence is small; the effect is greatest at low frequencies--above 1.5 Hertz it is negligible.

The two-dimensional gust amplitude ratios are very significantly different from the 1-D ratios, even at low frequencies. The difference increases with frequency.

Theoretical maximum coherency for 1-D turbulence is 1.0. For 2-D turbulence it can be below 0.01 in the frequency range plotted. The difference in phase angle between 1-D and 2-D turbulence is usually small when the response amplitudes are reasonably large.

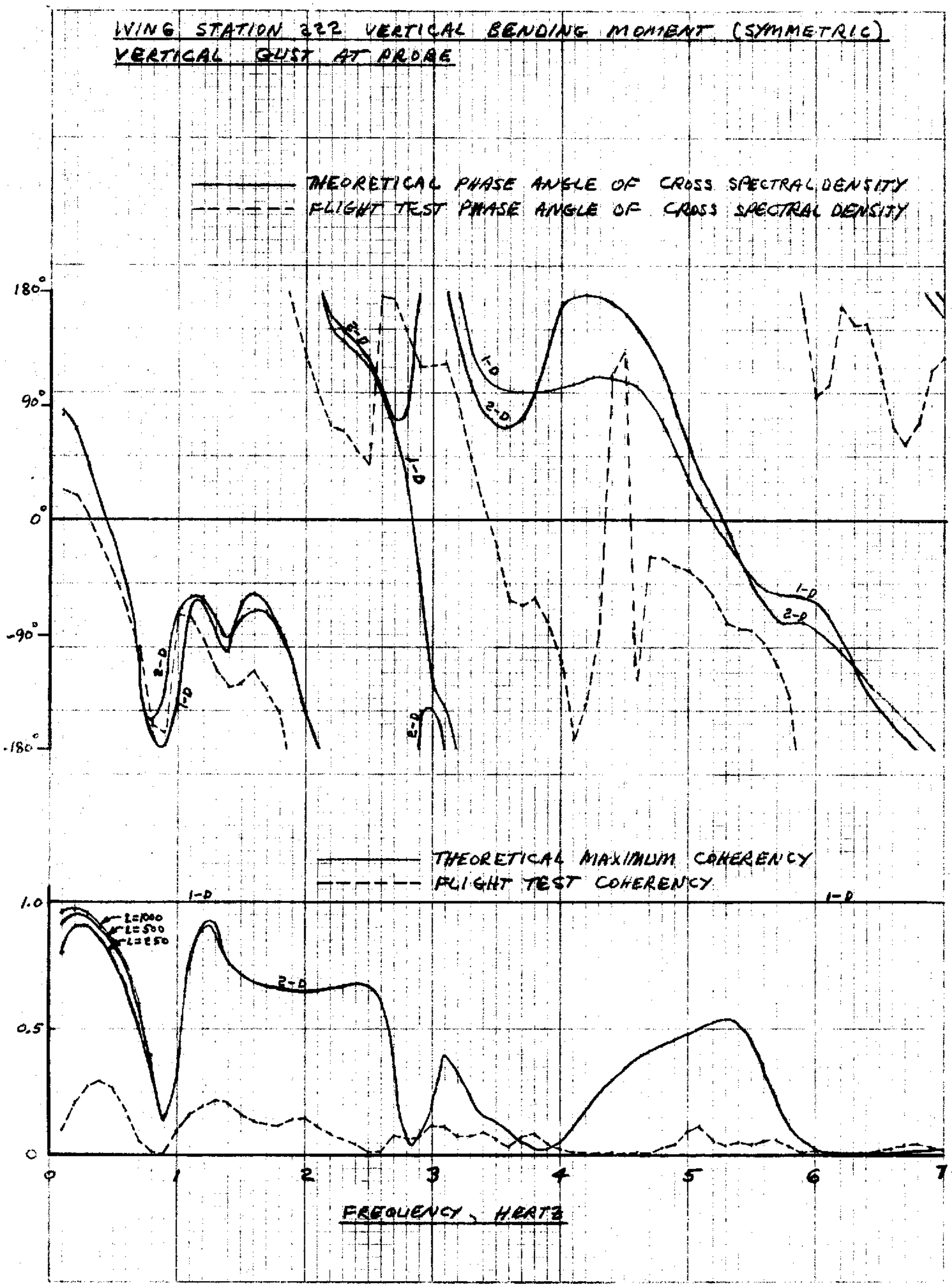
WING STATION 222 VERTICAL BENDING MOMENT (SYMMETRIC)
VERTICAL GUST AT PROBE
THEORETICAL PHASE ANGLE OF CROSS SPECTRAL DENSITY
FLIGHT TEST PHASE ANGLE OF CROSS SPECTRAL DENSITY
180°
90°
0°
-90°
-180°
1-D
2-D
THEORETICAL MAXIMUM COHERENCY
FLIGHT TEST COHERENCY
1.0
0.5
0
L=1000
L=500
L=250
0
1
2
3
4
5
6
7
FREQUENCY, HERTZ

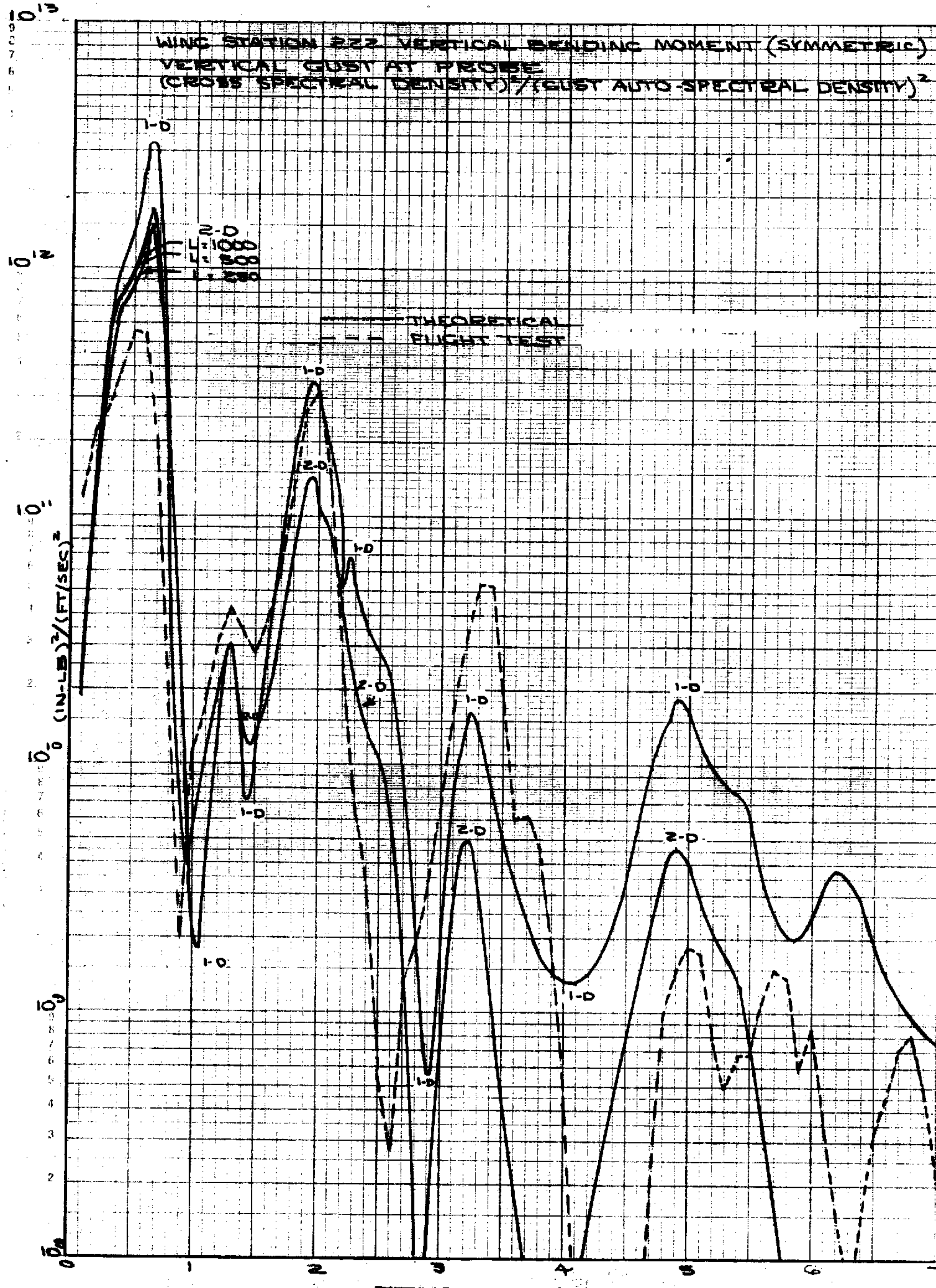

WING STATION 222 VERTICAL BENDING MOMENT (SYMMETRIC)
VERTICAL GUST AT PROBE
(CROSS SPECTRAL DENSITY)²/(GUST AUTO-SPECTRAL DENSITY)²
THEORETICAL
FLIGHT TEST
1-D
2-D
L=1000
L=500
L=250
(IN-LB)²/(FT/SEC)²
FREQUENCY, HZ

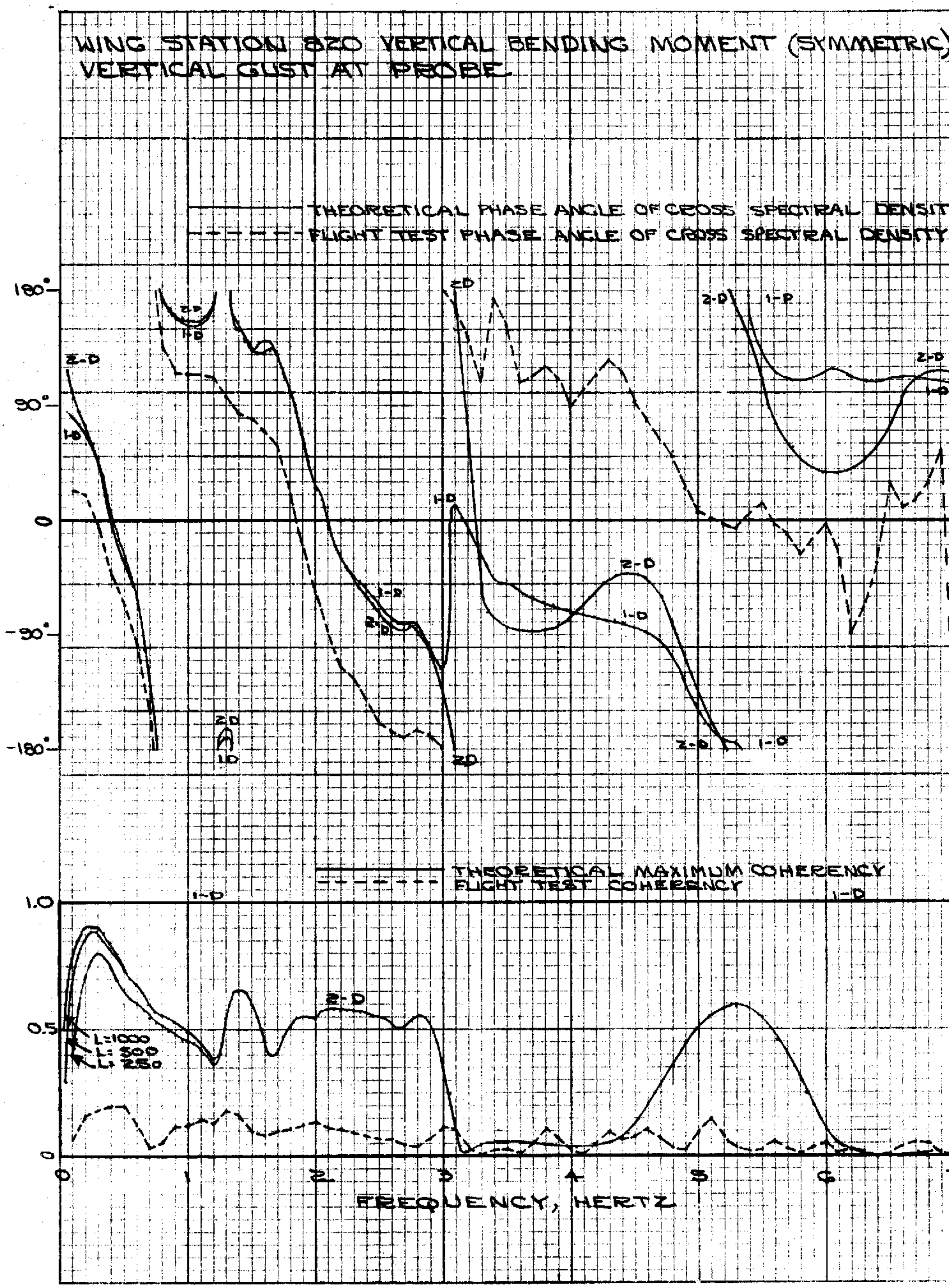
WING STATION 820 VERTICAL BENDING MOMENT (SYMMETRIC)
VERTICAL GUST AT PROBE
THEORETICAL PHASE ANGLE OF CROSS SPECTRAL DENSITY
FLIGHT TEST PHASE ANGLE OF CROSS SPECTRAL DENSITY
180°
90°
0
-90°
-180°
2-D
1-D
THEORETICAL MAXIMUM COHERENCY
FLIGHT TEST COHERENCY
1.0
0.5
0
L=1000
L=500
L=250
0
1
2
3
4
5
6
7
FREQUENCY, HERTZ

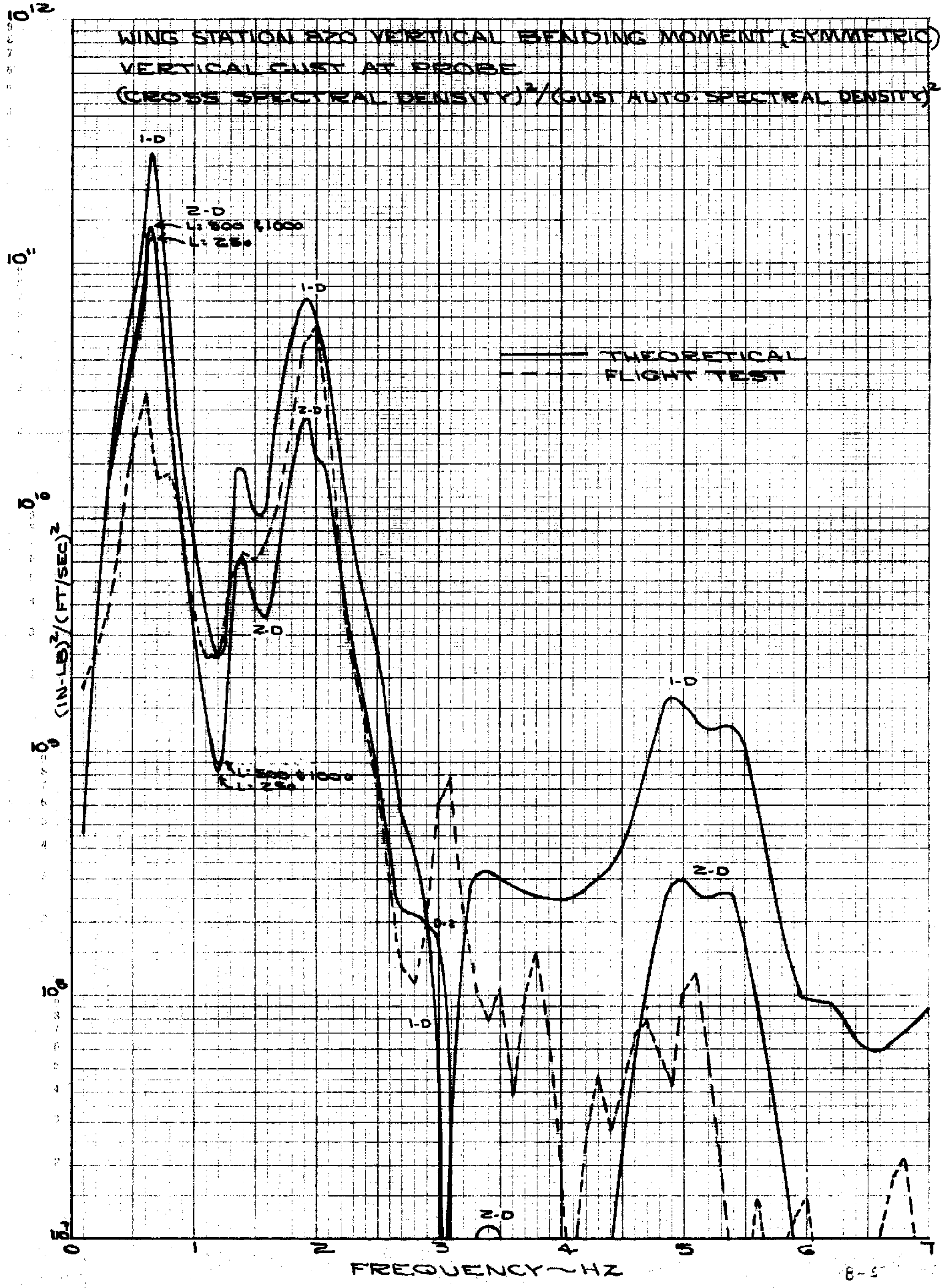

WING STATION 820 VERTICAL BENDING MOMENT (SYMMETRIC)
VERTICAL GUST AT PROBE
(CROSS SPECTRAL DENSITY)²/(GUST AUTO SPECTRAL DENSITY)²
THEORETICAL
FLIGHT TEST
1-D
2-D
L: 500 & 1000
L: 250
(IN-LB)²/(FT/SEC)²
FREQUENCY ~ HZ

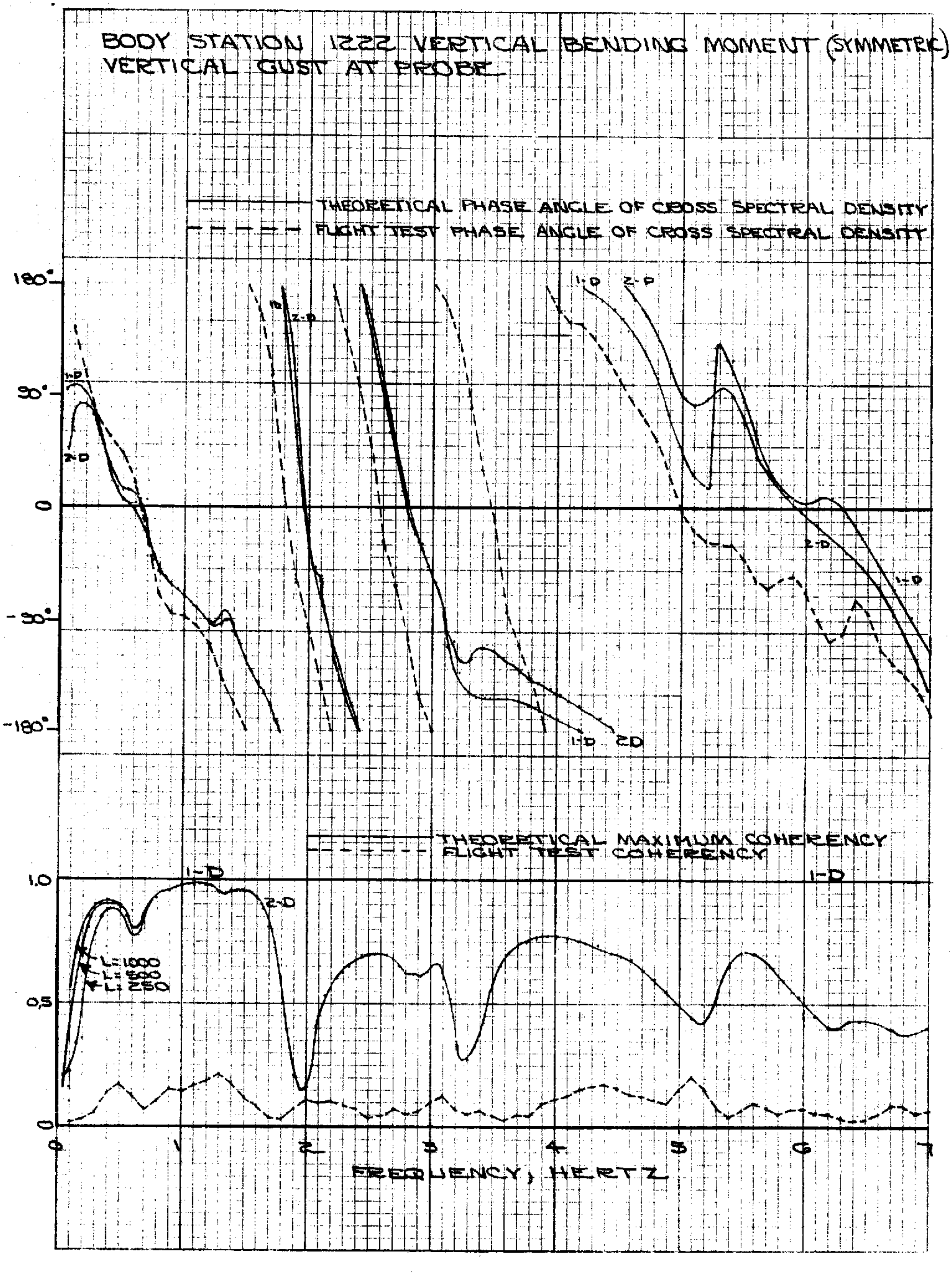

BODY STATION 1222 VERTICAL BENDING MOMENT (SYMMETRIC)
VERTICAL GUST AT PROBE
THEORETICAL PHASE ANGLE OF CROSS SPECTRAL DENSITY
FLIGHT TEST PHASE ANGLE OF CROSS SPECTRAL DENSITY
180°
90°
0
-90°
-180°
1-D
2-D
THEORETICAL MAXIMUM COHERENCY
FLIGHT TEST COHERENCY
1.0
0.5
0
L=1000
L=500
L=250
0
1
2
3
4
5
6
7
FREQUENCY, HERTZ

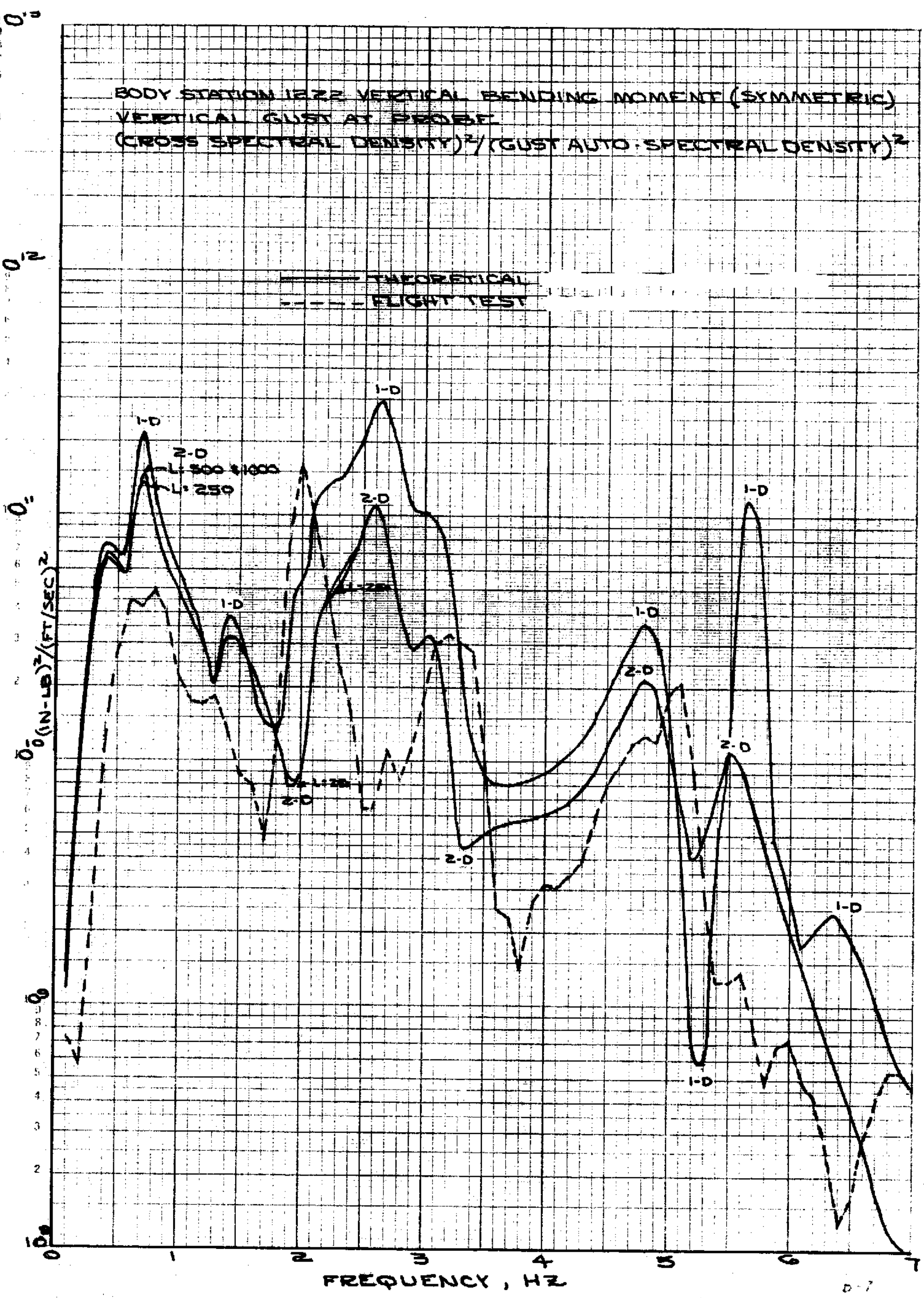

BODY STATION 1222 VERTICAL BENDING MOMENT (SYMMETRIC)
VERTICAL GUST AT PROBE
(CROSS SPECTRAL DENSITY)²/(GUST AUTO SPECTRAL DENSITY)²
THEORETICAL
FLIGHT TEST
1-D
2-D
L: 500 & 1000
L: 250
10^{8}
10^{9}
10^{10}
10^{11}
10^{12}
10^{13}
(IN-LB)²/(FT/SEC)²
0
1
2
3
4
5
6
7
FREQUENCY, HZ

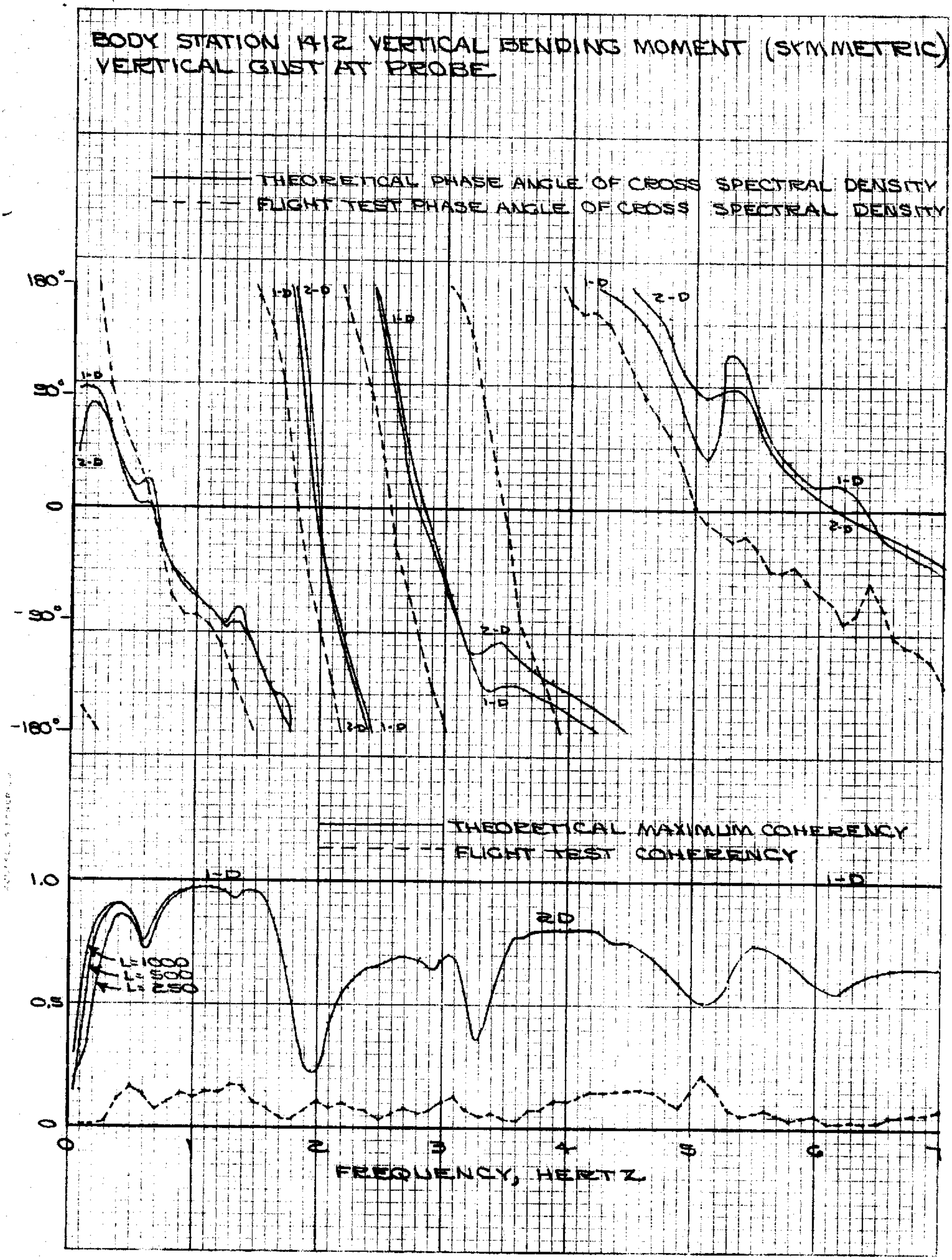
BODY STATION 1412 VERTICAL BENDING MOMENT (SYMMETRIC)
VERTICAL GUST AT PROBE
THEORETICAL PHASE ANGLE OF CROSS SPECTRAL DENSITY
FLIGHT TEST PHASE ANGLE OF CROSS SPECTRAL DENSITY
180°
90°
0
-90°
-180°
1-D
2-D
THEORETICAL MAXIMUM COHERENCY
FLIGHT TEST COHERENCY
1.0
0.5
0
L=1000
L=500
L=250
2D
0
1
2
3
4
5
6
7
FREQUENCY, HERTZ

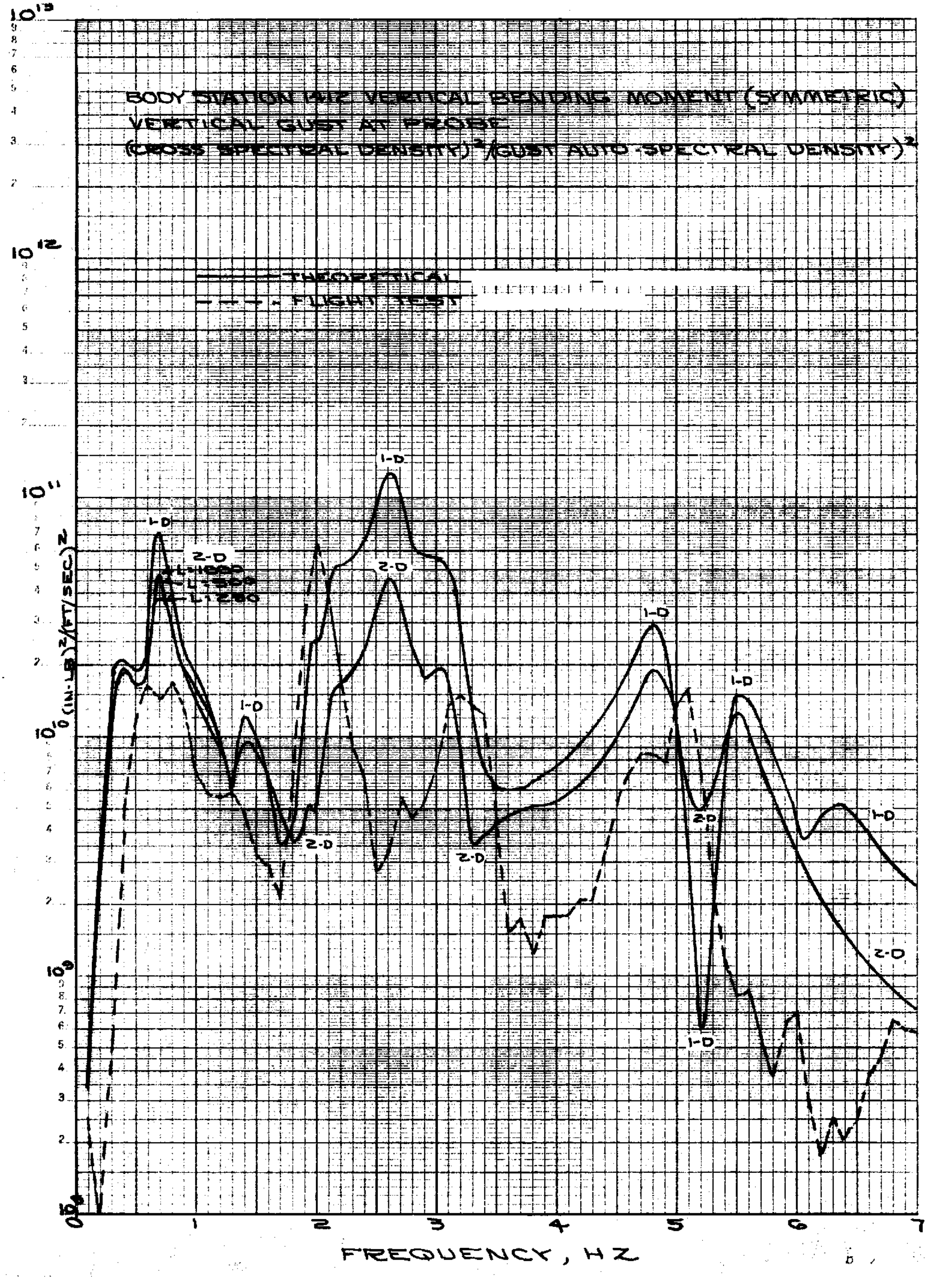

BODY STATION 1412 VERTICAL BENDING MOMENT (SYMMETRIC)
VERTICAL GUST AT PROBE
(CROSS SPECTRAL DENSITY)² /(GUST AUTO-SPECTRAL DENSITY)²
THEORETICAL
FLIGHT TEST
1-D
2-D
L-1000
L-500
L-250
$(IN-LB)^2/(FT/SEC)^2$
FREQUENCY, HZ

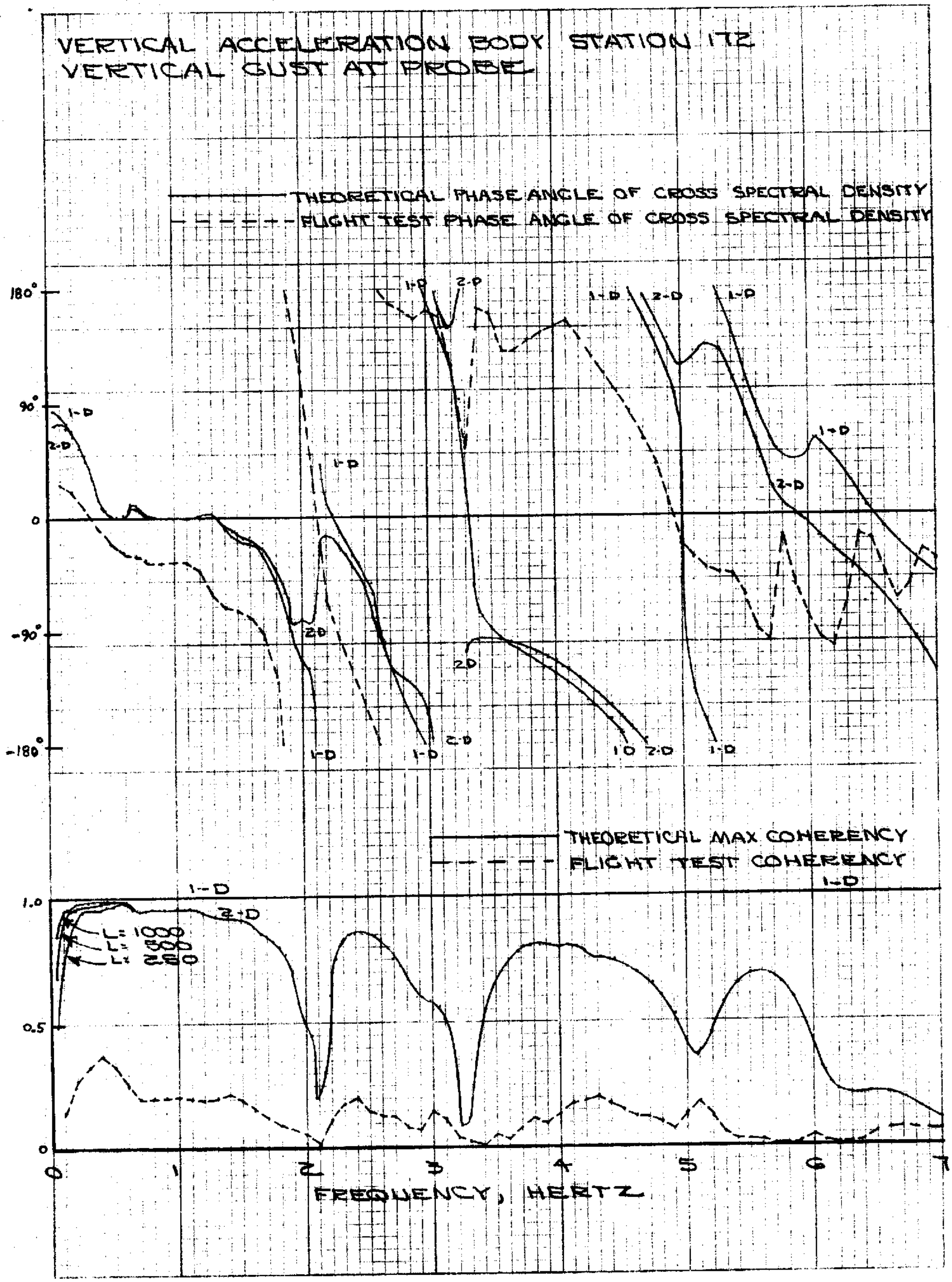

VERTICAL ACCELERATION BODY STATION 172
VERTICAL GUST AT PROBE
THEORETICAL PHASE ANGLE OF CROSS SPECTRAL DENSITY
FLIGHT TEST PHASE ANGLE OF CROSS SPECTRAL DENSITY
180°
90°
0
-90°
-180°
1-D
2-D
THEORETICAL MAX COHERENCY
FLIGHT TEST COHERENCY
1.0
0.5
0
L: 1000
L: 500
L: 250
0
1
2
3
4
5
6
7
FREQUENCY, HERTZ

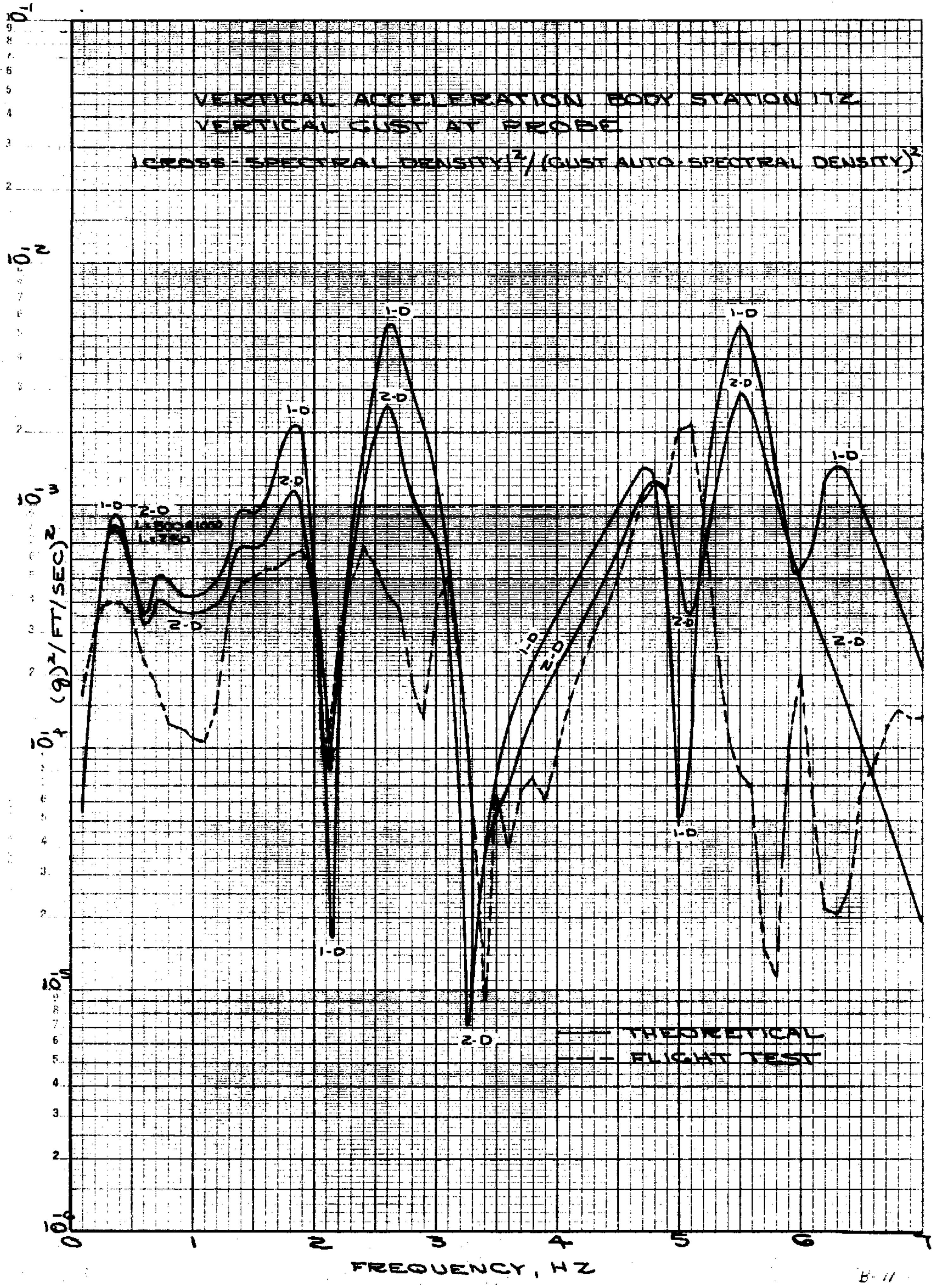

VERTICAL ACCELERATION BODY STATION 172
VERTICAL GUST AT PROBE
|CROSS-SPECTRAL DENSITY|²/(GUST AUTO-SPECTRAL DENSITY)²
(g)²/(FT/SEC)²
FREQUENCY, HZ
1-D
2-D
1:1500 & 1000
1:750
THEORETICAL
FLIGHT TEST

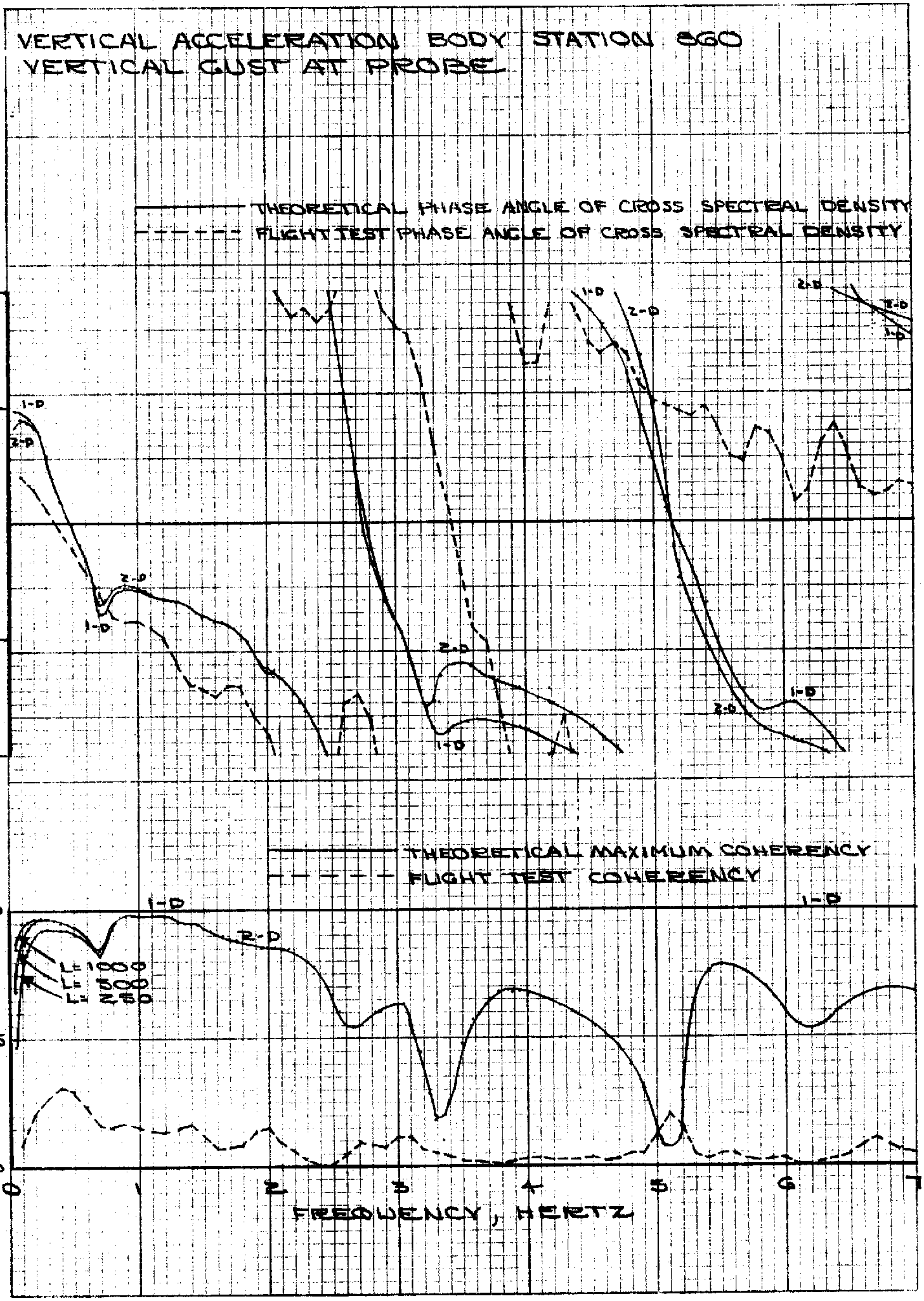
VERTICAL ACCELERATION BODY STATION 860
VERTICAL GUST AT PROBE
THEORETICAL PHASE ANGLE OF CROSS SPECTRAL DENSITY
FLIGHT TEST PHASE ANGLE OF CROSS SPECTRAL DENSITY
180°
90°
0
-90°
-180°
1-D
2-D
THEORETICAL MAXIMUM COHERENCY
FLIGHT TEST COHERENCY
1.0
0.5
0
L=1000
L=500
L=250
0
1
2
3
4
5
6
7
FREQUENCY, HERTZ

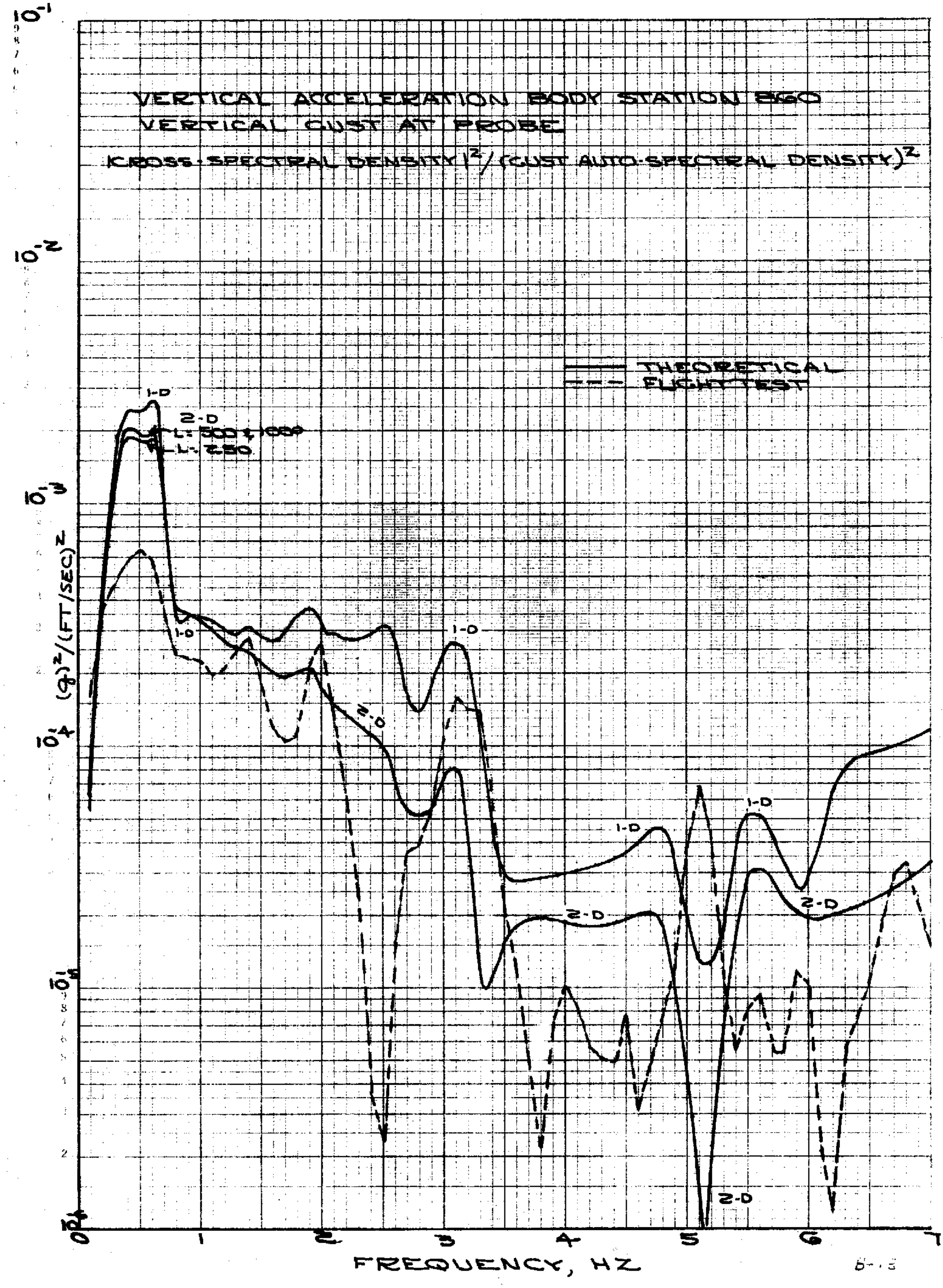

VERTICAL ACCELERATION BODY STATION 860
VERTICAL GUST AT PROBE
|CROSS-SPECTRAL DENSITY|²/(GUST AUTO-SPECTRAL DENSITY)²
THEORETICAL
FLIGHT TEST
1-D
2-D
L=500 & 1000
L=250
$(g)^2/(FT/SEC)^2$
FREQUENCY, HZ
0
1
2
3
4
5
6
7
10^{-1}
10^{-2}
10^{-3}
10^{-4}
10^{-5}
10^{-6}

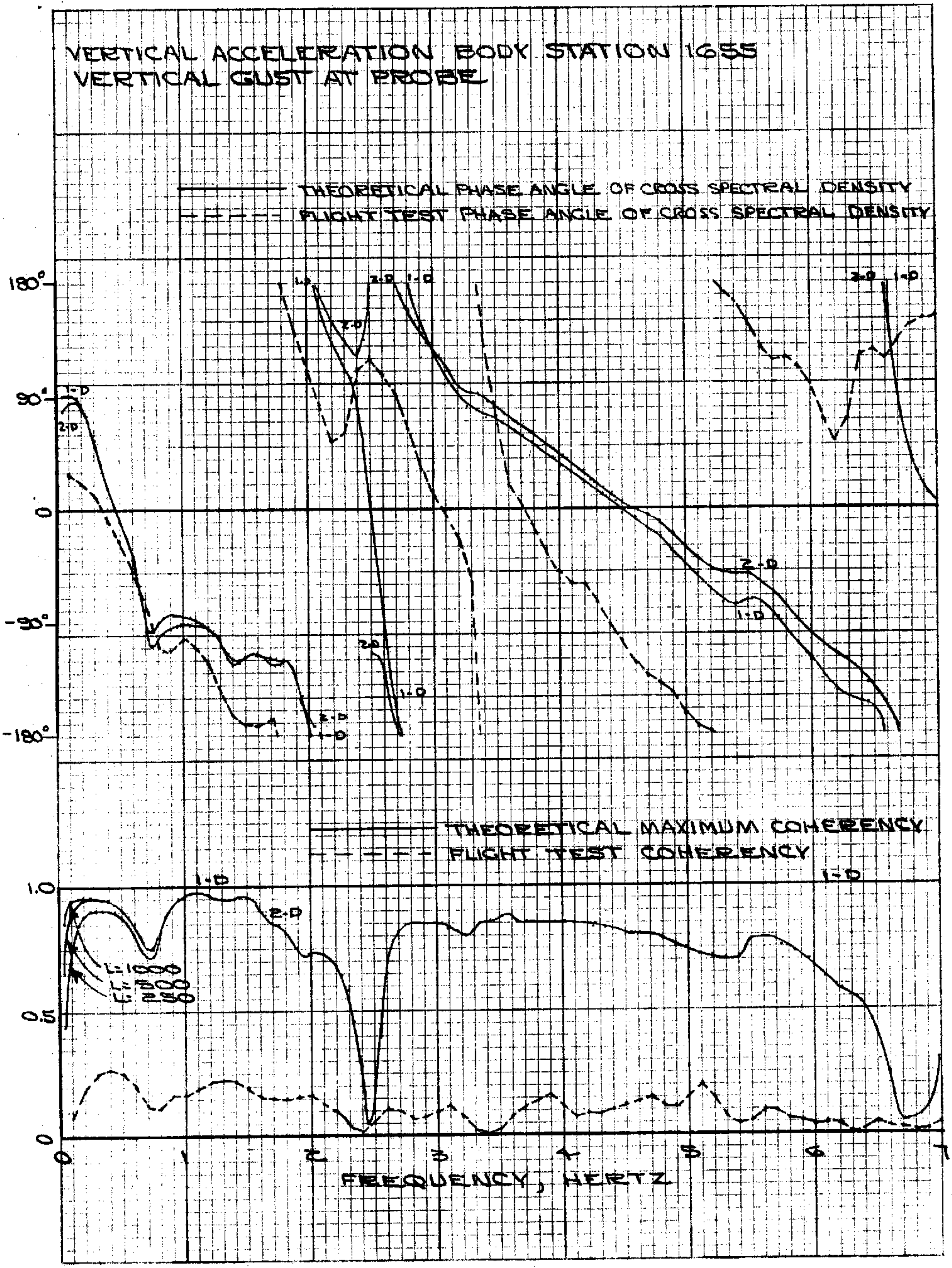
VERTICAL ACCELERATION BODY STATION 1655
VERTICAL GUST AT PROBE
THEORETICAL PHASE ANGLE OF CROSS SPECTRAL DENSITY
FLIGHT TEST PHASE ANGLE OF CROSS SPECTRAL DENSITY
180°
90°
0
-90°
-180°
1-D
2-D
THEORETICAL MAXIMUM COHERENCY
FLIGHT TEST COHERENCY
1.0
0.5
0
L=1000
L=500
L=250
0
1
2
3
4
5
6
7
FREQUENCY, HERTZ

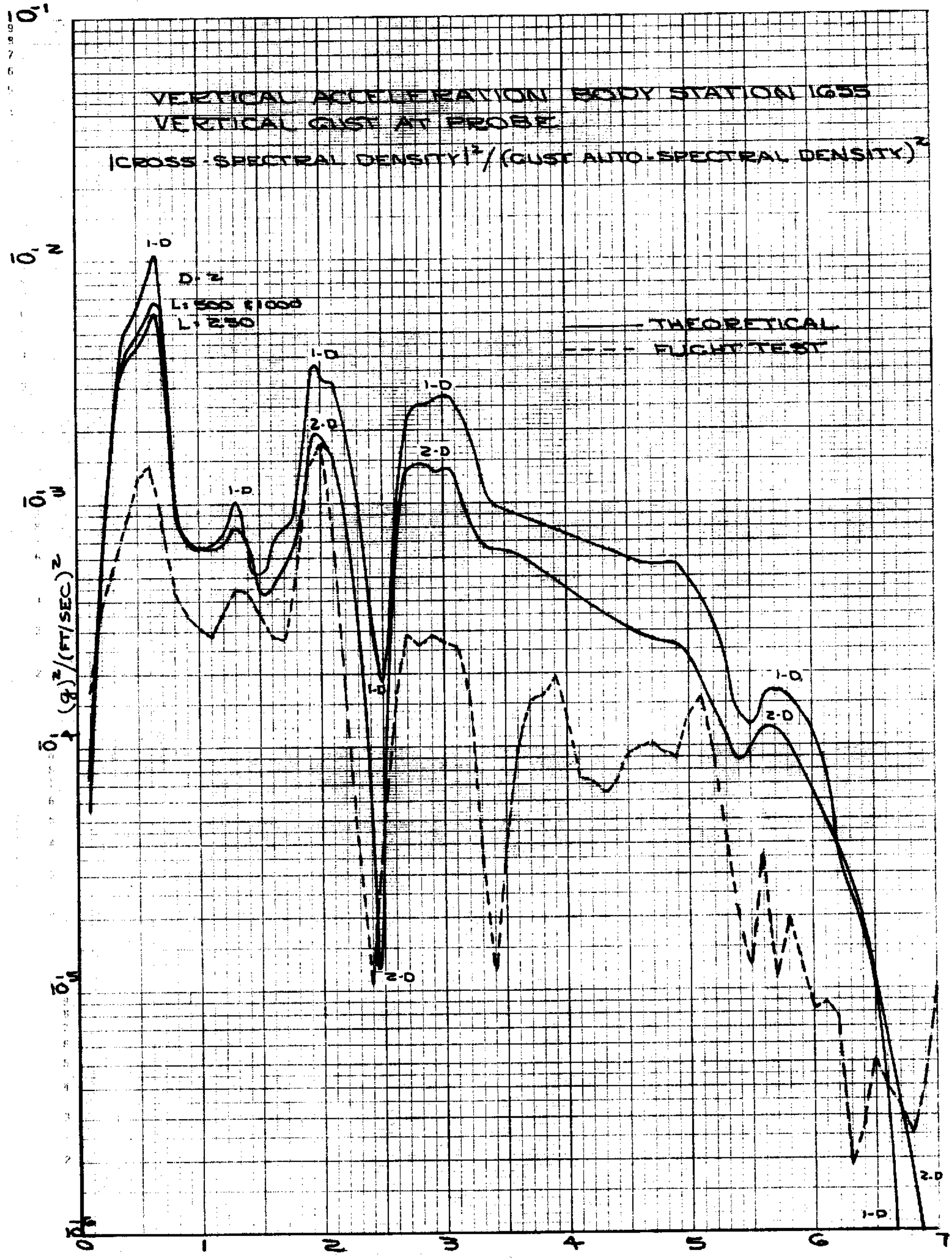

VERTICAL ACCELERATION BODY STATION 1655
VERTICAL GUST AT PROBE
|CROSS-SPECTRAL DENSITY|² / (GUST AUTO-SPECTRAL DENSITY)²
D=2
L=500 & 1000
L=250
THEORETICAL
FLIGHT TEST
1-D
2-D
(g)²/(FT/SEC)²
FREQUENCY, HZ

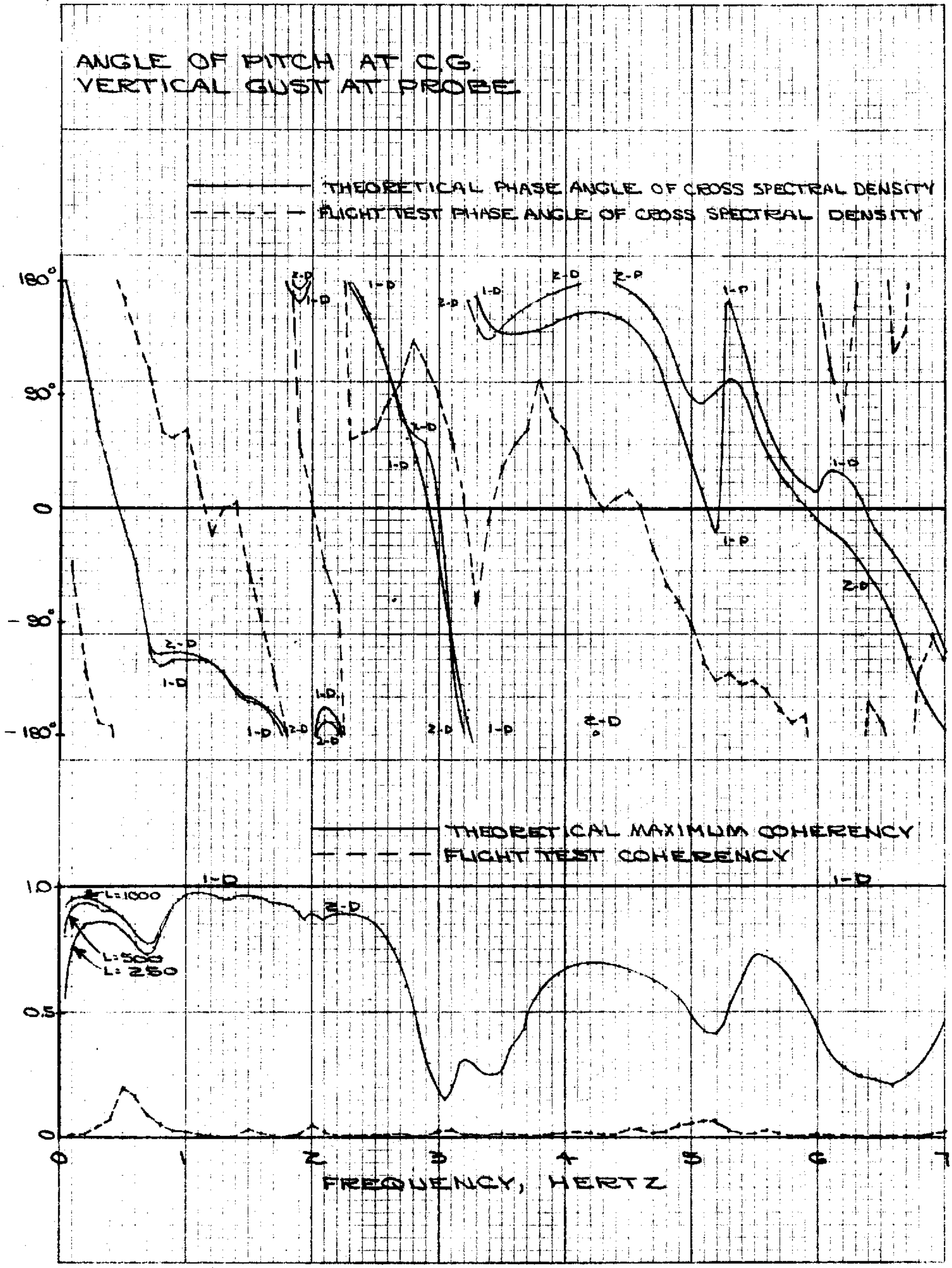

ANGLE OF PITCH AT C.G.
VERTICAL GUST AT PROBE
THEORETICAL PHASE ANGLE OF CROSS SPECTRAL DENSITY
FLIGHT TEST PHASE ANGLE OF CROSS SPECTRAL DENSITY
180°
90°
0
-90°
-180°
1-D
2-D
THEORETICAL MAXIMUM COHERENCY
FLIGHT TEST COHERENCY
1.0
0.5
0
L=1000
L=500
L=250
0
1
2
3
4
5
6
7
FREQUENCY, HERTZ

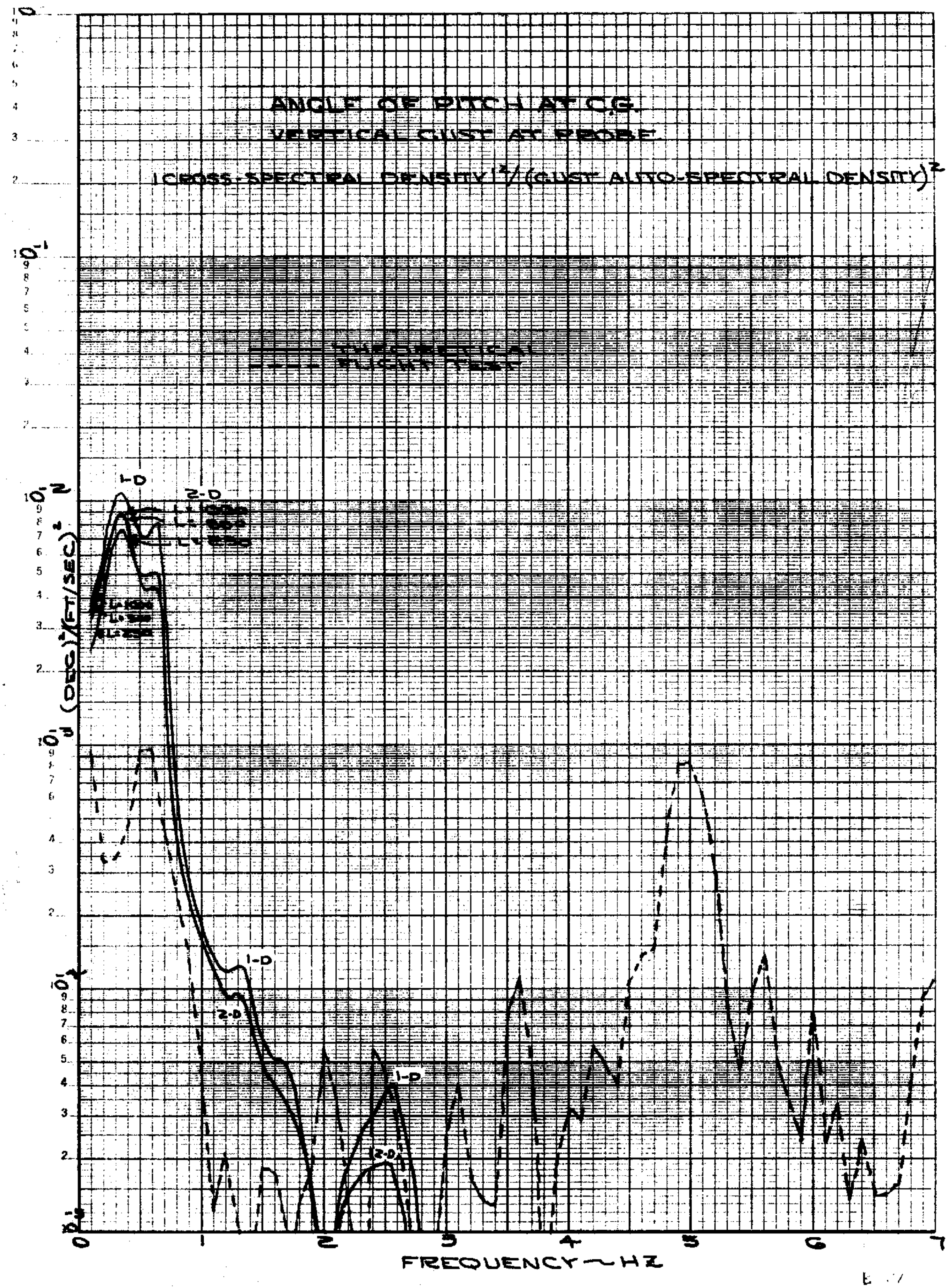

ANGLE OF PITCH AT C.G.
VERTICAL GUST AT PROBE
|CROSS-SPECTRAL DENSITY|²/(GUST AUTO-SPECTRAL DENSITY)²
THEORETICAL
FLIGHT TEST
1-D
2-D
(DEG)²/(FT/SEC)²
FREQUENCY ~ HZ

Attachment (C)

CHOICE OF THEORETICAL GUST SPECTRA

Reference Boeing Document D3-7763-4, B-52 Aeroelastic Model -- Frequency Response Function Data

The auto-spectral density of the gust for the flight test data is taken from the above reference and plotted in Figure C-1. Spectra for three scale length, L = 250, 500 and 1000 feet, based on the von Karman turbulence model are also shown. The three scale lengths were chosen to bracket the range expected in low level flight. RMS levels, σ_w , were chosen so the truncated RMS values (from 0.1 to 7.0 Hertz) would be the same as in flight test. The spectrum for L = 500 feet is a good overall fit to the flight test data, but no strong argument can be offered that any particular L would be a "best" fit.

It was assumed that the two-dimensional features of the flight test gust spectrum would be adequately described by a von Karman spectrum, scale length 500 feet.

COMPARISON OF ANALYTICAL AND TEST GUST SPECTRA

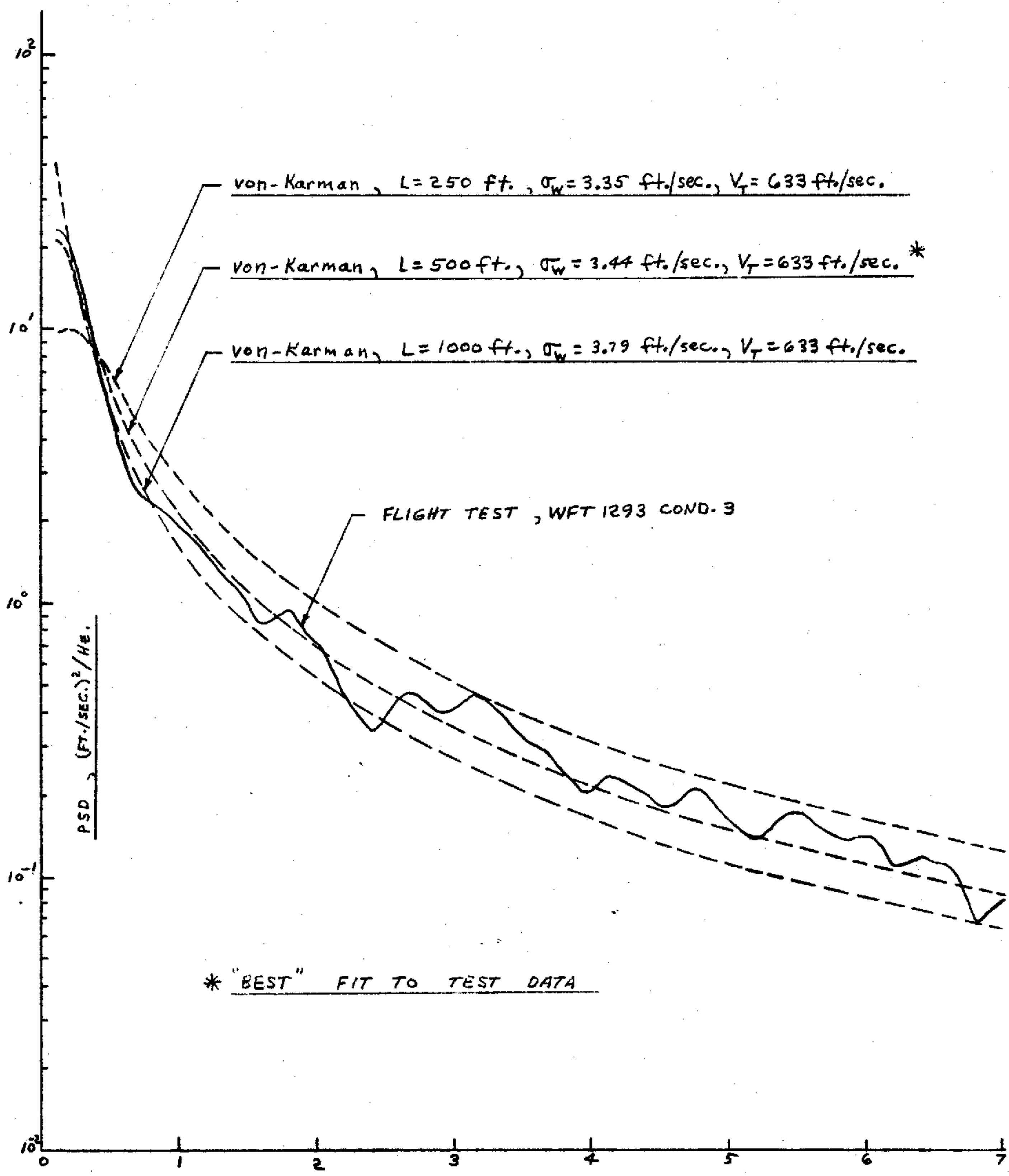

FIGURE C-1

Attachment (D)

SUMMARY OF SPECTRAL RELATIONSHIPS AND NOMENCLATURE

References:

(a) Boeing Document D3-7060-2, B-52C-F Dynamic Response and Loads Survey (Volume II) - WFT 1293

(b) Bendat, J. S. and Piersol, A. G., "Measurement and Analysis of Random Data," John Wiley and Sons, Inc., New York, 1966

Nomenclature

t = time, seconds

τ = correlation lag time, seconds

f = frequency, Hertz

$x(t)$, $y(t)$ = two quantities, for example CG - acceleration and gust velocity, which were measured and recorded continuously during flight through turbulence.

$R_{xy}(\tau)$ = cross-correlation function of $x(t)$ and $y(t)$

$R_{xx}(\tau)$, $R_{yy}(\tau)$ = auto-correlation functions of $x(t)$ and of $y(t)$

$G_{xy}(f)$ = cross-spectral density function of $x(t)$ and $y(t)$

$G_{xx}(f)$, $G_{yy}(f)$ = auto-spectral density functions of $x(t)$ and of $y(t)$

$\gamma^2_{xy}(f)$ = Coherence function of $x(t)$ and $y(t)$

$H_{x/y}(f)$ = Frequency response function, x (output) due to y (input)

Details of the flight test data handling and the planning and justification of parameter choices are found in the Boeing document referenced above. Only items important to this report are included here. The nomenclature used is the same as used by J. Bendat and A. Piersol in the second reference, above. The relationship of these parameters is listed below.

Standard Formulae

$$R_{xy}(\tau) = \frac{1}{t_{max.}} \times \int_0^{t_{max.}} x(t)\, y(t+\tau)\, dt$$

Note $R_{yx}(\tau) = R_{xy}(-\tau)$.

$R_{xx}(\tau)$ = as above, but with x replacing y.

$R_{yy}(\tau)$ = as above, but with y replacing x.

$$G_{xy}(f) = 2 \times \int_{-\tau_{max.}}^{\tau_{max.}} R_{xy}(\tau)\, e^{-i 2\pi f \tau}\, d\tau$$

Note $G_{yx}(f)$ = complex conjugate of $G_{xy}(f)$.

$G_{xx}(f)$ = as above, but using $R_{xx}(\tau)$.

$G_{yy}(f)$ = as above, but using $R_{yy}(\tau)$.

$$\gamma^2_{xy}(f) = \frac{|G_{xy}(f)|^2}{G_{xx}(f)\,G_{yy}(f)}$$

$$|H_{x/y}(f)|^2 = \frac{|G_{xy}(f)|^2}{G_{yy}(f)^2}$$, if y(t) is the vertical gust and there are no spanwise gust variations

$$|H_{x/y}(f)|^2 = \frac{G_{xx}(f)}{G_{yy}(f)}$$, if as above, and if there are no pilot inputs and no noise in the measurement of x(t).

Phase angle of $H_{xy}(f) = \arctan\left[\frac{\text{Imaginary part of } G_{xy}(f)}{\text{Real part of } G_{xy}(f)}\right]$ = phase angle of $G_{xy}(f)$.

Note phase angle of $G_{yx}(f)$ = -phase angle of $G_{xy}(f)$.

See Attachment (E), "Method of Response Calculations with Spanwise Gust Variations," for the calculation of the response spectral densities when there are multiple, partially coherent, inputs.

METHOD OF RESPONSE CALCULATIONS WITH SPANWISE GUST VARIATIONS

The frequency response of a load "L" to vertical gusts can be written as:

$$L(\omega) = \lfloor H_1(\omega) \quad H_2(\omega) \quad \cdots \quad H_n(\omega) \rfloor \begin{Bmatrix} w_1(\omega, x_1, y_1) \\ w_2(\omega, x_2, y_2) \\ \vdots \\ w_n(\omega, x_n, y_n) \end{Bmatrix}$$

where there are "n" gust reference stations with streamwise/spanwise coordinates x_i, y_i.

Each reference gust is assumed to directly affect only a local area of the airplane. Frequency responses for the load "L" due to each of the gusts must be known. A similar problem exists for one-dimensional turbulence when penetration effects must be considered -- the gusts "w_i" then are independent of the spanwise distance y.

The spectral density of the load is given by

$$G_{LL}(\omega) = \lfloor H_i(\omega) \rfloor \left[G_{ww}(\omega, x_i - x_j, y_i - y_j) \right] \left(\lfloor H_i(\omega) \rfloor \right)^{*T} \quad \triangleright 1$$

where the i, j element of the square n x n matrix $[G_{ww}]$ is the cross-spectral density of gusts at points (xi, yi) and (xj, yj).

The effects of the streamwise coordinate x (penetration effect) can be isolated as is the case with one-dimensional turbulence. An element of the $[G_{ww}]$ matrix can be written

$$G_{ij}(\omega, x_i - x_j, y_i - y_j) = e^{-\frac{i\omega(x_i - x_j)}{V}} \bar{G}_{ij}(\omega, y_i - y_j)$$

where $\bar{G}_{ij}$ is real and found as follows:

$$\bar{G}_{ij} = \frac{1}{\pi} \int_0^\infty R\left(\sqrt{\left(\frac{\tau V}{L}\right)^2 + \left(\frac{y_i - y_j}{L}\right)^2}\right) \cos(\omega\tau)\, d\tau$$

$R(\frac{\tau V}{L})$ is the one-dimensional auto-correlation function for vertical gusts, V is the true airspeed, L is the scale of turbulence.

von Karman $\quad R(z) = .5925\left(\frac{z}{1.339}\right)^{\frac{1}{3}} \left[K_{\frac{1}{3}}\left(\frac{z}{1.339}\right) - \frac{1}{2}\left(\frac{z}{1.339}\right) K_{\frac{2}{3}}\left(\frac{z}{1.339}\right) \right]$

The integration can be performed and the results expressed as follows:

$$\bar{G}_{ij} = \frac{.3165 L}{V} \left(\frac{-\mathcal{U}^{11/6} K_{\frac{1}{6}}(\mathcal{U}\sqrt{1+\gamma^2})}{(1+\gamma^2)^{11/12}} + \frac{(1+\frac{8}{3}\gamma^2)\mathcal{U}^{5/6} K_{\frac{5}{6}}(\mathcal{U}\sqrt{1+\gamma^2})}{(1+\gamma^2)^{17/12}} \right) \quad \triangleright 2$$

where $\quad \mathcal{U} = \frac{|y_i - y_j|}{1.339 L}, \quad \gamma = 1.339 \frac{L\omega}{V}$

Notice the elements of the $[G_{ww}]$ matrix must be computed for both left and right sides of the airplane, even if only symmetric responses are wanted. Antisymmetric responses to vertical gusts can as easily be computed.

1▷ The cross-spectral density of two loads can be computed by letting the pre- and post-multiplying H's be for two different loads.

2▷ This expression is given in D. Sawdy's thesis. See Attachment (A) reference c. It is identified as $\hat{\Phi}_{33}(r_2, \Omega_1)$.

Attachment (F)

EQUATIONS OF MOTION AND RESPONSE EQUATIONS

References:
(a) Boeing Document D3-7763-1, B-52 Aeroelastic Model -- Summary report
(b) Boeing Document D3-7763-3, B-52 Aeroelastic Model -- Equations of Motion and Response Equations -- Data

Errata: D3-7763-3, pages 1-237 and 1-238, Matrix $[C]_{WG}$ and Matrix $[D]_{WG}$ were erroneously documented for the wrong response stations. All documented wing load calculations were correct, however. The corrected pages for this document are attached.

The equations of motion used for the theoretical responses of this study were in the following form (LaPlace Domain):

$$\left(s^2[N_2] + s[N_1] + [N_0] + s\,\phi(s)[\bar{R}_2] + \phi(s)[\bar{R}_3]\right)\{q(s)\} + \frac{1}{V}\psi(s)[\bar{R}_1]\ \{w_i(s, x_i, y_i)\}$$

The form and coefficients are identical to those published in references a and b with the following exceptions:

- for convenience, the coefficients are for real-time derivatives instead of (Vt/b_r) derivatives.
- The gust coefficients have been combined into a single $[\bar{R}_1]$ matrix. Gust velocities "w_i" are at the following reference stations:

Body Station	Buttock Line	
-108.3	0.	(reference gust, probe)
100.0	0.	(forward body ref.)
509.2	±111.0	(wing ref.)
675.9	±333.0	(wing ref.)
842.6	±555.0	(wing ref.)
1009.3	±777.0	(wing ref.)
1176.0	±999.0	(wing ref.)
1500.0	0.0	(aft body ref.)
1572.0	±90.0	(horizontal tail ref.)
1729.0	±260.0	(horizontal tail ref.)

Note that right side and left side gusts are not identical. Only the symmetric part of the airplane response is being computed, since the flight test responses were averaged (1/2 left plus 1/2 right) and then correlated with the gust.

The responses were calculated from the following equations:

$$\{\text{Responses}(s)\} = \left([C_{MD}] + s^2[\Phi]\right)\{q(s)\} + [C_W]\{w_i(s, x_i, y_i)\}$$

Using the mode displacement method of computing bending moments for the wing and body of the B-52 gives answers identical to about 3 decimal places with the answers of the load summation method. The mode displacement coefficients were used here for convenience. If the number of elastic modes were to be reduced to fewer than thirty, we would recommend using the documented load summation coefficients.

Coefficient matrices for the equations of motion and response equations are attached.

MATRIX 'NZ..' 34 BY 34 COEFFICIENTS FOR $s^2 \{g(s)\}$

ROW 1

7.75155E-01	-1.14538E-02	5.98009E-06	1.26801E-03	4.59801E-04
-9.57155E-04	-2.05266E-04	4.53954E-06	1.48698E-04	1.04168E-03
-1.51021E-03	1.94793E-03	3.07990E-04	2.36041E-05	3.18423E-05
3.58117E-04	1.86473E-04	2.97714E-04	4.14403E-04	2.17573E-04
5.59334E-04	3.39858E-04	-7.06653E-05	1.11022E-04	-2.48988E-05
-3.51856E-05	-1.12128E-05	8.14362E-05	-8.15911E-06	5.77597E-05
-6.41565E-05	5.30283E-06	1.49582E-06	5.71295E-06	

ROW 2

-1.14528E-02	4.35030E 00	1.33266E-03	-9.34277E-04	-6.83285E-04
-2.33715E-03	-1.45521E-03	-3.31874E-04	-3.95243E-03	-3.02490E-03
3.80043E-03	-1.66731E-03	1.12921E-04	1.01824E-04	-1.25879E-05
-5.35817E-04	-1.37627E-03	-2.64014E-03	-2.16034E-03	-5.40216E-04
-3.52190E-03	-1.66562E-03	-7.53728E-04	8.76656E-04	1.17419E-04
1.51438E-04	-1.29079E-05	-5.93319E-04	6.47450E-05	-1.15684E-04
-5.53055E-05	4.93977E-05	-1.18201E-05	-4.76153E-05	

ROW 3

5.98005E-06	1.33266E-03	2.71469E-02	6.09546E-04	3.76789E-04
-2.46371E-04	-3.29953E-05	-2.56959E-06	-1.30299E-04	-2.52565E-04
3.33336E-04	1.47113E-06	-1.19652E-04	-3.50498E-05	2.05709E-06
1.47723E-04	-7.67119E-05	4.36700E-04	-1.92327E-04	1.17833E-04
-6.44245E-05	-4.37526E-05	-2.72914E-04	-2.30791E-05	4.25743E-06
1.02055E-05	6.16252E-05	-2.80330E-05	2.76860E-05	8.78031E-06
1.55496E-05	2.46119E-06	-1.00842E-06	-1.96392E-06	

ROW 4

1.26801E-03	-9.34277E-04	6.09546E-04	1.33803E-01	5.07696E-04
-9.27766E-06	5.91259E-05	1.83087E-05	-7.14653E-06	-2.44154E-04
3.52034E-04	3.61224E-04	-5.10670E-06	-6.36254E-05	7.00646E-06
2.48763E-04	-3.21887E-05	5.31165E-04	-9.99274E-05	1.02599E-04
1.12254E-04	6.05771E-05	-3.07246E-04	-3.57105E-05	5.45002E-06
3.58415E-06	3.71933E-05	-9.60926E-06	2.05410E-05	1.62909E-05
5.42234E-06	1.10090E-05	-2.48995E-06	6.05175E-06	

ROW 5

4.59801E-04	-6.83285E-04	3.76789E-04	5.07696E-04	5.39800E-02
1.74993E-04	9.36675E-05	2.06191E-05	3.85070E-05	-2.48568E-04
4.10757E-04	2.16290E-04	1.62884E-05	-5.38715E-05	3.51085E-06
1.81537E-04	-1.76976E-05	3.91032E-04	-5.87578E-05	1.33627E-04
3.61517E-05	7.87638E-05	-1.90371E-04	-2.96264E-05	4.64642E-06
1.29055E-05	2.21443E-05	-4.15373E-06	1.59410E-05	1.33706E-05
9.37423E-06	5.37710E-06	1.61424E-06	1.20673E-05	

ROW 6

-9.57155E-04	-2.33719E-03	-2.46371E-04	-9.27766E-06	1.74993E-04
1.11125E-01	4.37004E-04	7.60299E-05	4.13838E-04	-4.14303E-04
5.66529E-04	3.14041E-05	3.02546E-04	-8.29827E-05	-1.07757E-05
7.45983E-05	9.65849E-05	3.73703E-04	1.40431E-04	8.37338E-05
-4.51974E-05	3.61116E-04	1.34440E-05	-5.80491E-05	1.75888E-06
-2.51165E-05	-5.68105E-06	3.56126E-05	2.17848E-06	2.37606E-05
3.10505E-05	1.58118E-05	7.38656E-07	-4.61209E-06	

MATRIX '…'   34 BY   34

ROW 7

-3.09264E-04	-1.45521E-03	-3.28853E-05	5.81259E-05	9.36675E-05
4.37004E-04	3.06930E-02	2.65568E-05	1.51380E-04	-1.52560E-04
3.00546E-04	6.02471E-05	8.25867E-05	-3.35922E-05	-2.05929E-06
6.09553E-05	3.34203E-05	1.52764E-04	4.22831E-05	4.80653E-05
-1.89806E-05	1.34436E-04	-1.26640E-05	-3.17732E-05	1.34116E-05
-6.29562E-06	-7.12007E-06	1.22091E-05	1.32763E-06	8.07291E-06
7.67351E-06	5.58244E-06	5.08596E-07	-2.03316E-06	

ROW 8

4.53954E-04	-3.31874E-04	-2.56959E-06	1.83087E-05	2.06191E-05
7.69359E-05	2.66569E-05	6.90051E-03	2.89104E-05	-2.33239E-05
4.36346E-05	1.45684E-05	1.57388E-05	-5.93368E-06	-3.89970E-07
1.06398E-05	7.01538E-06	3.34079E-05	8.79015E-06	9.76020E-06
1.07091E-06	2.39220E-05	-3.68036E-06	-6.36098E-06	2.74826E-07
-1.93527E-06	2.94200E-07	2.57761E-06	3.25563E-07	1.85786E-06
1.61071E-06	5.53781E-07	2.33295E-07	-2.86675E-07	

ROW 9

1.49699E-04	-3.95243E-03	-1.20299E-04	-7.14653E-06	3.85070E-05
4.13938E-04	1.51380E-04	2.99104E-05	2.00882E-02	2.64393E-05
3.89340E-05	5.77575E-05	7.08940E-05	-2.08287E-05	-2.17304E-06
3.37043E-05	9.27520E-05	1.88309E-04	9.85647E-05	3.79368E-05
1.49527E-05	1.37667E-04	4.33590E-05	-6.15316E-05	-8.04733E-06
-2.10347E-05	-1.07537E-05	2.91461E-05	-5.16942E-06	9.27004E-06
1.41417E-05	1.07336E-06	1.46714E-06	-7.50723E-06	

ROW 10

1.04166E-03	-3.07490E-03	-2.52565E-04	-2.44194E-04	-2.48568E-04
-4.14303E-04	-1.52560E-04	-2.33239E-05	2.64293E-05	5.71779E-07
-9.98430E-04	-1.92757E-04	-1.61929E-05	8.02358E-05	-5.51410E-06
-3.71630E-04	8.47787E-05	-3.25901E-04	8.55861E-05	-1.20902E-04
1.83337E-04	-1.38512E-04	1.36911E-04	7.26417E-06	-1.87770E-05
-1.94377E-05	7.25805E-06	3.13956E-05	-2.09714E-05	-7.40666E-06
-1.34644E-05	-1.95262E-05	1.24530E-06	1.33155E-05	

ROW 11

-1.51071E-03	3.80943E-03	3.33336E-04	3.92034E-04	4.10357E-04
6.64539E-04	3.00546E-04	4.76246E-05	2.88340E-05	-8.98430E-04
1.54735E-01	3.37546E-04	9.06471E-05	-1.27783E-04	4.68787E-06
3.55566E-04	-1.07313E-04	5.33248E-04	-1.12443E-04	1.98367E-04
-1.93634E-04	1.87411E-04	-1.54658E-04	-1.58207E-05	3.63374E-05
3.10463E-05	-4.19696E-05	-2.66323E-05	2.64499E-05	1.93318E-05
3.97324E-05	3.15845E-05	-1.75791E-06	2.46116E-06	

ROW 12

1.94793E-03	-1.66731E-03	1.43113E-06	3.61224E-04	3.16280E-04
3.14041E-05	6.02471E-05	1.45684E-05	9.77975E-05	-1.92757E-04
3.37546E-04	7.40798E-02	3.60687E-05	-8.75784E-05	3.68158E-05
5.56984E-04	1.01852E-04	3.00839E-04	-3.47345E-06	2.27573E-04
1.89391E-05	-4.46545E-05	-5.44580E-05	-1.27750E-05	-3.29980E-05
-1.47497E-06	-1.41205E-04	1.59052E-05	1.55919E-05	7.78746E-05
-3.29973E-06	2.31127E-05	8.99872E-07	1.25688E-05	

MATRIX 'N2..' 34 BY 34

ROW 13

3.07990E-04	1.12921E-04	-1.19692E-04	-5.10670E-06	1.62884E-05
3.02546E-04	8.25867E-05	1.57388E-05	7.08940E-05	-1.61929E-05
9.96471E-05	2.60687E-05	3.59333E-02	-2.79302E-06	-7.23373E-06
-5.15183E-05	9.34560E-05	-1.11681E-04	-6.08142E-06	-1.55457E-05
-3.31447E-05	8.68363E-05	-3.57986E-05	2.44403E-05	-1.91383E-05
-2.26296E-05	-1.32721E-05	6.77162E-06	-5.79815E-06	4.99608E-06
-3.10130E-05	4.69445E-06	5.23367E-07	-1.05373E-05	

ROW 14

3.26041E-05	1.01824E-04	-3.59498E-05	-6.36254E-05	-5.38715E-05
-9.35927E-05	-3.35922E-05	-5.93268E-06	-2.08297E-05	8.02358E-05
-1.27793E-04	-8.75784E-05	-2.79302E-06	6.15447E-03	-2.18336E-06
-6.26185E-05	1.78407E-06	-6.98774E-05	3.08311E-06	-3.09590E-05
6.76575E-06	-1.76894E-05	1.87841E-05	8.84404E-06	-1.30415E-06
-9.80395E-07	7.72099E-06	-3.10874E-07	-3.21849E-06	-3.15505E-06
-2.56336E-05	-3.46819E-06	2.74269E-07	5.32392E-06	

ROW 15

3.18433E-05	-1.25879E-05	2.05709E-06	7.00646E-06	3.51085E-06
-1.07757E-05	-2.05929E-06	-3.88970E-07	-2.17304E-06	-5.51410E-06
4.69282E-06	3.68159E-05	-7.23373E-06	-2.18336E-06	3.05356E-03
1.85365E-05	-9.22921E-07	6.69791E-06	-2.73909E-07	6.28203E-06
4.00296E-06	-5.01158E-06	-5.91668E-07	-3.14435E-07	-3.54364E-07
1.04684E-06	-4.85522E-06	6.23851E-08	7.47311E-07	4.44418E-07
-1.23364E-06	2.89469E-07	-1.23750E-07	1.51552E-06	

ROW 16

2.58117E-04	-5.25817E-04	1.47723E-04	2.48763E-04	1.81537E-04
7.45982E-05	6.09553E-05	1.06298E-05	3.37042E-05	-2.71630E-04
3.55566E-04	5.56984E-04	-9.15183E-05	-6.26198E-05	1.85365E-05
1.70104E-02	-2.59251E-05	2.64101E-04	-2.16639E-07	1.42253E-04
7.49818E-06	2.57790E-05	-6.20162E-05	-3.32267E-05	3.24347E-06
1.50289E-05	-4.30855E-05	1.06723E-06	1.60486E-05	1.08549E-05
2.27004E-06	1.15014E-05	-9.80282E-07	-1.04325E-05	

ROW 17

1.66473E-04	-1.37627E-03	-7.67119E-05	-3.21887E-05	-1.76976E-05
9.65849E-05	3.34203E-05	7.01538E-06	9.77520E-05	8.47787E-05
-1.07313E-04	1.01857E-04	8.34560E-05	1.78407E-06	-9.33971E-07
-3.98251E-05	8.89212E-04	5.92211E-06	4.65212E-06	7.07752E-07
-1.64054E-05	-1.65530E-05	-1.55295E-05	7.90477E-06	4.47441E-06
4.63653E-07	-5.82357E-07	1.23943E-05	-5.41350E-06	5.01205E-06
-3.69512E-06	2.88887E-07	2.59345E-07	2.99952E-08	

ROW 18

3.92714E-04	-2.64014E-03	4.36700E-04	5.31165E-04	3.81032E-04
7.73703E-04	1.59764E-04	3.34079E-05	1.88309E-04	-2.25901E-04
5.33245E-04	3.00838E-04	-1.11681E-04	-6.98774E-05	6.69791E-06
3.64101E-04	5.92211E-06	3.25075E-02	-7.99915E-05	2.65510E-04
6.15331E-05	1.16308E-04	-2.03044E-04	-1.18895E-04	3.14718E-05
-1.45069E-05	6.80145E-05	3.84483E-06	1.17887E-05	2.52862E-05
1.34946E-04	5.67736E-06	-3.54021E-07	-1.37470E-05	

MATRIX 'N2..'   34 BY   34

ROW 19

4.14403E-04	-2.16034E-03	-1.92327E-04	-9.99274E-05	-5.87578E-05
1.40431E-04	4.22831E-05	8.79015E-06	9.85647E-05	8.55861E-05
-1.13443E-04	-3.47345E-06	-6.08142E-06	3.08311E-06	-2.73909E-07
-3.16635E-07	4.65212E-06	-7.99915E-05	1.20289E-02	-2.19454E-05
5.06342E-05	8.76917E-05	1.04021E-04	-4.89778E-06	3.26577E-05
3.27485E-05	1.00947E-05	2.17484E-05	-7.96682E-06	3.15980E-06
-1.43205E-05	-3.53529E-06	-1.07866E-07	-1.55979E-06	

ROW 20

2.17573E-04	-5.49216E-04	1.17833E-04	1.92599E-04	1.32637E-04
5.37238E-05	4.80653E-05	9.76020E-06	3.79368E-05	-1.20902E-04
1.98267E-04	2.27573E-04	-1.55457E-05	-3.08590E-05	6.28203E-06
1.42953E-04	7.07752E-07	2.65510E-04	-2.19454E-05	1.51525E-03
2.74133E-05	5.23544E-05	-9.99498E-05	-2.72979E-05	1.96176E-06
8.48627E-07	-5.30375E-06	5.18910E-07	5.91958E-06	6.09809E-06
7.69823E-06	5.26474E-06	1.93315E-07	5.18920E-06	

ROW 21

9.58374E-04	-2.53190E-03	-6.44242E-05	1.13254E-04	3.61517E-05
-4.51934E-05	-1.88906E-05	1.03091E-06	1.48527E-05	1.83227E-04
-1.93634E-04	7.99201E-05	-3.31447E-05	6.76575E-06	4.00256E-06
7.49815E-06	-1.64054E-05	6.15331E-05	8.06342E-05	2.74133E-05
1.63555E-02	2.73449E-05	-2.98030E-06	1.59474E-05	-5.62505E-06
3.34200E-06	9.46606E-06	2.00623E-05	-5.57326E-06	2.94114E-06
1.14294E-05	-4.66443E-07	-8.79274E-07	2.44942E-05	

ROW 22

3.29555E-04	-1.66562E-03	-4.27526E-05	6.05771E-05	7.97638E-05
3.61116E-04	1.24436E-04	2.29220E-05	1.27667E-04	-1.38512E-04
1.87411E-04	-4.46545E-05	8.68363E-05	-1.78834E-05	-5.01158E-06
3.57790E-05	-1.65530E-05	1.16309E-04	8.76917E-05	5.23544E-05
3.72449E-05	1.80039E-02	-9.65393E-05	-1.05238E-05	-6.81529E-06
-6.29592E-06	2.75384E-05	1.99683E-05	-2.50259E-06	1.39126E-06
-7.12736E-06	3.13031E-06	-5.81852E-07	-2.24708E-05	

ROW 23

-7.56653E-05	-7.53728E-04	-2.72814E-04	-3.07246E-04	-1.90371E-04
1.34440E-05	-1.36440E-05	-3.69036E-06	4.32590E-05	1.36911E-04
-1.54695E-04	-5.44590E-05	-3.57986E-05	1.87841E-05	-5.91668E-07
-6.30162E-05	-1.55395E-05	-2.03044E-04	1.04021E-04	-9.99488E-05
-2.98030E-06	-9.65393E-05	1.60549E-02	-2.07925E-06	-2.50385E-06
-1.56031E-05	-5.13511E-05	1.56873E-05	-1.07030E-05	2.23014E-06
3.70955E-05	-8.81819E-07	-3.06787E-07	6.66958E-06	

ROW 24

1.11033E-04	8.76656E-04	-2.39791E-05	-3.57105E-05	-2.96264E-05
-5.90481E-05	-3.17732E-05	-6.36088E-06	-6.15316E-05	7.26417E-06
-1.59207E-05	-1.37750E-05	2.44403E-05	8.34404E-06	-3.14435E-07
-3.32267E-05	7.89477E-06	-1.19985E-04	-4.89778E-06	-2.72979E-05
1.59474E-05	-1.05238E-05	-2.07925E-06	4.91686E-03	1.40032E-05
2.76517E-05	2.57370E-05	-6.98107E-06	4.60476E-07	-1.48086E-05
1.57677E-05	2.41050E-06	-2.25397E-07	9.24333E-06	

MATRIX INV.. 34 BY 34

ROW 25

-3.49095E-05	1.17419E-04	4.25743E-06	5.45002E-06	4.64642E-06
1.75988E-06	1.34116E-06	2.76826E-07	-8.04723E-06	-1.87770E-05
3.63214E-05	-3.39880E-05	-1.91383E-05	-1.30415E-06	-3.54364E-07
3.24747E-06	4.42441E-06	3.14718E-05	3.26577E-05	1.96176E-06
-5.62505E-06	-6.81529E-06	-2.50385E-06	1.40022E-05	1.01109E-03
3.66058E-05	3.09029E-05	-3.73666E-06	-9.43502E-07	1.02603E-06
-3.73942E-06	1.47407E-07	-1.24005E-06	-2.13737E-06	

ROW 26

-2.51856E-05	1.81638E-04	1.02098E-05	2.58415E-06	1.28099E-06
-2.51165E-05	-8.28562E-06	-1.92523E-06	-2.10347E-05	-1.94277E-05
2.30463E-05	-7.47497E-06	-2.26296E-05	-9.89035E-07	1.04684E-06
1.50295E-05	4.63657E-07	-1.45069E-05	2.27495E-05	8.48627E-07
3.34200E-06	-6.29292E-06	-1.56031E-05	2.76517E-05	3.66058E-05
6.67125E-04	2.29680E-05	-5.11704E-06	1.22923E-06	-3.14839E-07
-5.20360E-06	2.49832E-07	-1.17493E-06	2.11903E-06	

ROW 27

-1.12125E-05	-1.20979E-05	6.16252E-05	2.71193E-05	2.21443E-05
-5.63105E-06	-7.12007E-06	2.94200E-07	-1.07537E-05	7.25806E-06
-4.16564E-05	-1.41205E-04	-1.32221E-05	7.72099E-06	-4.85922E-06
-4.90855E-05	-5.82357E-07	6.80145E-05	1.00947E-05	-9.20375E-06
9.44606E-06	2.75384E-05	-5.13511E-05	2.52270E-05	3.09029E-05
2.20680E-05	5.88829E-03	-4.24527E-06	4.04093E-06	3.04494E-06
4.32020E-05	-9.84174E-07	-8.69741E-07	-5.67347E-06	

ROW 28

9.14763E-05	-5.93219E-04	-2.80330E-05	-9.60826E-06	-4.15273E-06
3.56126E-05	1.22091E-05	2.57261E-06	2.91441E-05	2.13956E-05
-2.66323E-05	1.68092E-05	6.77162E-06	-3.10874E-07	6.23851E-08
1.06723E-06	1.32043E-05	3.84483E-06	2.17484E-05	9.18910E-07
3.00623E-05	1.98683E-05	1.56873E-05	-6.98107E-06	-3.73666E-06
-5.11304E-06	-4.24527E-06	1.82556E-04	-5.20144E-06	5.95426E-06
-3.42060E-06	6.49774E-08	-5.27128E-07	6.79660E-09	

ROW 29

-5.15911E-06	6.47450E-05	2.76860E-05	2.05419E-05	1.59410E-05
3.17848E-06	1.32763E-06	3.25563E-07	-5.16942E-06	-2.09214E-05
3.64455E-05	1.55919E-05	-5.79815E-06	-3.21849E-06	7.47311E-07
1.40486E-05	-5.41350E-06	1.17887E-05	-7.96682E-06	5.91958E-06
-5.57226E-06	-2.50259E-06	-1.07020E-05	4.60426E-07	-9.43502E-07
1.23923E-06	4.04093E-06	-5.49144E-06	2.00355E-04	1.40477E-06
-1.91890E-06	1.21028E-06	2.27206E-07	-1.90312E-07	

ROW 30

5.77557E-05	-1.15684E-04	8.78931E-06	1.62909E-05	1.32706E-05
3.37606E-05	8.07291E-06	1.85786E-06	9.27004E-06	-7.40666E-06
1.92319E-05	2.78246E-05	4.99608E-06	-2.15505E-06	4.44418E-07
1.08545E-05	5.11205E-06	2.52862E-05	3.15980E-06	6.09809E-06
2.94114E-06	1.79126E-06	2.23014E-06	-1.48086E-06	1.02603E-06
-3.14839E-07	3.04494E-06	5.96426E-06	1.40477E-06	3.27051E-04
3.71385E-07	1.99539E-06	-1.81899E-07	1.02500E-07	

MATRIX 'A2..' 34 BY 34

ROW 31

-6.41669E-05	-9.52508E-05	1.55486E-05	5.42234E-06	9.37423E-06
2.10505E-05	7.67351E-06	1.61071E-06	1.41417E-05	-1.34644E-05
3.87324E-05	-3.29973E-06	-2.10130E-05	-2.56336E-06	-1.23364E-06
2.27004E-06	-2.68512E-06	1.34948E-04	-1.43235E-05	7.68823E-06
1.14294E-05	-7.12736E-06	2.70098E-05	1.57877E-05	-2.73842E-06
-5.20360E-06	4.32020E-05	-3.43060E-06	-1.91890E-06	3.71388E-07
5.36704E-07	8.93126E-06	-2.07921E-07	2.19354E-06	

ROW 32

5.30283E-06	4.93977E-05	2.46119E-06	1.10090E-05	9.37710E-06
1.58115E-05	5.58244E-06	9.53781E-07	1.07336E-06	-1.95262E-05
3.15845E-05	2.31127E-05	4.69445E-06	-3.46819E-06	2.89469E-07
1.15014E-05	2.88887E-07	5.67736E-06	-3.53529E-06	5.26474E-06
-4.66443E-07	3.13031E-06	-9.81819E-07	2.41050E-06	1.47407E-07
2.40832E-07	-9.84174E-07	6.49774E-08	1.31038E-06	1.99539E-06
5.93126E-06	4.31972E-04	5.19151E-08	-8.80366E-07	

ROW 33

3.60225E-07	-4.13710E-06	-5.66663E-07	-2.31753E-06	1.70657E-06
3.52230E-07	3.43940E-07	1.98536E-07	1.05459E-06	8.94610E-07
-1.33781E-06	6.74908E-07	3.87555E-07	2.71574E-07	-1.22406E-07
-5.50435E-07	2.50367E-07	-2.66200E-07	-2.10194E-07	1.94636E-07
-1.06532E-06	-1.18137E-06	-5.22957E-07	-7.96545E-08	-1.09169E-06
-1.06030E-06	-7.76497E-07	-5.11665E-07	2.13942E-07	-1.66755E-07
-2.36535E-07	8.92036E-08	5.30910E-06	0.0	

ROW 34

5.71295E-06	-4.76153E-05	-1.86392E-06	6.05175E-06	1.20673E-05
-4.61210E-06	-3.03216E-06	-2.86675E-07	-7.50723E-06	1.33155E-05
3.46116E-06	1.25688E-05	-1.05373E-05	5.33382E-06	1.51552E-06
-1.04325E-05	2.99952E-08	-1.37470E-05	-1.55979E-06	5.19920E-06
2.44947E-05	-3.24708E-05	6.66558E-06	9.24333E-06	-3.13737E-06
2.11903E-06	-5.67347E-06	6.79660E-09	-1.80312E-07	1.02500E-07
2.19354E-06	-8.80366E-07	0.0	6.23474E-05	

MATRIX 'M1..' 34 BY 34 *COEFFICIENTS FOR s{q(s)}*

ROW 1

2.91724E-02	-6.21381E-01	-6.00573E-03	1.12019E-01	4.57720E-02
-4.69481E-02	-1.10753E-02	-1.47312E-03	-1.96004E-02	7.31614E-02
-4.77120E-02	5.12165E-02	1.37316E-02	-1.13860E-03	3.62123E-03
-4.61300E-03	1.83685E-02	-2.43229E-02	-7.83445E-02	2.19838E-02
1.37099E-01	-9.56576E-02	-5.30536E-02	-1.49151E-02	-3.90082E-02
-2.85973E-02	-5.26729E-02	-1.47278E-02	1.12250E-03	-1.64664E-02
-1.02992E-02	2.49306E-03	5.04209E-02	7.43074E-03	

ROW 2

4.41972E-02	1.37856E 00	1.71046E-02	-2.41593E-01	-9.58405E-02
-3.47085E-03	-3.69747E-02	-9.16686E-03	-1.20277E-01	-1.82448E-01
2.54273E-01	-2.66210E-01	-2.66187E-01	5.92526E-04	3.89503E-03
9.59761E-02	-1.22846E-01	-3.10027E-02	3.11639E-01	-5.75728E-02
1.74370E-02	1.96588E-01	2.52235E-01	1.83352E-01	2.54138E-01
3.21676E-01	1.64842E-01	1.06701E-01	-2.21364E-02	7.55817E-02
-7.00155E-03	8.12877E-03	-3.92720E-02	-1.16030E-02	

ROW 3

-2.40537E-03	6.83227E-03	2.56465E-02	4.62537E-02	2.01442E-02
-1.67661E-02	1.32192E-03	2.59185E-04	-4.39938E-03	-5.50413E-03
7.72435E-03	-2.02711E-02	-1.11008E-02	-1.56447E-03	-2.26642E-04
5.60924E-03	-7.07604E-03	1.69026E-02	1.76973E-02	1.06783E-02
2.33014E-02	8.40671E-03	-2.89120E-02	-9.41357E-03	1.80394E-02
1.11643E-02	6.73669E-03	4.50129E-03	-8.94387E-03	-2.41249E-03
-9.30447E-03	-7.56935E-04	-2.19263E-03	6.98446E-05	

ROW 4

3.21351E-03	-1.05055E-01	3.77837E-03	1.42569E-01	3.38176E-02
-2.93915E-02	2.06645E-03	4.19583E-04	-1.88390E-03	1.59149E-03
4.55180E-03	-7.77315E-03	-4.37526E-03	-2.69010E-03	1.00981E-04
7.90866E-03	-2.81232E-03	2.13890E-02	1.75306E-03	2.06499E-02
3.77312E-02	5.27871E-03	-5.29744E-02	-2.08763E-02	1.08175E-02
3.08644E-03	-1.35105E-02	3.83157E-04	-1.17235E-02	-5.09671E-03
-1.66343E-02	-1.15565E-03	-9.87979E-04	1.43231E-03	

ROW 5

1.04711E-02	-4.00620E-02	1.91328E-03	4.24270E-02	5.06853E-02
-1.56525E-02	3.48457E-03	4.24233E-04	2.11168E-03	-4.46300E-03
6.77771E-03	-3.72901E-03	-1.13440E-03	-1.78118E-03	-4.71640E-05
6.09683E-03	-1.57903E-03	1.56637E-02	1.99149E-03	1.29411E-02
1.07096E-02	1.23716E-02	-3.11287E-02	-1.41722E-02	6.71023E-03
2.04147E-03	-1.04063E-02	-1.38582E-06	-7.56224E-03	-6.08858E-03
-1.16565E-02	-1.12842E-03	-5.56345E-04	1.12756E-04	

ROW 6

6.27783E-03	5.85068E-02	-3.96077E-03	-1.80587E-02	-7.70622E-03
9.64965E-03	1.25396E-02	1.72602E-03	2.70018E-02	-2.17120E-02
7.37899E-03	1.73359E-02	2.16148E-02	-9.08907E-04	-8.64073E-04
3.40322E-03	8.49129E-03	8.28516E-03	-1.49179E-02	4.11357E-03
-7.36859E-03	4.57141E-02	-7.01815E-03	-1.87322E-02	-1.34634E-02
-1.57362E-02	-2.17846E-02	-7.37949E-03	4.44374E-04	-7.32977E-03
-7.69719E-03	-1.45894E-03	2.90328E-03	-4.48851E-03	

MATRIX 'N1..' 34 BY 34

ROW 7

1.42361E-03	2.60952E-02	-9.11438E-04	1.57048E-03	5.86560E-04
2.15359E-03	2.84533E-02	6.69910E-04	1.03315E-02	-7.59691E-03
4.37804E-03	6.46949E-03	7.91062E-03	-6.84592E-04	-2.91652E-04
2.13560E-03	2.90829E-03	7.13452E-03	-5.15883E-03	3.95889E-03
-2.42027E-02	1.73444E-02	-7.84304E-03	-9.09099E-03	-4.05805E-03
-5.33159E-03	-1.11974E-02	-3.01163E-03	-1.28016E-03	-3.80230E-03
-4.67264E-03	-8.57616E-04	1.00976E-03	-1.55669E-03	

ROW 8

4.40915E-04	2.79261E-03	-1.46926E-04	1.06759E-03	4.43595E-04
3.79010E-04	8.09649E-04	5.41992E-03	1.80743E-03	-8.99847E-04
1.97872E-04	1.12161E-03	1.51998E-03	-1.19355E-04	-5.78782E-05
2.34342E-04	6.15746E-04	1.21301E-03	-1.25139E-03	8.00972E-04
-3.63166E-03	2.57093E-03	-1.96952E-03	-1.85750E-03	-8.92110E-04
-1.15232E-03	-1.93042E-03	-6.33330E-04	-7.28068E-04	-7.59508E-04
-7.39589E-04	-1.50222E-04	2.11119E-04	-2.58520E-04	

ROW 9

1.33933E-02	1.87887E-02	-1.23259E-03	2.07143E-03	6.07296E-04
7.97678E-03	6.43435E-03	1.07012E-03	3.52470E-02	2.04144E-03
-6.91274E-03	1.45697E-02	1.65326E-02	-3.12395E-04	-4.68565E-04
-2.77259E-03	7.98241E-03	7.14779E-03	-1.53795E-02	3.39315E-03
-2.83810E-02	7.43357E-03	-1.12175E-02	-1.28328E-02	-1.41206E-02
-1.35491E-02	-1.47610E-02	-7.47833E-03	1.08856E-03	-5.55975E-03
-5.91462E-04	-1.30919E-03	2.91066E-03	-1.64670E-03	

ROW 10

4.13268E-03	-6.85523E-02	-2.96311E-04	7.58872E-04	1.17582E-04
1.09114E-02	-5.07165E-03	-5.27247E-05	-4.07808E-03	9.79099E-03
-3.47763E-02	6.94982E-03	6.59595E-03	1.90132E-03	5.38426E-05
-1.43244E-02	7.40903E-03	-1.99898E-02	-1.95824E-02	-9.05731E-03
2.97968E-02	-4.94264E-02	5.83814E-03	5.57337E-03	-1.73089E-02
-1.17186E-02	1.75631E-02	-5.30916E-03	8.87032E-03	2.61435E-03
1.65863E-02	1.74339E-03	2.71697E-03	3.50805E-03	

ROW 11

3.17569E-03	1.08101E-01	-4.67664E-04	1.36708E-03	6.26112E-04
-1.55579E-02	8.43835E-03	3.17302E-04	8.79381E-03	-4.36883E-02
2.39581E-01	-7.34562E-03	-1.10269E-02	-3.00246E-03	2.03646E-04
2.22693E-02	-9.20803E-03	3.39669E-02	2.17732E-02	1.57629E-02
-4.19470E-02	7.31620E-02	-9.49980E-03	-8.97088E-03	2.22958E-02
1.48668E-02	-2.81790E-02	6.20682E-03	-1.38654E-02	-5.88713E-03
-2.40827E-02	-3.09033E-03	-3.51378E-03	-2.28245E-03	

ROW 12

-5.18974E-03	-1.56083E-01	-3.03025E-03	1.24643E-02	3.55680E-03
-3.39141E-02	-1.35771E-03	-1.13651E-03	1.38458E-03	1.41198E-02
1.36767E-02	1.74816E-01	7.52353E-03	-1.37869E-03	1.82385E-03
3.77384E-03	8.39712E-03	3.55174E-02	-2.39737E-02	1.80693E-02
1.68716E-02	-7.90409E-03	-2.15858E-02	-5.14746E-03	-1.25433E-02
-5.71625E-03	-6.13847E-02	-9.50398E-03	-5.15016E-03	-1.34524E-02
-1.98716E-02	-6.05745E-03	3.30403E-03	4.25964E-03	

MATRIX 'N1..' 34 BY 34

ROW 13

-4.24203E-03	-3.97174E-02	-1.92486E-03	-4.48005E-03	-2.07107E-03
8.94256E-04	2.15906E-03	1.89609E-04	5.41708E-03	-6.55845E-03
-3.24124E-03	1.33783E-02	9.84504E-02	-2.33440E-05	-3.45342E-04
-2.50700E-03	6.50960E-03	-7.89022E-03	-1.04423E-02	-1.12445E-03
-2.02826E-02	4.93492E-03	-1.44905E-03	-3.63670E-03	-8.43303E-03
-7.95344E-03	-5.77037E-03	-6.22684E-03	4.53196E-03	-2.99576E-03
4.94790E-04	1.14829E-03	2.64846E-03	-1.46434E-03	

ROW 14

-1.17030E-04	-1.45699E-03	-1.69265E-05	-3.19734E-03	-1.28664E-03
2.27971E-03	-1.00126E-03	-5.69239E-05	-1.51255E-03	2.16047E-03
-4.00315E-03	-1.27756E-03	-5.10309E-05	1.40515E-02	-5.99303E-05
-3.00125E-03	1.42337E-04	-4.49448E-03	-1.37227E-04	-2.60943E-03
2.52250E-03	-5.15145E-03	3.73380E-03	2.27034E-03	-7.86398E-04
-3.31356E-04	5.41125E-03	1.53882E-04	1.56922E-03	1.37827E-03
3.10537E-03	5.36707E-04	5.40651E-05	4.00646E-05	

ROW 15

1.13399E-04	-2.85735E-03	-1.17925E-05	2.11299E-04	4.19167E-05
-7.30535E-04	-1.90300E-04	-5.22145E-05	-3.05366E-04	7.01134E-04
7.07105E-04	7.04685E-04	-5.50617E-04	-3.77000E-05	9.01076E-03
4.71864E-04	-6.39108E-05	7.95227E-04	-2.14322E-04	5.01893E-04
1.42559E-03	-5.11061E-04	-2.37990E-04	1.83913E-04	3.61445E-05
2.63344E-04	-1.67832E-03	3.67443E-05	-2.84951E-04	-2.01721E-04
-7.78317E-04	-3.11368E-04	-2.67591E-05	2.62993E-04	

ROW 16

1.10548E-03	-8.12179E-03	3.48513E-04	1.21361E-02	4.65811E-03
-1.21031E-02	1.55988E-03	-1.92511E-04	1.87078E-03	-1.45865E-03
1.73634E-02	6.60719E-03	-5.76178E-03	-1.40902E-03	8.07814E-04
5.12812E-02	-2.20222E-03	2.05643E-02	1.09828E-03	1.18399E-02
4.69440E-03	1.27940E-02	-1.36898E-02	-5.70054E-03	4.14064E-03
4.12995E-02	-2.66875E-02	1.05131E-03	-7.81017E-03	-5.09441E-03
-1.56143E-02	-3.35871E-03	-9.59205E-04	1.14932E-03	

ROW 17

1.94294E-05	-1.76398E-02	-2.86759E-04	-6.94836E-04	-4.76145E-04
2.55649E-03	9.82459E-04	2.00733E-04	3.84892E-03	4.25022E-03
-5.32132E-03	8.78730E-03	7.96187E-03	1.66366E-04	-8.00584E-05
-2.04326E-02	9.69377E-03	-1.05049E-03	-9.08530E-03	8.70211E-05
-8.30286E-03	-7.33489E-03	-5.99295E-03	-7.33694E-04	-6.62036E-03
-5.58719E-03	-4.78953E-03	-9.65702E-03	4.37042E-03	-4.39800E-03
3.23429E-03	-7.97201E-04	1.50557E-03	1.44186E-05	

ROW 18

2.41538E-04	-1.38376E-03	2.18080E-03	3.81367E-02	1.65926E-02
-6.57366E-03	5.49658E-03	9.02523E-04	7.08686E-03	-4.74445E-03
9.19827E-04	-3.71562E-03	4.50700E-03	-1.61868E-03	-5.33751E-04
3.56301E-03	1.00379E-04	1.58576E-01	-2.06515E-03	2.37411E-02
3.91361E-03	2.76074E-02	-5.66573E-02	-2.64377E-02	5.52129E-03
-3.16437E-03	-1.52925E-02	-3.36600E-03	-1.61194E-02	-1.52087E-02
-9.57224E-03	-8.95299E-03	-2.41654E-04	-1.15039E-03	

MATRIX 'N1..' 34 BY 34

ROW 19

-3.20026E-04	9.54441E-03	-3.56772E-04	-4.98259E-03	-2.16635E-03
2.94406E-03	4.88217E-04	5.43863E-05	1.52060E-03	-8.55590E-04
6.55180E-04	1.28108E-03	1.88558E-03	1.20859E-04	-8.02913E-05
-9.00121E-04	-3.07878E-04	-2.30105E-02	4.13009E-02	-2.07934E-03
-5.86266E-03	-5.54414E-04	5.49163E-03	6.29784E-04	-1.26207E-03
-4.53606E-04	1.19131E-04	7.05695E-04	9.78101E-04	1.59815E-03
2.37055E-04	6.93762E-04	-1.76989E-03	-3.20724E-04	

ROW 20

-3.55795E-05	-2.13174E-02	4.80801E-04	1.49887E-02	6.26575E-03
-6.80309E-03	1.45705E-03	1.11643E-04	1.58873E-03	-1.04015E-03
4.52665E-03	3.21367E-03	9.23918E-05	-9.37615E-04	1.84188E-04
4.26068E-03	3.90358E-05	1.46125E-02	-1.63771E-03	1.52110E-02
4.35260E-03	8.60531E-03	-1.02451E-02	-8.66367E-03	1.90120E-03
1.70767E-04	-1.35683E-02	-1.09114E-03	-5.47055E-03	-5.36956E-03
-5.75691E-03	-2.23297E-03	5.55925E-07	2.94994E-04	

ROW 21

5.50680E-06	-1.28957E-01	5.10780E-04	2.26659E-02	9.36729E-03
-3.49031E-03	-5.40625E-03	-6.17339E-04	-1.01583E-02	1.98264E-02
-1.56437E-02	4.24335E-03	-3.80679E-03	1.96452E-04	6.14817E-04
-2.13416E-03	-5.44005E-04	-4.85330E-02	-1.04539E-02	3.60838E-03
1.13882E-01	-3.52639E-02	-1.20155E-02	-1.00441E-03	-4.66948E-03
-2.53533E-03	-1.95642E-03	2.02935E-03	-2.04883E-03	-3.73984E-04
-1.31316E-02	1.60511E-04	-5.11577E-04	4.45996E-03	

ROW 22

-3.36856E-04	2.69511E-02	-1.13223E-03	1.12625E-04	3.36129E-04
2.61059E-03	5.63861E-03	7.43704E-04	9.69536E-03	-1.74136E-02
4.39473E-03	3.49702E-03	6.44069E-03	-1.03213E-03	-4.23327E-04
5.86420E-03	-4.54413E-04	1.98659E-03	-2.43733E-03	5.51005E-03
-2.79382E-02	1.18711E-01	-1.23464E-02	-1.38659E-02	-1.15586E-03
-4.98873E-03	-7.49020E-03	1.44954E-03	-4.17891E-03	-3.00872E-03
-1.12429E-02	-1.87925E-04	-1.04904E-04	-5.06963E-03	

ROW 23

1.22000E-04	7.62490E-02	-2.14919E-03	-3.26752E-02	-1.43462E-02
3.14354E-03	-1.40034E-03	-3.98686E-04	1.40231E-03	2.79957E-03
3.03505E-03	5.56703E-03	1.40546E-03	1.33138E-03	1.57261E-04
-4.37455E-03	-3.18425E-05	-1.31983E-02	-5.12334E-03	-1.19048E-02
-1.31783E-02	-7.12151E-03	1.17548E-01	1.40670E-02	-8.98033E-03
-3.45192E-03	1.45546E-03	3.07734E-03	5.53643E-03	7.33820E-03
1.27776E-02	1.68480E-03	4.10521E-04	8.53185E-04	

ROW 24

-9.94141E-05	-5.55025E-03	-2.57457E-04	-8.63810E-03	-3.70996E-03
-1.77301E-02	-2.91741E-03	-5.47116E-04	-5.68442E-03	-5.78958E-04
2.57870E-03	-2.38443E-03	-6.16295E-03	4.07275E-04	3.40280E-04
1.29817E-03	-8.73380E-04	-9.11894E-03	4.13349E-03	-4.06294E-03
5.98275E-03	-4.60194E-03	1.01857E-02	3.80091E-02	4.06738E-03
5.59772E-03	6.50438E-03	-3.73348E-05	7.88933E-03	2.03954E-03
2.83404E-03	3.51496E-04	-1.39052E-03	4.85213E-04	

MATRIX 'A1..' 34 BY 34

ROW 25

9.25357E-05	2.09633E-02	8.02622E-04	1.62898E-03	9.09855E-04
-2.33206E-03	-4.32453E-04	-1.10024E-04	-2.81654E-03	-4.95749E-03
6.05648E-03	-7.92571E-03	-5.81152E-03	-2.03759E-04	-1.99008E-05
2.11245E-03	-2.31313E-03	2.74349E-03	8.02169E-03	5.84417E-04
1.71869E-03	4.20255E-03	-1.06269E-03	2.95469E-03	1.50351E-02
7.03551E-03	5.95453E-03	2.07413E-04	-8.30065E-04	-1.77485E-05
-1.47709E-04	-6.22967E-05	-2.53864E-03	-2.32840E-04	

ROW 26

-4.99016E-05	1.43892E-02	6.75391E-04	9.55375E-05	1.22254E-04
-2.84803E-03	-1.01466E-03	-2.31954E-04	-3.34067E-03	-2.67480E-03
5.69327E-03	-5.08012E-03	-5.73825E-03	-1.29847E-04	1.46278E-04
2.24491E-03	-2.24794E-03	8.73554E-04	7.18707E-03	5.89560E-05
3.78055E-03	7.58503E-04	9.13268E-04	4.27307E-03	7.48107E-03
1.11774E-02	3.91230E-03	4.38594E-04	-3.49695E-04	5.09073E-04
-1.23260E-03	-5.56366E-05	-2.13562E-03	3.58211E-04	

ROW 27

-1.95719E-04	2.77446E-02	1.37022E-03	3.33601E-03	2.11367E-03
6.28595E-03	-8.17044E-04	2.51842E-04	-3.44742E-03	-2.54529E-03
-9.94126E-03	-1.43557E-02	-2.94550E-03	5.47779E-04	-5.79349E-04
-3.43843E-03	-2.02865E-03	-4.53171E-03	7.71341E-03	-3.70904E-03
3.90538E-03	-9.40921E-04	-3.35448E-03	1.92724E-03	6.69682E-03
3.90002E-03	6.49381E-02	7.59530E-04	1.20633E-03	1.91955E-03
6.89870E-03	8.53509E-05	-1.79356E-03	-2.51634E-03	

ROW 28

-1.09959E-05	-1.82213E-04	-1.53376E-05	-1.71803E-04	-7.49368E-05
1.44449E-04	-1.45591E-05	2.10026E-06	2.41954E-05	1.52927E-04
-3.49479E-04	1.34949E-04	8.62439E-05	1.07891E-05	9.33879E-07
-5.14690E-05	-3.33006E-04	-5.17498E-04	-6.66505E-05	-1.76411E-04
4.41503E-04	2.47557E-04	1.01070E-03	-6.53081E-04	-1.04610E-03
-9.84705E-04	-6.97913E-04	2.45322E-03	-3.17502E-04	5.24969E-04
-3.09059E-04	1.28075E-04	-3.80770E-04	1.61643E-05	

ROW 29

5.21186E-05	-6.47355E-04	-9.13929E-05	-9.48972E-04	-4.08566E-04
4.57601E-04	-9.41189E-05	-5.60337E-06	-3.88444E-05	3.56685E-04
-4.92330E-04	4.34677E-04	3.93681E-04	4.78235E-05	-1.37786E-06
-3.53175E-04	3.43365E-04	-2.19584E-03	-2.29518E-04	-8.07542E-04
-6.69726E-04	-1.60792E-03	1.26300E-03	5.75679E-04	-1.86914E-04
2.15732E-06	6.06197E-04	-4.52979E-04	2.48290E-03	3.03185E-04
1.38905E-04	3.59540E-04	3.56425E-04	1.19385E-04	

ROW 30

-3.20039E-05	2.49584E-03	3.58673E-05	-9.20109E-04	-3.77977E-04
1.97663E-04	-1.83672E-04	-2.68358E-05	-4.06145E-04	-8.48841E-05
3.56986E-04	-8.61631E-04	-6.33194E-04	3.70454E-05	-2.63646E-06
-1.01698E-04	-4.36499E-04	-1.42200E-03	7.67848E-04	-7.53363E-04
3.43644E-04	-5.37699E-04	2.10922E-03	6.28613E-04	2.57984E-04
2.55060E-04	9.34670E-04	6.63513E-04	1.99629E-04	3.56942E-03
3.25639E-04	3.93569E-04	-2.65413E-04	1.17337E-04	

MATRIX 'N1..' 34 BY 34

ROW 31

-5.70497E-05	9.01598E-03	1.25627E-04	-2.49601E-03	-9.68060E-04
3.13517E-03	-1.72409E-04	7.32211E-05	2.46973E-04	7.47641E-04
-4.51384E-03	-3.32840E-03	8.04480E-04	4.72807E-04	-7.94207E-04
-2.97871E-03	4.30145E-04	3.66458E-03	-8.37399E-04	-1.35020E-03
1.25729E-04	7.11926E-04	4.41641E-04	2.47286E-03	-1.21724E-03
-9.33706E-04	7.94720E-03	-4.72947E-04	4.96058E-05	-1.58610E-04
5.78217E-03	-5.51225E-04	1.91408E-04	-1.50605E-03	

ROW 32

-1.90003E-05	-2.70256E-03	-7.64756E-05	1.08648E-04	1.54001E-05
-6.76553E-04	5.62875E-05	-2.94077E-05	3.64277E-05	-7.94629E-04
1.09205E-03	-7.21092E-05	-4.87692E-06	-7.50257E-05	-1.89943E-05
2.00381E-04	-1.35666E-04	-1.54007E-03	4.63209E-05	-1.19241E-04
-3.76718E-04	7.57571E-04	6.75700E-04	2.43558E-04	1.40662E-04
1.82255E-04	-6.47684E-04	1.52751E-04	7.95821E-05	2.25579E-04
5.16141E-04	5.50798E-03	-5.16765E-06	-1.80878E-04	

ROW 33

0.0	-5.63024E-04	-2.49119E-05	-2.36130E-05	-1.53965E-05
7.65733E-05	2.87358E-05	5.84089E-06	1.10334E-04	1.17482E-04
-1.49640E-04	7.24957E-04	1.95763E-04	3.86098E-06	-1.88466E-06
-6.64991E-05	8.73929E-05	-3.67927E-05	-2.55154E-04	4.64262E-07
-1.30778E-04	-8.78730E-05	-3.70258E-05	-5.82920E-05	-2.21602E-04
-1.81765E-04	-1.57606E-04	-6.09524E-05	3.24900E-05	-3.07659E-05
1.59750E-05	-3.54123E-07	3.09753E-04	0.0	

ROW 34

0.0	-2.65649E-03	1.30713E-05	2.86790E-04	9.81133E-05
-3.57720E-04	-1.74191E-04	-3.05117E-05	-2.93991E-04	6.77612E-04
5.44459E-05	2.99120E-04	-1.96984E-04	1.84870E-06	3.83426E-05
8.89351E-06	3.81729E-06	1.36480E-05	-1.51002E-04	5.52842E-05
1.34503E-03	-1.06767E-03	1.54857E-04	1.81531E-04	-6.13757E-05
9.03586E-05	-5.51721E-04	1.76517E-07	1.41727E-05	2.36624E-05
-2.13152E-04	-2.17409E-05	0.0	1.32302E-03	

MATRIX NO. 1   34 BY 34   *COEFFICIENTS FOR* $\{q(5)\}$

ROW 1

0.0	-1.70456E 00	-5.06982E-02	-3.40411E-02	-1.61321E-02
-9.27820E-02	-2.57924E-02	-7.56463E-03	-8.71560E-02	-1.68761E-01
4.59400E-02	1.24830E-01	2.27688E-01	4.55243E-03	-8.11876E-03
-1.01293E-01	-6.20738E-03	1.12026E-01	1.04311E-01	-4.06583E-03
-5.10058E-02	-8.58178E-02	-3.42793E-02	-2.27889E-02	-1.62588E-02
1.52612E-02	-3.05844E-03	5.21049E-03	6.91847E-03	-1.70340E-02
1.49535E-02	5.45875E-03	0.0	0.0	

ROW 2

0.0	-2.58247E 00	-5.13736E-02	-2.59414E-02	-1.24075E-02
-4.94929E-01	-1.54672E-01	-3.97117E-02	-5.00419E-01	-7.93110E-01
3.48166E-01	7.41868E-01	1.27554E 00	2.53377E-02	-4.23336E-02
-5.83075E-01	-1.51020E-02	6.26361E-01	4.36018E-01	-2.46581E-02
-2.99188E-01	-4.95633E-01	-1.45310E-01	-1.96137E-01	-1.12163E-01
1.04451E-01	-6.53151E-03	4.02301E-02	3.80998E-02	-9.99203E-02
9.53155E-02	5.34496E-02	-1.59515E 00	-1.06026E 00	

ROW 3

0.0	1.57493E-01	4.71303E-01	2.98883E-02	1.91076E-03
-3.41297E-03	-1.20092E-03	-1.71403E-04	-3.44048E-03	-8.43010E-04
4.24075E-03	2.07931E-03	4.99634E-03	8.58712E-05	-1.25629E-04
-3.71579E-03	5.04978E-04	2.52594E-03	-1.96852E-03	-1.53015E-04
-1.60907E-03	-2.32013E-03	5.78126E-04	-2.52078E-03	-1.00253E-03
8.65378E-04	2.49096E-04	4.32578E-04	1.17463E-04	-4.77185E-04
3.52044E-04	3.25003E-04	-7.06727E-02	5.46499E-03	

ROW 4

0.0	-1.29227E-01	-3.32163E-03	8.27370E 00	-9.24655E-04
-1.41918E-02	-4.31441E-03	-1.14364E-03	-1.42426E-02	-2.35909E-02
1.00157E-02	1.86416E-02	3.30478E-02	6.49247E-04	-1.15859E-03
-1.50895E-02	-4.86552E-04	1.66512E-02	1.29536E-02	-6.50828E-04
-9.04567E-03	-1.31680E-02	-4.41927E-03	-4.70029E-03	-2.91882E-03
3.63941E-03	-2.40170E-04	5.87387E-04	1.00849E-03	-2.62280E-03
3.27919E-03	1.44935E-03	-6.70972E-02	1.15845E-01	

ROW 5

0.0	-6.11837E-02	-1.59527E-03	-9.65175E-04	5.51516E 00
-6.53932E-03	-1.98586E-03	-5.27391E-04	-6.58160E-03	-1.09475E-02
4.64799E-03	8.45861E-03	1.51477E-02	2.98751E-04	-5.36589E-04
-6.94459E-03	-2.26990E-04	7.80668E-03	6.32491E-03	-3.05610E-04
-3.78298E-03	-6.22008E-03	-2.15117E-03	-2.17654E-03	-1.35146E-03
1.24372E-03	-1.23792E-04	4.63287E-04	4.80284E-04	-1.24888E-03
1.09330E-03	6.93356E-04	-4.38049E-02	3.97423E-02	

ROW 6

0.0	-3.66819E-01	-1.02008E-02	-7.11535E-03	-3.66960E-03
1.64686E 01	-9.32553E-03	-2.62227E-03	-3.00472E-02	-5.70793E-02
1.36840E-02	7.30457E-02	1.15306E-01	2.40907E-03	-3.88376E-03
-5.18622E-02	-2.74085E-03	5.64395E-02	4.52258E-02	-2.13163E-03
-2.69067E-02	-4.63946E-02	-1.54915E-02	-1.59010E-02	-9.78132E-03
5.73918E-03	-9.45500E-04	3.55555E-03	3.89116E-03	-9.91819E-03
8.64744E-03	5.16293E-03	2.18386E-01	-1.42473E-01	

MATRIX 'NC..' 34 BY 34

ROW 7

0.0	-8.31826E-02	-2.29589E-03	-1.64671E-03	-8.79232E-04
-7.76927E-03	4.34187E 00	-6.33095E-04	-7.12703E-03	-1.38212E-02
2.74974E-03	1.99146E-02	3.08270E-02	6.49868E-04	-1.02539E-03
-1.38394E-02	-7.49123E-04	1.49341E-02	1.17059E-02	-5.63083E-04
-7.11001E-03	-1.22592E-02	-4.01336E-03	-4.32275E-03	-2.60371E-03
3.64310E-03	-2.38685E-04	9.69192E-04	1.05153E-03	-2.67989E-03
2.33141E-02	1.37544E-02	8.19508E-02	-6.97095E-02	

ROW 8

0.0	-2.57633E-02	-7.07192E-04	-4.95032E-04	-2.58173E-04
-2.41402E-03	-7.03113E-04	1.12636E 00	-2.25510E-03	-4.25974E-03
1.02011E-03	5.58929E-03	8.90690E-02	1.84326E-04	-2.95863E-04
-3.56560E-03	-2.05735E-04	4.31570E-03	3.42672E-03	-1.62534E-04
-2.06255E-03	-3.56033E-03	-1.17532E-02	-1.23772E-03	-7.56397E-04
7.54017E-04	-7.00442E-05	2.76541E-04	2.99598E-04	-7.65250E-04
6.67218E-04	3.97165E-04	1.66621E-02	-1.21565E-02	

ROW 9

0.0	-7.82574E-02	-1.63704E-03	-1.36734E-03	-9.59723E-04
-1.61523E-02	-4.83127E-03	-1.30913E-03	5.21690E 00	-2.75923E-02
4.51647E-03	5.03861E-02	7.61457E-02	1.61659E-03	-2.45704E-03
-3.42449E-02	-1.67820E-02	3.61508E-02	2.50548E-02	-1.39545E-03
-1.76950E-02	-3.07039E-02	-9.96088E-03	-1.19316E-02	-6.77230E-03
7.02863E-03	-3.39180E-04	2.65355E-03	2.67933E-03	-6.97733E-03
5.01349E-03	3.46429E-03	3.15125E-01	-1.17495E-01	

ROW 10

0.0	-2.41476E-01	-5.74629E-03	-4.05235E-03	-2.32189E-03
-3.65257E-02	-1.09825E-02	-2.95602E-03	-3.47709E-02	2.01099E 01
1.65700E-02	8.87750E-02	1.40190E-01	2.93442E-03	-4.66245E-03
-6.36177E-02	-2.85550E-03	6.94602E-02	5.12266E-02	-2.72962E-03
-3.50484E-02	-5.95515E-02	-1.98712E-02	-2.24382E-02	-1.34314E-02
1.33567E-02	-6.76133E-04	5.02473E-03	5.09216E-03	-1.32769E-02
1.16827E-02	6.86299E-03	3.36083E-01	2.71722E-01	

ROW 11

0.0	-1.85559E-01	-6.09297E-03	-3.94358E-03	-1.60678E-03
-9.49992E-04	-1.50620E-05	-8.79353E-05	-1.63528E-03	-4.26813E-03
6.30045E 01	-1.55344E-02	-3.44314E-02	-5.27781E-04	5.83754E-04
1.05491E-03	3.33116E-04	-7.67662E-03	3.24148E-03	3.23923E-04
3.56287E-03	6.96008E-03	-6.49208E-04	5.17369E-03	1.63536E-03
-3.44881E-03	-3.90823E-04	-1.07707E-03	-7.75287E-04	2.08794E-03
-1.67419E-03	-7.75583E-04	-4.82608E-01	2.00421E-02	

ROW 12

0.0	3.03241E-01	9.23991E-03	6.99934E-03	3.55251E-03
1.87097E-02	5.06299E-03	1.54239E-03	1.76893E-02	4.02869E-02
-6.98402E-03	6.89353E 01	-9.94533E-02	-2.02980E-03	3.37185E-03
4.35154E-03	2.72935E-03	-5.90253E-02	-6.45651E-02	2.29523E-03
3.09757E-02	5.44739E-02	2.35267E-02	1.58296E-02	1.31031E-02
-1.16561E-02	1.41973E-03	-4.05725E-03	-4.77306E-03	1.24481E-02
-1.15955E-02	-6.93375E-03	6.49828E-01	1.17206E-01	

MATRIX 'NC..' 34 BY 34

ROW 13

0.0	2.47865E-01	7.29439E-03	5.97735E-02	3.26296E-03
3.22711E-02	6.20225E-03	1.83020E-03	2.10297E-02	4.74213E-02
-5.76622E-03	-7.65705E-02	4.27934E 01	-2.94523E-03	4.59849E-03
5.97455E-02	2.57745E-03	-7.95546E-02	-8.15926E-02	3.25431E-03
4.44798E-02	7.73023E-02	3.15835E-02	2.50292E-02	1.92376E-02
-1.77134E-02	1.34063E-02	-6.38240E-03	-7.05907E-03	1.86502E-02
-1.74010E-02	-1.01943E-02	5.66484E-01	-7.88389E-02	

ROW 14

0.0	6.83816E-03	2.07146E-04	1.69404E-04	8.25920E-05
4.75610E-04	1.90426E-04	3.91971E-05	4.60228E-04	1.04161E-03
-1.94379E-04	-1.42191E-03	-2.43313E-03	8.47469E 00	9.21105E-05
1.17003E-03	7.31649E-05	-1.63014E-03	-1.72755E-03	6.80999E-05
9.84057E-04	1.65408E-03	7.29241E-04	5.04653E-04	4.17928E-04
-3.73267E-04	7.14858E-05	-1.23996E-04	-1.42275E-04	3.82196E-04
-3.61525E-04	-2.17469E-04	1.12787E-02	8.51108E-04	

ROW 15

0.0	-6.62598E-03	-1.81421E-04	-1.47459E-04	-8.22523E-05
-9.03621E-04	-2.32253E-04	-6.54206E-05	-7.83803E-04	-1.61186E-03
3.44990E-04	2.44193E-03	4.07235E-03	9.00744E-05	5.59831E 00
-1.93735E-03	-1.05566E-04	2.54677E-03	2.39856E-03	-1.08273E-04
-1.52944E-03	-2.57075E-03	-1.03961E-03	-8.80224E-04	-6.58351E-04
6.11101E-04	-1.93226E-05	2.23045E-04	2.33110E-04	-6.27442E-04
5.55955E-04	3.45728E-04	-5.51719E-03	1.51503E-02	

ROW 16

0.0	-6.45941E-02	-1.89963E-03	-1.73582E-03	-1.00387E-03
-7.11206E-03	-1.97327E-03	-5.85997E-04	-6.71956E-03	-1.59370E-02
1.59111E-03	2.93217E-02	4.80923E-02	1.09709E-03	-1.75944E-03
3.69122E 01	-1.38512E-03	3.12327E-02	3.16510E-02	-1.31724E-03
-1.84743E-02	-3.17167E-02	-1.30140E-02	-1.06144E-02	-8.15487E-03
7.56706E-03	-3.84993E-04	2.75196E-03	2.97379E-03	-7.93956E-03
7.47296E-03	4.35623E-03	-1.94623E-01	1.91826E-03	

ROW 17

0.0	-1.12522E-03	-5.16771E-06	7.25859E-06	1.07704E-05
-5.39819E-04	-1.75977E-04	-4.30449E-05	-6.41864E-04	-1.00093E-03
6.51077E-04	3.77690E-04	1.20454E-03	2.62988E-05	-5.68173E-05
-4.70434E-04	1.74096E 00	1.20779E-03	1.39137E-03	-5.80903E-05
-9.47665E-04	-1.34481E-03	-6.31493E-04	-4.66191E-04	-4.11288E-04
3.26863E-04	1.99305E-06	1.14859E-04	1.13297E-04	-3.22337E-04
3.17955E-04	2.00063E-04	2.81854E-01	1.51925E-03	

ROW 18

0.0	-1.41133E-02	-5.50009E-04	-1.25680E-04	5.08302E-05
3.69661E-03	1.12434E-03	3.02141E-04	4.04384E-03	8.74909E-03
-1.99396E-03	-1.75206E-02	-3.09024E-02	-6.96175E-04	1.15672E-03
1.54056E-02	8.11697E-04	9.30253E 01	-2.04162E-02	1.10107E-03
1.75004E-02	2.74883E-02	1.18639E-02	1.01833E-02	7.91569E-03
-7.41074E-03	-3.36057E-04	-2.83055E-03	-2.77862E-03	7.75190E-03
-7.53055E-03	-4.39820E-03	-1.03663E-01	8.63264E-03	

MATRIX *NC..* 34 BY 34

ROW 19

0.0	1.92837E-02	9.97508E-05	-1.74791E-04	-1.93689E-04
8.60954E-03	2.82742E-03	6.88884E-04	1.02947E-02	1.56344E-02
-1.06073E-02	-5.56335E-03	-1.90970E-02	-3.66558E-04	8.44803E-04
1.05635E-02	2.22122E-04	-1.76817E-02	3.78212E 01	1.00435E-03
2.19210E-02	2.80110E-02	1.49110E-02	8.41435E-03	7.92202E-03
-4.72874E-03	-8.52703E-04	-2.47100E-03	-1.89198E-03	5.95869E-03
-6.05510E-03	-3.54880E-03	-7.29322E-01	-6.06415E-02	

ROW 20

0.0	2.31315E-03	7.44966E-05	4.36052E-05	1.61735E-05
-1.54733E-05	-7.54296E-06	-1.27565E-06	-2.06704E-05	-6.10954E-05
-2.60095E-05	4.61427E-04	7.47515E-04	1.67294E-05	-2.57838E-05
-3.72931E-04	-1.81573E-05	5.44794E-04	4.07265E-04	6.53203E 00
-4.09041E-04	-6.90529E-04	-2.28609E-04	-3.44520E-04	-2.24826E-04
2.37931E-04	5.77976E-06	1.06953E-04	1.10553E-04	-2.98652E-04
2.91395E-04	1.55971E-04	1.52454E-02	2.20950E-02	

ROW 21

0.0	-3.21766E-04	1.02805E-04	9.77583E-05	1.09078E-08
-1.74500E-03	-5.60584E-04	-1.43585E-04	-1.76703E-03	-2.87067E-03
9.39146E-04	5.72342E-03	9.33323E-03	1.55110E-04	-2.78223E-04
-4.36254E-03	-1.27587E-04	5.32728E-03	4.60620E-04	-3.96451E-04
9.18130E 01	-6.48397E-03	-4.93796E-04	-6.31681E-03	-3.29364E-03
3.63742E-03	8.85702E-04	1.41378E-03	1.41494E-03	-3.96813E-03
3.93055E-03	2.06069E-03	-4.02029E-01	4.59167E-01	

ROW 22

0.0	1.96828E-02	4.54756E-04	4.17938E-04	1.58720E-04
-4.74503E-04	-2.58207E-04	-5.73919E-05	-1.06739E-03	-1.93269E-03
1.01810E-03	4.64737E-03	9.39498E-03	1.72744E-04	-3.41836E-04
-4.99834E-03	-1.83729E-04	8.42052E-03	3.93500E-03	-6.03116E-04
-8.95594E-03	1.10435E 02	-4.27334E-03	-8.29772E-03	-5.44918E-03
5.47188E-03	1.09150E-03	2.08060E-03	2.00174E-03	-5.78929E-03
5.81570E-03	3.36276E-03	-2.93479E-01	-4.28242E-01	

ROW 23

0.0	-7.01169E-03	-9.72462E-06	1.86277E-04	1.23802E-04
-3.71346E-03	-9.71852E-04	-3.17933E-04	-3.18436E-03	-3.96605E-03
3.47933E-03	6.02401E-05	2.37779E-03	-1.67898E-05	-7.02475E-05
-1.29312E-03	1.41973E-04	1.66050E-03	-3.62853E-03	-2.58972E-04
-4.07683E-03	-4.16752E-03	1.09500E 02	-4.48781E-03	-2.54790E-03
2.52337E-03	1.13930E-03	8.29862E-04	6.15658E-04	-2.05158E-03
2.15094E-03	1.25592E-03	-1.42732E-01	6.19953E-02	

ROW 24

0.0	5.80885E-03	5.38448E-05	-9.74408E-05	-9.83728E-05
1.53540E-03	5.29045E-04	1.20674E-04	1.84502E-03	2.02662E-03
-2.33553E-03	2.61773E-03	2.78555E-03	8.53175E-05	-8.60901E-05
-1.39562E-03	-1.92659E-04	2.14271E-03	3.35553E-03	-8.35037E-05
-2.17257E-05	-1.87048E-03	-5.62431E-05	4.19678E 01	-6.03633E-04
9.03994E-04	-4.02786E-04	6.84290E-04	9.15153E-04	-2.23493E-03
2.16679E-03	1.05068E-03	-2.56312E-01	7.24787E-02	

MATRIX INC.. 34 BY 34

ROW 25

0.0 -4.82263E-03 -1.45997E-04 -8.04292E-05 -4.12172E-05
-1.33350E-04 -2.77551E-05 -1.19368E-05 -1.29255E-04 -1.92866E-04
1.00902E-04 2.29073E-04 4.29363E-04 -3.66527E-06 -4.80053E-06
-3.03435E-04 -6.28945E-06 3.66003E-04 -5.79889E-04 -6.47234E-05
-4.69206E-04 -8.26939E-04 2.39825E-04 -1.29748E-03 1.06598E 01
8.78821E-04 1.52117E-04 4.48416E-04 4.87593E-04 -1.33038E-03
1.35417E-03 6.76422E-04 -6.15949E-01 -2.43898E-02

ROW 26

0.0 3.91579E-03 1.17679E-04 9.11907E-05 4.97626E-05
-1.78275E-04 -9.98334E-05 -2.13141E-05 -3.33765E-04 -3.83090E-04
3.74900E-04 -1.78318E-04 -1.10795E-04 -2.11709E-06 3.98786E-08
6.54111E-05 2.74954E-05 -3.29148E-04 -3.49114E-04 3.42754E-05
3.65634E-05 5.51465E-04 -1.57715E-04 7.98072E-04 4.02840E-04
7.90091E 00 5.40000E-05 -3.67836E-04 -4.52598E-04 1.16872E-03
-1.17287E-03 -6.23079E-04 -5.04508E-01 3.16227E-02

ROW 27

0.0 1.08517E-02 3.36137E-04 2.24419E-04 1.13459E-04
3.75326E-04 6.33635E-05 2.37260E-05 1.51008E-04 3.95896E-04
1.40946E-04 -6.99352E-04 -6.50231E-04 -7.70523E-06 6.71076E-06
1.57529E-04 2.03510E-05 2.17443E-04 3.35168E-04 -1.23939E-05
-1.00342E-03 -1.10909E-03 -1.01228E-03 1.21842E-04 -3.64224E-04
6.53809E-05 7.47289E 01 -5.79225E-05 -1.37170E-04 2.37839E-04
-3.35893E-04 4.78268E-05 -4.33284E-01 -2.17649E-01

ROW 28

0.0 6.37473E-04 4.01080E-05 4.25756E-05 2.50510E-05
-3.47093E-04 -8.65602E-05 -1.95468E-05 -3.06936E-04 -3.74866E-04
3.66035E-04 -1.49845E-04 2.05595E-05 -3.97584E-06 -3.33057E-06
-3.52837E-05 3.17730E-05 1.62296E-05 -1.80398E-04 -6.50128E-06
-9.07779E-05 9.19057E-05 2.77751E-05 -1.07526E-05 3.56807E-05
-7.31940E-05 8.17174E-05 3.03268E 00 -1.11762E-04 3.80825E-04
-3.57619E-04 -2.19948E-04 -3.26209E-01 -8.40529E-05

ROW 29

0.0 -3.04533E-03 -9.41475E-05 -6.34781E-05 -3.32414E-05
-1.09733E-04 -3.84336E-05 -9.49102E-06 -9.43353E-05 -2.05515E-04
3.57092E-05 3.19783E-04 3.03575E-04 4.62082E-07 -5.38991E-06
-9.72568E-05 -3.15128E-06 -4.09074E-05 -4.01918E-04 -7.25058E-06
9.73687E-05 3.19015E-04 2.95166E-04 -1.47266E-04 5.40423E-05
-3.11129E-05 1.12676E-04 -5.71548E-05 3.80539E 00 2.07837E-04
-1.83461E-04 -2.31083E-04 1.18163E-01 5.11346E-03

ROW 30

0.0 1.86590E-03 5.81182E-05 4.35349E-05 2.77692E-05
1.30769E-04 3.67187E-05 1.14984E-05 1.39867E-04 3.14474E-04
-3.84915E-05 -3.91773E-04 -6.65057E-04 -4.67900E-06 1.82720E-05
3.67630E-04 5.35377E-06 -1.37837E-04 4.78958E-04 2.27801E-05
6.87314E-05 -3.34436E-04 -3.30181E-04 2.43040E-04 -7.77230E-05
9.38841E-05 -2.41457E-04 1.64062E-04 3.59070E-04 6.75329E 00
5.45194E-04 5.79067E-04 -1.13153E-01 9.28994E-03

MATRIX 'INC..'   34 BY 34

ROW 31

0.0	3.33346E-03	7.96570E-05	2.25097E-06	-3.20691E-06
7.66124E-04	8.65969E-05	2.03579E-05	2.59929E-04	2.00948E-04
-2.95550E-04	5.16524E-04	8.01498E-04	1.30795E-05	-2.76854E-05
-3.78676E-04	-2.68268E-05	4.36383E-04	1.65279E-04	-3.71571E-05
-3.75871E-04	-2.02246E-04	-4.04819E-06	-3.28134E-04	-7.93179E-05
1.87491E-05	2.47985E-04	-1.50310E-04	-2.19745E-04	5.51184E-04
1.25165E 02	-5.07772E-04	7.58708E-02	-8.11716E-02	

ROW 32

0.0	1.19436E-03	2.34774E-05	2.94170E-06	-1.62330E-06
1.16625E-04	3.87073E-05	9.20825E-06	1.14059E-04	1.01976E-04
-1.19115E-04	1.41372E-04	2.30020E-04	7.55385E-06	-1.10468E-05
-1.27254E-04	-1.44333E-05	2.42957E-04	3.09936E-04	-6.65020E-06
-7.25303E-05	-1.47040E-04	-9.08239E-05	6.40481E-05	5.91550E-05
-7.14156E-05	-3.56869E-05	-3.42132E-05	-3.11252E-05	1.22834E-04
-1.41537E-04	1.41725E 01	-6.76595E-03	-8.65619E-03	

ROW 33   COLUMN 33   8.20546E-03

ROW 34   COLUMN 34   1.00513E-02

MATRIX 'RB2.' 34 BY 34 COEFFICIENTS FOR $s\phi(s)\{g(s)\}$

ROW 1

7.06220E-01	-1.20233E 00	2.44749E-02	1.59794E-01	6.39883E-02
-1.00466E-01	-2.49563E-02	-1.36087E-02	-6.62433E-03	1.09129E-01
-1.34059E-01	1.44461E-01	2.23793E-02	1.43768E-03	2.29624E-03
1.15057E-02	2.58545E-02	1.16692E-02	-2.03521E-02	2.59009E-02
1.44205E-01	-3.62539E-02	-4.61999E-02	3.67488E-03	-1.95183E-02
-1.37870E-02	-2.02219E-02	-1.13857E-04	5.90264E-04	-3.02452E-03
-7.54869E-03	2.35923E-03	4.44962E-03	9.16815E-03	

ROW 2

-4.04232E-01	5.16601E 00	7.04620E-02	-1.31035E-01	-8.04492E-02
-2.94360E-01	-1.26976E-01	-2.79184E-02	-3.06759E-01	-2.16940E-01
2.68445E-01	-1.70698E-01	-1.44444E-01	8.00188E-03	4.29111E-03
3.34972E-02	-1.63902E-01	-1.79079E-01	-2.51629E-03	-4.36129E-02
-4.12684E-02	-2.52339E-02	5.20384E-02	1.22612E-01	9.39323E-02
5.60575E-02	4.60376E-02	1.04689E-03	-3.50116E-03	1.32017E-02
-1.27486E-02	6.43917E-03	-2.71983E-02	1.41304E-03	

ROW 3

5.61101E-02	3.46295E-02	4.77085E-02	6.50300E-02	3.49246E-02
-2.77945E-02	-3.70730E-03	-2.37519E-04	-1.21096E-02	-1.27261E-02
1.67178E-02	-3.75712E-03	-1.22069E-02	-2.63447E-03	1.87923E-04
1.17299E-02	-9.51340E-03	2.97653E-02	-3.99959E-03	1.14570E-02
1.56545E-02	-1.09707E-03	-2.78250E-02	-3.83004E-03	6.72594E-03
4.84145E-03	7.46502E-03	-1.04040E-04	-1.14173E-03	-1.44433E-04
-2.24941E-03	2.56223E-04	-1.60582E-03	5.61544E-04	

ROW 4

3.61903E-02	-1.56016E-02	2.28671E-02	4.34228E-02	2.56740E-02
1.90311E-02	4.23669E-02	9.75254E-04	-2.22953E-03	-1.71181E-02
2.66153E-02	1.55521E-02	-1.39706E-03	-3.89276E-03	4.52896E-04
1.49239E-02	-3.55581E-03	1.95967E-02	-2.65839E-03	1.09447E-02
1.01463E-02	2.68547E-03	-1.80933E-02	-4.51809E-03	3.09189E-03
1.55430E-03	-5.66072E-04	-1.33137E-04	-8.73922E-04	-5.46495E-04
-3.36715E-03	4.58537E-04	-5.61279E-04	2.70305E-04	

ROW 5

1.91999E-02	-3.73134E-02	1.84452E-02	3.30463E-02	2.04752E-02
6.55007E-03	5.76946E-03	1.15674E-03	2.17436E-03	-1.55340E-02
2.37754E-02	1.07403E-02	9.94532E-05	-3.31354E-03	2.06510E-04
1.15890E-02	-1.86703E-03	1.92841E-02	-1.66049E-03	9.00072E-03
3.09559E-02	6.26855E-03	-1.44386E-02	-4.76189E-03	1.95619E-03
4.91174E-04	-1.03698E-03	-1.15150E-04	-7.09250E-04	-5.32750E-04
-2.46106E-03	2.87513E-04	-2.99129E-04	-1.44570E-04	

ROW 6

-3.98563E-02	-2.11398E-01	-7.44075E-03	4.97733E-03	1.17443E-02
6.59249E-02	2.57617E-02	4.35374E-03	3.12756E-02	-2.84442E-02
4.35317E-02	1.94874E-02	2.05901E-02	-5.40316E-03	-4.64717E-04
1.09546E-02	1.02284E-02	1.93231E-02	1.99060E-03	8.43122E-03
-3.59132E-02	2.98917E-02	-5.43382E-03	-1.95664E-02	-3.75337E-03
-5.40333E-03	-1.00433E-02	-2.94433E-04	-1.85712E-04	-1.36070E-03
-2.87242E-03	4.12563E-04	1.56513E-03	-2.36325E-03	

MATRIX 'PP3.'   34 BY   34

ROW   7

-3.71533E-02	-9.17894E-02	-1.25175E-03	2.75286E-03	3.78709E-03
1.63288E-02	6.58540E-03	1.21064E-03	9.54078E-03	-6.25599E-03
5.99255E-02	7.24434E-03	5.48954E-03	-1.45970E-03	-8.80677E-05
3.39234E-03	3.42986E-03	8.40911E-03	2.56756E-04	2.06249E-03
-6.50590E-03	8.66783E-03	-2.41680E-03	-3.18512E-03	-1.37757E-03
-1.78424E-03	-3.17765E-03	-1.09300E-04	-1.11692E-04	-4.85065E-04
-5.35791E-04	1.37793E-05	5.16848E-04	-5.81731E-04	

ROW   8

1.64833E-03	-1.56297E-02	-5.10289E-05	1.45283E-03	1.18987E-03
3.12958E-03	1.35031E-03	2.46728E-04	1.80641E-03	-1.06971E-03
1.79780E-03	2.06506E-03	1.16866E-03	-3.28311E-04	-2.73909E-06
8.43707E-04	7.31412E-04	1.62684E-03	-1.34133E-05	7.45894E-04
-5.79489E-04	1.44300E-03	-7.39612E-04	-6.86566E-04	-2.93333E-04
-2.87741E-04	-6.50342E-04	-2.36624E-05	-2.35531E-05	-1.05614E-04
-1.66809E-04	1.52526E-05	1.10302E-04	-7.91998E-05	

ROW   9

3.36367E-02	-2.10958E-01	-4.58026E-03	4.03459E-03	2.37896E-03
1.07807E-02	5.03017E-03	1.08595E-03	1.29167E-02	8.57463E-03
-1.05907E-02	1.36360E-02	7.62077E-03	-3.50074E-04	-4.21814E-05
-1.42490E-04	8.40143E-03	9.93185E-03	-4.86725E-04	2.63897E-03
2.35317E-04	4.03980E-03	-2.75392E-03	-3.39402E-03	-3.86929E-03
-3.74943E-03	-3.55109E-03	-2.49306E-04	1.39701E-04	-7.52980E-04
6.52164E-04	-2.37792E-04	1.13578E-03	-3.52411E-05	

ROW   10

8.26256E-03	-1.06942E-01	-1.85385E-02	-2.01337E-02	-1.41402E-02
-3.10559E-03	-3.09938E-03	-4.76055E-04	3.00541E-03	2.54960E-02
-3.56834E-02	-5.67839E-02	5.93539E-03	3.42501E-03	-4.81662E-04
-1.67405E-02	7.06654E-03	-1.99346E-02	3.42812E-04	-8.56894E-03
7.51575E-03	-1.30912E-02	9.29578E-03	2.06392E-03	-3.52479E-03
-3.21415E-03	3.67178E-03	-5.11975E-05	1.02697E-03	2.59812E-04
2.53372E-03	-1.05749E-04	8.77164E-04	2.53414E-04	

ROW   11

-5.20839E-02	1.09934E-01	2.67591E-02	3.48903E-02	2.13880E-02
2.43546E-02	1.36333E-02	2.03070E-03	6.88615E-03	-4.30194E-02
6.49496E-03	-3.84468E-03	-3.69573E-03	-5.22656E-03	-1.60655E-04
1.39430E-02	-9.19862E-03	4.39162E-02	-1.16173E-03	1.26267E-02
-3.10794E-02	3.00322E-02	-1.41154E-02	-5.75198E-03	4.74411E-03
2.70625E-03	-3.78750E-03	4.17075E-05	-1.68003E-03	-6.42322E-04
-1.81319E-03	1.64426E-04	-5.17634E-04	-2.08883E-03	

ROW   12

1.03975E-01	-1.25593E-01	1.31059E-02	3.72235E-02	2.02701E-02
-3.35665E-03	1.42076E-03	4.33383E-04	8.19659E-04	-4.57560E-03
1.76397E-02	5.44402E-02	-3.52686E-04	-3.98191E-03	1.65936E-03
2.28599E-02	4.71794E-03	3.09818E-02	-5.61639E-03	1.56827E-02
1.67227E-02	-2.14379E-03	-1.41109E-02	3.93318E-04	2.99752E-04
1.41073E-03	-1.40939E-02	-9.43530E-04	-1.01253E-03	-1.43744E-03
-3.36447E-03	-8.59608E-07	4.63047E-05	2.02644E-03	

MATRIX 'RR2.' 34 BY 34

ROW 13

1.02956E-02	3.30600E-02	-4.07223E-03	-2.36975E-03	-9.99462E-04
4.29326E-03	9.47002E-04	1.08918E-04	-6.57425E-04	-3.05300E-03
3.94593E-03	3.50423E-03	5.90034E-03	-5.43458E-05	-5.88680E-05
-1.14143E-03	3.19993E-03	-6.58167E-03	-4.01494E-04	-9.89770E-04
-2.97988E-03	2.81591E-03	-3.93092E-04	3.33451E-03	9.64224E-04
8.52811E-04	-5.02002E-04	-4.65757E-04	4.55891E-04	-9.20363E-05
-1.22768E-03	4.55016E-04	-1.35457E-04	-2.30739E-04	

ROW 14

1.04381E-04	9.19045E-03	-2.44823E-03	-4.25642E-03	-3.11296E-03
-2.14466E-03	-1.81664E-03	-3.05207E-04	-1.57492E-03	3.93952E-03
-6.28735E-03	-3.51825E-03	-1.76998E-04	7.82673E-04	-7.66285E-05
-2.98051E-03	7.88911E-05	-5.05720E-03	1.98126E-04	-1.98393E-03
1.12406E-03	-2.28229E-03	1.86269E-03	9.93403E-04	-1.64133E-04
-2.91262E-05	1.29333E-03	2.96562E-05	1.80989E-04	1.52369E-04
4.09112E-04	-5.76164E-06	-3.77305E-07	6.58671E-05	

ROW 15

2.39705E-04	-2.20039E-03	3.74521E-04	5.87220E-04	3.75560E-04
-3.30641E-06	9.42553E-05	1.62846E-05	9.27123E-05	-2.04877E-04
6.52643E-04	7.10572E-04	-2.15761E-04	-9.28696E-05	3.01409E-05
4.83210E-04	-4.27618E-05	1.09152E-03	-9.65342E-05	3.53167E-04
2.34453E-04	-4.72274E-05	-2.29407E-04	-1.25896E-04	5.42613E-06
2.13621E-05	-3.15276E-04	-2.39633E-06	-3.71538E-05	-2.19378E-05
-5.72484E-05	-1.58186E-05	-2.54137E-07	3.39597E-05	

ROW 16

2.74508E-02	-6.99011E-02	1.14106E-02	2.13299E-02	1.28261E-02
-2.23161E-04	3.12678E-03	6.02104E-04	3.13890E-03	-7.71742E-03
1.53534E-02	2.13599E-02	-3.14395E-03	-2.67330E-03	6.99768E-04
1.36373E-02	-1.06518E-03	2.23896E-02	-1.64114E-03	9.08052E-03
4.41855E-03	3.12677E-03	-7.06947E-03	-3.57331E-03	-1.93553E-04
1.03527E-04	-6.64802E-03	3.13462E-05	-8.59699E-04	-6.13837E-04
-1.67560E-03	-1.76130E-04	6.90195E-05	6.50421E-04	

ROW 17

9.51513E-03	-9.71556E-02	-5.44568E-03	-2.33359E-03	-1.26572E-03
7.02319E-03	2.42846E-03	5.07805E-04	6.65898E-03	5.97756E-03
-1.55649E-03	6.69827E-03	5.88569E-03	1.23360E-04	-7.19548E-05
-3.12179E-03	7.53918E-03	3.46273E-04	-3.83469E-04	3.26077E-05
-1.68390E-03	-1.38987E-03	-1.23195E-03	5.64305E-05	-8.68207E-04
-9.22168E-04	-8.03463E-04	-7.51675E-04	4.43965E-04	-4.96341E-04
4.35574E-04	-1.34720E-04	4.80180E-04	-8.25548E-06	

ROW 18

4.74480E-02	-2.03065E-01	2.56474E-02	4.75943E-02	2.71440E-02
5.46413E-04	5.20976E-03	1.44695E-03	7.52313E-03	-4.03772E-03
9.83433E-03	1.84231E-02	-1.21285E-03	-3.09598E-03	2.62873E-04
1.20875E-02	1.52483E-03	4.92359E-02	-4.91713E-03	1.56417E-02
1.29319E-02	9.96542E-03	-2.59871E-02	-9.21522E-03	3.08316E-04
-1.56605E-03	1.29630E-03	-3.09680E-04	-1.50690E-03	-1.47847E-03
1.27315E-03	-4.74581E-04	2.92942E-04	-1.37583E-04	

MATRIX 'RB2.' 34 BY 34

ROW 19

4.55816E-02	-2.55601E-01	-1.80206E-02	-7.89122E-03	-5.20710E-03
1.32953E-02	4.18574E-03	9.43501E-04	1.37138E-02	1.66755E-02
-2.07607E-02	1.74165E-02	1.03372E-02	5.57438E-04	5.42891E-05
-3.14620E-03	8.19235E-03	-5.46578E-03	6.77567E-04	-8.76229E-04
5.22137E-03	1.88411E-03	6.75537E-03	-2.78974E-03	-7.40859E-03
-6.21673E-03	-6.86995E-03	2.96885E-04	4.71680E-04	-4.55406E-04
1.83802E-04	3.33972E-05	1.86632E-03	3.48643E-04	

ROW 20

7.60604E-03	-2.44490E-02	4.76156E-03	8.92108E-03	5.64180E-03
2.34465E-03	1.84545E-03	3.67856E-04	1.51530E-03	-3.94100E-03
6.86223E-03	6.43177E-03	-3.03974E-04	-1.08303E-03	1.69108E-04
4.56879E-03	9.70173E-06	9.81385E-03	-8.47699E-04	2.82661E-03
1.36802E-03	3.40531E-03	-5.12411E-03	-1.79507E-03	2.96010E-04
1.71195E-05	-1.32211E-03	-7.13522E-05	-3.16928E-04	-2.97728E-04
-6.25790E-04	-3.09536E-05	-4.56962E-06	3.01459E-05	

ROW 21

-6.48655E-02	-1.13555E-01	-1.54201E-02	-1.28117E-02	-2.37653E-03
4.24698E-02	1.31186E-02	2.23309E-03	1.62038E-02	-7.36630E-03
1.40492E-02	-2.16640E-03	1.02258E-02	-1.67064E-03	-5.08482E-04
-1.36990E-03	4.28048E-03	-3.56494E-04	2.22292E-03	-3.74521E-04
-9.75982E-03	6.78163E-03	4.67952E-03	-7.24676E-03	-3.90713E-03
-4.93269E-03	-2.78222E-03	4.15699E-04	8.31509E-05	-2.60503E-04
-5.38034E-04	1.64699E-05	1.18742E-03	-1.31501E-03	

ROW 22

8.53383E-02	-1.94479E-01	4.23247E-04	1.12169E-02	2.89245E-03
-1.24645E-02	-3.05670E-03	-1.68687E-04	3.48355E-03	1.78507E-02
-2.83081E-02	1.14974E-02	3.08385E-03	1.24056E-03	1.37691E-04
-1.95134E-02	3.34580E-03	8.03457E-05	-8.09093E-04	1.66713E-03
1.22792E-02	3.41502E-03	-6.13190E-03	-1.35607E-03	-4.88022E-03
-3.48929E-03	-1.23309E-03	5.22540E-04	2.59398E-04	-2.91078E-04
-8.56841E-04	4.86526E-06	9.65530E-04	6.99550E-04	

ROW 23

3.27152E-02	-1.24999E-01	-2.32623E-03	-2.47976E-03	-2.47046E-03
-3.64195E-03	-3.73857E-05	7.92617E-05	6.08236E-03	1.10964E-02
-1.24339E-02	9.40091E-04	6.49058E-04	9.52046E-04	-9.27779E-05
-3.51622E-03	2.30179E-03	7.55698E-03	-4.41286E-04	-6.88494E-04
1.44950E-03	8.83691E-04	5.51810E-03	-7.00222E-04	-3.52574E-03
-2.82921E-03	-2.99505E-03	3.64774E-04	-2.15778E-04	-1.54995E-04
2.74098E-03	-3.33861E-04	7.31720E-04	1.18127E-04	

ROW 24

1.15538E-02	-5.11260E-02	2.41418E-03	5.13339E-03	2.88985E-03
1.67567E-03	1.15151E-03	2.70749E-04	2.37321E-03	1.65350E-03
-1.64269E-03	-9.52916E-04	2.04809E-03	9.36789E-06	-1.34320E-04
-1.23053E-03	1.61650E-03	3.80110E-03	-6.57255E-04	5.42884E-04
1.09556E-03	2.75078E-03	-3.52819E-03	-1.64308E-04	-3.41645E-04
-3.06559E-04	5.71391E-04	-3.26443E-04	9.48475E-05	-3.36957E-04
-1.97750E-04	-4.45467E-06	1.74710E-04	-1.88274E-04	

MATRIX 'RR2.' 34 BY 34

ROW 25

1.23079E-02	-1.12299E-01	-8.11680E-03	-4.79784E-03	-2.78465E-03
7.43009E-03	2.35559E-03	4.97326E-04	7.07695E-03	7.20377E-03
-9.14255E-03	6.87817E-03	4.82536E-03	2.36558E-04	-3.34456E-05
-1.85574E-03	4.88880E-03	-1.08752E-03	3.32591E-04	-4.77783E-04
3.40845E-04	-5.09576E-05	2.47500E-03	-1.25024E-03	-2.58458E-03
-3.30706E-03	-2.11020E-03	-7.23629E-04	2.80440E-04	-3.11214E-04
6.19662E-04	-7.34375E-05	7.90247E-04	4.83262E-05	

ROW 26

9.63127E-03	-9.37735E-02	-4.28773E-03	-1.80015E-03	-9.70882E-04
5.85476E-03	2.09033E-03	4.42442E-04	5.77167E-03	5.37729E-03
-6.44976E-03	3.10946E-03	3.67133E-03	1.80251E-04	-9.23721E-05
-1.89885E-03	3.71527E-03	1.14877E-03	4.81483E-05	-3.86805E-05
1.53221E-04	9.35076E-04	4.30846E-04	-1.12285E-03	-1.84467E-03
-1.65041E-03	-1.35959E-03	-2.03784E-04	2.26729E-04	-2.57744E-04
2.38388E-04	-6.96472E-05	5.82790E-04	-4.48095E-05	

ROW 27

1.80378E-02	-7.25402E-02	-3.61550E-03	9.19084E-03	6.11796E-03
1.19902E-02	4.64172E-03	9.28604E-04	4.87994E-03	-5.09859E-03
5.49658E-03	3.20778E-02	4.53244E-03	-2.09979E-03	4.30004E-04
5.77356E-03	3.05872E-03	-7.36761E-04	4.82808E-04	4.25186E-03
3.54733E-03	-4.36780E-05	-4.71509E-03	-3.49587E-03	-1.06765E-03
-1.37827E-03	-2.41171E-03	-2.25645E-04	-5.83663E-05	-5.57593E-04
-1.67140E-03	7.50446E-05	4.34126E-04	2.65296E-04	

ROW 28

1.03460E-03	-9.55873E-02	-4.44409E-03	-8.81909E-04	-4.01502E-04
5.43589E-03	2.37929E-03	5.00907E-04	6.04852E-03	4.85193E-03
-5.88676E-03	5.97509E-03	4.21213E-03	-3.11482E-05	-3.49491E-05
-3.64727E-04	4.52495E-03	1.28582E-03	-8.90584E-05	4.38167E-04
3.01228E-04	4.57133E-04	-6.17895E-05	-1.43633E-03	-2.10530E-03
-3.03547E-03	-1.95403E-03	-9.54943E-06	1.37669E-04	-2.82745E-04
2.04340E-04	-1.07011E-04	5.50806E-04	7.28945E-06	

ROW 29

1.60144E-03	1.94175E-02	6.10172E-03	7.57648E-03	4.52033E-03
-3.09509E-03	6.75429E-05	2.15858E-05	-1.61042E-03	-4.22617E-03
6.36896E-03	7.34012E-04	-2.33344E-03	-6.68874E-04	1.02512E-04
3.20934E-03	-2.16853E-03	6.19976E-03	-4.97796E-04	2.30713E-03
1.20424E-03	1.09811E-03	-3.55674E-03	-8.32661E-04	1.07533E-03
9.33619E-04	1.39029E-04	-5.23632E-06	-2.70457E-04	-4.40178E-05
-5.17357E-04	2.16337E-05	-2.30361E-04	4.39501E-05	

ROW 30

1.27595E-02	-5.45202E-02	1.36002E-03	5.62726E-03	3.38244E-03
3.93517E-03	1.74845E-03	3.79053E-04	3.04716E-03	2.71546E-04
9.05999E-04	6.11782E-03	1.75905E-03	-5.56446E-04	7.19904E-05
1.96346E-03	3.08104E-03	6.14084E-03	-7.17791E-04	2.30775E-03
1.37734E-03	1.37618E-03	-3.07040E-03	-1.35179E-03	-5.71382E-04
-7.33196E-04	-1.38125E-03	-9.86470E-05	-1.06417E-04	-2.96007E-04
-1.75419E-04	-3.68706E-05	2.04476E-04	4.08773E-05	

MATRIX 'PP2.' 34 BY 34

ROW 31

9.05605E-03	8.67332E-03	4.48465E-03	7.54953E-03	4.84884E-03
4.59031E-04	1.29063E-03	2.10509E-04	2.46085E-04	-6.77369E-03
6.07654E-03	8.01869E-03	-1.18056E-03	-1.15148E-03	2.35212E-04
6.18688E-03	-1.38543E-03	7.68093E-03	-2.90918E-04	3.51899E-03
-5.41476E-04	4.47720E-03	-4.24342E-03	-8.29660E-04	4.02938E-04
4.02066E-04	-3.77137E-04	2.66376E-06	-4.66167E-04	-3.26092E-04
1.95746E-04	-1.49461E-04	-1.07914E-04	-1.38019E-04	

ROW 32

1.26227E-03	-4.49342E-03	9.05048E-04	7.12616E-04	6.13607E-04
1.39542E-04	4.39020E-04	6.02212E-05	7.70497E-04	-1.03510E-03
1.99657E-03	2.05406E-03	-2.72176E-04	-2.16435E-04	5.79272E-05
1.25274E-03	2.42920E-04	3.93247E-03	-2.87106E-04	9.84725E-04
-3.29601E-04	1.30370E-03	-6.35943E-04	1.58471E-05	3.39425E-05
9.33641E-05	-6.98854E-04	-6.15839E-05	-1.35405E-04	-1.31399E-04
3.07314E-04	-9.10736E-05	-2.22638E-06	-3.84501E-05	

ROW 33

3.14862E-05	-2.66481E-04	-1.46345E-05	-7.06539E-06	-4.05956E-06
3.10541E-05	7.40274E-06	1.54149E-06	2.33965E-05	2.14700E-05
-2.84014E-05	2.93282E-05	2.41307E-05	4.89043E-07	-2.41217E-07
-7.97511E-06	1.33394E-05	-2.87109E-06	-2.06394E-05	2.27104E-08
-8.39616E-06	-4.12510E-06	1.02523E-06	-1.23732E-05	-2.44049E-05
-2.04078E-05	-1.73214E-05	-4.57818E-06	2.82925E-06	-2.85117E-06
2.32441E-06	-9.32067E-08	4.02968E-06	0.0	

ROW 34

1.94702E-04	-1.93305E-04	1.27321E-06	2.55762E-05	-1.13179E-06
-1.03579E-04	-3.35343E-05	-5.50319E-06	-3.09033E-05	6.36655E-05
-6.20355E-05	9.91782E-05	-3.01443E-05	9.70132E-07	5.39514E-06
2.97603E-05	2.15749E-07	-3.07751E-05	-2.37094E-06	5.42770E-06
6.91635E-05	-8.83184E-05	1.61377E-05	5.17016E-06	-3.55229E-06
6.05566E-06	-4.39669E-05	4.13622E-07	2.54170E-06	2.08664E-06
-3.04113E-05	-3.83289E-06	0.0	3.43865E-05	

MATRIX 'PPP.' 34 BY 34 *COEFFICIENTS FOR* $\phi(s)\ \{g(s)\}$

ROW 1

0.0	-4.12650E 01	-3.45862E-02	8.92631E 00	3.66230E 00
-3.63347E 00	-7.32827E-01	-9.19969E-02	-1.36638E 00	4.63476E 00
-3.70012E 00	2.98401E 00	1.17527E 00	-9.18709E-02	1.29113E-01
-5.39258E-01	1.35470E 00	-1.30132E 00	-4.62310E 00	1.60836E 00
9.38994E 00	-6.33204E 00	-5.43064E 00	-1.23845E 00	-2.18430E 00
-1.73215E 00	-2.70135E 00	-1.26907E 00	1.10735E-01	-1.28032E 00
-4.39077E-01	1.43957E-01	2.11562E 00	1.44019E 00	

ROW 2

0.0	2.36255E 01	6.05641E-01	-1.13561E 01	-4.55752E 00
-3.30339E 00	-3.40533E 00	-6.84981E-01	-9.15034E 00	-7.62333E 00
1.17364E 01	-1.23946E 01	-1.45430E 01	1.09433E-01	3.59026E-01
4.93309E 00	-8.20030E 00	-2.74335E 00	1.52647E 01	-2.78284E 00
9.91073E 00	6.86998E 00	1.43292E 01	9.77105E 00	1.25599E 01
1.17053E 01	5.47658E 00	9.07580E 00	-7.32265E 00	5.21086E 00
-1.94123E 00	6.00240E-01	-1.30493E 01	2.09017E-01	

ROW 3

0.0	-3.37856E 00	2.44613E-01	3.31042E 00	1.43036E 00
-1.25923E 00	3.52053E-02	7.31013E-03	-3.90998E-01	-1.39918E-01
3.69656E-01	-1.09317E 00	-6.69561E-01	-1.04238E-01	-3.31820E-02
3.57327E-01	-4.80836E-01	9.07690E-01	8.11880E-01	7.07927E-01
2.05160E 00	2.74615E-01	-1.83323E 00	-6.45954E-01	9.68528E-01
5.94083E-01	2.37027E-01	3.78119E-01	-5.92898E-01	-1.09744E-01
-6.03586E-01	1.75702E-02	-7.69136E-01	8.95028E-02	

ROW 4

0.0	-2.11463E 00	7.18949E-02	1.75722E 00	7.33854E-01
-9.60564E-01	1.52467E-01	3.12099E-03	6.93052E-02	-3.98549E-01
9.63789E-01	-1.14834E-01	-3.99418E-01	-9.99604E-02	9.84411E-03
4.39491E-01	-1.74459E-01	7.78716E-01	2.10237E-01	6.33203E-01
4.33418E-01	8.35356E-01	-1.08925E 00	-5.02407E-01	4.26195E-01
2.49473E-01	-8.89616E-01	1.02493E-01	-4.16871E-01	-2.33662E-01
-5.95987E-01	1.93343E-02	-2.72431E-01	4.21780E-02	

ROW 5

0.0	-1.12186E 00	5.91673E-02	1.44904E 00	6.09327E-01
-6.63249E-01	1.78825E-01	1.44124E-02	1.72465E-01	-3.57116E-01
5.90119E-01	-6.27279E-02	-6.49402E-02	-8.07793E-02	4.77232E-04
3.22604E-01	-9.28184E-02	7.01176E-01	1.26943E-01	5.25061E-01
8.13954E-02	7.72473E-01	-1.02389E 00	-5.31707E-01	2.81945E-01
1.16213E-01	-6.81866E-01	3.29828E-02	-3.28535E-01	-2.26467E-01
-5.04899E-01	-1.93269E-02	-1.41203E-01	-2.30244E-02	

ROW 6

0.0	2.32883E 00	-1.25716E-01	8.05179E-02	9.53646E-03
7.76991E-02	5.82822E-01	6.60508E-02	1.21208E 00	-8.67106E-01
6.73352E-01	1.12576E 00	1.06891E 00	-8.40529E-02	-2.30713E-02
3.65139E-01	5.02220E-01	7.98705E-01	-7.42735E-01	4.80611E-01
-2.97263E 00	1.81096E 00	-9.77265E-01	-9.48131E-01	-5.80906E-01
-6.55679E-01	-1.71558E 00	-5.46667E-01	-3.56095E-02	-5.35985E-01
-6.05355E-01	-1.07675E-01	7.63883E-01	-3.73854E-01	

MATRIX 'RR3.' 34 BY 34

ROW 7

0.0	2.17089E-01	-2.90559E-02	1.71660E-01	6.68229E-02
1.49935E-02	1.53945E-01	1.99956E-02	3.24332E-01	-1.41062E-01
5.37559E-02	3.43848E-01	3.30371E-01	-2.22558E-02	-6.02812E-03
4.78643E-02	1.68491E-01	2.77184E-01	-2.75450E-01	1.75746E-01
-6.78505E-01	3.95310E-01	-4.21647E-01	-3.23218E-01	-1.98656E-01
-2.22742E-01	-4.72399E-01	-1.34531E-01	-1.98323E-02	-1.88272E-01
-1.88089E-01	-5.86726E-02	2.53119E-01	-9.19734E-02	

ROW 8

0.0	-9.04699E-02	-5.88827E-03	6.91072E-02	2.71814E-02
-1.99115E-02	3.03481E-02	3.47094E-03	6.28853E-02	-2.01502E-02
1.97582E-02	7.92525E-02	6.68061E-02	-5.83257E-03	-5.88901E-04
1.29589E-02	3.60206E-02	5.50239E-02	-6.62158E-02	4.32523E-02
-1.10717E-01	6.78150E-02	-9.58317E-02	-6.71423E-02	-4.26332E-02
-4.57661E-02	-1.19810E-01	-3.95047E-02	-5.81347E-03	-4.15136E-02
-4.05555E-02	-7.83124E-03	5.39551E-02	-1.25379E-02	

ROW 9

0.0	-1.96542E 00	-3.98937E-02	4.84517E-01	1.93389E-01
6.92098E-02	9.72429E-02	2.17637E-02	2.99344E-01	4.03021E-01
-5.74991E-01	6.43458E-01	5.99882E-01	-1.66722E-03	-5.37093E-03
-1.80142E-01	4.05439E-01	1.15454E-01	-7.50115E-01	1.62096E-01
-2.13407E-01	-4.05370E-01	-7.42134E-01	-3.74727E-01	-5.47204E-01
-4.97755E-01	-4.63125E-01	-4.18862E-01	1.21297E-01	-2.91750E-01
-1.17036E-02	-8.14973E-02	5.69944E-01	-5.38768E-03	

ROW 10

0.0	-4.82787E-01	-7.75317E-02	-9.27276E-01	-3.97211E-01
5.86925E-01	-9.53547E-02	-6.74825E-04	2.40190E-02	4.81883E-01
-9.25825E-01	2.96290E-01	4.19489E-01	7.05481E-02	-1.58597E-02
-4.73589E-01	3.36281E-01	-8.78464E-01	-5.49260E-01	-4.89284E-01
-2.47969E-01	-9.96473E-01	6.93149E-01	3.57259E-01	-5.62311E-01
-3.96857E-01	5.09652E-01	-2.88936E-01	4.48247E-01	9.70383E-02
7.70660E-01	1.20964E-01	4.48621E-01	4.10033E-02	

ROW 11

0.0	3.04324E 00	1.01630E-01	1.27779E 00	5.74368E-01
-3.93749E-01	3.44433E-01	4.42648E-02	3.43626E-01	-1.19907E 00
8.51235E-01	-6.24757E-01	-7.31539E-01	-1.00590E-01	-2.05429E-02
5.79106E-01	-3.87556E-01	1.44218E 00	7.40626E-01	7.18834E-01
-7.93983E-01	2.31709E 00	-1.45397E 00	-9.27038E-01	7.38749E-01
3.21863E-01	-2.14607E-01	3.12907E-01	-6.57741E-01	-2.53667E-01
-9.43659E-01	-2.31683E-01	-4.81566E-01	-3.29329E-01	

ROW 12

0.0	-5.90030E 00	1.33484E-02	1.74243E 00	7.05259E-01
-1.06760E 00	-1.44740E-02	-2.05297E-02	-1.06434E-01	3.58599E-01
3.42726E-01	6.79891E-01	-3.83418E-02	-7.64783E-02	4.77137E-02
3.80355E-01	1.92515E-01	1.17143E 00	-5.37298E-01	8.68021E-01
1.26730E 00	-4.46683E-02	-1.71975E 00	-4.11975E-01	2.01903E-02
1.38307E-02	-1.51335E 00	-3.26386E-01	-3.42947E-01	-5.95980E-01
-6.65154E-01	-2.44159E-01	8.80209E-02	3.17850E-01	

MATRIX 'RR2.' 24 BY 24

ROW 13

0.0	-6.01755E-01	-3.91795E-02	-2.07496E-01	-9.20811E-02
-6.69354E-02	-1.08459E-02	-9.08581E-03	-2.37844E-02	-1.52785E-01
1.37999E-01	1.48744E-01	2.39317E-02	-2.44720E-03	6.46134E-02
4.42710E-02	1.17856E-01	-2.92515E-01	-6.59388E-02	-5.53069E-02
-2.50022E-01	4.69269E-02	1.12570E-01	1.68258E-01	1.87319E-02
3.18390E-02	-7.62348E-02	-1.59876E-01	1.42239E-01	-5.55511E-02
-1.77344E-02	2.58820E-02	-4.09992E-03	-3.76528E-02	

ROW 14

0.0	-6.05988E-03	-5.07652E-03	-1.92542E-01	-8.00412E-02
9.09597E-02	-4.46757E-02	-4.02828E-03	-6.53823E-02	7.95515E-02
-1.20987E-01	-3.68440E-02	-1.71258E-02	1.46253E-02	-7.22522E-04
-6.83793E-02	3.27035E-03	-1.99757E-01	-3.80566E-04	-1.12284E-01
9.30519E-02	-2.00807E-01	2.01357E-01	1.16211E-01	-2.79317E-02
-2.04597E-03	1.82957E-01	8.56412E-03	6.78135E-02	6.12780E-02
1.18955E-01	2.73263E-02	1.12815E-03	1.04669E-02	

ROW 15

0.0	-1.34805E-02	1.53628E-03	2.70446E-02	1.12460E-02
-1.04134E-02	2.94715E-03	3.22065E-04	3.84278E-03	-6.01647E-04
7.10499E-03	2.43276E-03	-1.12210E-03	-1.48808E-03	1.98615E-04
6.65215E-03	-1.78162E-03	3.95298E-02	-1.21457E-03	1.87058E-02
9.45069E-03	1.81655E-02	-3.63658E-02	-1.66100E-02	3.81805E-03
5.36679E-04	-2.19219E-02	1.18382E-05	-1.32036E-02	-1.00191E-02
-1.12036E-02	-6.52649E-03	-7.82578E-04	5.37010E-03	

ROW 16

0.0	-1.60397E 00	3.83585E-02	1.05688E 00	4.37341E-01
-4.99637E-01	7.78162E-02	4.53617E-03	7.98870E-02	5.36725E-02
2.62973E-01	1.98791E-01	-1.86027E-02	-5.16670E-02	1.44108E-02
3.36753E-01	-3.68708E-02	8.47641E-01	-1.04801E-01	5.09403E-01
4.43814E-01	3.18181E-01	-5.62925E-01	-4.49136E-01	6.35554E-02
5.17173E-03	-7.74114E-01	4.44606E-03	-3.20197E-01	-2.48043E-01
-4.78311E-01	-1.32524E-01	1.00602E-02	1.02251E-01	

ROW 17

0.0	-5.55977E-01	-3.48841E-02	-3.34962E-02	-2.22195E-02
1.13695E-01	4.57764E-02	9.30308E-03	1.74355E-01	1.92048E-01
-3.65469E-01	3.93807E-01	3.54053E-01	7.32757E-03	-4.07311E-03
-1.21150E-01	3.22963E-01	-4.20634E-02	-3.96513E-01	2.84534E-02
-3.81463E-01	-3.15266E-01	-2.68846E-01	-2.69592E-02	-2.70605E-01
-2.24347E-01	-1.86472E-01	-3.89653E-01	1.92515E-01	-1.93088E-01
1.41741E-01	-3.41029E-02	2.98297E-01	-1.29318E-02	

ROW 18

0.0	-3.94104E 00	1.01659E-01	2.51750E 00	1.07506E 00
-6.62537E-01	1.46947E-01	3.12475E-02	1.14313E-01	7.14099E-01
-3.43562E-01	2.74946E-02	2.07096E-01	-7.91899E-02	-9.09832E-03
1.30936E-01	7.90142E-02	1.24846E 00	-3.55529E-01	8.97048E-01
1.05042E 00	3.05247E-01	-2.46236E 00	-1.08344E 00	6.87633E-02
-1.85753E-01	-6.14101E-01	-1.67510E-01	-4.84453E-01	-5.40359E-01
-3.55133E-01	-1.38594E-01	1.35531E-01	-1.95329E-02	

MATRIX 'RP3.' 34 BY 34

ROW 19

0.0	-2.68674E 00	-1.16937E-01	-1.85352E-01	-1.05955E-01
2.22097E-01	4.97218E-02	1.11483E-02	3.32636E-01	5.82534E-01
-6.90982E-01	1.01876E 00	7.55929E-01	2.29318E-02	2.52751E-03
-2.74863E-01	4.48437E-01	-3.21186E-01	-1.10660E 00	-4.56180E-02
-3.67604E-01	-6.48168E-01	-6.22209E-02	-2.06506E-01	-9.15954E-01
-7.12588E-01	-6.59360E-01	-3.62220E-01	2.39537E-01	-1.58794E-01
1.36909E-01	-2.29669E-03	6.48204E-01	5.44700E-02	

ROW 20

0.0	-4.44427E-01	1.43991E-02	4.04036E-01	1.70147E-01
-1.61578E-01	4.54354E-02	4.70814E-02	5.19822E-02	-4.62108E-02
1.00062E-01	4.55972E-02	1.44255E-02	-2.27546E-02	1.72995E-03
9.08342E-02	-1.97729E-04	3.22429E-01	-2.69717E-02	2.11244E-01
6.98373E-02	2.16398E-01	-4.52260E-01	-2.12427E-01	4.92226E-02
3.15463E-05	-2.72611E-01	-2.38937E-02	-1.22673E-01	-1.18917E-01
-1.95030E-01	-4.32906E-02	-1.90723E-03	4.70561E-03	

ROW 21

0.0	3.79015E 00	-1.13798E-01	-1.06651E 00	-4.67044E-01
5.18684E-01	3.36113E-01	3.90196E-02	9.14107E-01	-5.86339E-01
3.95311E-01	5.88926E-01	6.92585E-01	-1.35901E-02	-2.96637E-02
-2.12569E-02	2.45906E-01	1.58432E-01	-3.92427E-01	-5.17115E-02
-2.35956E 00	1.12460E 00	4.07218E-01	-3.13233E-01	-5.09837E-01
-4.73517E-01	-7.46013E-01	-1.90689E-01	7.98244E-02	-9.05161E-02
1.43956E-01	6.42235E-02	5.28412E-01	-2.07345E-01	

ROW 22

0.0	-4.95638E 00	2.46327E-03	1.06111E 00	4.45233E-01
-1.57983E-01	-1.13950E-01	-9.11790E-05	-1.68782E-01	8.57163E-01
-1.02615E 00	4.31107E-01	2.99306E-01	9.48441E-03	1.08228E-02
-2.14363E-01	2.02162E-01	-3.95554E-01	-6.89821E-01	1.19445E-01
1.23709E 00	-1.15135E 00	-8.11982E-01	-3.36329E-01	-4.71377E-01
-4.05104E-01	-8.46964E-02	-1.34561E-01	6.55248E-02	-1.08775E-01
-1.83904E-01	-1.62145E-02	4.27949E-01	1.08771E-01	

ROW 23

0.0	-1.32727E 00	-3.27231E-03	3.22263E-01	1.39328E-01
1.71113E-01	-9.29691E-02	1.31080E-02	5.12587E-02	4.16408E-01
-7.27666E-01	1.56552E-01	2.84119E-01	2.65801E-02	-8.71854E-02
-2.39947E-01	1.42499E-01	2.30935E-02	-4.21996E-01	-1.81839E-02
3.09122E-01	-4.71157E-01	-3.08113E-01	-1.69126E-01	-3.72155E-01
-3.36335E-01	2.46994E-01	-8.61103E-02	4.60030E-02	-5.50141E-02
1.87082E-01	-9.02957E-02	3.21929E-01	2.00265E-02	

ROW 24

0.0	-6.75096E-01	8.48500E-03	3.80590E-01	1.66706E-01
-7.41414E-02	3.15189E-02	1.02906E-02	4.42905E-02	3.73493E-02
-2.58717E-01	1.65845E-02	1.28403E-01	-3.81715E-03	-7.35541E-03
-4.25893E-02	7.20279E-02	-2.01777E-02	-1.20786E-01	6.06388E-02
4.26950E-02	-3.32135E-02	-3.92556E-01	-1.61175E-01	-4.98442E-02
-9.04009E-02	1.22590E-01	-9.06625E-02	1.26625E-02	-7.84883E-02
-2.14829E-02	-2.08039E-02	8.97738E-02	-3.02698E-02	

MATRIX [illegible] 34 BY 34

ROW 25

0.0	-7.10146E-01	-4.04200E-02	-1.48598E-01	-7.41922E-02
1.57157E-01	2.82116E-02	7.05059E-03	1.87062E-01	2.40235E-01
-2.99474E-01	4.45533E-01	3.67088E-01	1.17740E-02	-1.98441E-03
-1.42526E-01	2.41414E-01	-8.34944E-02	-4.76837E-01	-2.61442E-02
-3.06518E-01	-2.88107E-01	-6.03170E-02	-7.16376E-02	-3.87145E-01
-3.02169E-01	-2.64154E-01	-2.36641E-01	1.36737E-01	-1.02741E-01
1.12808E-01	-1.27994E-02	3.78254E-01	7.85117E-03	

ROW 26

0.0	-5.02579E-01	-2.47062E-02	2.72348E-02	7.45427E-03
1.30429E-01	4.34010E-02	1.09999E-02	1.52607E-01	1.61327E-01
-3.04923E-01	2.76385E-01	2.95269E-01	6.98127E-03	-6.03227E-03
-1.18411E-01	1.81146E-01	-5.19107E-02	-3.40454E-01	-1.75009E-04
-2.26398E-01	-1.82566E-01	-1.96246E-01	-1.22537E-01	-2.70578E-01
-2.26466E-01	-9.57737E-02	-1.87550E-01	9.17734E-02	-9.22830E-02
7.57517E-02	-1.62493E-02	2.80154E-01	-7.08067E-03	

ROW 27

0.0	-1.05338E 00	-5.41976E-02	6.65776E-02	-4.66850E-03
-3.27582E-01	9.30240E-02	-5.96749E-03	2.40459E-01	-1.42718E-03
5.77019E-01	6.43616E-01	1.94086E-01	-3.95905E-02	2.06529E-02
1.92419E-01	1.50740E-01	2.60079E-01	-3.43983E-01	2.32920E-01
-3.57728E-01	1.72312E-01	-8.04187E-02	-1.05240E-01	-2.02631E-01
-1.02930E-01	-1.20393E 00	-1.75571E-01	-3.10608E-02	-1.73352E-01
-2.03733E-01	2.71557E-02	2.28164E-01	4.08423E-02	

ROW 28

0.0	-6.04527E-01	-3.05019E-02	3.00969E-02	5.16849E-03
8.81805E-02	4.77525E-02	9.24556E-03	1.65680E-01	1.65078E-01
-2.32513E-01	3.28787E-01	3.05916E-01	3.27493E-03	-3.27613E-03
-9.59829E-02	2.16924E-01	-9.15300E-03	-3.61783E-01	2.58928E-02
-2.53592E-01	-1.86227E-01	-2.00690E-01	-1.18360E-01	-2.94450E-01
-2.53682E-01	-2.42145E-01	-2.15504E-01	9.64873E-02	-1.23114E-01
6.12218E-02	-2.08654E-02	2.85132E-01	1.16633E-03	

ROW 29

0.0	-9.35733E-02	2.94186E-02	3.43030E-01	1.48688E-01
-1.58449E-01	1.25505E-02	4.76391E-04	-3.78763E-02	-8.60755E-02
1.42075E-01	-1.45367E-01	-1.71503E-01	-1.72930E-02	1.15577E-03
9.29390E-02	-1.02361E-01	2.14821E-01	1.46761E-01	1.30185E-01
2.01924E-01	1.96559E-01	-2.38613E-01	-1.10609E-01	1.63260E-01
1.06676E-01	-4.42806E-02	8.89491E-02	-1.28632E-01	-1.78392E-02
-1.42871E-01	-1.41823E-02	-1.27072E-01	7.04389E-03	

ROW 30

0.0	-7.45549E-01	-2.43136E-03	3.07707E-01	1.27165E-01
-7.96051E-02	3.81623E-02	5.87043E-03	7.71646E-02	5.74559E-02
-6.92358E-02	1.52452E-01	1.29340E-01	-1.11421E-02	-2.80674E-04
4.21515E-02	9.62686E-02	1.60126E-01	-1.74237E-01	1.31036E-01
1.49152E-02	5.36134E-03	-3.71453E-01	-1.61513E-01	-8.65200E-02
-1.01305E-01	-2.17400E-01	-1.13673E-01	-2.19134E-02	-1.24282E-01
-6.70918E-02	-3.38978E-02	1.11721E-01	6.49312E-03	

MATRIX 'PP3.' 34 BY 34

ROW 31

0.0	-5.29153E-01	1.30552E-02	3.30947E-01	1.24539E-01
-2.25003E-01	1.57015E-02	-2.77144E-03	-1.26950E-02	-3.94991E-02
2.07803E-01	5.84233E-02	-9.78242E-02	-2.17646E-02	1.13301E-02
1.51679E-01	-6.11443E-02	3.26958E-01	3.60760E-02	2.01063E-01
1.98361E-01	2.17251E-01	-3.13855E-01	-1.23894E-01	8.96071E-02
7.25963E-02	-3.20980E-01	4.79827E-02	-1.43674E-01	-7.72827E-02
-2.95893E-01	-6.58450E-02	-6.35495E-02	-2.28814E-02	

ROW 32

0.0	-7.37557E-02	3.98450E-03	7.66846E-02	3.35728E-02
-1.75768E-02	4.63603E-03	1.43375E-03	3.68231E-03	8.57470E-03
-2.81855E-02	1.33707E-02	3.94366E-03	-1.87290E-03	9.44798E-04
1.49710E-02	9.16298E-03	1.21608E-01	-1.48682E-02	5.46385E-02
3.52705E-02	3.93255E-02	-1.47685E-01	-4.59462E-02	6.59888E-03
-4.10859E-03	-2.32919E-02	-1.99166E-02	-2.94570E-02	-4.30285E-02
-4.59455E-02	-4.01064E-02	2.74949E-03	-6.09036E-03	

ROW 33

0.0	-1.83977E-03	-8.15865E-05	-7.75466E-05	-5.06700E-05
2.53024E-04	9.49449E-05	1.93077E-05	3.65411E-04	3.90084E-04
-5.60241E-04	7.56436E-04	6.61990E-04	1.32297E-05	-6.47846E-06
-7.38430E-04	3.44570E-04	-1.19333E-04	-8.45191E-04	1.84550E-06
-4.77847E-04	-3.39187E-04	-1.75658E-04	-2.96130E-04	-7.27307E-04
-6.00636E-04	-5.05191E-04	-2.75759E-04	1.45794E-04	-1.41197E-04
5.74956E-05	-1.10926E-05	6.73408E-04	0.0	

ROW 34

0.0	-1.13766E-03	5.85133E-05	1.24231E-03	4.26137E-04
-1.52883E-03	-7.47885E-04	-1.30450E-04	-1.26054E-03	2.91493E-03
3.15907E-04	1.35872E-03	-8.45927E-04	9.07493E-06	1.63639E-04
3.14103E-05	1.63036E-05	9.10226E-05	-6.50491E-04	2.37063E-04
4.93574E-03	-4.59394E-03	6.65111E-04	7.77680E-04	-2.61755E-04
3.39485E-04	-2.33666E-03	-8.33651E-07	5.51426E-05	9.07589E-05
-8.73959E-04	-9.28912E-05	0.0	1.28310E-03	

MATRIX 'XWR,' 1 BY 10 BODY STATIONS , GUST REFERENCE STATIONS

ROW 1

-1.08200E 02	1.00000E 02	5.09200E 02	6.75900E 02	8.42600E 02
1.00930E 03	1.17600E 03	1.50000E 03	1.57200E 03	1.72900E 03

```
MATRIX 'YWR.'     1 BY   10   BUTTOCK LINES , GUST REFERENCE STATIONS

ROW    1
 0.0             0.0             1.11000E 02   3.33000E 02   5.55000E 02
 7.77000E 02     9.99000E 02     0.0           9.00000E 01   2.60000E 02
```

MATRIX 'BRIW' 34 BY 10 COEFFICIENTS FOR $\frac{1}{V}\psi(s)\{w_\perp(s,\kappa_0 q)\}_{\frac{1}{2}Left+\frac{1}{2}Right}$

ROW 1

0.0	1.09952E 00	1.07583E 01	8.66250E 00	7.49412E 00
6.26510E 00	3.94289E 00	6.05029E-01	2.99002E 00	1.25158E 00

ROW 2

0.0	2.80562E 00	1.31862E 01	6.79612E 00	-2.25120E 00
-6.43154E 00	-9.66253E 00	-1.22315E 00	-1.90766E 01	-8.08598E 00

ROW 3

0.0	-3.62619E-02	-4.77204E-02	2.14373E-01	8.77768E-01
1.76387E 00	2.01630E 00	-1.21131E-01	-1.07013E 00	-4.71906E-01

ROW 4

0.0	1.24931E-01	7.11414E-01	2.31806E-01	1.94928E-01
-8.55063E-02	1.60918E 00	4.40613E-03	-3.68302E-01	-1.77895E-01

ROW 5

0.0	5.76221E-02	2.08574E-01	-6.46500E-02	-1.49818E-01
4.29440E-02	1.36792E 00	3.55151E-03	-1.88315E-01	-9.47936E-02

ROW 6

0.0	3.17487E-01	-2.62937E-01	-1.17024E 00	-2.45531E 00
-1.31162E 00	1.23966E 00	4.93215E-02	1.02004E 00	5.11463E-01

ROW 7

0.0	7.58811E-02	-1.13607E-01	-2.60993E-01	-5.89196E-01
-1.97306E-01	4.26535E-01	7.30147E-03	3.35459E-01	1.72019E-01

ROW 8

0.0	2.32643E-02	1.91691E-02	-2.18329E-02	-8.47475E-02
-4.00380E-02	1.09730E-01	2.49897E-03	7.16926E-02	3.64318E-02

ROW 9

0.0	1.31935E-01	-4.27617E-02	1.16810E-01	2.45909E-02
3.69236E-01	3.57368E-01	-5.36781E-02	7.16656E-01	4.24019E-01

ROW 10

0.0	3.03614E-01	2.65232E-01	-3.47337E-01	5.62430E-01
1.96645E-01	-1.08472E 00	-6.21385E-02	5.38500E-01	3.60940E-01

ROW 11

0.0	4.81114E-02	-5.00625E-01	-1.53348E 00	-1.84093E 00
1.15639E-01	1.69164E 00	1.37446E-01	-5.42571E-01	-4.21920E-01

ROW 12

0.0	-1.78699E-01	1.57502E 00	1.55486E 00	1.20381E 00
-1.59626E-01	1.59876E 00	-1.24541E-01	-7.63595E-02	2.52833E-01

ROW 13

0.0	-1.77469E-01	9.45899E-01	3.25626E-01	-4.65158E-01
-1.28765E-01	-7.16230E-02	-7.01956E-02	-1.89632E-01	1.81412E-01

```
MATRIX 'RR1W'      24 BY    10

ROW   14
 0.0           -4.01651E-03   4.02184E-02   4.16734E-02   9.80477E-02
 3.16288E-02   -2.57761E-01  -2.82164E-03  -2.42201E-03   4.70387E-03

ROW   15
 0.0            5.79865E-03  -1.69842E-02  -1.39224E-02   2.36223E-02
-7.14312E-03    2.94760E-02   8.27324E-04   9.20173E-04  -2.48917E-03

ROW   16
 0.0            4.81243E-02  -1.28167E-01   3.78767E-01   2.66840E-01
-5.19782E-02    1.01834E 00   1.64697E-02   8.38510E-02  -6.36813E-02

ROW   17
 0.0            1.83699E-03  -2.54253E-02  -1.47037E-02  -3.40666E-03
-1.24145E-03    2.78858E-03  -7.01776E-04   2.03907E-01   3.94148E-01

ROW   18
 0.0           -8.36976E-04   2.69803E-01  -2.76556E-01   6.63829E-01
 1.29781E 00    1.71483E 00   1.49503E-02   2.02366E-01   6.93597E-02

ROW   19
 0.0           -2.82008E-02   5.24771E-01   4.59068E-01   1.52527E-01
-3.58853E-02   -1.14205E-01   8.91713E-03   1.31526E 00   3.85303E-01

ROW   20
 0.0           -7.54780E-04   1.93190E-02  -1.41653E-03   1.91276E-02
 3.47869E-02    3.76434E-01  -1.55837E-03  -3.51513E-03  -3.08664E-04

ROW   21
 0.0            1.16579E-02  -6.80476E-01  -1.59577E 00  -1.11350E 00
-1.41902E 00   -4.07935E-02  -1.13362E-02   9.57093E-01   2.07320E-01

ROW   22
 0.0           -1.00416E-02   5.70760E-01   1.43866E 00   4.31368E-01
 1.54982E 00    1.37785E-01  -9.64116E-03   6.99988E-01   1.58004E-01

ROW   23
 0.0            1.44901E-02  -1.34906E-01  -2.61109E-01   4.05865E-01
 5.97868E-01    7.41138E-02  -7.47829E-03   5.34541E-01   1.10894E-01

ROW   24
 0.0           -6.93194E-03   9.08557E-02  -9.37682E-02  -1.68148E-01
 4.74582E-01    1.91587E-01   1.13308E-03   1.06419E-01   7.35679E-02

ROW   25
 0.0            3.40451E-03   1.97763E-02   3.39652E-02   6.73198E-02
-8.87649E-02   -7.14970E-02   1.41812E-03   5.28795E-01   2.29566E-01

ROW   26
 0.0           -7.85660E-04  -6.80885E-02  -9.90071E-02  -3.32420E-02
 1.35120E-01    6.11546E-03  -2.13013E-03   3.89691E-01   1.71991E-01
```

```
MATRIX 'RBIW'    34 BY    10

ROW   27
 0.0            -7.79897E-03   2.79417E-01   8.22827E-01   1.52233E-02
-9.85334E-01     4.62830E-01  -3.05273E-03   3.17106E-01   1.40340E-01

ROW   28
 0.0             2.00483E-04  -3.15190E-02  -8.36389E-03   6.48079E-03
 1.47151E-02     5.15526E-02  -9.37955E-04   3.28817E-01   2.42845E-01

ROW   29
 0.0             1.27815E-03  -3.25288E-02  -2.76405E-02   5.04758E-02
 9.20390E-02     3.65993E-01   1.76718E-03  -1.38007E-01  -1.16759E-01

ROW   30
 0.0             3.41357E-04   1.06564E-01   1.00879E-02   4.95238E-02
 9.55490E-02     2.59836E-01  -2.21127E-03   1.12802E-01   1.11187E-01

ROW   31
 0.0            -5.19278E-03   4.49450E-02   4.67474E-01  -1.36479E-01
-1.09850E-01     3.90473E-01   1.85933E-03  -5.22625E-02  -7.51478E-02

ROW   32
 0.0            -1.13609E-03  -3.40640E-02   5.40844E-04  -1.59620E-02
 3.26104E-02     8.51178E-02   9.17209E-05  -7.76603E-03   1.32785E-02

ROW   33 THE NON-ZERO ELEMENTS ARE
       9     1.46675E-03          10     3.73012E-04

ROW   34 THE NON-ZERO ELEMENTS ARE
       4     5.95735E-03           5     5.41923E-03
```

MATRIX 'C.MT' 9 BY 34 *OUTPUT COEFFICIENTS FOR {q(s)}*

ROW 1 IS ZERO.

ROW 2 *VERTICAL BENDING MOMENT BODY STA. 1222*

0.0	0.0	1.63146E 07	3.33983E 07	2.21260E 07
-2.05857E 08	-7.56957E 07	-1.66617E 07	-3.05199E 08	-3.48310E 08
4.73183E 08	-5.75248E 08	-4.42584E 08	-1.97434E 07	9.74605E 06
1.61446E 08	2.77739E 07	1.09722E 06	-3.27431E 08	-3.11227E 07
-6.29866E 08	-4.55827E 08	-4.27405E 08	-3.00516E 08	-3.69507E 08
2.30607E 08	2.70282E 08	-1.04619E 08	-1.93296E 08	3.60875E 08
-3.79205E 08	6.36154E 07	0.0	0.0	

ROW 3 *VERTICAL BENDING MOMENT BODY STA. 1412*

0.0	0.0	9.71900E 06	2.04774E 07	1.46212E 07
-1.93251E 08	-4.78468E 07	-1.04259E 07	-2.01601E 08	-2.36516E 08
3.21511E 08	-4.85815E 08	-4.11546E 08	-1.47114E 07	6.98990E 06
1.50977E 08	1.15891E 07	7.12891E 07	2.80768E 08	-1.78304E 07
-2.05055E 08	-2.10078E 08	-3.16605E 08	6.72431E 07	-7.92005E 07
2.64376E 07	5.67839E 06	-5.32135E 07	-4.78218E 07	1.08903E 08
-1.57344E 07	1.88735E 07	0.0	0.0	

ROW 4 *VERTICAL BENDING MOMENT WING STA. 222*

0.0	0.0	-5.87327E 07	1.93257E 07	5.29874E 07
2.31236E 08	5.44810E 07	1.23263E 07	-5.63300E 07	-6.06850E 07
3.97201E 08	-3.11376E 08	1.17319E 08	8.24360E 06	-1.11946E 07
-2.04143E 08	1.90597E 06	2.91209E 08	-1.36784E 08	-5.26052E 06
9.13857E 07	1.85966E 07	2.34096E 08	-3.07846E 07	8.46708E 07
-5.62305E 07	-2.51392E 07	-9.95712E 06	-4.26392E 06	1.66863E 07
-7.05651E 07	1.59916E 07	0.0	0.0	

ROW 5 *VERTICAL BENDING MOMENT WING STA. 820*

0.0	0.0	-1.77744E 07	-3.31249E 07	-3.23114E 07
-1.19763E 08	-2.79317E 07	-4.73327E 06	8.87272E 06	4.35976E 07
-6.16593E 06	6.94701E 07	-7.13155E 07	-4.75610E 06	-1.87854E 06
1.59076E 07	3.80330E 05	1.80634E 08	-1.56584E 07	-3.70325E 06
-8.13344E 06	-1.71452E 08	1.80484E 08	-3.07854E 07	2.78934E 07
-1.77454E 07	-1.63346E 07	-8.67376E 06	-2.37582E 07	1.19106E 06
3.39721E 08	8.60862E 07	0.0	0.0	

ROWS 6 THROUGH 8 ARE ZERO.

ROW 9 *ANGLE OF PITCH, FUSELAGE AT C. G.*

0.0	-5.72958E 01	-1.72406E 00	-9.68820E-01	-3.71712E-01
-3.17813E 00	-6.56352E-01	-1.79658E-01	-2.70141E 00	-3.94537E 00
3.70761E 00	-5.22291E 00	-4.89009E 00	-1.74529E-01	1.27811E-01
3.03516E 00	1.22584E-01	-1.62852E 00	-4.10512E 00	-8.78130E-02
-5.64550E-01	6.13099E-01	7.65810E-01	-1.75750E 00	-3.57990E-01
6.14216E-01	5.91184E-01	4.19153E-01	4.12242E-01	-1.05414E 00
1.26933E 00	0.0	0.0	0.0	

MATRIX 'CCHT' 9 BY 34 *OUTPUT COEFFICIENTS FOR* $s^2\{q(s)\}$

ROWS 1 THROUGH 5 ARE ZERO.

ROW 6 *VERTICAL ACCELERATION BODY STA. 172*

-3.34787E-01	-1.80337E 00	-5.48016E-03	-4.89789E-02	-2.29846E-02
-1.64968E-01	-4.35038E-02	-1.25993E-02	-1.05302E-01	-2.05261E-01
2.31921E-02	1.73751E-01	2.44903E-01	5.09208E-03	-8.03608E-03
-9.90829E-02	-4.93760E-03	9.39497E-02	7.17286E-02	-3.56720E-03
-3.33003E-02	-5.04604E-02	-1.85004E-02	-1.44701E-02	-9.62878E-03
1.33537E-03	8.73529E-05	1.92429E-03	1.80499E-03	-4.51382E-03
3.47437E-03	1.04028E-03	0.0	0.0	

ROW 7 *VERTICAL ACCELERATION BODY STA. 860*

-3.26788E-01	-2.09871E-02	4.24929E-02	-2.05465E-02	-1.01125E-02
-1.39281E-02	1.94753E-03	-3.90173E-04	4.22545E-02	3.31523E-02
-9.07745E-02	1.96195E-02	-1.70545E-02	5.76669E-04	2.59900E-04
1.21070E-02	-1.16307E-03	-4.45759E-03	4.18809E-02	4.26057E-04
-1.70938E-02	-2.03394E-02	-2.99383E-02	7.89560E-03	-8.32524E-03
2.88092E-02	3.56529E-03	-2.04833E-03	-3.55343E-03	5.86380E-03
-5.73099E-03	2.36842E-05	0.0	0.0	

ROW 8 *VERTICAL ACCELERATION BODY STA. 1655*

-3.36787E-01	2.03859E 00	1.30533E-01	4.13870E-02	7.10908E-02
-1.13776E-01	-3.73869E-02	-7.98916E-03	-7.90951E-02	-5.87127E-02
5.66518E-02	1.30432E-02	2.61952E-02	4.17467E-04	-1.85854E-04
-1.31375E-02	1.02205E-02	-1.61677E-02	-1.10803E-01	2.10799E-04
-7.07415E-02	-5.72481E-02	-4.43717E-02	3.06124E-04	-1.04040E-02
1.66936E-03	3.65807E-03	3.66253E-03	-6.28682E-03	9.10880E-03
-5.94493E-03	3.12627E-03	0.0	0.0	

ROW 9 IS ZERO.

MATRIX 'CW..' 5 BY 10 OUTPUT COEFFICIENTS FOR $\{w_g(s; x_i, y_i)\}$

VERTICAL GUST VELOCITY AT PROBE

ROW 1 COLUMN 1 8.33333E-02

ROWS 2 THROUGH 5 ARE ZERO.

MATRIX 'C-WG'

ROW 40 VERTICAL BENDING MOMENT W.S. 222

9.83602E 02	-9.92690E 02	2.71720E 02	-1.83727E 01	-3.04338E 01
-9.10490E 01	-1.99154E 01	-4.46431E 00	1.26331E 01	1.00688E 01
-5.71607E 01	1.94112E 01	-5.76000E 00	-3.53306E-01	4.67621E-01
7.87398E 00	-5.00373E-02	-5.97675E 00	2.53654E 00	6.76427E-02
-9.40287E-01	-1.75855E-01	-1.98883E 00	2.10072E-01	-4.52173E-01
2.65497E-01	1.14982E-01	3.23150E-02	1.27921E-02	-4.68622E-02
1.75919E-01	-2.82901E-02	0.0	0.0	

ROW 48 VERTICAL BENDING MOMENT W.S. 820

1.68686E 02	-3.52060E 02	8.22525E 01	3.14922E 01	1.35935E 01
4.67421E 01	1.02104E 01	1.71429E 00	-1.98988E 00	-7.23366E 00
8.87332E-01	-4.33076E 00	3.50138E 00	2.03838E-01	7.84704E-02
-6.13133E-01	-9.98478E-03	-3.70604E 00	2.90372E-01	4.76186E-02
8.37784E-02	1.62130E 00	-1.53335E 00	2.10078E-01	-1.48961E-01
8.37864E-02	7.47111E-02	2.81499E-02	7.12765E-02	-3.34501E-03
-5.96380E-01	-1.53153E-01	0.0	0.0	

MATRIX 'D-WG'

ROW 40) *VERTICAL BENDING MOMENT W.S. 222*

4.29099E-03	2.43610E-01	1.20628E 00	2.24028E 00	3.27428E 00
4.30829E 00	5.34229E 00	6.37629E 00	7.41030E 00	8.44430E 00
1.54391E-02	3.38232E-01	5.25772E-01	5.25772E-01	5.25772E-01
5.25772E-01	5.25772E-01	5.25772E-01	5.25772E-01	5.25772E-01
0.0				

VERTICAL BENDING MOMENT W.S. 820

ROW 43 THE NON-ZERO ELEMENTS ARE

6	3.97896E-02	7	7.53572E-01	8	1.78916E 00
9	2.82476E 00	10	3.86035E 00	16	1.02681E-01
17	5.63281E-01	18	5.63281E-01	19	5.63281E-01
20	5.63281E-01				

COORDINATION SHEET

TO	3-7560 - G. O. Thompson - MS 16-18	**NO.**	3-7560-70-76
		ITEM NO.	
GROUP INDEX	Flight Controls Analysis Staff	**DATE**	12-31-70
SUBJECT	CONTROL TECHNOLOGY SUPPORT PROVIDED AT NASA-LANGLEY RESEARCH CENTER	**MODEL**	

1.0 INTRODUCTION AND SUMMARY

Work described in this report was performed at NASA-Langley Research Center through the cooperative efforts of Harley Brixey (Boeing-Wichita) and David Gray (NASA-Langley) in support of flutter suppression research conducted by Maynard Sandford (NASA-Langley).

Purpose of the work assignment was to provide technical support in mechanizing a flutter suppression control system for a NASA 1/17 scale wing aeroelastic model approximating a SST type wing. Two major areas of work were (1) hardware mechanization of a surface positioning control system and (2) analog mechanization of a NASA flutter suppression feedback control law developed by Dr. Nissim.

The specified flutter suppression feedback control law commands control surface deflections as a function of wing deflections independent of frequency. The mechanization effort goal was to develop a physical system which would accomplish the control system objective with minimum frequency dependence over the frequency range 5 to 25 Hz.

A general sketch of the flutter suppression control system is shown in Figure 1. The feedback control law is mechanized on a general purpose analog computer. Photocells are used as angular deflection sensors on both the motor shaft and control surface. Control surface actuation torque is provided by a high performance electrical torque motor. Torque is transmitted from the externally mounted torque motor to the control surface through a precision fitted mechanical linkage. Two miniature accelerometers are used as wing motion sensors.

End to end frequency response of the complete flutter suppression system deviates from the desired system frequency response as much as ±10 degrees phase and ±10 percent gain. Leading phase and reduced gain occurs at the low end of the frequency band because of low frequency attenuation filtering. Lagging phase and increased gain occurs at the high end of the frequency band because of resonance effects in the surface positioning control system. Gain and phase deviations cross zero between 10 and 15 Hz and result in a reasonably accurate mechanization at the expected flutter frequency of 12 Hz.

Complete system performance evaluations will be accomplished on the final system prior to tunnel testing.

2.0 SURFACE POSITIONING CONTROL SYSTEM

A block diagram of the surface positioning control system is shown in Figure 2. The objective of this system is to provide almost ideal transfer characteristics (zero phase shift and constant gain) between electrical command (δ_c) and control surface deflection (δ_s) for a primary frequency band of 5 to 25 Hz with a desired large amplitude capability of ±12 degrees deflection at 12 Hz and minimum low amplitude distortion.

To even approach ideal transfer characteristics requires a position system frequency bandwidth much broader than the primary frequency band stated above. Both broad bandwidth and minimum low amplitude distortion are achieved with a high gain position feedback loop. A high gain loop utilizing feedback from the surface could not be stabilized because of linkage dynamics. Feedback from the motor shaft photocell is used to form the high gain position loop and feedback from the surface is integrated and used for a surface trim loop. In addition to providing low frequency surface trim, the trim loop provides low frequency attenuation filtering (washout). The surface positioning transfer function approximation shown in Figure 2 is based on preliminary testing data and observations. Linkage dynamics are dependent on how precisely the couplings are fitted. Backlash contributes low amplitude distortion and phase lag. Linkage resonance, which appears to be directly related to the amount of backlash, contributed significant amplitude and phase deviations at 25 Hz. It appears that non-perfect mechanical linkage will be the primary contributor to surface positioning inaccuracy.

Figure 3 shows a mechanization schematic for the surface positioning control system. This system is scaled such that a 10 volt analog input commands 20 degrees surface deflection. The motor has mechanical stops at ±30 degrees and the trim loop is limited (with Zenner diodes) so the maximum bias on the motor will not restrict the large amplitude capability of the system.

2.1 Hardware Testing

Preliminary testing was performed with a breadboard setup of the actual hardware that will be used later in a wing model flutter suppression system. The hardware included a high performance torque motor, power amplifier, photocell angular position sensors, numerous operational amplifiers, and a mechanical linkage system between the torque motor and surface. Maynard Sandford designed and fabricated the mechanical linkage system. David Gray selected the electrical hardware and designed electrical circuits which offered both convenience and flexibility in the control system synthesis.

2.2 Torque Motor

Torque motor data as specified by the manufacturer is listed below:

K_i = 13 oz-in/amp
R_a = .74 ohm
J_m = .003 oz-in-sec^2
K_b = .0917 Volts/Rad/Sec

L ≤ 200 uh
Friction = 4 oz-in
Weight = 26 lbs

The motor has a permanent magnet stator and a shell type wire wound rotor with minimum inductance. Based on data listed above the approximate transfer function between armature voltage and motor shaft angular position is:

$$\frac{\Theta_M}{V_a} = \frac{57.3\ K_i/R_a\ J_m}{S(S + K_b K_i/R_a J_m)} = \frac{3.36 \times 10^5}{S(S + 537)} \quad \left(\frac{\text{DEG}}{\text{VOLT}}\right)$$

Figure 4 shows normalized frequency responses of the torque motor as a function of input voltage amplitude. A theoretical linear frequency response for the motor is also shown. Some effort was expended trying to determine a nonlinear math model for the motor and the source of the nonlinearities. The phase and gain characteristics for the small amplitude input are attributed to a spring effect in the motor which is probably caused by residual magnetism. Friction effects in the form of low gain and less phase lag are apparent in the intermediate amplitude characteristics. The large amplitude characteristics show that a second order linear model is not sufficient for the motor. The large amplitude data was used as the worst case for loop stability purposes and requirements for electrical compensation were determined graphically.

2.3 Electrical Compensation

Figure 5 shows the electrical compensation used in the forward path of the motor position loop and the measured frequency response for this compensation. Compensation is used to improve loop stability by providing leading phase in the frequency region where the open loop frequency response crosses zero db. This crossing occurs at approximately 250 Hz for the compensated loop.

2.4 Motor Positioning Performance

Actual motor positioning control system data is compared to ideal characteristics in Figure 6. This data shows maximum deviations of 1.5% gain and 7.7 degrees phase at a .1 degree amplitude. Frequency response data was obtained with a transfer function analyzer. The angular position voltage waveform was monitored on an oscilloscope to observe sinusoidal quality and noise level. Noise on the waveform was approximately 10 mv peak to peak and the waveform remained reasonably sinusoidal down to .01 degree amplitude.

Loop resonance information was obtained through small amplitude step response. A one degree step command resulted in 70 percent peak overshoot which corresponds to approximately .1 damping ratio. Resonant frequency is approximately 250 Hz. Large amplitude steps cause amplifier saturation in the forward path and current limiting in the power supplies that drive the power amplifier. Hard saturation results in an undesirable limit cycle near 85 Hz. Even though a limit cycle was observed during experimental testing, it is not expected to occur as a result of flutter suppression commands.

2.5 Angular Position Sensor

A sketch of photocell current-voltage characteristics and method of application as angular position sensor is shown in Figure 7. Theoretically, short-circuit current is a linear function of illumination level and open-circuit voltage varies logarithmically. Each angular position sensor is composed of two similar photocell segments which operate across loading resistance into differential inputs of an operational amplifier.

Some sample calibration data for the motor position photocell is presented in Figure 8. This data is within 1 percent of the linear reference over the ±25 degree range. Such accuracy over this frequency range is neither obtainable nor required of the surface trim photocell.

3.0 FLUTTER SUPPRESSION FEEDBACK CONTROL LAW

The flutter suppression feedback control law that was specified by Dr. Nissim is presented in Figure 9. This control law commands control surface deflection as a frequency independent function of wing deflections and requires both in phase and quadrature phase components. Miniature accelerometers are used to obtain wing acceleration information which is processed on an analog computer (EAI 580) to produce a surface command which approximates the specified command.

Figure 10 shows a block diagram of the control law mechanization. There are two major mechanization problems: (1) accurate double integration over the desired frequency band (5 to 25 Hz) results in very high low frequency gain, (2) period measuring, which is used in obtaining a frequency independent quadrature phased signal, contributes a transient time lag to amplitude change due to variations in frequency.

An analog mechanization diagram for the control law is shown in Figure 11. Nominal potentiometer settings are given in Table I.

Preliminary evaluation indicates that the extremely high gain between accelerometer and control surface at one radian per second frequency is tolerable with normal noise present but must be reduced to accommodate low frequency transients resulting from wing transient effects on accelerometer resonance and null shift.

Gain adjustment of the quadrature phased signal has a nominal rise time of .25 seconds. This speed of response is believed to be sufficient since it occurs in the secondary channel. Theoretical and experimental data for the period measuring mechanization are compared in Table II.

4.0 CONCLUSIONS AND RECOMMENDATIONS

The motor positioning control system operates with sufficient accuracy at amplitudes equal to or greater than .1 degree over a 5 to 25 Hz frequency band. The photocell used in the motor positioning loop is a good angular position sensor. The photocell located on the control surface provides a signal adequate for the surface trim loop. The limit cycle observed during testing is not expected to occur as a result of flutter suppression commands.

Analog simulation of the flutter suppression feedback control law will require further study. Additional attenuation filtering is needed at low frequencies to accommodate accelerometer transients. A high quality multiplier is needed to maintain sufficient accuracy in the secondary channel for low amplitude signals.

Prepared by Harley D. Brixey
Harley D. Brixey

Approved by Gerald E. Bergmann
Gerald E. Bergmann

cc: 7500 - CFNewberry - MS 16-36
NASA - AGRainey - Langley

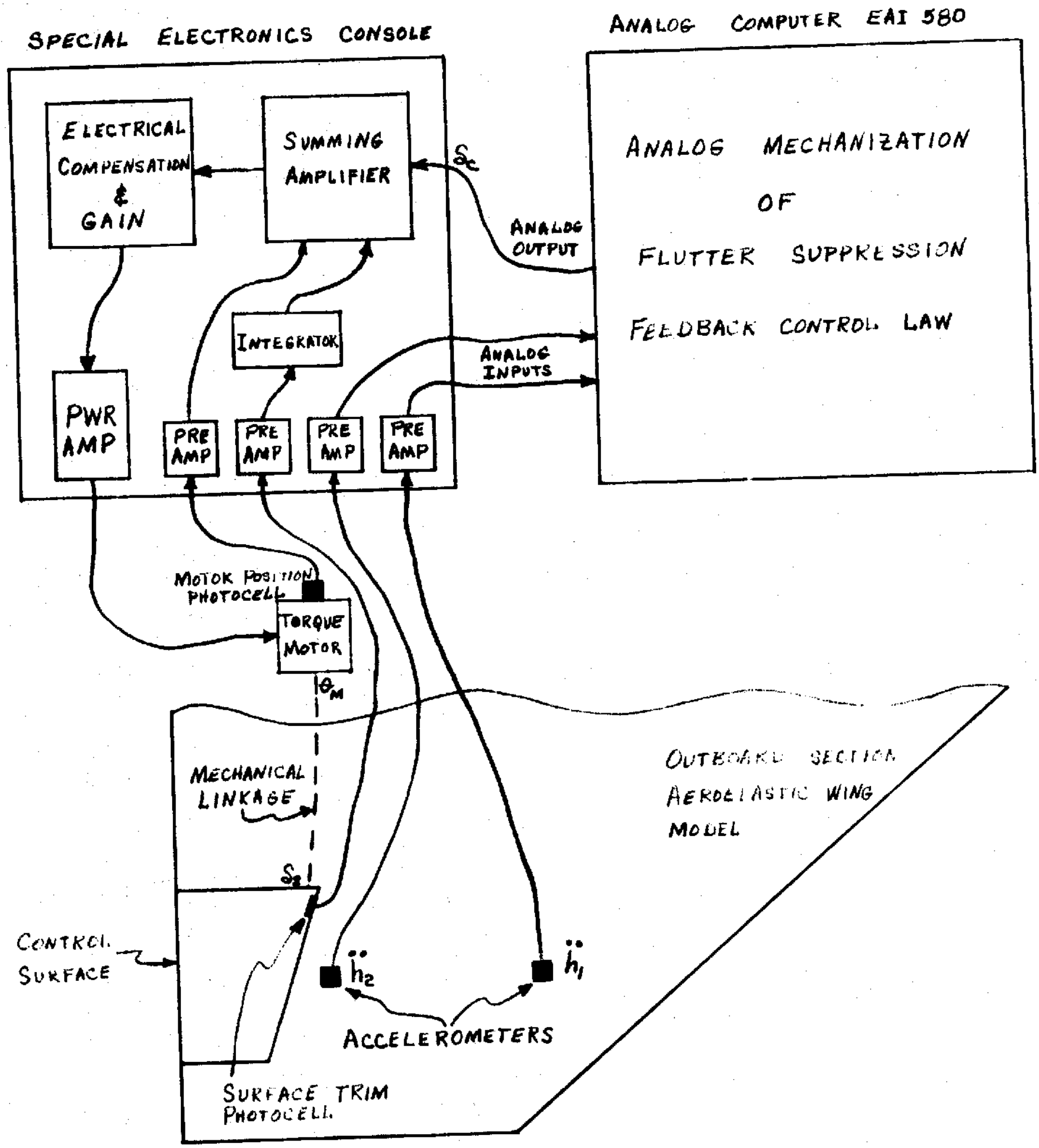

FLUTTER SUPPRESSION SYSTEM SKETCH

FIGURE 1

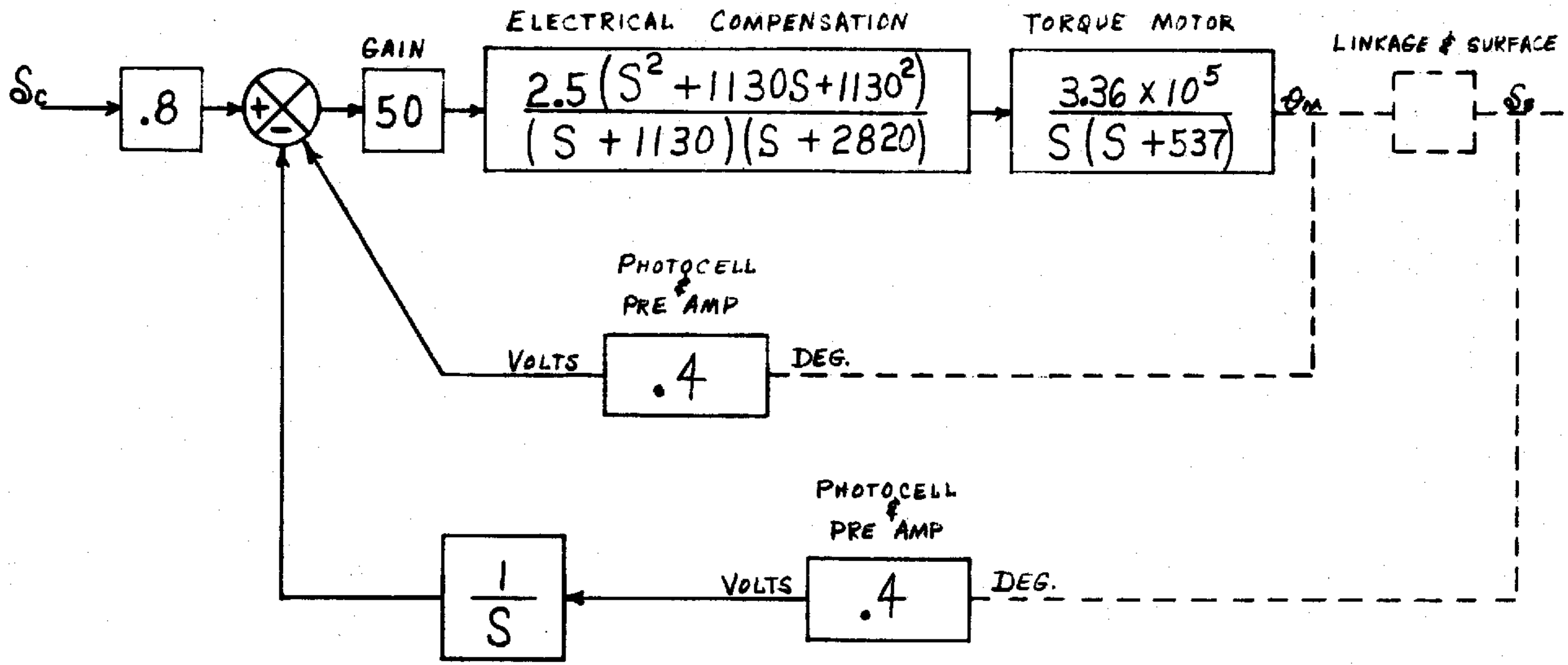

MOTOR POSITIONING SYSTEM — TRIM~WASHOUT — LINKAGE BACKLASH — LINKAGE & SURFACE DYNAMICS

$$\frac{\delta_s}{\delta_c} \cong \left[\frac{2(1570^2)}{S^2 + 314S + 1570^2}\right] \bullet \left[\frac{S}{S+1}\right] \bullet \left[\text{LINKAGE BACKLASH}\right] \bullet \left[\frac{\omega_n^2}{S^2 + 2\zeta\omega_n S + \omega_n^2}\right] \left(\frac{\text{DEG}}{\text{VOLT}}\right)$$

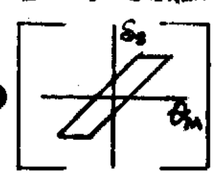

SURFACE POSITIONING CONTROL SYSTEM

FIGURE 2

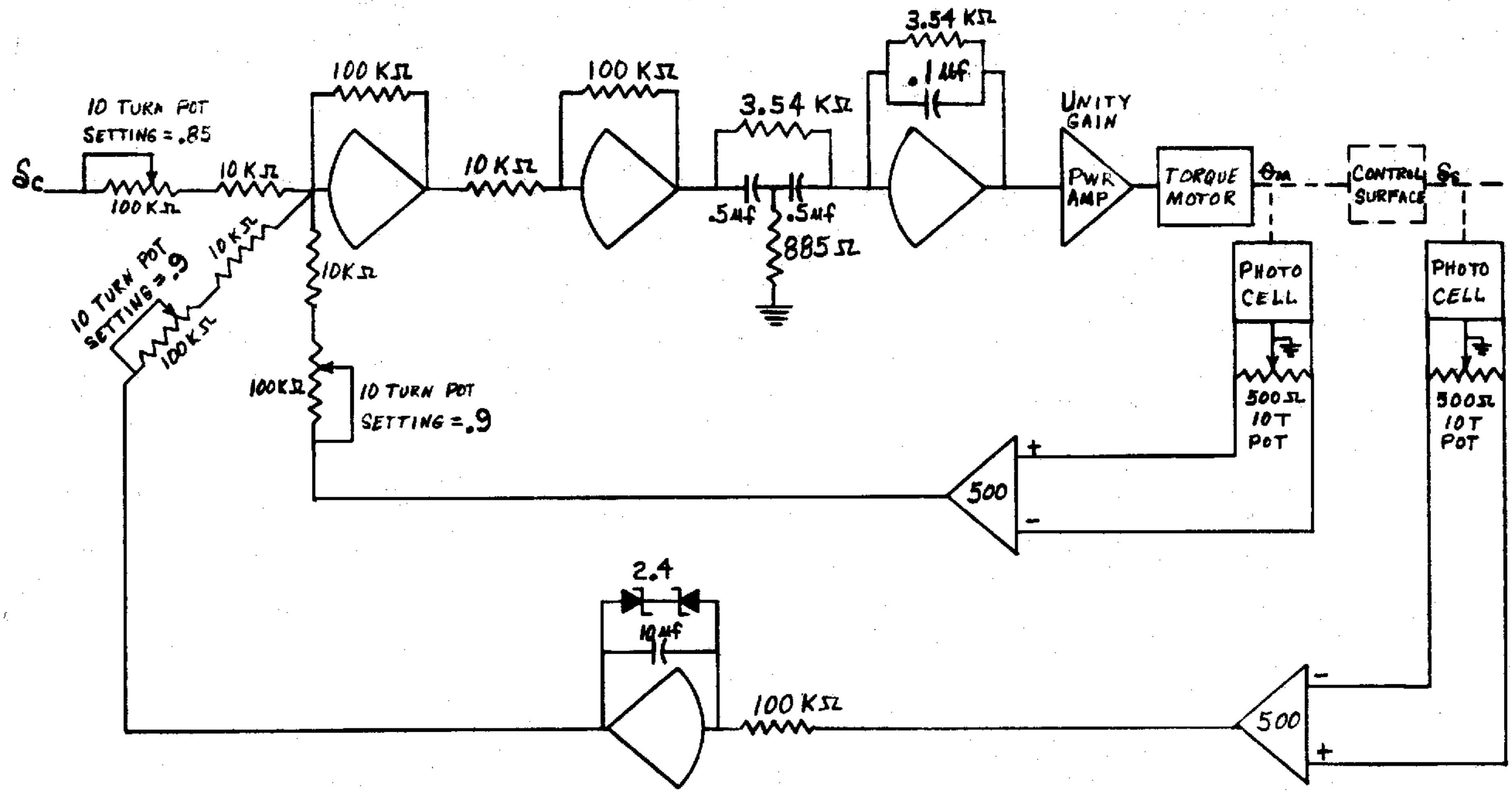

SURFACE POSITIONING CONTROL SYSTEM

FIGURE 3

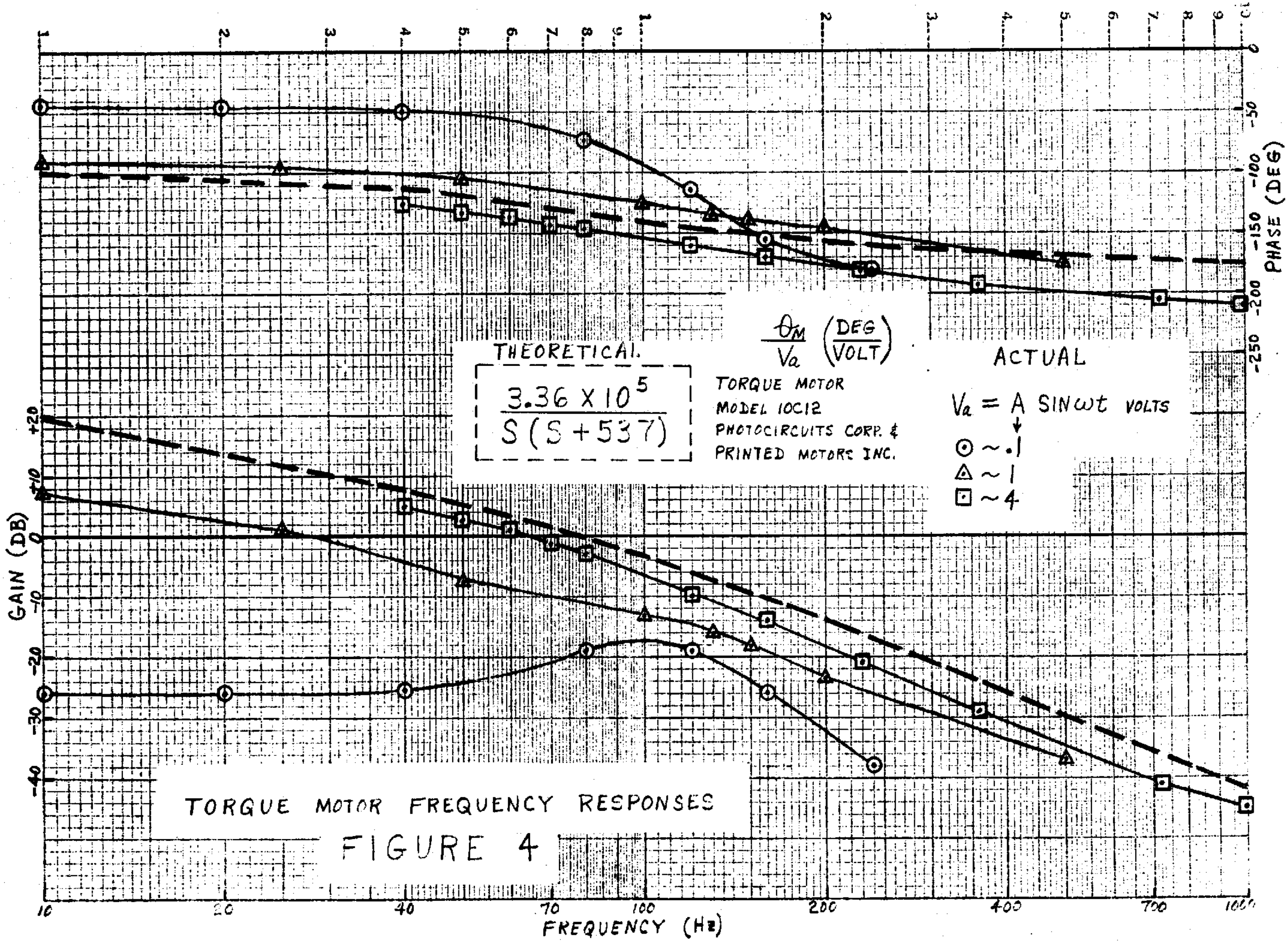

TORQUE MOTOR FREQUENCY RESPONSES

FIGURE 4

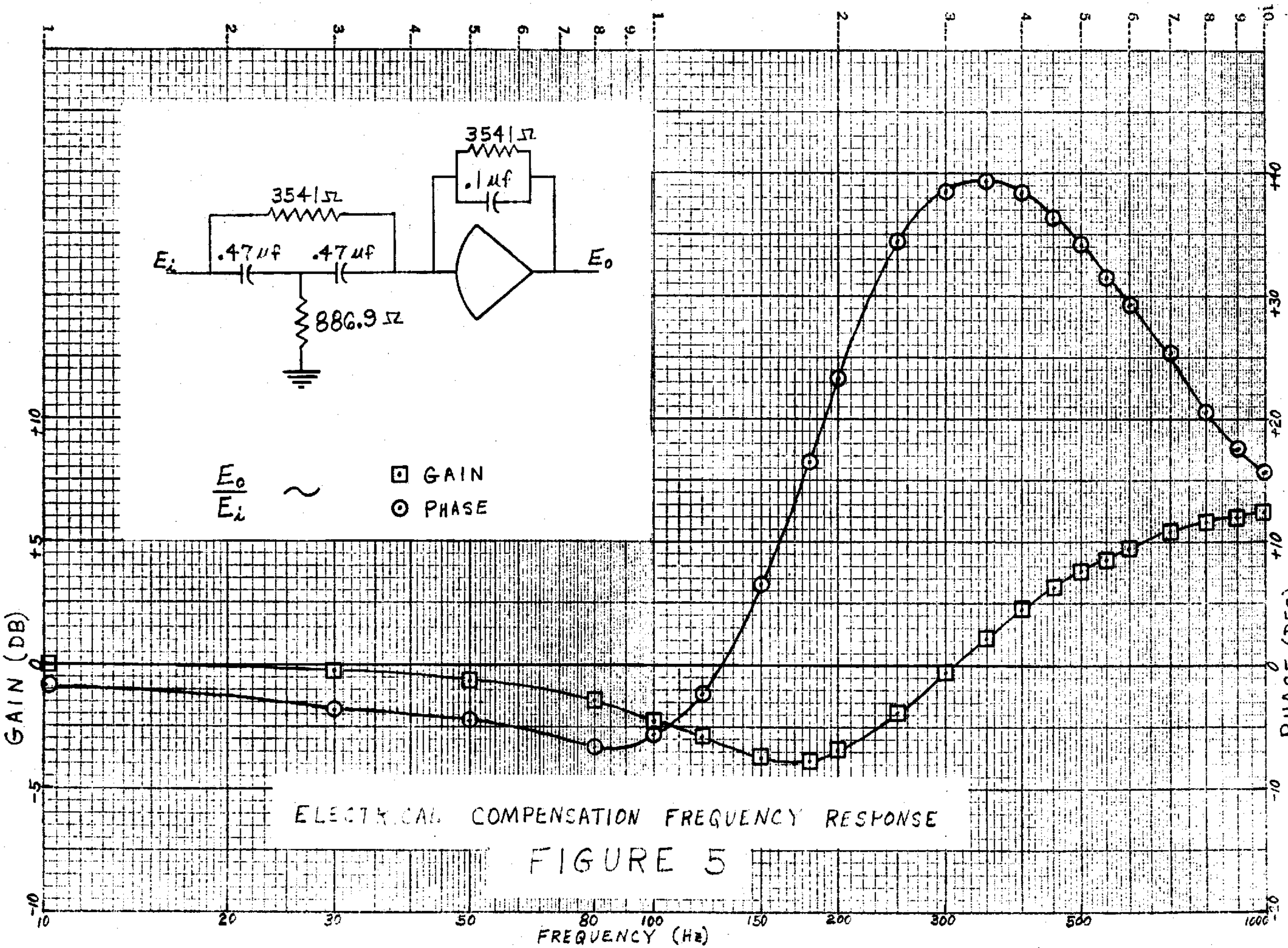

ELECTRICAL COMPENSATION FREQUENCY RESPONSE

FIGURE 5

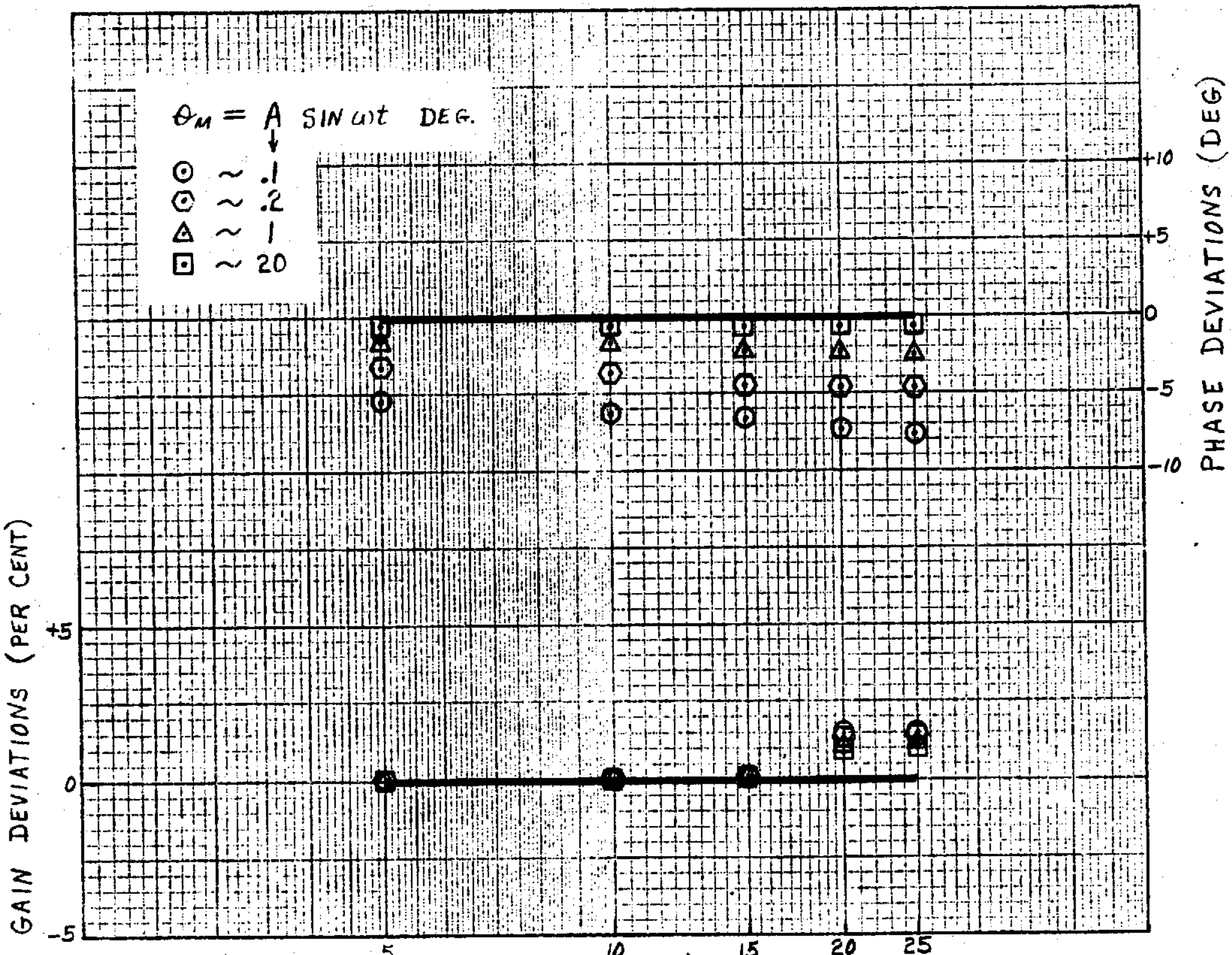

FREQUENCY RESPONSE COMPARISON OF ACTUAL MOTOR POSITIONING CONTROL SYSTEM TO AN IDEAL SYSTEM

FIGURE 6

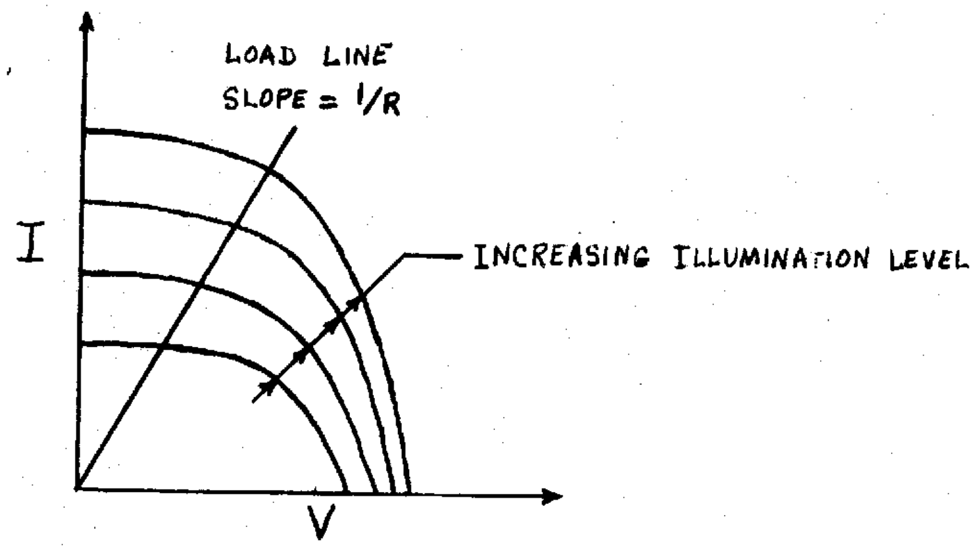

CURRENT – VOLTAGE CHARACTERISTICS

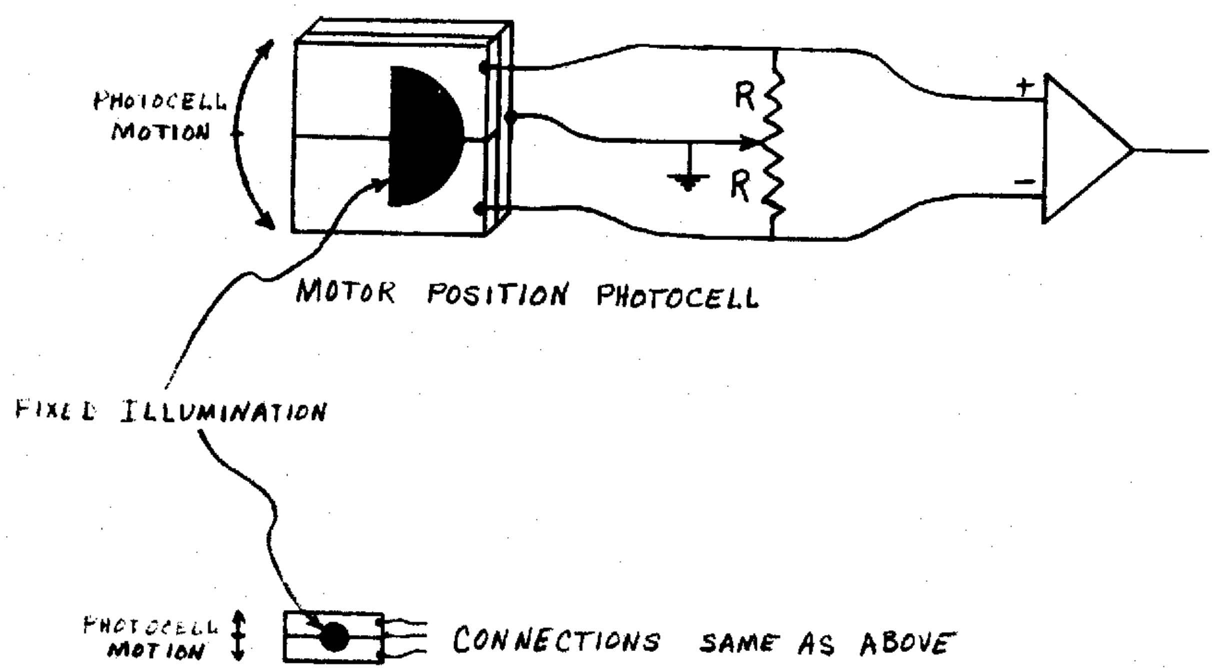

SURFACE TRIM PHOTOCELL

PHOTOCELL CHARACTERISTICS AND APPLICATIONS SKETCH

FIGURE 7

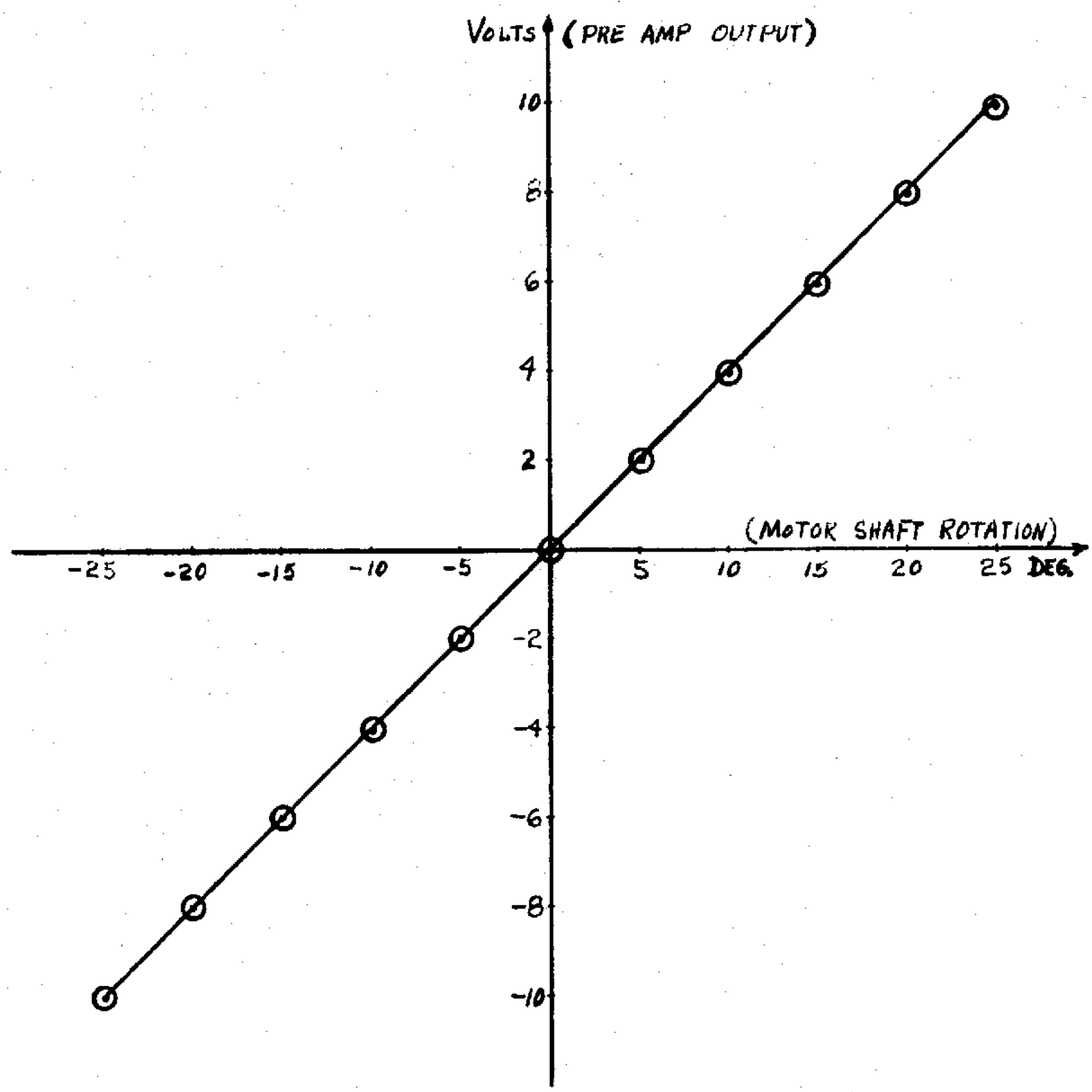

MOTOR POSITION PHOTOCELL CALIBRATION DATA

FIGURE 8

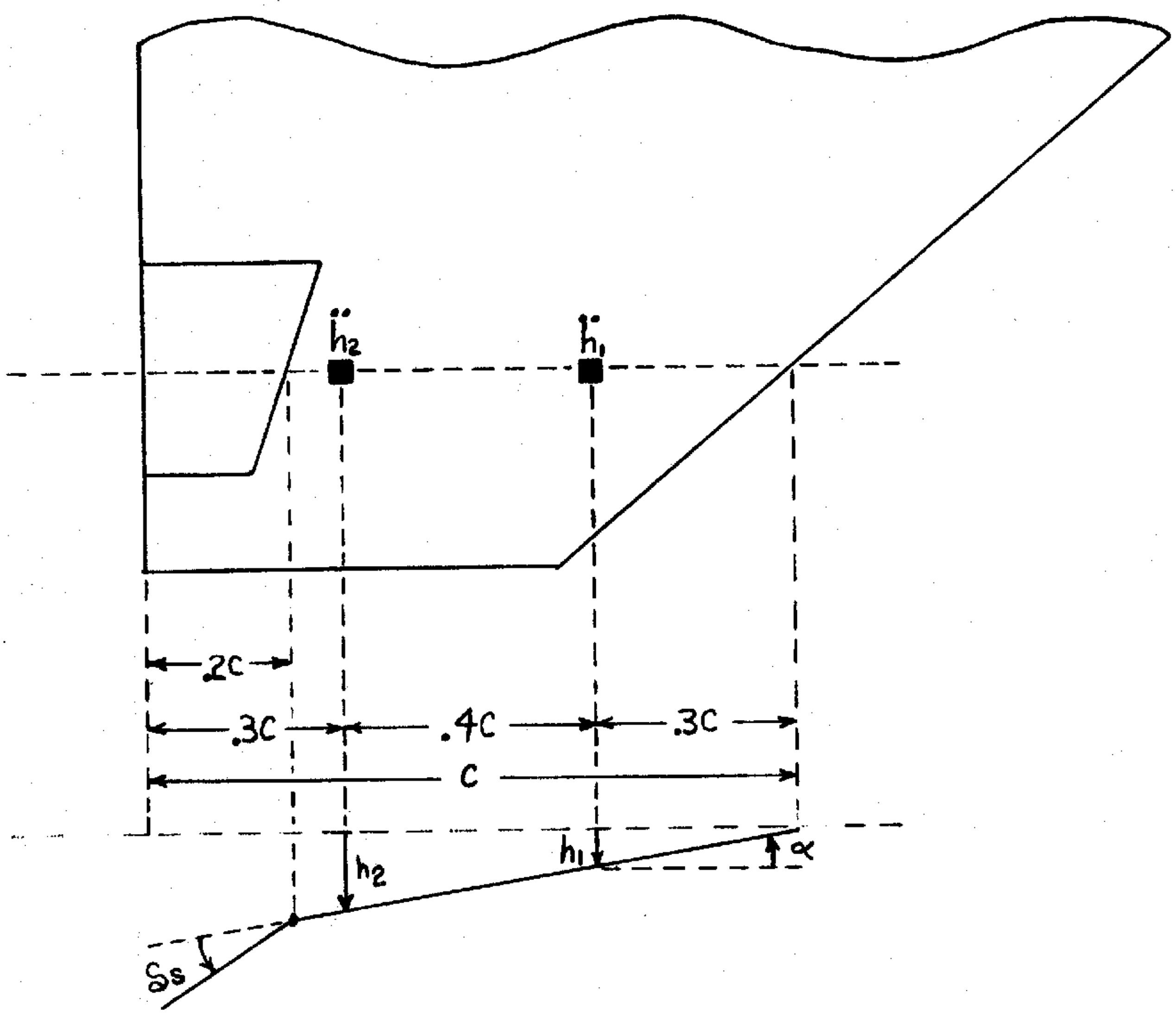

$$\delta_s\,(DEG) = 57.3\left[(-.7 + J.7)\frac{h_1}{c} + (-1.9 + J.1)\alpha\right]$$

ALTERNATE FORM

$$\left[(4.05 + J.45)\frac{h_1}{c} + (-4.75 + J.25)\frac{h_2}{c}\right]$$

FLUTTER SUPPRESSION FEEDBACK CONTROL LAW

FIGURE 9

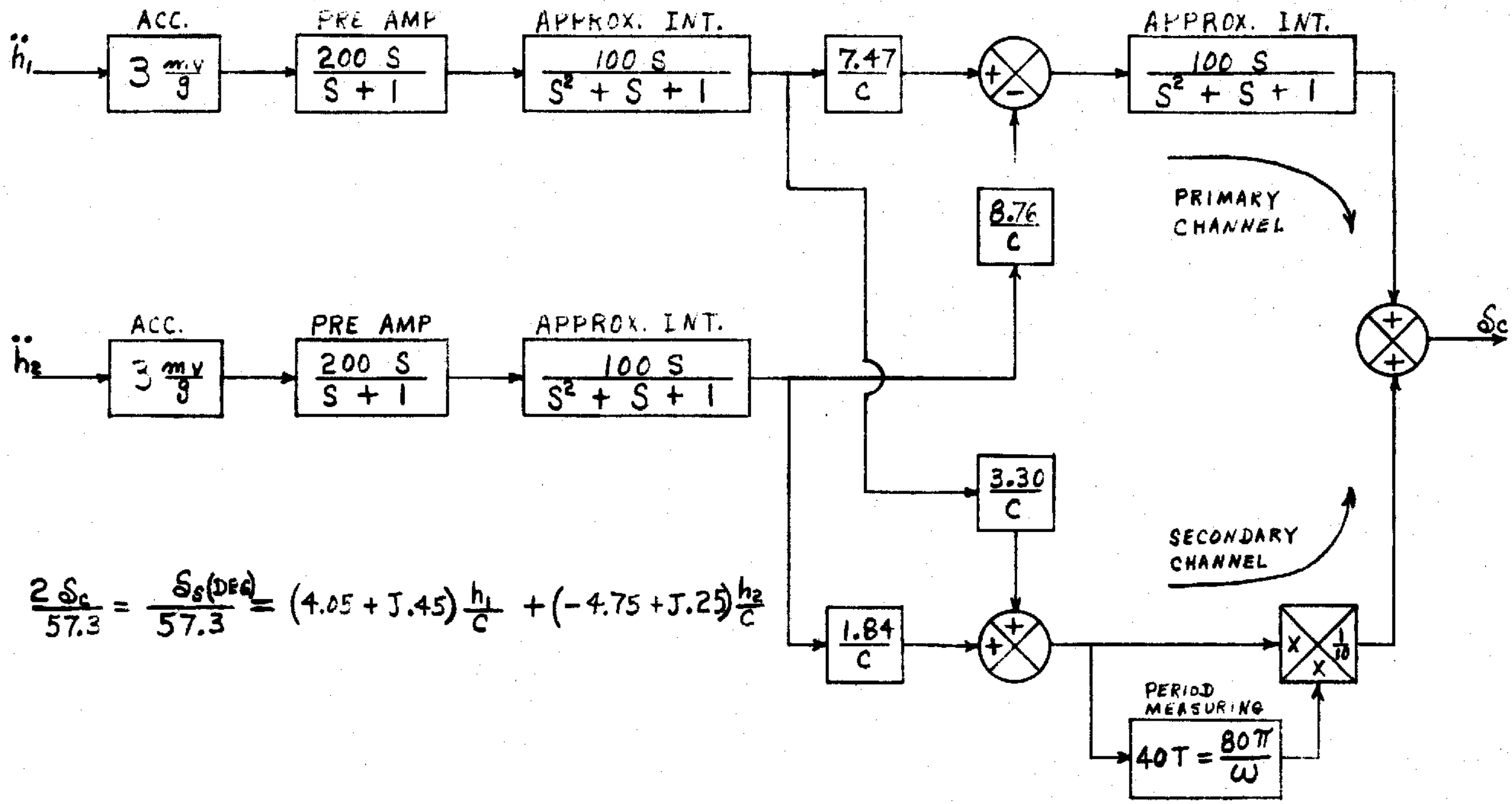

FLUTTER SUPPRESSION FEEDBACK CONTROL LAW

FIGURE 10

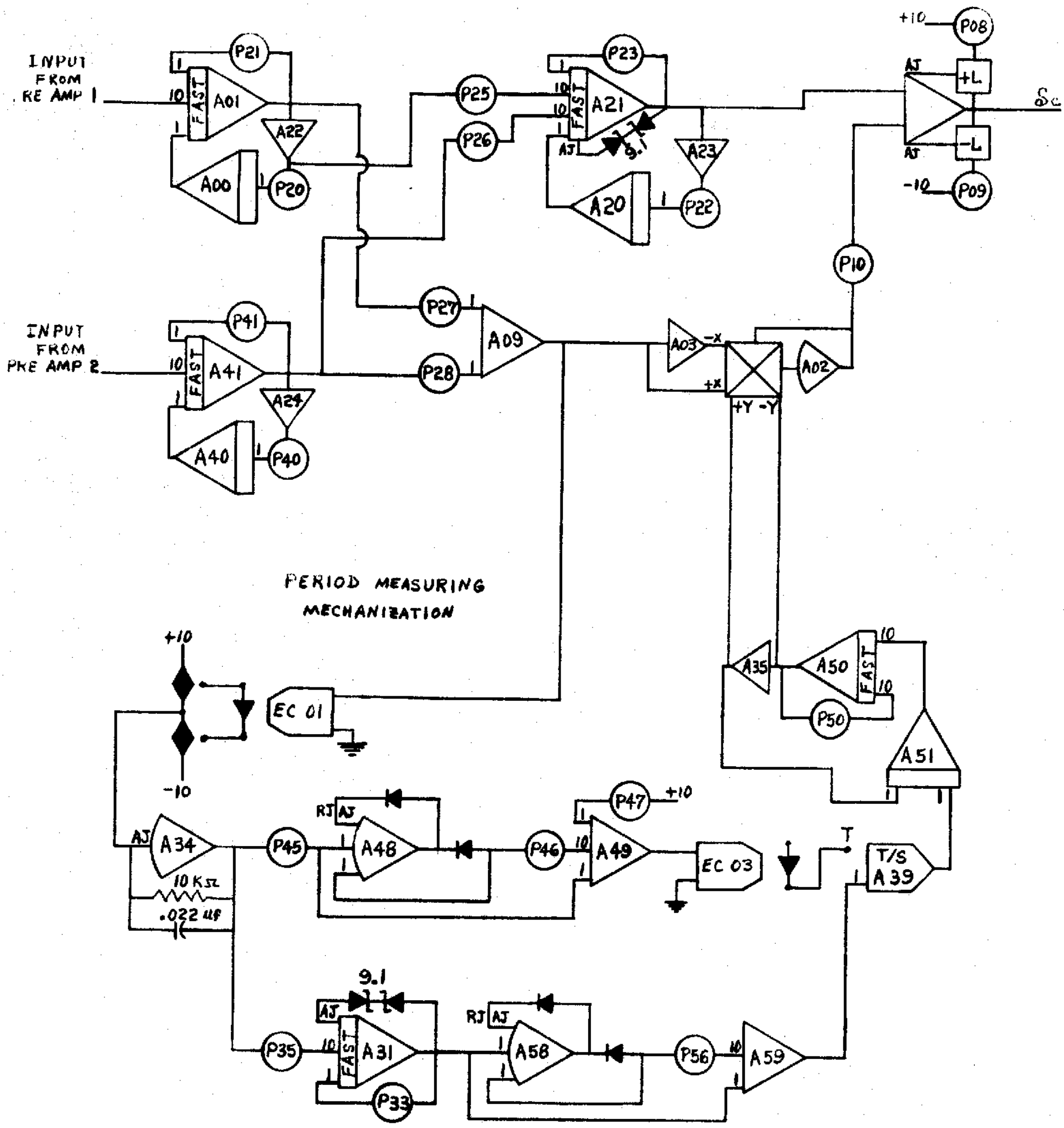

FLUTTER SUPPRESSION FEEDBACK CONTROL LAW

FIGURE 11

TABLE I

ANALOG POTENTIOMETER SETTINGS

IDENTIFICATION	SETTING	IDENTIFICATION	SETTING
P08	*	P28	.254**
P09	*	P33	.5
P10	.5	P35	.16***
P20	.1	P40	.1
P21	.1	P41	.1
P22	.1	P45	.8
P23	.1	P46	.2
P25	.515**	P47	.4
P26	.604**	P50	.2
P27	.455**	P56	.2

*Variable limits on flutter system authority

**Based on $\bar{c}$ of 14.5 inches

***Adjust to give 4 volts out of A35 in response to steady state 10 cps input to analog system

TABLE II

PERIOD MEASURING MECHANIZATION DATA

INPUT	A Sin ωt	.05 Sin ωt	10 Sin ωt
FREQUENCY (Hz)	THEORETICAL OUTPUT	MEASURED OUTPUT	MEASURED OUTPUT
0	∞	9.3	9.3
5	40T=8.000 VOLTS	40T=7.86 VOLTS	40T=7.87 VOLTS
6	6.667	6.64	6.65
7	5.714	5.73	5.73
8	5.000	5.02	5.02
9	4.444	4.46	4.47
10	4.000	4.00	4.00
11	3.636	3.62	3.63
12	3.333	3.32	3.321
13	3.077	3.05	3.055
14	2.857	2.82	2.828
15	2.667	2.64	2.636
16	2.500	2.47	2.473
17	2.353	2.32	2.320
18	2.222	2.19	2.190
19	2.105	2.07	2.072
20	2.000	1.97	1.969
21	1.905	1.876	1.877
22	1.818	1.785	1.785
23	1.739	1.705	1.706
24	1.667	1.635	1.635
25	1.600	1.565	1.566